Stony Brook University

The Semicircular Canals of Birds and Non-Avian Theropod Dinosaurs

A Dissertation Presented

by

Justin Scott Sipla

to

The Graduate School

in Partial Fulfillment of the Requirements for the Degree of

Doctor of Philosophy

in

Anatomical Sciences

Stony Brook University

August 2007

Stony Brook University

The Graduate School

Justin Scott Sipla

We, the dissertation committee for the above candidate for the Doctor of Philosophy degree, hereby recommend acceptance of this dissertation.

Catherine A Forster, Ph.D. – Dissertation Advisor
Associate Professor
Department of Anatomical Sciences

William L. Jungers, Ph.D. – Chairperson of Defense
Professor
Department of Anatomical Sciences

Jack T. Stern, Ph.D. – Dissertation Advisor
Professor
Department of Anatomical Sciences

James M. Clark, Ph.D. – Outside Member
Professor
Department of Biological Sciences
George Washington University

This dissertation is accepted by the Graduate School

Lawrence Martin
Dean of the Graduate School

Abstract of the Dissertation

The Semicircular Canals of Birds and Non-Avian Theropod Dinosaurs

by

Justin Scott Sipla

Doctor of Philosophy

in

Anatomical Sciences

Stony Brook University

August 2007

The invasion of aerial habits by primitive birds involved massive reorganization of neurological and sensory systems, many of which are coordinated in the brain by vestibular cues from the semicircular canals. These organs sense angular accelerations experienced by the head and body with every movement. Canal signals are combined with visual and somatosensory inputs and are used to generate a wide-range of reflexive behaviors necessary for stabilizing gaze, maintaining posture, and coordinating body movements.

This dissertation focuses on understanding the relationship between locomotor behavior and vestibular function in birds and non-avian theropod dinosaurs, both from a comparative and functional perspective. Widespread use of noninvasive computed tomography (CT) has opened great possibilities for visualizing canal structures, which are often preserved in fossil specimens. The otic capsules of 178 species of extant birds and

15 species of non-avian theropods were CT scanned and the vestibular structures reconstructed and measured from digitally prepared volumes.

The morphology of the semicircular canals in non-avian theropods and many flightless birds is shown to reflect their status as bipedal cursors, while the pattern seen in volant avians is found to correlate strongly with different flying behaviors. Independent measures of aerobatic maneuverability, such as wing loading, also correlate with canal morphology, demonstrating that, at least in flying birds, larger and thus more sensitive canals are possessed by agile species flying at slower speeds. Freed in air from the need for intermittent contact with a surface substrate, birds can employ a wider repertoire of body movements during locomotion, including forms of rotation that would be improbable on land. In the absence of somatosensory cues from postural interactions with the ground, it is argued that these movements place increased demands on the vestibular system of avian fliers.

Investigation into the size and shape of avian semicircular canals permits evaluation of the mode of flight employed by primitive avialans, like *Archaeopteryx*, shedding light on some of the broader neurophysiological adaptations to flight behavior that characterize bird evolution.

In preparing this dissertation, my wife Kathryn was a constant support, as in all things.

She endured my labors with patience, confidence, and love.

This work is dedicated to her.

Table of Contents

List of Figures

List of Tables

Acknowledgements

I am greatly indebted to Fred Spoor for his mentorship. I was introduced to Fred by Callum Ross at the 2001 annual meeting of the American Association of Physical Anthropologists (AAPA) in Kansas City, a few months before I started graduate school. I originally came to Stony Brook to document kinematic patterns of head movement associated with locomotion in primates, for the purpose of testing biophysical models of semicircular canal function. Discussions with Cathy Forster soon shifted my interest to bird and dinosaur vestibular evolution. Cathy became my main advisor, and I am forever grateful to her for the wisdom, guidance, and inspiration she imparted to me on a daily basis. Cathy gave me the freedom to take this project wherever it needed to go.

Investigations described in this text began in January, 2003, following a two-week crash course in computed tomography at University College London with Fred Spoor. The journey ever since has been marked by all the hazards and rewards of scientific inquiry: frustration, excitement, defeat, and the occasional victory. I am indebted to many who helped along the way. Had it not been for the great and sympathetic interest of several advisors, colleagues, friends, and curators, far too many to name here, I would not be in a position to report on the majority of animals included in this work.

As I'm sure many graduate students at Stony Brook have said over the years, Bill Jungers was instrumental in getting the statistics right. I could not have finished this project without his help. Many sincere thanks to Jack Stern and Jim Clark for joining my committee at the zero hour, and for tackling all the burdens and responsibilities that came with doing so. Their comments vastly improved this manuscript.

I am exceedingly grateful to Peter Capainolo, Carl Mehling, and Walter Joyce, who tirelessly helped in the retrieval of taxa from the collections at AMNH Ornithology, AMNH Vertebrate Paleontology, and Yale Peabody Museum, respectively. Very special acknowledgement must be given to Mark Norell (AMNH), who granted access to many unique theropod specimens from Mongolia and China. Of course, I would not have been able to collect a single datum were it not for the help of the medical imaging staff at Stony Brook University Hospital, where the CT scans were primarily generated: Charlie Mazzarese, Herriot Nicoleau, Lou Caronia, and Wayne Mattera. My friend and cohort Justin Georgi has been a constant ally in these investigations. The value of our daily discussions about semicircular canal function can hardly be overestimated.

Much love and gratitude are due my parents for their constant support and encouragement. Lastly, and most importantly, I am indebted to my wife Kathryn. Though she forgot to recite the "in sickness and in health" vow during our wedding ceremony, she has stuck by me through it all. I am grateful to her every day, for every thing.

This research was generously supported by grants from the Jurassic Foundation and Frank M. Chapman Memorial Fund (American Museum of Natural History, Dept. of Ornithology).

Introduction

In vertebrates, the sensation of motion is experienced at the nonconscious level by the vestibular system, composed of the semicircular canals, otolith organs, and associated structures. This bilateral network of membranous tubes and vesicles is embedded in the labyrinth of the avascular, bony otic capsule of birds, mammals, and all other tetrapods. The sensory receptors of the vestibular system, or end organs, supply afferent axons to the eighth cranial nerve (vestibulo-cochlear nerve), which transmits a frequency code of impulses to the brain stem regarding angular and linear forces experienced by the head in motion. This information is combined centrally with visual and proprioceptive inputs and used to generate a wide-range of reflexive behaviors necessary for stabilizing gaze, maintaining posture, and coordinating body movements. This complex control system even regulates certain autonomic functions, adjusting heart and respiratory rates in response to rapid changes in posture. More generally, these systems function to maintain the sense of balance.

Anatomical differences in the size of vestibular organs have long been argued to indicate differences in vestibular function. For centuries, researchers have sought knowledge of the structural differences of the vestibular system in various animals, to address a wide range of clinical, evolutionary, and anatomical questions. Until recently, however, observing the vertebrate labyrinth typically required mould-injection casting and destructive sectioning of the otic capsule, something often disallowed on rare specimens, especially fossils. Today, widespread use of noninvasive computed tomography (CT) has opened great possibilities for visualizing labyrinthine structures

preserved in hard tissues. Specimens can be borrowed from museum collections for short durations, scanned, and returned without alteration. Furthermore, data generated from CT scans are stored electronically as digital media, creating a permanent record of the specimen that can be shared easily among investigators.

The focus in this dissertation will be on part of the organ of balance, the semicircular canal system, because it is the comparative, functional and evolutionary morphology of this part that is increasingly well understood. The size of the semicircular canals is directly related to the sensitivity of the angular motion sensors, and this property has been linked to degree of locomotor agility in numerous animal groups. A major goal of the present study is to describe semicircular canal size variation in a large comparative sample of extant birds and extinct theropod dinosaurs—the closest relatives of birds—using computed tomography. This is done to assess patterns of inner ear design associated with powered flight, and to identify neurophysiological specializations associated with detecting motion during aerial locomotion and aerobatics. How and when did the bird labyrinth acquire its unique characteristics, and what, if anything, can this tell us about the origin of flight? To answer these questions, representatives from nearly every extant bird order and several extinct theropod orders are examined herein, comprising the largest known inventory of comparative bird and dinosaur semicircular canal size data so far assembled.

The dissertation is structured into five chapters. Chapter 1 introduces the reader to the anatomy and physiology of the vestibular system to establish principles of canal function applicable to bird and non-avian dinosaur evolution. Chapter 2 reviews the evolutionary origin of birds and current hypotheses about the origin of avian flight,

followed by a review on the aerodynamics of flapping flight. Particular attention is given to morphological factors of wing shape that influence flight performance, namely wing loading and aspect ratio. Hypotheses and methods are detailed in Chapter 3. Results of the research conducted in this dissertation are presented in Chapter 4, followed by a discussion of the findings. Chapter 5 is a synthesis of the original research conducted and presented in this dissertation, with comments on directions for future work. Finally, Appendix 1 compiles the raw morphometric data obtained for the dissertation, as well as sources of data collected by other authors, and Appendix 2 summarizes the taxonomic rank of all bird specimens used in the foregoing analyses.

Chapter 1:
Anatomy and Function of the Vestibular System

This chapter provides an overview of the vestibular system and its anatomical and functional components, with emphasis placed on the semicircular canals, the part of the system that responds to angular forces. The reader is introduced to the anatomy, physiology, and physics of the semicircular canals to establish principles of canal function applicable to bird and non-avian dinosaur evolution.

1.1. Historical perspective

> "It is not easy to say where this sense [of motion] exists; whether in the muscle only, or in the joints and sinews and integuments, or in the whole frame altogether."
>
> — Herbert Mayo (1837)

The great majority of work undertaken in vestibular research stems from a clinical need to treat human balance disorders. Conditions such as vestibular neuronitis (inflammation of the eighth cranial nerve due to infection), Ménière's disease (increase in volume and pressure of endolymph in the inner ear), and benign paroxysmal positional vertigo (abbreviated BPPV; caused by the accumulation of displaced otoconia in the semicircular ducts), can have profound, debilitating effects on human well-being. Diseases of the end organs that sense motion, or damage to central vestibular pathways

that carry motion impulses, can result in vertigo, imbalance, pathological nystagmus, tinnitus, progressive hearing loss, and a constellation of related symptoms.

It is no surprise, then, that medical practitioners since antiquity have sought information on the nature of balance perception. In the second century AD, prominent Greek physician Galen examined the inner ear and decided that its complicated system of fluid-filled passages and cavities resembled the mythical 'labyrinthos' constructed by Daedalus for King Minos, who needed it to imprison his wife's son, the Minotaur (cited in Hawkins and Schacht, 2005). Galen's examinations did not go much further, and for centuries the vestibular system was believed to be part of the organ of hearing.

It wasn't until the early nineteenth century, after rigorous description of the vestibular organs by renaissance anatomists, that a role in balance perception became known. Erasmus Darwin, Charles' grandfather, wrote extensively about vertigo in his *Zoonomia* (1796). Therein, he relates an experiment (cited in Cohen, 1984) in which he looks steadily at the ceiling while rotating himself until he becomes vertiginous. He then stops and pitches his head downward, noting that the experience of vertigo continued long after the time of head pitch. Some twenty years later, Czech anatomist Jan Evangelista Purkyně (also written Purkinje) repeated this experiment and recognized that the head movements must have excited discreet sensors within the skull capable of detecting movement around different axes (1820), though he incorrectly believed that such motions were detected by movements of the cerebellum within the posterior cranial fossa (for a description of Purkinje's experiments of nystagmus and vertigo, see Grüsser, 1984).

At about the same time, French anatomist Marie-Jean-Pierre Flourens recognized that the semicircular canals were dissociated from the perception of hearing. Flourens (1824) reported that destructive sectioning of the semicircular canals in pigeons affected the animal's posture, equilibrium, and locomotor capabilities, but not its hearing. He also demonstrated that by stimulating a semicircular canal nerve, eye movements were invoked in the plane of the canal (Flourens, 1824, 1830).

In the latter part of the nineteenth century it was discovered simultaneously by three separate investigators—Ernst Mach, Josef Breuer, and Alexander Crum-Brown—that sensation of angular motion relied on inertial forces perceived by the semicircular canals (Mach, 1873; Breuer, 1874; Crum-Brown, 1874). It was Crum-Brown who noted that each semicircular canal could sense motion about one axis and in one direction only. Therefore, he concluded, "six semicircular canals are required, in three pairs, each pair having its two canals parallel (or in the same plane) and with their ampullae turned opposite ways" (1874). While Mach, Breuer, and Crum-Brown shared the basic discovery of *where* angular motion was detected in the skull, evidence of *how* the semicircular canals functioned remained unknown until J.R. Ewald's experiments with pigeon semicircular canals (Ewald, 1892; reviewed in Cohen and Raphan, 2004). Using injected air to mechanically indent the semicircular ducts, Ewald initiated endolymph flow within the duct lumen and observed that head and eye movements could be induced in the plane of the affected duct. He also noted that within each duct, one direction of fluid flow had an excitatory effect on nerve transmission, while the opposite direction had an inhibitory effect.

Vestibular science flourished during the twentieth century and continues to the present day, particular in the fields of neurophysiology and biophysics. Considerable attention has been placed on understanding the morphophysiology of the vestibular end organs, the biomechanics of their function, and the complex interactions of the vestibular system with the head-neck sensorimotor system, in particular those processes underlying vestibular control of eye, neck, and spinal reflexes. The following sections explore these functions in greater detail.

1.2. Evolution and anatomy of vestibular end organs

The vestibular end organs were one of the first sensory systems established in vertebrate evolution and arose early in the evolution of the lineage, possibly as a modification of the basic neuromast organ present in fish lateral line systems (van Bergeijk, 1966; Baird 1974; Fritzsch, 1988; Northcutt, 1989). Fish and larval amphibians use the lateral line to detect movement and vibration in the surrounding water, to avoid collisions and permit orientation relative to changing water currents, and to detect prey (Schellart and Wubbels, 1998). Vestibular organs and lateral line organs share many basic anatomical features. Both systems utilize an array of hair cells with cilia protruding into a gelatinous matrix, the cupula. Deflection of the cupula causes excitation of afferent neurons, informing the brain about the nature of the disturbance. Whereas the lateral line sensors are typically deployed in grooves running lengthwise down each side of the body in fish, vestibular organs are housed with the dense otic capsule of the inner ear. The presumed original function of the vestibular organs was to encode linear and rotational

movements experienced by the head during movement, as well as to provide the brain stem with information on head orientation relative to gravity, for the purpose of driving motor responses crucial to everyday function and survival.

Swedish physician Gustav Retzius greatly developed the comparative anatomy of the vertebrate labyrinth in two volumes of drawings called Das Gehörorgan der Wirbelthiere ("The Acoustic Organ of Vertebrates," 1881, 1884) and showed that the basic configuration of the vestibular sensors was similar from fish to mammals and reptiles. All gnathostome vertebrates were shown by Retzius to possess a vestibular apparatus comprised of three semicircular canals and three otolith organs (utricle, saccule, and lagena, the latter being lost in eutherian mammals) in each ear, with a variable number of additional sensory organs (termed papillae) not associated with either the canals or otolithic structures.

Retzius showed that agnathan (jawless) vertebrates possessed one or two vertical semicircular canals with their associated sensory epithelia (1881). In the case of the hagfish (Class Myxini), a single semicircular canal arises from the utricle and is considered homologous to the vertical (anterior and posterior) canals of gnathostome vertebrates (Lowenstein and Thornhill, 1970). In lampreys (Class Cephalaspidomorphi), the two vertical canals are distinct, arising jointly by common crus from the utricle, and conforming generally to the planar orientations of the vertical canals in gnathostomes. It is believed that the third (horizontal) canal was acquired during the early stages of gnathostome evolution (Lewis et al., 1985), transforming the primitive two-canal design into a complex three-dimensional sensor capable of tracking movements in all three rotational degrees of freedom (Fritzsch, 1987; Fritzsch and Beisel, 2001). This basic 3-

canal configuration is remarkably conserved in all gnathostomes, including reptiles and birds, though often extreme differences in the size and shape of these organs are reported (Spoor and Zonneveld, 1998; Spoor et al., 2002, 2007; Sipla et al., 2003, 2004; Georgi and Sipla, in press; Sipla and Spoor, in press).

1.2.1. Anatomical organization of the gnathostome labyrinth

In all non-eutherian vertebrates, each side of the mirror-symmetric vestibular system contains an ensemble of six hair cell clusters—arranged as three otolithic maculae and three semicircular duct cristae—located in the hard, avascular bony otic capsule of the cranium (Figure 1–1). The hair cell clusters are situated within a system of interconnected vesicles and tubes, the membranous labyrinth. The membranous labyrinth is composed of fibrous ectodermal epithelium and is suspended by fine trabecular filaments within a layer of laminar bone, the bony labyrinth, which invests the membranous labyrinth and separates it from the cancellous bone of the neurocranium (Gray, 1907, 1908) This is the condition found in all birds and mammals (Curthoys et al., 1977), though in lower vertebrates the bony labyrinth is often partly or totally cartilaginous.

Two distinct extracellular fluids are contained within the inner ear: endolymph and perilymph. Endolymph is compartmentalized within the membranous labyrinth, where it bathes the apical surfaces of the vestibular epithelium. This fluid is free to flow between the passages of the otolith organs and semicircular ducts, except where the passages are obstructed by sensory epithelia (such as by the cupula of the semicircular

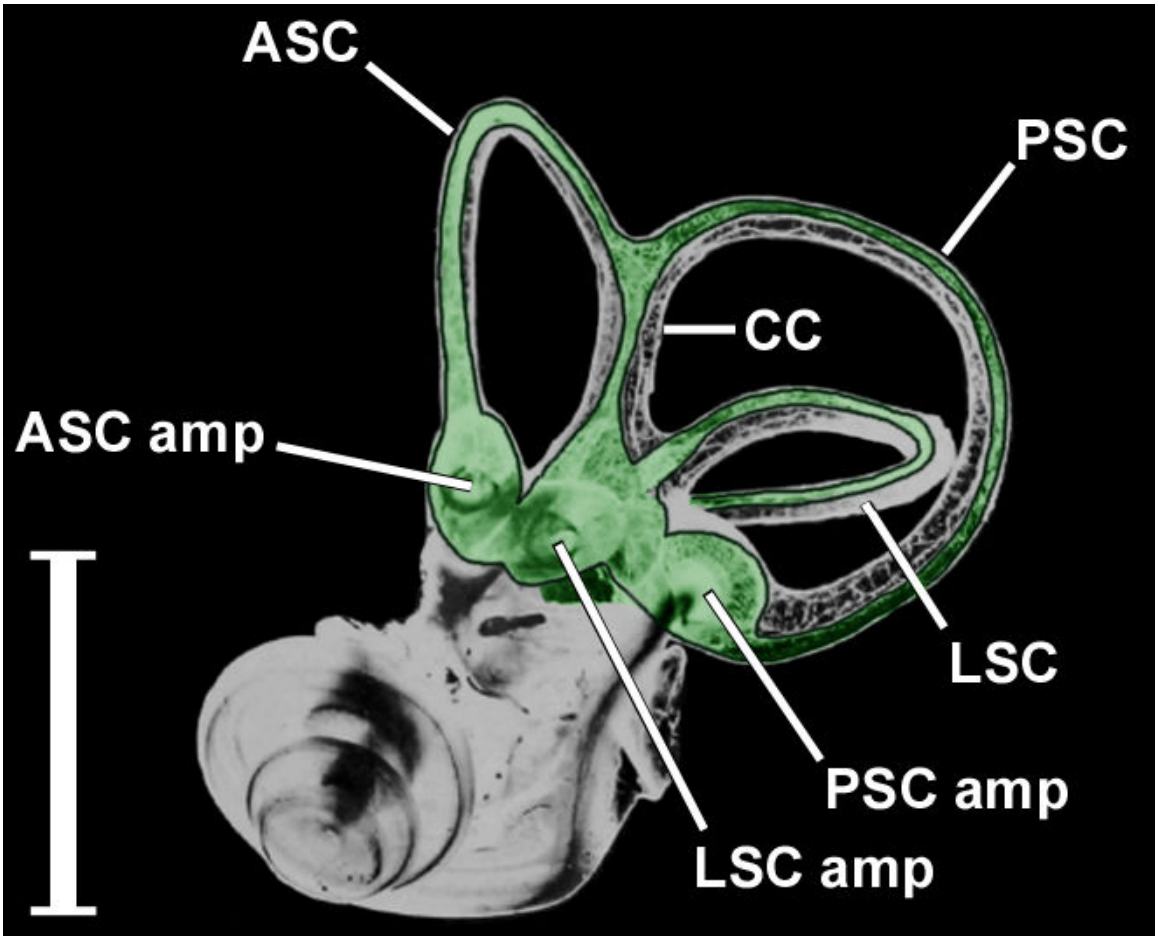

Figure 1–1. Generalized semicircular canal system. Lateral view of preparation of the inner ear of the yellow-faced baboon (*Papio cynocephalus*), showing the three semicircular canals and the membranous ducts (shaded green) enclosed along their outer border. Anterior is left. ASC = anterior semicircular canal; PSC – posterior semicircular canal; LSC – lateral semicircular canal; CC – common crus; ASC amp – anterior ampulla; PSC amp – posterior ampulla; LSC amp – lateral ampulla. Scale bar = 5 mm. Modified from Gray (1907).

crista) or other structures. Endolymph has an ionic composition rich in K^+ but deficient in Na^+ and Ca^{2+}. Immersing the membranous labyrinth and surrounding its basolateral epithelial surface is the perilymph. Perilymph is a more typical extracellular fluid in being Na^+ and Ca^{2+} rich but K^+ deficient, a chemical composition similar to that of cerebrospinal fluid (Goldberg and Hudspeth, 2000). Under normal circumstances, compartmentalization of endolymph (within) and perilymph (without) keeps the two fluids from mixing across the surface of the membranous labyrinth. Electrochemical gradients present across the apical (endolymphatic) face regulate the sensitivity of the mechanoreceptors associated with hair cell function (see section 1.3), whereas basolateral (perilymphatic) gradients modulate the tuning and resonance of hair cells as well as their synaptic transmission (reviewed in Steinacker, 2004; see also Goodman and Art 1996a, b).

1.2.2. The otolith organs

Within each ear, the otolith organs are three hair cell clusters specialized for the detection of linear accelerations. Located within the sacs of the membranous utricle, saccule, and lagena (the latter not present in eutherian mammals), these hair cell clusters are arranged in roughly elliptical patches, called *maculae*, firmly anchored to the internal surface of the membranous labyrinth between the substrate and the endolymphatic fluid (Wersäll and Bagger-Sjöbäck, 1974; Wilson and Melvill Jones, 1979). The ciliated bundles, or hairs, of the macular hair cells project into the endolymphatic space and directly contact the otolithic membrane, a gelatinous sheet that covers the entire sensory

macula. Each ciliated bundle is composed of numerous stereocilia arranged in ranks of increasing length and headed by a single, eccentrically located kinocilium. Embedded within the otolithic membrane are dense populations of fine calcium carbonate crystals, called *otoconia*. It is the presence of the otoconia (*lit.* "ear dust") that gives the otolith organs their name.

When the head of an organism undergoes a linear acceleration (translation) or change in the direction of gravity (tilt), the membranous labyrinth experiences the same movement because of its firm anchorage to the otic capsule by trabeculae. (There is no experimental data to suggest that the membranous labyrinth is capable of movement relative to the bony labyrinth; Rabbitt et al., 2004.) The otoconia, however, are free to shift within the highly deformable otolithic membrane. This causes an inertial deflection of the hair cell cilia, which increases or decreases the firing rate of neural outputs, depending on the orientation of hair cells within the macula and the direction of shear of the stereocilia (Jaegar et al., 2002). The magnitude of the response is graded with the amplitude of stimulation.

Combined orientation of hair cells in the paired utricular, saccular, and lagenar maculae are capable of tracking any possible linear movements within the physiological range (Loe et al., 1973; Anderson et al., 1978; Angelaki and Dickman, 2000). Neural output from the otolithic maculae is sustained during continuous deflection of the hair bundle (Goldberg and Fernández, 1971; Hudspeth and Gillespie, 1994; Eatock, 2000), providing the brain stem with constant information on linear and gravito-inertial acceleration. When a person lies down to sleep in a moving train, for instance, they

perceive that they are still moving forward and lying down (with the head tilted accordingly) eight hours later when they awake.

1.2.3. The semicircular canals

The semicircular canals[1] are the primary sensors adapted to the detection of angular head movements. Angular accelerations (the rate of change of angular velocity over time) are experienced by the head whenever it is turned or tilted, during oscillatory movements of the body, and during the wide repertoire of movements associated with vertebrate locomotion. In the case of limbed tetrapods, head accelerations can occur as the result of intermittent contact with a terrestrial substrate, as during walking, running, or leaping, or as the result of continuous contact with an aqueous or aerial medium, as during swimming or flight.

To sense these movements, three slender, toroidal semicircular ducts (anterior, posterior, and lateral) are located within each labyrinth, arranged in roughly orthogonal planes (Figure 1–1). The endolymph-filled ducts are continuous at both ends with the membranous utricle, though fluid cannot flow freely around the complete duct circuit. Instead, the endolymphatic space is interrupted by a gelatinous mucopolysaccharide membrane resembling a diaphragm, the *cupula*, which spans the cross-sectional area of each duct in a dilated region called the *ampulla*. At the base of each ampulla is a raised ridge of hair cells and supporting cells, the *crista ampullaris*. Ciliated bundles consisting

[1] Following the Terminologia anatomica (Federal Committee on Anatomical Terminology, 1998) the term ‘semicircular canal’ refers to the bony morphology of the labyrinth, and the term ‘semicircular duct’ to the membranous duct inside the canal. The term ‘semicircular canal system’ covers the entire functional unit including both bony and soft-tissue aspects.

of several stereocilia and a single kinocilium project from the apical surface of the ampullary cristae and extend across the subcupular space (Helling et al., 2000). The tip of the kinocilium is embedded a few micrometers into the cupula (Hillman, 1977).

When the head experiences an angular acceleration, endolymph inside the semicircular ducts undergoes relative movement with respect to the duct wall. Because of its inertia, the endolymph lags behind the rotation of the bony and membranous labyrinths, and therefore rotates within the semicircular duct in a direction opposite that of the head (Camis, 1930; basic principles reviewed in Wilson and Melvill Jones, 1979). This fluid motion is resisted by the viscoelastic properties of the cupula, which prevents endolymph from flowing around it (Hillman and McLaren, 1979; cf. Damiano, 1999). As the endolymph presses against the cupular surface in the direction of its rotation, the cupula is deformed with a maximum displacement near its center (in line with the center of the duct lumen) and a minimum displacement around its periphery (McLaren and Hilllman, 1979; Yamauchi et al., 2002).

Stereocilia within the crista ampullaris are oriented in one direction, such that all hair cells in a given ampulla are maximally excited by angular rotation in a single direction and inhibited by rotation in the opposite direction (Wersäll and Bagger-Sjöbäck, 1974; Blanks et al., 1975, 1985; Estes et al., 1975; Reinsine et al., 1988; Dickman, 1996). Labyrinthine geometry is organized in such a way that the semicircular ducts in each ear are aligned in approximately orthogonal planes in three-dimensional (3D) space (Gray 1907, 1908; Wersäll and Bagger-Sjöbäck, 1974). Pairs of ducts on opposite sides of the skull tend to parallel one another, and when activated generate outputs of opposite sign (referred to as a “push-pull” operational mode; Graf, 1988). That is, when angular motion

occurs within the plane of a coplanar pair, the endolymph is displaced in opposite directions with respect to their ampullae. Depending on the direction, one ampullary sensor is excited, increasing its neural firing rate (spikes/s), while the other is inhibited, decreasing its output. The functional coplanar pairs are right anterior-left posterior (RALP), left anterior-right posterior (LARP), and right lateral-left lateral (RLLL). For the vertical canals (RALP and LARP), displacement of the cupula away from the utricle (ampullofugal flow) is excitatory (Wilson and Melvill Jones, 1979) and increases the number of spikes encoded by the afferent canal nerve. For the lateral canals (RLLL), displacement of the cupula toward the utricle (ampullopetal flow) is excitatory (ibid.). By combining input from each of the canal pairs, the brain creates a representation of the vector describing the instantaneous speed of angular head movement relative to 3D space (Graf, 1988).

This morphology enables the three ampullary organs to mechanically decompose any 3D movement experienced by the head into three individual components, one component carried by each afferent canal nerve (first proposed by Mach, 1875; cited in Rabbitt, 1999). Because the canals are not perfectly toroidal and do not lie in perfectly flat planes (Oman et al., 1987), and because endolymph conduits are hydrodynamically shared by all three canals in the utricular vestibule and common crus (Muller and Verhagen, 1988a, b), interactions between the canals are complicated and driven by pressure gradients (Rabbitt et al., 1998). Recordings from afferent canal nerves show that the direction yielding a maximum excitatory response from a given nerve is not the same as the direction that nulls the other two canals in the same labyrinth, and these directions differ from the anatomical canal planes by as many as 10 degrees or more (Estes et al.,

1975; Reinsine et al., 1988; Dickman, 1996; reviewed in Rabbitt, 1999). The important point here is that a movement in the maximal response direction of a given canal will excite to some degree its sister canals. Therefore, this direction cannot be used to perfectly parse an input rotation into discreet vectorial components, one carried by each nerve. To investigate this problem, Rabbit (1999) developed a mathematical model to describe endolymph flow and cupular dynamics in a hydrodynamically interconnected labyrinth using the oyster toadfish (*Opsanus tau*) as a model animal. Rabbitt determined the null planes of the three canals and derived the prime rotational direction for each canal by plotting the intersections of its sisters' null planes. He found that the prime directions are non-orthogonal and not aligned with the anatomical canal planes or the directions that elicit maximal response. This complex vectorial decomposition underlies the directional coding of movement by the canals. Because the prime directions are highly sensitive to the morphology of the membranous vestibular organs, sensitivity to different directions is predicted to vary between species according to their unique locomotor habits. However, the specific numeric coordinates for any given labyrinth cannot be extrapolated from theory without a complete 3D reconstruction of the membranous geometry plus experimental data on firing rate modulation from each ampullary nerve (Rabbitt, 1999).

Although the physical stimulus of the semicircular canals is angular acceleration, the neural output from the sensory cells in the ampulla is interpreted as velocity by the central nervous system (Mayne, 1950, 1965). Put another way, endolymph flow in the semicircular duct causes a volume displacement of the cupula that is proportional to angular head velocity. Consequently, the semicircular canal system in vertebrates is

adapted to function as a band-pass angular velocity transducer, capable of measuring the velocity of an animal's transient head movements within a range of frequencies and to the accuracy defined by the lower and upper corners of the frequency response curve.

1.2.4. Other vestibular sensors

A number of additional vestibular sensors not associated with either the otolithic organs or semicircular canals are present in several but not all groups of vertebrates, namely the basilar papilla, papilla neglecta, and amphibian papilla (Lewis et al., 1985). At various points in gnathostome evolution, these extra sensors have assumed different exteroceptive functions, typically as hearing organs specialized for the detection of sound waves and/or substrate-borne vibrations. The basilar papilla is adapted as an auditory organ in tetrapods (Fritzsch, 1987), further modified as the spiral cochlea in eutherian mammals (van Bergeijk, 1966). The papilla neglecta serves as a sensor of vibratory and auditory stimuli in fish (Lowenstein and Roberts, 1951; Fay et al., 1975; Corwin, 1981), but has been experimentally determined in turtles to work as a rotation sensor encoding between angular acceleration and angular jerk (Brichta and Goldberg, 1998). The amphibian papilla is an accessory auditory organ unique to amphibians, which may be derived from the papilla neglecta of more primitive gnathostomes (Fritzsch and Wake, 1988).

1.3. Transduction of mechanical energy into neural signals

The neuroepithelium of each vestibular organ is composed of specialized receptor cells, called hair cells, and supporting cells (Wersäll and Bagger-Sjöbäck, 1974; Hunter-Duvar and Hinojosa, 1984). All of the hair cells found in the vestibular apparatus, whether in the utricular maculae, semicircular duct cristae, or the cochlea, share a similar form and function. Hair cells originate from the surface ectoderm of the membranous labyrinth and project their hair bundles, or cilia, into the endolymph bath at the apical aspect of the cell (Hudspeth, 2000). The endolymph is kept perfectly isolated from the extracellular perilymph at the basolateral surface of the hair cell by tight junctions.

The hair bundle serves as the receptor apparatus for mechanical stimuli. It is composed of a single eccentrically located kinocilium and several specialized microvilli, the stereocilia, arranged in ranks of increasing length. Each bundle is morphologically polarized in the direction of the kinocilium, such that application of a positive mechanical stimulus—specifically, a bundle displacement toward the kinocilium—elicits an excitatory electrical response in afferent nerves by gating mechanically sensitive ion channels at the tips of the stereocilia (Flock, 1964; Hudspeth, 1982; Howard and Hudspeth,1988; Assad et al., 1991; Pickles and Corey, 1992). Stereocilia tips are connected to each other by an elastic element, the gating spring, which is linked to the ion channel gate (Corey and Hudspeth 1983; Howard and Hudspeth, 1988). Pushing a bundle in the positive direction stretches the gating spring, applying force to the gate and increasing its probability of opening. The kinocilium is not directly involved in

mechanoelectrical transduction (Hudspeth and Jacobs, 1979) and is known to degenerate during development in the hair bundles of the mammalian cochlea.

Deformation of the semicircular canal cupulae or otolithic membrane translates the input stimulus (angular acceleration or linear acceleration, respectively) into deflection of the hair bundles. Hair cell deflection causes depolarization or hyperpolarization of the hair cell membrane potential, depending on the direction of movement (Lowenstein and Wersäll, 1959). Because about 15% of a hair cell's transduction channels are open at rest, the unstimulated receptor exhibits a resting potential of about –60 mV (Hudspeth, 2000). A positive bundle deflection (toward the kinocilium) opens additional channels and depolarizes the hair cell plasma membrane due to the influx of cations (Corey and Hudspeth, 1979; Ohmori, 1985). The principle cation responsible for carrying the transduction current is K^+, which is found in high concentration in endolymph, but there is also a contribution from inward passing Ca^{2+} cations (Ricci and Fettiplace, 1998). The transduction currents open voltage-gated Ca^{2+} channels in the basolateral membrane, permitting influx of calcium from the extracellular medium (Hudspeth, 2000). As with most other synapses, intracellular calcium binds to vesicles containing excitatory neurotransmitter (believed to be glutamate), inducing transmitter release across the presynaptic membrane and subsequent depolarization of the postsynaptic afferent nerve terminal, increasing its firing rate (ibid.). Conversely, a negative bundle deflection (away from the kinocilium) will close transduction channels in the stereocilia and hyperpolarize the hair cell membrane. This closes voltage-gated Ca^{2+} channels, inhibiting transmitter release and reducing afferent nerve firing rate.

Chemical transmission in all hair cells is mediated by ribbon synapses, special electron-dense lamellae in the presynaptic cytoplasm oriented at right angles to the presynaptic membrane (Smith and Sjöstrand, 1961; reviewed in Sterling and Matthews, 2005). The ribbons provide a shuttle zone for the exocytotic release of neurotransmitter across the presynaptic membrane and are capable of very high transmitter release rates over long periods (von Gersdorff, 2001). This is an important feature of hair cells and retinal photoreceptor cells which release transmitter in response to small graded potential changes, unlike most neurons which release transmitter as the result of a regenerative action potential.

Another interesting feature of hair cells is found in the process of adaptation, the change in responsiveness (decay) of the bundle during periods of sustained deflection, resulting in lower rate of neurotransmitter release (Eatock, 2000). It is posited that adaptation relieves the gating springs of the stereocilia, freeing the transduction channels to respond to novel stimuli that emerge relative to ongoing background stimuli (ibid.). In this manner, hair cell adaptation works to fine-tune the receptor potentials and transduction currents of the cell to better match the frequency content of sustained head movements.

Because all of the hair cells in a semicircular canal ampulla are oriented in the same direction, the entire crista is maximally excited by the same direction of motion. The morphological polarization of the utricular and saccular maculae is more complex, with different groups of hair bundles polarized in all possible directions within the plane of each macula (Spoendlin, 1966). Stimuli at right angles to a bundle's axis of polarity produce no change in resting potential, but obliquely-directed stimuli produce a graded

change in potential, proportional to the vectorial projection of the stimulus along the bundle's axis of polarity (Hudspeth, 2000). In the case of the semicircular canals, the difference in frequency coding between coplanar canal cristae is interpreted by the brain as a head rotation (Graf, 1988). In the case of the otolith organs, the brain is provided with a redundant representation of the magnitude and orientation of any linear acceleration in the horizontal and vertical planes (Spoendlin, 1966).

1.3.1. Hair cell types

The vestibular end organs of tetrapods are supplied by two types of hair cells (Wersäll and Bagger-Sjöbäck, 1974). Type I hair cells have a goblet-shaped cell body in synaptic contact with the calyx ending of a single afferent fiber of the eighth cranial nerve (Wersäll, 1956). These types of hair cells are present in amniotes but not in amphibians or fish (Lysakowski, 1996). The calyceal ending of the afferent fiber surrounds almost the entire basolateral surface of the Type I hair cell (Wersäll and Bagger-Sjöbäck, 1974), except in squamates where it is restricted to the lower part of the cell's neck (Jørgensen, 1988). As with all hair cells, transmission is mediated by ribbon synapses in the presynaptic cytoplasm of the hair cell (Smith and Sjöstrand, 1961). However, the inner face of the calyx ending also invaginates into the hair cell at various points, reducing the width of the intercellular space for reasons that are poorly understood (Goldberg, 1996). Because of the long apposition and tight conformity of the calyx to the hair cell, currents originating in the hair cell can directly influence the membrane potential of the afferent nerve ending (an example of ephaptic transmission) and vice

versa, an effect that is entirely separate from (but less effective than) the process of chemical transmission (ibid.). Multiple ribbon synapses are made with each calyx, typically >10 (e.g., Goldberg et al., 1990), and it has been estimated that a calyx ending receives approximately three times as much synaptic input from its hair cell than does a Type II cell (e.g., Baird et al., 1988).

Type II hair cells are cylindrical in shape and are defined by their lack of calyx endings (Wersäll, 1956). This hair cell type is similar to hair cells found in other neuromast organs (such as the cochlea and lateral line) and is found in all vertebrate species including anamniotes (Lysakowski, 1996). Instead of a single afferent calyx ending, Type II hair cells are innervated by bouton endings from multiple afferent and efferent nerve fibers. Each Type II cell typically makes one or very few ribbon synapses with each of their afferent boutons (Goldberg et al., 1990).

In mammals, both type I and type II fibers are found throughout the ampullary cristae and otolithic maculae (Wersäll J, Bagger-Sjöbäck; Lysakowski, 1996). In eureptilians (squamates and archosaurs, including birds), type I hair cells are restricted to the central zones of the cristae and to the striola (a curved border running across the surface of the macula), but type II hair cells are widely distributed as in mammals (reviewed in Lysakowski and Goldberg, 2004). The functional effects of this distinction are unknown.

1.3.2. Afferent signaling and efferent control

The vestibular component of the eighth cranial nerve transmits all frequency coded impulses from vestibular afferents to the brain stem. Cell bodies of the primary vestibular afferent neurons reside in the vestibular (Scarpa's) ganglion, which is present as a swelling of the vestibular nerve within the internal acoustic meatus. Peripheral processes form synaptic contact with Type I and Type II hair cells of the vestibular end organs. Individual primary vestibular afferent fibers typically summate input from multiple hair cells (e.g., Boyle et al. 1991). Central processes project to the vestibular nuclei of the brain stem, with some fibers passing directly to the cerebellum (via the juxtarestiform body) for integration (Brodal, 1974).

As stated previously, mechanical deflection of a hair bundle in the positive direction generates a postsynaptic potential in primary afferent fibers. This increases the discharge frequency (spike rate) of primary afferents, but the response is not uniform. Individual fibers exhibit a range of temporal responses to bundle deflection across the frequency spectrum of head movements (Boyle et al., 1991). While some afferents respond with temporal dynamics that faithfully match the angular velocity of the head with high gain, other neurons adapt with a gain decline spanning several orders of magnitude within an individual animal (Goldberg and Fernández, 1971), a phenomenon resulting from the nature of synaptic contacts between hair cells and afferents (Highstein et al., 1996; Holstein et al., 2004). Here, *gain* (sensitivity to stimulus) is measured as the ratio of afferent impulses/sec per magnitude of angular head velocity/sec. The phase of the response—that is, the temporal match between peak afferent discharge and peak

stimulus velocity—can also be shifted in time due to afferent modulation (Highstein et al., 2005). This type of signal processing takes place after head movements are mechanically decomposed into directional components by the hair bundles (a process that is strongly dependent on the position of the labyrinth with respect to the excitatory rotation vector). As a result, a temporal mismatch is created between the mechanical input to the hair bundles and the nonmechanical encoding of spikes by the afferent nerve (a process that is strongly dependent on synaptic connections). In some afferents, this "post-mechanical" signal adaptation can cause a velocity-sensitive hair bundle deflection to be converted to an acceleration-sensitive first-order afferent signal. Even greater disparities between mechanical and afferent response are noted at higher stimulus frequencies (ibid.).

Given the morphological differences that exist between hair cell types and synaptic contacts, the degree of postsynaptic afferent signal processing likely varies between phylogenetic groups and even between closely related species. Caution must therefore be exercised when interpreting the mechanical bandwidth attunements of the semicircular canal system to the movement criteria of species (see section 1.4.3). Although input velocities are directionally and temporally coded by the hair bundles with high fidelity (mechanical gain), the output waveform transmitted to the brain stem by afferent nerves is heavily processed (afferent gain). To summarize, it is difficult to conclude much about afferent gain on the basis of mechanical gain. (For a more comprehensive treatment of nonmechanical signal processing by afferent nerves, the reader is referred to Highstein et al., 2005.)

Efferent neurons also play a role in signal processing. These neurons originate in the brain stem and project back to the basolateral surface of the vestibular end organs, synapsing with type II hair cells and some afferent nerve endings including the calices of type I hair cells and the boutons of both types (Lysakowski and Goldberg, 2004). Activation of efferent fibers excites the afferents of some hair cells while inhibiting others, with specific patterns varying greatly between species. This provides a mechanism by which the brain stem can further alter the discharge sensitivity of individual hair cells, though the effects of these inputs are largely unknown (Goldberg and Hudspeth, 2000).

1.4. Functional morphology of the semicircular ducts

Because the membranous labyrinths are tethered to the skull, angular acceleration of the head induces endolymph flow within the semicircular ducts. This generates an inertial force within the endolymph and a compensatory displacement of the cupula and hair cell bundles. Deflection of the stereocilia generates a receptor potential in the hair cells of the cristae, modulating transmitter release. Depolarization or hyperpolarization of primary vestibular afferent fibers generates or inhibits action potentials which encode parameters of angular acceleration, interpreted as velocity by the central nervous system over a range of frequencies. Combined vestibular inputs from all six sensors enable vertebrates to maintain equilibrium and spatial orientation while locomoting freely in their environments.

The waveform of signals encoded by the ampullary hair bundles receives as its *input* a signal governed by the macromechanical interaction of several variables: (1) frequency and direction of the input rotational stimulus, (2) fluid-dynamical properties of the endolymph, (3) structure of the cupula, and (4) size and shape of the duct parts. This section reviews the basic macromechanical principles governing endolymph flow, with special attention given to the physical parameters of semicircular duct parts that influence response characteristics of the system. Finally, existing comparative evidence for semicircular canal size variation in vertebrates is reviewed and implications drawn for inferring specializations in birds and non-avian dinosaurs. Because of the gross anatomical similarity of canal structures in gnathostome vertebrates, the physical principles underlying canal function are broadly applicable to all species.

1.4.1. Basic fluid mechanics

Early work (e.g., Ewald, 1892) demonstrated that artificial fluid flow in the semicircular duct lumen resulted in neural stimulation of vestibular afferents. But the question of how, or if, head movements could generate fluid movements in the ducts waited on the attention of classical physicists.

Lorente de Nó (1927) was the first to derive a mathematical expression for endolymph flow within the semicircular ducts. Lorente de Nó modeled the dynamics of endolymph flow in a single, perfectly circular duct with no cupula, and was able to describe the biophysics of fluid flow in response to a step change in head angular velocity (cited in Rabbitt et al., 2004). (It was assumed by Lorente de Nó that endolymph flow in

a narrow duct would be quickly stopped by frictional damping.) Wilhelm Steinhausen (1931) made the important discovery that the cupula completely filled the lumen of the ampulla and prevented endolymph from flowing around it, though he believed that the cupula was hinged upon the crista and moved in the manner of a swing door (the cupula is better described as a diaphragmlike structure that deforms maximally at the center [Hillman and McLaren, 1979; Yamauchi et al., 2002]). Steinhausen also observed that deflection of the cupula accurately followed the flow of endolymph when subjected to angular rotation in the pike fish. These critical observations enabled Steinhausen to model the semicircular canal system as a heavily damped torsion pendulum, in which the inertial term of the second order differential equation of motion is derived from the mass of endolymph, the damping term from the viscosity of endolymph, and the restoring force from the elasticity of the cupula.

Steinhausen's torsion-pendulum equation provided a firm theoretical hypothesis for canal function, one that remains relevant today. Though Steinhausen did not establish the values of the constants of his equation, and was therefore unable to prove the hypothesis, this was soon determined experimentally by Van Egmond and coworkers in a series of influential papers (1948, 1949) and subsequently upheld by the extensive work of others (e.g., Van Buskirk et al., 1976; Oman et al., 1987; Damiano, 1999). These later investigators improved upon the basic Steinhausen model, giving a more realistic description of labyrinth mechanics than the torsion pendulum theory. Van Buskirk and colleagues (1976) developed a mathematical model for the unsteady fluid-dynamic response of the semicircular canals that accounted for the effects of the utricle and the elastic properties of the cupula (reviewed in Van Buskirk, 1987). Oman and co-workers

(1987) developed a rigorous hydrodynamical theory that accounted for the nonuniform geometry of the semicircular ducts. Damiano (1999) incorporated a modern theory of cupular ultrastructure, one that accounts for the porosity of the cupular membrane, noting that porosity had little effect on the macromechanical behavior of the model within the physiological range of rotational frequencies (though possibly contributing to mechanical adaptation at low frequencies). Despite their added complexity, the basic predictions of these models are strikingly similar. All produce an overdamped second order system that behaves as an angular-velocity meter over a limited range of stimulus frequencies (the midband frequency range). Differences in the models are due mainly to the significance placed on the scale of labyrinth parts, mechanical properties of endolymph, and the behavior of the cupula during step or sinusoidal stimuli.

These seminal works modeled endolymph flow within a single semicircular duct circuit, this being a necessary simplification of biological reality since endolymph conduits are hydrodynamically interconnected in the utricle and crus commune. More recently, however, advances have been made in modeling fluid interactions in three-duct interconnected systems (e.g., Muller and Verhagen, 1988a, b; Rabbitt et al., 1995; Rabbitt, 1999). These models attempt to relate fluid displacements in the entire semicircular canal system to cupular volume displacements in all three ampullae. A key prediction of these models is that sensitivity of a particular duct to rotational stimuli is dependent on the dimensions of the other parts of the system (Muller and Verhagen, 1988a), specifically because endolymph flow in one duct entrains flow in the connected ducts. Another important prediction is the existence of optimal directions of rotation for each duct (Rabbitt, 1999). These directions are distinct from the direction of rotation that

will elicit maximal response of a duct's ampullary nerve, and distinct from the anatomical canal planes.

This underscores the point that the precise means by which the canals decompose angular movements into vectorial components—one carried by each of the three ampullary nerves—cannot be deduced by investigation of bony labyrinth geometry. This task requires, as a minimum, a three-dimensional model of the entire membranous labyrinth and recordings of activation patterns from each ampullary nerve in response to rotational stimuli. Although this approach is highly accurate, flow in a three-duct labyrinth is described by a cumbersome system of sixth order differential equations that, if solved, lead to unmanageable formulae for endolymph flow (e.g., Muller and Verhagen, 2002a). Moreover, such detailed information is not presently available for a wide range of vertebrate species. The investigations of Rabbitt et al. (1995) and Rabbitt (1999) are restricted to the labyrinth of the oyster toadfish (*Opsanus tau*). Simply stated, one cannot infer an organism's bias to detection of movements in preferred planes, if such a bias exists, on the sole basis of canal geometry.

Seeking generalizations that could be more broadly applicable to semicircular canal shapes across vertebrates, Muller and Verhagen (2002a, b, c) modeled endolymph flow in a pair of two-duct models using schematized labyrinths in a variety of configurations and rotation vectors designed to replicate shape diversity in the gnathostome vertical canals. They found that despite morphological coupling of duct circuits the physical behavior of the two-duct (and by inference, the three-duct) system provides no mechanical advantage or disadvantage to canal function relative to the one-duct model developed by Van Egmond et al. (1949). This permits us to make

generalizations about semicircular canal system function, specifically, because the physical parameters of the semicircular duct parts directly influence the response characteristics of the system in a way that is broadly applicable across endolymph models. These general trends are reviewed in the next subsection.

1.4.2. Significance of physical parameters

From the basic second order equation of motion developed by Steinhausen (1931), Van Egmond and colleagues formulated an equation of motion representing a balance of moments exerted on the endolymph, describing angular cupula- and head-movement following an input rotation (Van Egmond et al., 1949). An equivalent notation of this equation is provided by Melvill Jones and Milsum (1971), given here for a single duct model with a uniform duct radius:

$$J \cdot \varphi'' + b \cdot \varphi' + \mathrm{k} \cdot \varphi = J \cdot \alpha \cdot \Omega' \qquad (1)$$

where φ'', φ', and φ = angular acceleration, velocity, and displacement of the cupula respectively, Ω = angular velocity of the head, α = constant, J = polar moment of inertia of the endolymph, b = viscous torque of the endolymph per relative angular velocity, k = restoring torque of the cupula per angular displacement (reviewed in Muller, 1994). Note that $J = m \cdot R^2$, where m = mass and R = the circumferential radius of the duct circuit.

Muller (1990) gives an analogous equation balancing the forces acting on the endolymph:

$$M \cdot \ddot{x} + F \cdot \dot{x} + S \cdot x = a(t) \quad (2a)$$

where M = mass coefficient of endolymph inside the semicircular duct, F = friction coefficient of endolymph, S = elastic coefficient (stiffness) of the cupula, $\ddot{x}$, $\dot{x}$, and x = acceleration, velocity, and displacement of the endolymph respectively. Expressed in words, Muller's equation reads (from Muller, 2000):

"inertial forces + frictional forces + elastic forces = input rotation forces" (2b)

From equation 2a, the following time constants were derived by Muller (1990):

$$T1 = F/S \quad (3)$$

and

$$T2 = M/F \quad (4)$$

When a duct is rotated during a sinusoidal- or step-stimulus, the endolymph carries out an excursion with respect to the duct wall followed by a restoring movement to its starting position. The excursion and restoring movement are characterized by real-valued time constants *T1* and *T2* (equations 3, 4) (Muller, 2000). The short time constant (*T2*) is a measure of the response speed of the system; i.e., how long it takes for the

cupula to maximally displace following an input rotation. This quantity is a direct measure of the sensitivity of the ampullary organs; i.e., the longer it takes for endolymph to maximally displace within a duct, the higher the gain of the sensor. Sensitivity (gain) represents the ability of the sensor to resolve differences in angular acceleration and velocity (sensu Muller 1990, 1994, 1999). The long time constant (*T1*) measures the recovery time of the system; i.e., the time it takes the cupula to return to its original position after a deflection. The short time constant (T2) has a real time value of ~5 milliseconds in humans (Oman and Young, 1972). By contrast, the long time constant (*T1*) has a real time value of ~20 seconds (ibid.). Although natural movements do not occur over this time span, both the long and short time constants play a role in shaping the velocity band-pass characteristics of the sensor.

Any change in the physical dimensions of the duct parts will directly influence the response time and sensitivity of the sensor with a corresponding change in bandwidth. Response time increases with the size of the cross-sectional area of the duct lumen, and sensitivity increases with both the lumen size and the circumferential arc length of the duct, the latter often expressed by its radius of curvature (Figure 1–2: r and R, respectively). Recall that the semicircular canal system in vertebrates is adapted to function as a band-pass angular velocity transducer over a limited range of stimulus frequencies (Mayne, 1950). As we shall see, the lower corner frequency of the midband range is directly related to the long time constant (*T1*), while the upper corner frequency is related to the short time constant (*T2*) (Steinhausen, 1933; Wilson and Melvill Jones, 1979).

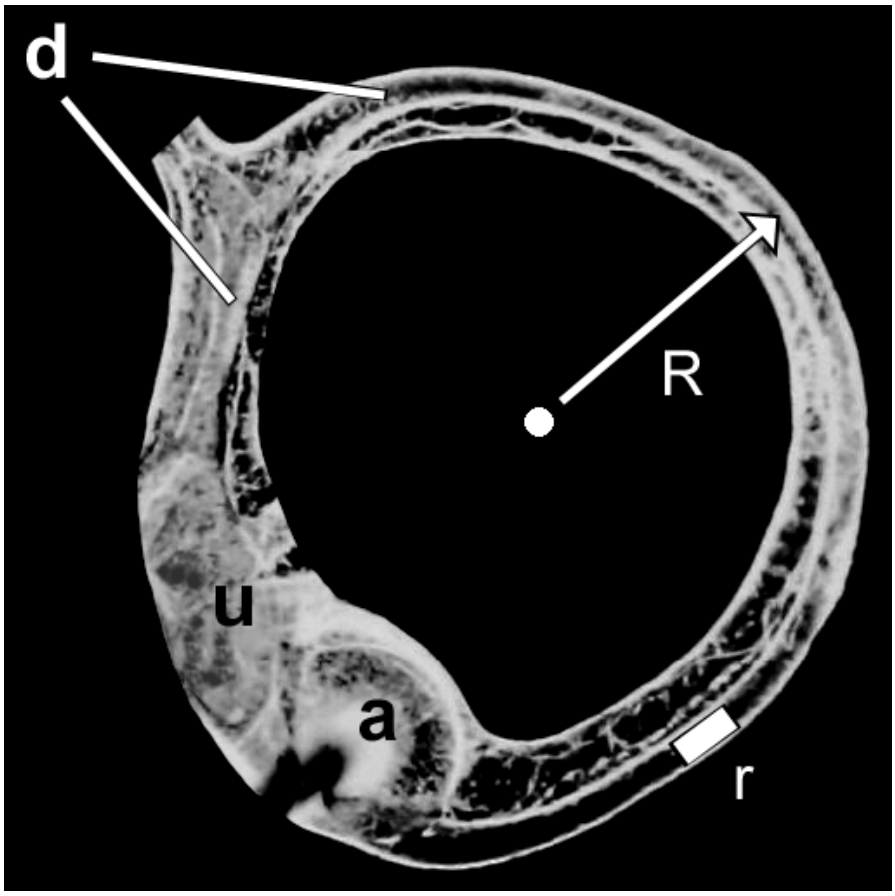

Figure 1–2. Detail of endolymph circuit. Detail of the posterior canal of the yellow-faced baboon (*Papio cynocephalus*) from Gray's (1907) preparation, demonstrating the parts of the endolymph circuit: d – the duct; a – the posterior ampulla; u – utricle. The cross-sectional area of the duct lumen (r) and radius of curvature (R) are also indicated.

Rabbitt and colleagues (2004) provide several simple equations that allow us to investigate the effects of changing canal dimensions on sensitivity and bandwidth. These equations are derived from their second-order differential equation describing endolymph flow in a single semicircular duct (equation 4.6 on page 162 of Rabbitt et al., 2004; not given here), which is very similar to the earlier model of Oman et al. (1987). Like the original Steinhausen torsion-pendulum model to which it is closely related (Steinhausen, 1933), the Rabbitt et al. (2004) equation is derived from the mass of endolymph, m, the damping term from the viscosity of endolymph, c, and the restoring force of the cupula, k. Once integrated numerically, these terms are approximated by Rabbitt et al.(2004) as:

$$m \approx \frac{\rho \ell}{A_d} \tag{5}$$

$$c \approx \frac{8\pi\mu\ell}{A_d^2} \tag{6}$$

$$k \approx \frac{8\pi\gamma h}{A_c^2} \tag{7}$$

where ρ is the density of endolymph, ℓ the circumferential arc length of the duct measured along its curved centerline (not exactly the same thing as arc radius of curvature, but related; cf. Figure 1–2: R), A_d is the cross-sectional area of the duct (Figure 1–2: r), μ is the dynamic viscosity of endolymph, γ is the shear stiffness of the cupula, h is the thickness of the cupula, and A_c is the area of the cupula (based on the lumen of the ampulla above the sensory epithelium). For a duct lying in a single plane, the inertial forcing coefficient "g" is approximated by Rabbitt et al. (2004) as:

$$g \approx 2\pi\rho R^2 \cos(\theta) \tag{8}$$

where R is the average arc radius of curvature of the duct (Figure 1–2: R), and θ is the angle formed between the canal plane and the angular rotation vector. From equations 5-8, the long and short time constants are obtained. Equation 9 gives the long time constant (τ_1):

$$\tau_1 \approx \frac{c}{k} \approx \frac{\mu \ell A_c^2}{\gamma h A_d^2} \tag{9}$$

and from this, the lower corner frequency (ω_1) of the velocity-sensitive bandwidth is derived:

$$\omega_1 = \frac{1}{\tau_1} \approx \frac{k}{c} \tag{10}$$

This is converted to frequency units by the equation (Richard Rabbit, personal communication):

$$f_1 = \omega_1 \cdot 2 \cdot \pi \text{ Hz} \tag{11}$$

Equation 12 gives the short time constant (τ_2):

$$\tau_2 \approx \frac{m}{c} \approx \frac{\rho A_d}{8\pi\mu} \tag{12}$$

and the upper corner frequency (ω_2):

$$\omega_2 = \frac{1}{\tau_2} \approx \frac{c}{m} \tag{13}$$

converted to frequency units by the equation (Richard Rabbit, personal communication):

$$f_2 = \omega_2 \cdot 2 \cdot \pi \text{ Hz} \tag{14}$$

For a sinusoidal stimulus, the mechanical gain of the sensor (sensitivity to stimulus) is proportional to g / c, where g is given in equation 8 and c in equation 6. Between the lower corner (ω_1) and upper corner (ω_2) cutoff frequencies, the model predicts that cupular volume displacements are in phase with and accurately match the angular frequency of head motion with high, relatively flat gain (Rabbitt et al., 2004). Above the upper corner frequency, the inertia of the endolymph attenuates the response within the slender portion of the duct, causing the system to act like a displacement transducer (seismometer). Below the lower corner frequency, cupular stiffness attenuates the response, causing the system to behave like an acceleration transducer (accelerometer) (sensu Rabbitt et al., 2004).

Assuming that the density and viscosity of endolymph, as well as the stiffness of the cupula, are equal for all vertebrate labyrinths (for a justification, see Oman, 1980, but note this is an obvious simplification), a uniform reduction in the size of the semicircular canals will increase the velocity-sensitive bandwidth by decreasing the short time constant (τ_2). Because the upper corner ω_2 is inversely proportional to constant τ_2 (equation 13), the upper corner is pushed to a higher frequency. Conversely, uniform

enlargements of the canals will decrease bandwidth. It has been noted elsewhere that while increasing the overall size of the labyrinth parts does increase gain, it does so at the expense of velocity-sensitive bandwidth (Highstein et al., 2005). Having a small labyrinth may therefore be optimal as a baseline for most vertebrates, which require compensatory and orienting adjustments of eye, neck, and trunk position over a wide bandwidth of head movements. In other words, gain alone may not be the factor optimized by the canal system, especially since there are post-mechanical mechanisms to adjust gain. Obtaining a flat velocity-sensitive response over the range of volitional head movements may be just as important. Muller (1999) argues, however, that in terms of size the average vertebrate canal system is both reasonably responsive and sensitive "for any size of animal and for any movements of it," relegating all variation in canal size to ontogenetic and phylogenetic aspects of brain growth and available endocranial space. From a comparative standpoint, a very different viewpoint emerges (section 1.4.3).

It is worthy to note that the long time constant (τ_1) is relatively insensitive to uniform changes in semicircular canal size because the geometric scaling factors cancel out in the numerator and denominator of equation 9. *Nonuniform* changes in canal size can have a substantial effect. For instance, increasing the arc length ℓ (cf., Figure 1–2: R) without increasing the lumen size A_d (Figure 1–2: r) or the size of the ampulla A_c will increase the gain of the sensor in proportion to R and increase bandwidth by extending the sensitivity to lower frequencies. This happens, specifically, because the viscous drag increases with no change in cupular stiffness, hence decreasing the lower frequency. Conversely, there would be no change in the upper corner frequency because the lumen

area is constant and the length change ℓ effects the mass and damping coefficients in the same way (Richard Rabbitt, personal communication).

Taking reliable measurements of these morphological variables requires fixation of the fragile membranous labyrinth soon after death by either dissection or serial sectioning (Curthoys and Oman, 1986, 1987; Lindenlaub et al., 1995). However, the bony semicircular canals which enclose the duct organs can be investigated easily using computed tomography and other techniques (Spoor et al., 2000; see Chapter 3). These techniques permit the accurate reconstruction and measurement of morphological variables of canal geometry, most importantly the arc length of the semicircular canal (which contains the semicircular duct and gives an approximation of its enclosed length). Arc length is a key property of evolutionary studies in that it has repeatedly been linked to locomotor behavior (e.g., Spoor and Zonneveld, 1998; Spoor et al., 2002; Sipla et al., 2003, 2004). In contrast, the lumen size of the bony canal is of limited functional significance because it does not adequately reflect the lumen size of the enclosed membranous duct in many groups of vertebrates (e.g., Gray, 1907, 1908; Ramprashad et al., 1984, 1986). Caution must therefore be exercised in interpreting the effects of changing canal size on temporal response dynamics of the system, because the biophysical models of canal function are based exclusively on the membranous duct. In the case of CT-based investigations, like this one, we are left with the measurement of the bony arc size as the sole morphometric variable of relevance.

Differences in the size of the individual duct organs relative to each other are functionally significant. In birds, the anterior duct is greatly enlarged in the medio-caudal direction, far exceeding the posterior duct in overall size (see Chapter 4). Qualitative

experiments with fluid-filled models demonstrate that the flow of endolymph in asymmetrical duct systems is very similar to flow in the symmetrical labyrinth, but that the overall impulse (change in momentum added to the endolymph) in the plane of the anterior duct is increased, owing to adverse pressure gradients that are particularly large in the common crus during pitch movements (Muller and Verhagen, 2002b). Anterior-posterior canal asymmetry, as deduced by Muller and Verhagen (ibid.) therefore increases overall system sensitivity. The same conclusion is reached from basic hydrodynamic theory, in that a length increase in the size of the anterior semicircular duct will extend the sensitivity of the sensor to lower frequencies, provided that lumen size and ampulla size do not change uniformly with arc size (Rabbitt et al., 2004).

Canal shape is also hypothesized to influence the dynamic response characteristics of the semicircular canal system (Muller and Verhagen, 2002a, b, c). Despite growing evidence suggesting a link between canal shape and the movement criteria of individual species (Georgi and Sipla, in press; Georgi, in prep), there are as yet no detailed models of the functional dependence of the canal system on canal shape. There are some basic observations that may prove useful, however. The endolymph models of Ten Kate et al. (1970) and Van Buskirk et al. (1976) indicate that a reduction in canal aspect ratio (the ratio height to width) may affect the sensitivity of the canal system by increasing the proportion of the overall endolymph circuit that is composed of utricular wall. Recall that the fluid circuits of the canals are hydrodynamically shared within the utricle. Because fluid resistance is less within the dilated utricle, overall frictional forces in such a system are reduced, resulting in greater sensitivity. Georgi and Sipla (in press) reported on canal shape variation among secondarily aquatic tetrapods

using Elliptical Fourier Analysis, observing that aquatic species typically possess vertical semicircular canals that are more dorsoventrally compact and anteroposteriorly elongate (lower aspect ratio) than their terrestrial relatives. The utricular component of the duct circuit in aquatic forms is therefore greater, possibly (but not unequivocally) indicative of increased sensitivity associated with aqueous habits. With no means of testing the adaptive significance of shape variation, size variation remains the feature of choice in the present study. The interested reader is referred to the doctoral dissertation of Justin Georgi (Dept. of Anatomical Sciences, Stony Brook University), who is investigating the shape effects of canal function across a large sample of secondarily aquatic vertebrates.

1.4.3. Attunement of the canals to the frequency spectra of movements

Comparative analyses of semicircular canal morphology date back to Gustaf Retzius (1881, 1884), who demonstrated that the gross anatomical structure of the canal system was phylogenetically ancient, occurring unaltered in basic form among all gnathostome vertebrates. Gray (1907, 1908) expanded greatly on the work of Retzius, publishing a detailed study of the membranous labyrinth of tetrapods, including measurements and stereoscopic photographs of dissected labyrinths for a wide range of species. To date, Gray's research contains some of the best descriptions of membranous duct morphology yet published.

Numerous comparative studies have since posited an association between the size of the semicircular canals and locomotor behavior (Gray, 1907, 1908; Tanturri 1933; Turkewitsch, 1934; Jones and Spells, 1963; Hadzislimovic and Savkovic, 1964; Matano

el al., 1985, 1986; Lindenlaub et al., 1995; Spoor and Zonneveld, 1998; McVean, 1999; Spoor et al., 2002, 2007; Sipla et al., 2003, 2004; Georgi and Sipla, in press). As Spoor (2003) points out, this association was made even before the function of the canals was discovered (citing Hopkins, 1906). It has been argued (Mayne, 1965; Wilson and Melvill Jones; 1979) that volitional angular head movements in vertebrates occur at frequencies that fall between the lower and upper corners of the velocity-sensitive portion of the canal bandwidth, the so-called midband frequency. Jones and Spells (1963) speculate that interspecific differences in duct dimensions are therefore due to functional attunements of the semicircular duct system "to match the likely patterns of head movements… according to size, shape and habitat of the animal" (p. 416). These attunements, they argue, are brought about mainly by changes to the internal lumen diameter (r) of the semicircular duct, which greatly influences the response speed of the sensor as well as the upper corner frequency, but also by adjusting the circumferential length of the duct (R) to appropriately match the lower corner to a flat bandwidth. Adjustments in canal size may therefore represent evolutionary attunements of the sensors to match the frequency content of an animal's normal head movements. Corresponding shifts in the range of cutoff frequencies, specific to each animal, are necessary to avoid over- and under-stimulation of the canals during the course of volitional movements.

In a seminal work, Jones and Spells (1963) observed that, among a comparative sample of 87 vertebrate species, duct dimensions scaled to body mass with negative allometry. In larger animals, where physical constraints impose slower head movements, they argued that a more sensitive duct organ was needed to maintain the dynamic response characteristics of the system. Even though the body size of larger animals likely

corresponds with reduced angular head accelerations, Spoor (2003) questioned whether the increase in canal arc size with body size represents a functional compensation for increased sluggishness, as suggested by Jones and Spells (1963). There is considerable variation in the size and shape of the semicircular canal system among species with the same body mass. Among these, it is the species with a more acrobatic behavior that tend to show canals with a larger arc size, not the slower-moving ones. This, it was argued, is because a larger arc size increases the sensitivity of the system, thus providing an accurate canal response that is required when navigating a three-dimensional environment in an agile and acrobatic way (Spoor et al., 2002, 2007; Spoor, 2003). This approach emphasizes that it is the interspecific deviations from the general scaling trend of vertebrates that are of interest, rather than the slope itself, as these represent attunements of the system to the movement criteria of individual species.

Unfortunately, very little information is available to characterize the frequency content of vertebrate head rotations. Such data is best obtained from kinematic analyses of head position during locomotor behavior. Specific ranges of angular head velocities and accelerations have been measured in humans (e.g., Grossman et al., 1988, Keshner and Peterson, 1992; King et al., 1992) but are unavailable for most other mammals and even fewer nonsynapsid tetrapods. Lacking such data, inferences can be made about the nature of head movements by considering factors that might affect head position during volitional behaviors. In the case of limbed tetrapods, angular head accelerations are most commonly experienced as a consequence of locomotion, resulting from intermittent contact with a terrestrial substrate or as the result of continuous contact with an aqueous or aerial medium.

Specific frequency patterns should be largely dependent on overall limb morphology, the type of gait, and the position of the head relative to the pectoral girdle. Generally speaking, it is expected that the movements of larger species should result in lower frequency limb and trunk oscillations, with correspondingly lower frequency head oscillations, than those of smaller species. Higher frequency perturbations undoubtedly result from intermittent limb contact with a substrate, such as during walking, running, and leaping. During these behaviors, animals experience a footfall-related pattern of discrete mechanical pulses of acceleration and deceleration. Ground reaction forces generated by touch-down of the supporting feet are transmitted to the axial skeleton, and thus to the inertially unstable head, inducing pitch-down rotations of the skull atop the neck. The extent to which these higher-frequency vibrations elicit canal responses is unconfirmed. It should be noted, however, that the anterior semicircular canal is more directionally sensitive to pitch-down movements of the head than either the posterior or lateral canal (Wilson and Melvill Jones; 1979). Any pitch-down movement will excite anterior canal afferents and inhibit posterior canal afferents because of the orientation of the hair bundles in the respective cristae (recall that ampullofugal flow of endolymph, away from the utricle, is excitatory for the vertical canals). “Ewald’s second law” states that excitation of a semicircular canal afferent neuron elicits a greater response to stimuli than does inhibition (Ewald, 1892; Baloh et al., 1977; Halmagyi et al., 1990). This is because the inhibited afferents in a coplanar pair of canals can only be driven from their resting discharge rate to 0 spikes per second, whereas the excited afferents can be driven to much higher levels. Anterior-posterior canal asymmetries in tetrapods may directly take advantage of Ewald’s second law to compensate for (possible) sensory overload

experienced during periods of intermittent ground contact, when rotational frequencies are highest. This may be especially true of volant birds that require precise locomotor control during banking (roll) and landing (pitch) maneuvers, both of which preferentially excite anterior canal afferents while inhibiting coplanar posterior canal afferents. Recall too that anterior-posterior canal asymmetry increases overall system sensitivity during pitch movements (Muller and Verhagen, 2002b), a morphological arrangement that is uniquely pronounced in birds.

Muller (1990, 1994) argued that the canal sensors are tuned to the detection of step angular velocity (natural steplike or "jerky" movements) and not sinusoidal angular velocity. The frequency content of step stimuli is more strongly dependent on the locomotor mode(s) employed by a species and the head movements associated with such modes, Muller argued, than for sinusoidal stimuli, which often occur below the fundamental frequency of the canal bandwidth. The contact of an animal's feet with a surface substrate during gait may produce such head movements (Keshner and Peterson, 1992, 1995; Keshner et al., 1995), as might the kinematics of certain feeding behaviors or the perturbations that result from sudden slips or trips. As Rabbitt and colleagues (2004) point out, however, "real stimuli are not ideal steps or steady sinusoids but rather consist of more complex wave forms" (p. 165), noting that the canal sensors respond well to changes in both step angular velocity and sinusoidal angular velocity below high frequencies (below ~10 Hz).

It has been suggested that the challenges of navigating a complex three-dimensional environment, such as an aerial, aquatic, or tunneled subterranean habit, may place increased demands on the vestibular system (Lindenlaub et al., 1995; McVean,

1999; Sipla and Spoor, in press; Georgi and Sipla, in press). Though the gravitational frame of reference is provided by the macular end organs, not the semicircular canals, the canals are necessary to sense external environmental factors (air gusts, water currents) that may rotate the organism unpredictably in any direction. The vestibular system will directionally code the vectors of all such movements, whereas an animal would primarily require feedback only regarding its own motion relative to the moving environment. Freed in air and water from the need for intermittent contact with a surface substrate, a wider repertoire of body movements is potentially possible, including forms of rotation that would be improbable on land. Hypothetically, such demands should result in a system of semicircular ducts with greater sensitivity.

Though kinematic data on head movement is lacking in most vertebrates, a large amount of data is available on morphological parameters that predict flight behavior, such as the shape of the wing and its loading aspects. This dissertation examines the relationship between semicircular canal size and degree of aerial maneuverability in birds, to look for putative correlations (e.g., Jones and Spells, 1963) between canal sensitivity and head rotations induced by volitional movements, here determined by wing theory (see Chapter 2).

1.5. Central processing of vestibular input and canal-mitigated reflexes

With the anatomical and functional components of the semicircular canal system described, it's now reasonable to ask, "What are the canals good for?"

Angular rotations are decomposed mechanically by the canal hair bundles into vectorial components, transmitting a frequency code of impulses to the brainstem via afferent nerves (following significant post-mechanical processing). There are two main targets for these afferent signals: the vestibular nuclei of the brainstem and the cerebellum (Brodal, 1974; Wilson and Melvill Jones, 1979; Ito, 1984). At both locations, sensory input from the vestibular end organs is integrated with somatosensory and visual sensory input, used to generate reflexive motor responses that are crucial for daily function and survival. These interactions also produce an internal representation of spatial orientation within the brain (Howard and Templeton, 1966; Schöne, 1984).While it is beyond the scope of this dissertation to review the extent of this complex control system (that being a task for many others), the principle vestibular subsystems and the reflexes they mitigate are briefly described.

1.5.1. Central processing

The central vestibular system (vestibular nuclei and cerebellum) receives frequency coded impulses from the vestibular end organs (semicircular canals and otolith organs). Vestibular nuclei on both sides of the brainstem are interconnected by a network of mutually inhibitory commissures (Hain and Helminski. 2007). These commissures permit communication between the two sides of the brain stem and facilitate the action of the "push-pull" system of coplanar canal pairs described in section 1.2.3.

In mammals, there are principally four vestibular nuclei located in the pontomedullary region of the brain stem: superior, medial, lateral, and descending

(inferior) (Brodal, 1974; Wilson and Melvill Jones, 1979). In birds, six principle nuclei have been recognized in chickens (Wold, 1976), pigeons (Boord and Karten, 1979; Dickman and Fang, 1996), and mallard ducks (Tellegen et al., 2001), with numerous smaller cell groups reported in chickens (Wold, 1976). The organization of the vestibular complex is remarkably similar in birds and mammals. Regardless of the number of cell clusters, these nuclei receive and process vestibular and extravestibular sensory input (proprioceptive, visual, tactile, and auditory) and make extensive efferent connections with the ocular motor nuclei (cranial nerves VI, IV, and III) and reticular activating system of the brain stem (Hain and Helminski. 2007). Parsimony optimization suggests that at least all amniotes share a similar morphology. These connections provide the basis for the vestibular reflexes described in the next two sections.

As a recipient of efferents from the vestibular nuclei, as well as direct projections from primary afferent vestibular neurons, the cerebellum serves to calibrate and sequence the timing of vestibular reflexes (Brodal, 1974; Ito, 1984). Cerebellar efferents are projected back to the vestibular nuclei, creating a feedback loop that allows for precise control of visual and postural reflexes (Brooks and Thatch, 1981). One structure of importance is the cerebellar *flocculus* (petrosal lobule), a small lobe projecting from the caudolateral corner of the vestibulocerebellum, the region of the cerebellum that primarily receives vestibular and reticular inputs. In many species of mammals, birds, and non-avian dinosaurs, the flocculus is relatively large and indents the medial surface of the adjacent braincase wall, forming a recess into the bony space enclosed by the arc of the anterior semicircular canal (subarcuate fossa). Among ornithodiran archosaurs, this indentation is often extensive, as reported for pterosaurs (Witmer et al., 2003) and many

species of birds and non-avian dinosaurs, suggesting that floccular tissue has extensively invaginated the adjacent bone. It has been suggested (e.g., Witmer et al. [2003], citing the principle of proper mass proposed by Jerison [1973]) that the size of the subarcuate fossa indicates the amount of neural tissue residing therein and inferentially the amount of signal processing performed by this part of the vestibulocerebellum. This may indicate that neural integration in the flocculus is especially important for these taxa. Because the developing flocculus invades the space surrounded by the anterior semicircular canal (and in some species of birds and non-avian dinosaurs extends into the territory of the posterior and lateral canals), it is possible that floccular development plays a causal role in determining the arc size of the canals. Jeffery and Spoor (2006) examined a postmortem sample of human and primate fetuses using MRI and found that floccular expansion is unlikely to be a determinant of canal size in these taxa. Specifically, the authors found that embryonic formation of the subarcuate fossa did not depend on the emergence of the petrosal lobule, but was induced by cartilage absorption at the center of the developing anterior semicircular canal. The fossa was only occupied by floccular tissue if the petrosal lobule of the paraflocculus subsequently grew into the space available. Fossae that remained empty gradually filled with bone and disappeared.

Specifically, the flocculus is involved in modulating the gain and phase dynamics of the optokinetic reflex (OKR) and vestibuloocular reflex (VOR), as well as the control of smooth pursuit eye movements (reviewed in De Zeeuw et al., 2004). The flocculus also plays a role in the reflex control of neck movements (De Zeeuw and Koekkoek, 1997). Because the flocculus receives inputs from the vestibular system, both structures are both spatially and functionally interrelated (Xiong and Nagao, 2002). Teasing apart

canal function, as it relates to size, from flocculus function, as it relates to size, is a task beyond the limits of this study. Such a task may be beyond the purview of comparative morphological techniques, requiring electrical monitoring of vestibular and floccular nuclei, combined with measurement of these structures.

Cerebellar nuclei project back to the vestibular nuclei in the brain stem, where they have an inhibitory influence (Ito, 1984). Outputs from the vestibular nuclei drive three primary vestibular reflexes: the vestibuloocular reflex (VOR), vestibulospinal reflex (VSR), and vestibulocollic reflex (VCR).

1.5.2. The vestibuloocular reflex (VOR) and optokinetic reflex (OKR)

The VOR serves to maintain stable vision during movements of the head. In response to a given head movement, the VOR is activated to keep eye orientation invariant relative to space by generating involuntary eye movements having the same amplitude, but in the opposite direction as the perceived head motion (Fuchs and Kimm, 1975; Keller, 1978). The VOR has two components. The angular VOR compensates for rotation, using direct inputs from the semicircular canals to activate extraocular muscles that move the eyes. The linear VOR compensates for translation, using otolith inputs to activate the eye muscles. Of the two, the angular VOR is primarily responsible for gaze stabilization when the object of regard is far from the observer. This is because each semicircular canal directly activates one muscle and inhibits one muscle in each eye when stimulated (e.g., Cohen et al., 1964). There is close alignment between the plane of each canal and the line of action of the muscles it activates and inhibits, and good

correspondence between the torque axes of these muscles and the canal plane (Ezure and Graf, 1984).

The main neural circuits for the angular VOR are fairly simple. For example, during a yawing head turn to the right, the right lateral semicircular canal is excited. This sends an excitatory input to the left abducens nucleus, which activates the left lateral rectus muscle, directly, and right medial rectus, indirectly via an input to the right oculomotor nucleus, causing a relative movement of both eyes to the left (the direction opposite the rotation). The left medial and right lateral recti are simultaneously inhibited, facilitating the leftward motion. It should be emphasized, though, that each reflexive movement of the eye is achieved by all six eye muscles working in tandem, receiving activation and inhibition commands from all six canals with high gain and minimal phase lag (Cohen et al., 1964). The gain of the VOR is defined as the ratio [eye angle] / [head angle] during a head turn. A gain of 1 therefore indicates a perfect match between head movement and compensatory eye movement. A gain of <1 produces retinal smear (degradation of visual acuity) during head movements. The cerebellum plays an important role in motor learning to correct the VOR when gain <1 (Robinson, 1976), particularly through floccular pathways (De Zeeuw et al., 2004).

A nonvestibular reflex that assists the VOR in stabilizing vision is the optokinetic reflex (OKR). When an animal navigates an environment of stationary surfaces and obstacles, a characteristic pattern of visual motion falls across the retina, referred to as “optic flow” (Gibson, 1954). In order to compensate for the motion of the visual field, signals are relayed from visual pathways to the accessory optic system and pretectal nuclei (Simpson, 1984, Simpson et al., 1988). Here, optokinetic responses are generated

and relayed to extraocular motor nuclei, using the relative velocity of the image falling on the retina to induce eye movements in the same direction and at the same velocity as the external environment. The effect is to stabilize vision, but while the VOR works to stabilize the eyes in 3D space, the OKR works to stabilize the eyes on the moving scene. The interaction between the VOR and OKR is still poorly understood (e.g., Schweigart et al., 2003), but it is worth noting that the gain and phase dynamics of both systems is under direct control by the cerebellar flocculus (De Zeeuw et al., 2004).

1.5.3. The vestibulospinal reflex (VSR) and vestibulocollic reflex (VCR)

Two additional vestibular reflexes, the VSR and VCR, serve to stabilize the body and the neck, respectively. These reflexes are highly integrated with proprioceptive and tactile inputs from the somatosensory system, in part because the vestibular system alone cannot provide accurate information about body position. The canal and otolith sensors respond to changes in head position, but are incapable of sensing the position of the limbs or the trunk. This is especially true when considering animals with extremely long necks, such as giraffes and ostriches, where the inertially unstable head is far removed from the body. Furthermore, head rotations can often provide ambiguous sensory cues to the brain stem; for example, a signal from the vertical semicircular canals about head pitch could result from a flexing of the head about the neck, or a flexing of the body about the waist (example adapted from Horak, 2007). The vestibular system cannot distinguish between these two inputs. In order to clarify the nature of the motion and to provide necessary information on the position of the body relative to its support surface, and the position of

body segments relative to each another, the CNS must rely on visual and somatosensory coordinates from multiple sources (reviewed by Horak and Macpherson, 1996). The visual system provides information on the movement of the head with respect to the surrounding environment, plus evidence about the direction of earth vertical. Proprioceptive inputs from muscle spindles and neurotendinous organs provide information on muscle stretch and tension, respectively, and joint receptors report on the static and dynamic aspects of kinesthesia.

All these multisensory inputs combine to form an internal representation of body position and posture at any given time, of which vestibular inputs are merely one factor among many. Vestibular inputs become dominant when stabilization of the trunk and head is critical for good performance (Horak, 2007). In environments that lack good somatosensory cues, vestibular inputs become even more important, such as when the body is unexpectedly perturbed. I suggest that aerial habits may increase reliance upon vestibular input, as flying animals lack a direct postural interface with a supporting substrate and frequently encounter unpredictable wind gusts and densely spaced in-flight obstacles (particularly true in the case of forest-navigating birds). Maintaining axial balance during rapid wing beating further requires that the head and body be stabilized in the pitch plane, requiring active control of neck and body extensors.

Numerous motor output pathways from the vestibular nuclei project to alpha motoneurons in the ventral horn of the spinal cord. The vestibulospinal reflexes (VSR) facilitate vestibular control of posture and stability in a gravity environment, by directly innervating extensor muscles of the trunk and limbs (Suzuki and Cohen, 1964; Dietz, 1992). The VSR is primarily activated when balance is disturbed or in response to sudden

drops. The reflex serves to restore equilibrium by minimizing the displacement of the body's center of mass, with the extensor motor response being proportional to head acceleration (e.g., Dietz et al., 1989).

Finally, the vestibulocollic reflexes (VCR) are a set of vestibular-induced reflexes that act directly on the neck musculature (reviewed in Peterson and Boyle, 2004). Because the head has a center of gravity located above its axis of rotation, it is inertially unstable and subject to motion whenever the body moves. Such uncontrolled motions interfere with the brain's ability to use vestibular information by introducing unwanted "noise" to the system, and could potentially exceed the range of compensatory motions accomplished by the VOR in stabilizing gaze. Furthermore, despite often large oscillations of the body and limbs that occur during locomotion, such as during running, hopping, or flapping flight, the position of the head is held relatively constant with respect to gravity (Pozzo et al., 1990; Strait and Ross, 1999; Sipla et al., 2002; Sipla, 2002). The primary function of the VCR is therefore to stabilize the head with respect to gravity during locomotion and postural control, either to simplify the interpretation of vestibular sensations or to facilitate stable gaze. VCR commands have an extremely short latency (< 100 ms) and are largely suppressed during voluntary head movements (Peterson and Boyle, 2004).

Recordings of the electromyographic (EMG) activation of neck muscles following stimulation of semicircular canal receptors provides direct evidence of the VCR pathways and specific muscle response patterns to vestibular stimulation (e.g., Wilson and Maeda, 1974; Shinoda et al., 1996). Shinoda and colleagues (1996) established activity patterns between the semicircular canals and four groups of neck

muscles: extensors, ventral flexors, lateral flexors, and rotators. Of particular note, the muscles of the extensor group (biventer cervicis, complexus, cervical multifidus, and rectus capitis posterior) were found to be directly excited by stimulation of the ipsilateral and contralateral anterior canal nerves and lateral canal nerves, and the same muscles were inhibited by stimulation of the posterior canal nerves. Pitch-down rotations of the head, such as during locomotion, are directly resisted by activation of anterior and lateral canal afferents, which excite neck extensors via VCR pathways to resist excessive head movement in this direction. This may explain why the anterior semicircular canals of bipedal dinosaurs are enlarged relative to quadrupeds, to provide greater input to neck extensors, since it has been hypothesized that such animals experience higher-frequency pitch-down rotations of the head associated with bipedal maneuvering (Sipla et al., 2004). It may also explain the gross enlargement of the anterior canal seen in birds (Gray, 1908; Jones and Spells, 1963; Sipla et al., 2003), which must resist pitching rotations of the head during the downstroke of flapping flight.

In conclusion, due to the multisensory integration of the vestibular system with multiple reflexive motor systems, the overall function of the semicircular canals should not be viewed in an isolated context, but as part of a feedback system incorporating all of these components.

Chapter 2:
The Biology of Flight and Vestibular Control

Birds are flying machines. Morphological specialization for flapping flight is the dominant theme of avian evolution, with many features of avian anatomy specifically adapted to facilitate locomotion in air. Flight requires, foremost, a light body to minimize energy expenditure during locomotion, while at the same time necessitating a rigid frame capable of withstanding aerial stresses. Toward this end birds have evolved compact bodies with light appendages, hollow bones, and efficient digestive systems. Unlike many other amniotes, every species of bird reproduces using external eggs, minimizing the time spent by females carrying weighty embryos in the body. Of course, the feathered forelimbs of birds are highly specialized flying structures, performing as an airfoil that generates lift when air flows around it. Flight muscles account for as much as 25% of avian body mass, and the entire skeleton is concentrated around a highly fused and balanced center. Lacking grasping forelimbs, birds must manipulate objects with the bill. Consequently, their heads are often placed on long necks with greater numbers of cervical vertebrae than other tetrapods (between 13 and 25, compared to 7 in mammals). In many species, the long neck also serves to separate the head from the oscillating body during wingbeats, creating a stable platform for the brain and primary sense organs, the "control center" of the avian machine. The avian flow-through respiratory system permits a unidirectional flow of air through the lungs, resulting in more oxygen being diffused into the blood with each breath cycle, while the avian heart is relatively larger and more efficient than all other similarly-sized vertebrates including mammals. These specializations enable birds to get into the air and stay aloft, often for long periods of

time. Albatrosses, for instance, are renowned for their ability to cover great distances soaring and gliding over the ocean waves, expending little energy while searching for widely distributed food sources. Recently, the bar-tailed godwit (*Limosa lapponica*) was shown to undertake the longest non-stop migratory flight of any bird, traveling some 11,000 kilometers from breeding grounds in Alaska directly over the Pacific Ocean to New Zealand and eastern Australia, a trip taking eight continuous days and nights of flight without stopping to rest or feed (Gill et al., 2005).

The ability to alter flight trajectory and speed (i.e., maneuvering) is of critical value to birds over a wide range of behaviors. In volant birds, the ability to locate and acquire prey, to avoid predators, and to execute courtship displays often strongly depends on aerial maneuverability. To orient and maneuver in three dimensions, continuous corrections in flight course are necessary over a wide range of time scales. These will depend on the volitional interests of the animal (where does it want to go?) as well as external factors such as air turbulence and the density of obstacles along the flight path. Directional changes are brought about by the interaction of aerodynamic forces—initiated by active wing control—and the inertial resistance of the body to turns. Banking maneuvers require constant, authoritative adjustments of wing and body position to prevent stalling.

To what degree, then, are the rotation sensors of the inner ear specialized for the detection of movements associated with aerial maneuvering? There are over 8,500 extant species of birds that fly, and each approaches the task in its own particular way. The volant faculties of birds vary tremendously between species, ranging widely from the dynamic soaring of albatrosses to the helicopter-like darting and hovering movements of

hummingbirds. Many species are secondarily terrestrial and lack the ability to fly, while others have become proficient divers and swimmers. The ability to fly has enabled birds to radiate into a wide range of ecological niches, spurring the acquisition of synapomorphies not related to flight, per se, but more directly associated with sexual display, feeding behavior, vocalization, and so on.

In this chapter, I review the topic of bird origins (section 1) and the basic aerodynamics of flapping flight (section 2), focusing on the mechanisms and wing morphologies associated with flight maneuverability. Core predictions and hypotheses tested by this dissertation are given immediately following (Chapter 3).

2.1. The origin of birds and evolution of avian flight

The origin of birds from theropod dinosaurs is well corroborated by over thirty years of anatomical, paleontological, and phylogenetic research (Ostrom, 1976; Gauthier, 1986; Chatterjee, 1997; Forster et al., 1998; Padian and Chiappe, 1998; Chiappe, 1995, 2001; Sereno, 1999; Norell et al., 2001; Holtz, 1994, 1998; Prum, 2002; Chiappe and Dyke, 2002; Clarke et al., 2002; Livesy and Zusi, 2006, 2007), supporting a phylogenetic position for birds within the maniraptoran coelurosaurs. The earliest assertions that birds are related to theropod dinosaurs came from Thomas Henry Huxley (1868, 1870) and were revitalized a century later by John H. Ostrom (1973, 1974, 1976) who specified a theropod-bird origin based primarily on his interpretation of the dromaeosaurid *Deinonychus* (Ostrom, 1969).

Thulborn (1984) and Gauthier (1986) were the first to formally generate explicit phylogenetic hypotheses linking theropods and birds, using phylogenetic systematics. Under Gauthier's analysis, Theropoda was redefined to include birds and all dinosaurs more closely related to birds by common ancestry than to sauropodomorphs. Within this cladistic framework, modern birds (some 10,000 living species, the most abundant diversity of any tetrapod group) are firmly nested within the maniraptoran coelurosaurs. Gauthier (1986) erected the clade name "Avialae" to include all descendents stemming from the first dinosaur with a feathered wing used for powered flight (clarified in Gauthier and de Queiroz, 2001), of which *Archaeopteryx* is considered the basalmost member. I will use that definition here, and use the terms "bird" and "avialan" to mean the same thing. The crown clade stemming from the most recent common ancestor of all palaeognath and neognath birds shall be referred to as "Neornithes." Since the clade Theropoda includes all birds, those taxa not included within Avialae will be referred to as non-avian theropods. While *Archaeopteryx* is the oldest occurring definitive avialan (but note recent challenges to the contrary; e.g., Mayr et al., 2005), dozens of later-occurring Mesozoic birds have been described since its initial discovery in 1855 (reviewed in Chiappe and Dyke, 2002). Today, numerous avialan taxa are known, detailing an extensive series of nodes along the line leading to crown Neornithes and the full acquisition of a modern flight apparatus (e.g., Padian and Chiappe, 1998; Chiappe, 2001).

2.1.1. Birds are theropod dinosaurs

Osteological evidence of the association between birds and theropods comes from many sources. This topic has been well-reviewed elsewhere (e.g., Witmer, 1991; Padian and Chiappe, 1998) and necessitates only a brief treatment here pertaining to the acquisition of flight characters.

Major characteristics considered important to bird flight include: hollow long bones (for body weight reduction); fused clavicles, or furcula, acting as a spacer between the glenoids to prevent the pectoral girdles from compressing during downstroke; rotary wrist joint, for deployment of a grasping manus (a pre-adaptation enabling the flight stroke); coracoid and sternum expansion (leading to a deep, keeled thorax providing greater attachment surface for flight muscles); feathers for flight control and increased airfoil surface (sensu Sereno, 1999); and greatly elongated forelimbs, especially in the manus (sensu Ostrom, 1969, 1976), also for increased airfoil surface. These characters, and others, arose piecemeal as part of a hierarchically nested pattern of character evolution in Theropoda, and, despite their uniqueness among living birds, none are today considered autapomorphic for Avialae.

All non-avian theropods were obligatory bipeds. The most basal putative theropods (e.g., *Eoraptor*, *Herrerasaurus*) are noted for having short forelimbs disengaged from the locomotor cycle (Gatesy and Dial, 1996a), and this condition is retained throughout the entire theropod lineage leading up to avialans. While there are often extreme forelimb and manual adaptations in some theropod lineages, including, for instance, marked reduction of forelimb length in tyrannosaurids (Holtz, 2004) and

abelisaurids (Carrano, 2007), and strangely stunted—some would say "grotesque" (Chiappe, 1995)—forelimbs in alvarezsaurids (Senter, 2005), there is no evidence that any theropods used their forelimbs for ground support. Freedom of the manus from the function of terrestrial progression created a reduced "locomotor module" in basal dinosaurs comprised of the hindlimb and tail (Gatesy and Dial, 1996a), a condition that would ultimately permit modification of the forelimb into a wing in basal birds. Thus did birds arrive at a condition unique among extant vertebrates, in that the forelimbs and hindlimbs each subserve independent locomotor systems. The hindlimb kinematics of Neornithes changed dramatically, in that the primary method of ground propulsion became driven by knee-flexion and large tibiotarsal displacements, rather than by hip-extension and femoral retraction as in crocodiles and non-avian theropods (Gatesy, 1995).

Long bone hollowing for weight reduction occurs early in theropod evolution, found in primitive theropods like *Ceratosaurus* and all higher taxa (Sereno, 1999). The presence of a furcula is also widely distributed across theropods (e.g., Chure and Madsen 1996; Makovicky and Currie, 1998; Norell et al., 1998; Tykoski et al., 2002). Evolution of a compound distal carpal joint (fused distal carpals 1 and 2) occurs in *Coelophysis* and tetanurans (Wagner and Gauthier, 1999; Sereno, 1999), and a semilunate distal carpal occurs uniquely in maniraptoran theropods (Gauthier, 1986; Padian and Chiappe, 1998; Chatterjee, 1998; Wagner and Gauthier, 1999). The semilunate carpal is a further refinement of the primitive compound carpal joint, bearing a crescentic articular surface proximally, called the trochlear carpalis in avialans (Wagner and Gauthier, 1999). Distally, the semilunate carpal caps metacarpals I and II, incorporating both rays

functionally into the wrist joint (ibid.). The function of the semilunate carpal is to permit sideways flexion of the wrist, either to facilitate seizing movements in maniraptorans or more likely to permit folding of the arm skeleton. There is well established homology between this structure in maniraptorans and Neornithes (where it later loses its identity as the manual bones become fused), and inheritance of this joint from maniraptorans by Avialae is believed to have made evolution of the flight stroke possible from a kinesiological standpoint (Padian and Chiappe, 1998).

In the popular imagination, no single feature so remarkably links birds to coelurosaurian theropods as the shared derived trait of feathers. For most of human history, feathers have been uniquely associated with living birds, and systematists have long considered feathers diagnostic for Aves (Linnaeus, 1758; cited in Gauthier and de Queiroz, 2001; in this definition, "Aves" is synonymous with "Neornithes"). There is now a significant body of evidence that featherlike integumentary structures evolved before Avialae, first appearing in non-avialan coelurosaurian theropods and progressing in complexity through multiple steps until the full deployment of a modern avian plumage including asymmetrical flight feathers, as ascribed to *Archaeopteryx* (e.g., Griffiths, 1996; Wellnhofer, 2004). Fossilized feathers are exceptionally rare and are typically preserved as carbonized traces (Davis and Briggs, 1995) or fossil imprints (Norell and Xu, 2005). Feathers probably originated as a modification of the basic reptilian scale (Rawles, 1963; Maderson, 1972, Maderson and Alibardi, 2000; but see Brush, 1996, 2000, for a molecular refutation of homology), most likely in connection with a homeothermic insulating function (Bock, 1986), brooding, or display, and only later were these structures exapted as an aerodynamic surface for flight function

("exaptation" sensu Gould and Vrba, 1982). Plumulaceous (downy) and/or pennaceous (contour) feathers or featherlike structures are today known or inferred for many coelurosaurian taxa including basal tyrannosauroids (Xu et al., 2004), compsognathids (Chen et al., 1998; Currie and Chen, 2001), alvarezsaurids (Schweitzer et al., 1999), therizinosaurids (Xu et al., 1999a), oviraptorosaurids (Ji et al., 1998, Zhou and Wang, 2000; Zhou et al., 2000), dromaeosaurids (e.g., Xu et al., 1999b, 2000, 2001, 2003), and early avialans like *Archaeopteryx* (e.g., Elzanowski, 2002) and *Confuciusornis* (Hou et al., 1995). Since I became a graduate student in 2001, the extent to which the coelurosaurian body became covered in feathers was limited only by the pace at which new Chinese fossils could be described, so that today many paleontologists view the presence of protofeathers as autapomorphic for all of Coelurosauria (e.g., Norell and Xu, 2005), even when such structures aren't preserved in fossils (but see Göhlich and Chiappe, 2006, and for a refutation see Butler and Upchurch, 2007). The appearance of filamentous proto-feathers in early compsognathids like *Sinosauropteryx* (Chen et al., 1998), and the subsequent hierarchical acquisition of vaned pennaceous feathers and asymmetrical flight feathers in higher taxa, has effectively decoupled the origin of feathers from the origin of flight and removed "feathers" as a synapomorphy of Neornithes.

In most phylogenetic analyses, Avialae is considered the sister taxon of the group Deinonychosauria, which is comprised of the advanced maniraptoran families Dromaeosauridae and Troodontidae (e.g., Gauthier, 1986; Sereno, 1999) (Figure 2–1).

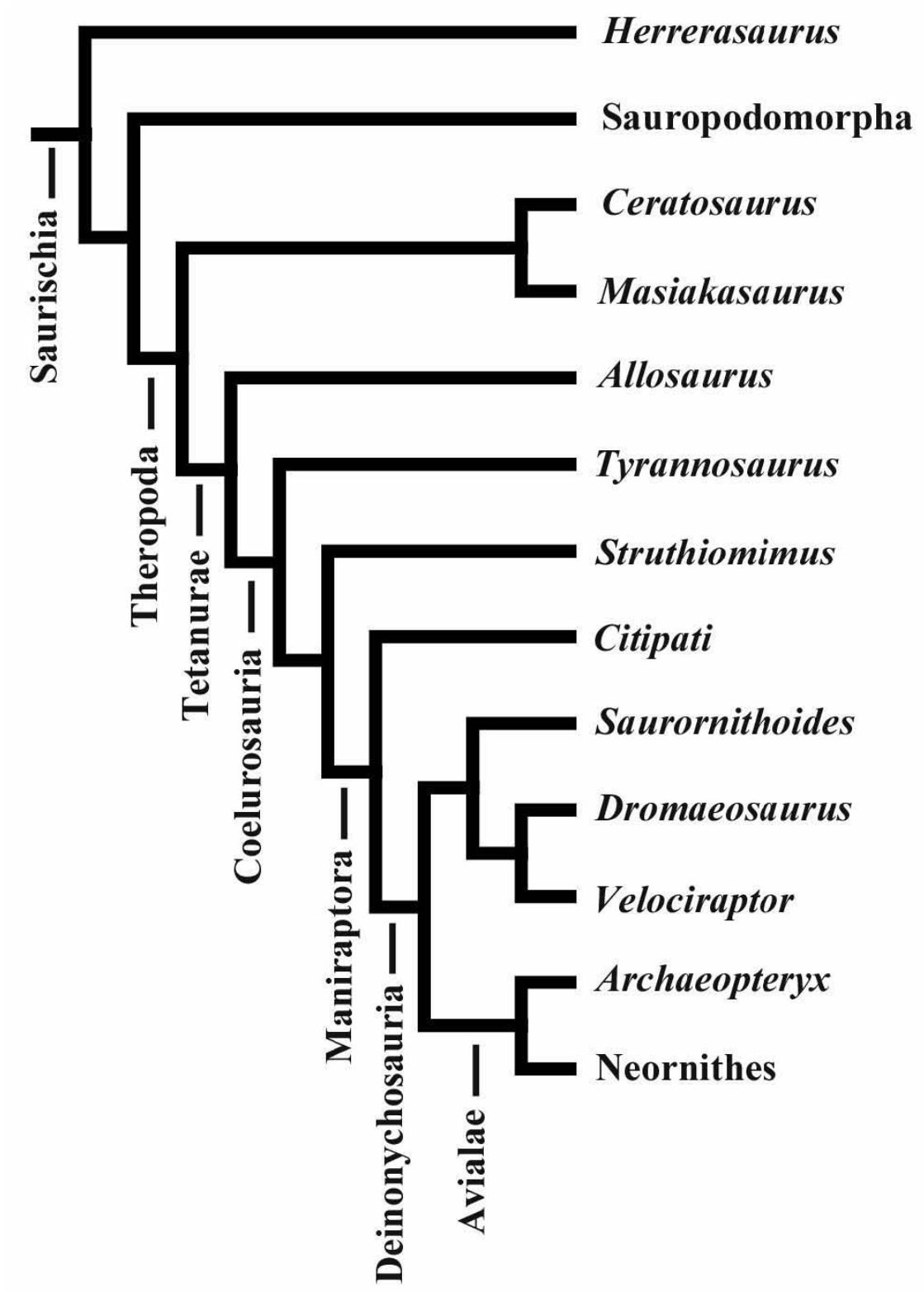

Figure 2–1. Summary phylogeny of Theropoda. A consensus phylogeny of theropod dinosaurs for the taxa in this study, modified from Padian and Chiappe (1998), Sereno (1999), and Norell et al. (2006).

As the basalmost member of Avialae, *Archaeopteryx* has received considerable attention since the initial discovery and description of an isolated carbonized feather from the Solnhofen Limestone, Germany, in 1861 (von Meyer, 1861), and was taken as early evidence of the kind of transitional forms anticipated just two years earlier by Darwin's theory of evolution by natural selection (1859). Few fossils have aroused as much interest in the popular imagination or had so profound an effect on interpretation of bird origins (Hecht, 1985). The Urvogel (German for "original bird") is today known from ten skeletal specimens (Mayr et al., 2005, 2007) referred to the genus *Archaeopteryx*. The taxonomic history of this genus is complex, with specimens assigned multiple different species names by different authors (e.g., Elzanowski, 2002; Mayr, 2005). As my analysis will be restricted in focus to the inner ear of the first discovered and coincidentally largest skeleton, the "London specimen" (BMNH 37001), I make no distinction between the numerous species names proposed for *Archaeopteryx* and refer to all members of this genus as *Archaeopteryx lithographica* (von Meyer, 1861). Senter and Robins (2003) advocate a similar view on the basis that the proportional differences among *Archaeopteryx* specimens often used to separate them can be explained by ontogenetic effects, though they recognize the distinctness of the genus *Wellnhoferia* (Elzanowski, 2001) on the basis of derived pedal and caudal characteristics.

Archaeopteryx has a mosaic of theropod and bird features, many that relate directly to flight function. Most of the body is covered in feathers of modern aspect, including highly asymmetrical flight feathers in the wing, and broad symmetrical tail feathers (Elzanowski, 2002), indicating that both the wing and tail were used for lift generation (Gatesy and Dial, 1996b). Asymmetry of the vanes of flight feathers, caused

by the outer (anterior) vane being narrower than the inner (posterior) vane, create pitching moments with each downstroke, necessary to keep the wing surface closed by pressing the feathers tightly together in areas of overlap (RÅ Norberg, 1985), and the presence of vane asymmetry indicates an aerodynamic function (Feduccia and Tordoff, 1979). There are no quill knobs in the ulna as indicated for *Rahonavis*, a hypothesized sister taxon (Forster et al., 1998), but neither are quill knobs a feature shared by all extant birds that can fly (Edington and Miller, 1941). Despite recent assertions to the contrary (Senter, 2006), the scapula is typically reconstructed as being oriented in a dorsal position with glenoid facing ventrolaterally, permitting elevation of the humerus above the dorsum (e.g., Ostrom, 1976; Jenkins, 1993).

Vazquez (1992) reported on the flight mechanics of the wrist in birds, using mallard ducks (*Anas platyrhynchos*) as a model, and showed that the joint configuration of the avian wrist was extraordinarily adapted for flight. Vazquez showed that during downstroke, when lift and thrust is generated, the manus is prevented from hyperpronation by the cuneiform, which transmits forces from the carpometacarpus (the fused carpus and manus unit in birds) to the ulna. During maneuvering and gliding, the manus is prevented from supination by interlocking of the carpometacarpus with the scapulolunar, allowing the wing to be secured in place while fully extended. During upstroke of slow, maneuvering flight, when the wing surface must be retracted and brought close to the side of the body, Vazquez showed that the pronounced articular ridge of the distal ulna and orientation of the cuneiform permit the manus to re-orient from the plane of the wing to the plane of the body (ibid). Vazquez noted, “There are important implications here for both the flight capabilities of the fossil *Archaeopteryx* and for the

evolution of powered flight" (1992: 266). Importantly, he called attention to the absence of articular facets on the cuneiform and scapulolunar elements of *Archaeopteryx* that characterize higher avian taxa, and questioned whether *Archaeopteryx* could fly using the same kinematics employed by modern birds in flapping flight.

Unlike more derived birds, *Archaeopteryx* retained a toothed jaw of small, conical teeth and a long bony tail (Elzanowski, 2002). The cranial cavity of *Archaeopteryx* is completely filled by the brain, and the optic lobes (mesencephalic tectum) are expanded and lateralized (Jerison, 1973; Bühler, 1985; Dominguez et al., 2004), as is typical for modern birds (Pearson, 1972). With a body mass estimate of 468 g (Elzanowski, 2002) and an endocephalic volume estimated at between 1.6 ml (Dominguez et al., 2004) and 1.76 ml (Hopson, 1977), the London specimen of *Archaeopteryx* has an encephalization index intermediate between birds and diapsid reptiles, though "appreciably closer to birds" (p. 668, Dominguez et al., 2004). It is unclear whether brain enlargement in *Archaeopteryx* is related to acquisition of flying behavior, arboreal habits, or some other aspect of environment (Jerison, 1973), though some (Dominguez et al., 2004) have speculated that *Archaeopteryx* has a brain adapted for flight, inferring that the overall enlargement of the brain and the proportions of the semicircular canals indicate bird-like spatial sensory capabilities. This is a tenuous assertion, since the relationship of bird canal size to flying behavior had not been previously demonstrated except by preliminary conference data (Sipla et al., 2003).

Shortly after the appearance of *Archaeopteryx* in the fossil record, major modifications to the avian bauplan appear rapidly in the earliest Cretaceous. The pygostyle—i.e., caudal vertebrae fused into a single ossification, for attachment of

retrices in birds—occurs in *Confuciusornis*, a well-represented species from the earliest Cretaceous of northern China (Hou et al., 1995). Alular feathers (comprising the bastard wing) enabling flight control at lower airspeeds are documented in the early enantiornithine *Eoalulavis*, from the Early Cretaceous of Spain (Sanz et al., 1996). Other members of the large enantiornithine radiation demonstrate a fully opposable hallux for perching, indicating that birds occupied arboreal habitats extending far back into the Cretaceous (Padian and Chiappe, 1998). The hallux of *Archaeopteryx* is also described as opposable but somewhat elevated, with a limited capacity for grasping (Elzanowski, 2002).

Among ornithurine birds, there is a large radiation of secondarily flightless species, the well-known Hesperornithiformes (Chiappe, 1995). These toothed, foot-propelled divers are common in the Late Cretaceous of North America, eastern Europe, and western Asia (ibid.). The less known Ichthyornithiformes constitute a clade of tern-like birds with proficient flying abilities (Padian and Chiappe, 1998, Clarke, 2004). Both groups retained teeth, with the toothless avian bill not being fully established until the appearance of Neornithes. For a summary of preneornithine evolution, the reader is referred to Chiappe (2001) and Chiappe and Dyke (2002).

2.1.2. Extant bird diversity

Extant birds (Neornithes) are the most speciose of all terrestrial vertebrates (some 10,000 species in over 2,000 genera), with representatives inhabiting all major biogeographic regions of the world.

Relationships among extant birds are highly contentious, in part because few sister group relationships are supported by ordinal phylogenies, and because of difficulties inherent to rooting the avian tree with distantly related archosaur taxa (i.e., Crocodylia). Most analyses recognize two primary groups within Neornithes, whether morphological or molecular characters are used: Paleognathae (ratites and tinamous) and Neognathae (all other extant birds) (Cracraft, 1981; Sibley and Ahlquist, 1990; Mindell et al., 1997; Cracraft et al., 2004; Livezey and Zusi, 2007). Relationships within the ratites are unsettled in the literature because of continued conflict between morphological and molecular data (Cracraft et al., 2004). Higher level systematics of the neognathan assemblage remain difficult, but some general relationships are supported.

Figure 2–2 is a summary phylogenetic hypothesis for extant avian orders modified from Livezey and Zusi (2007). Within Neognathae, there is another well-supported divergence between the sister clades Galloanserae (comprised of megapodes, guans, pheasants, and their allies [gamefowl] and ducks, geese, swans, and allies [waterfowl]) and Neoaves (all other neognaths). Further consensus on avian ordinal relationships is relatively insecure, and conflicting alternative topologies are common between morphological and molecular methods (see reviews in Sibley and Ahlquist, 1990; Cracraft et al., 2004; Livezey and Zusi, 2007). High diversification rates in some lower-level avian clades but not others further compound the difficulties in obtaining secure phylogenetic hypotheses (Phillimore et al., 2006).

Recently, Livezey and Zusi (2007) published a morphologically based phylogeny of higher order relationships of Neornithes, finding relatively stable clades for several groups, with the majority of nodes being highly supported. ‘Total evidence’ approaches

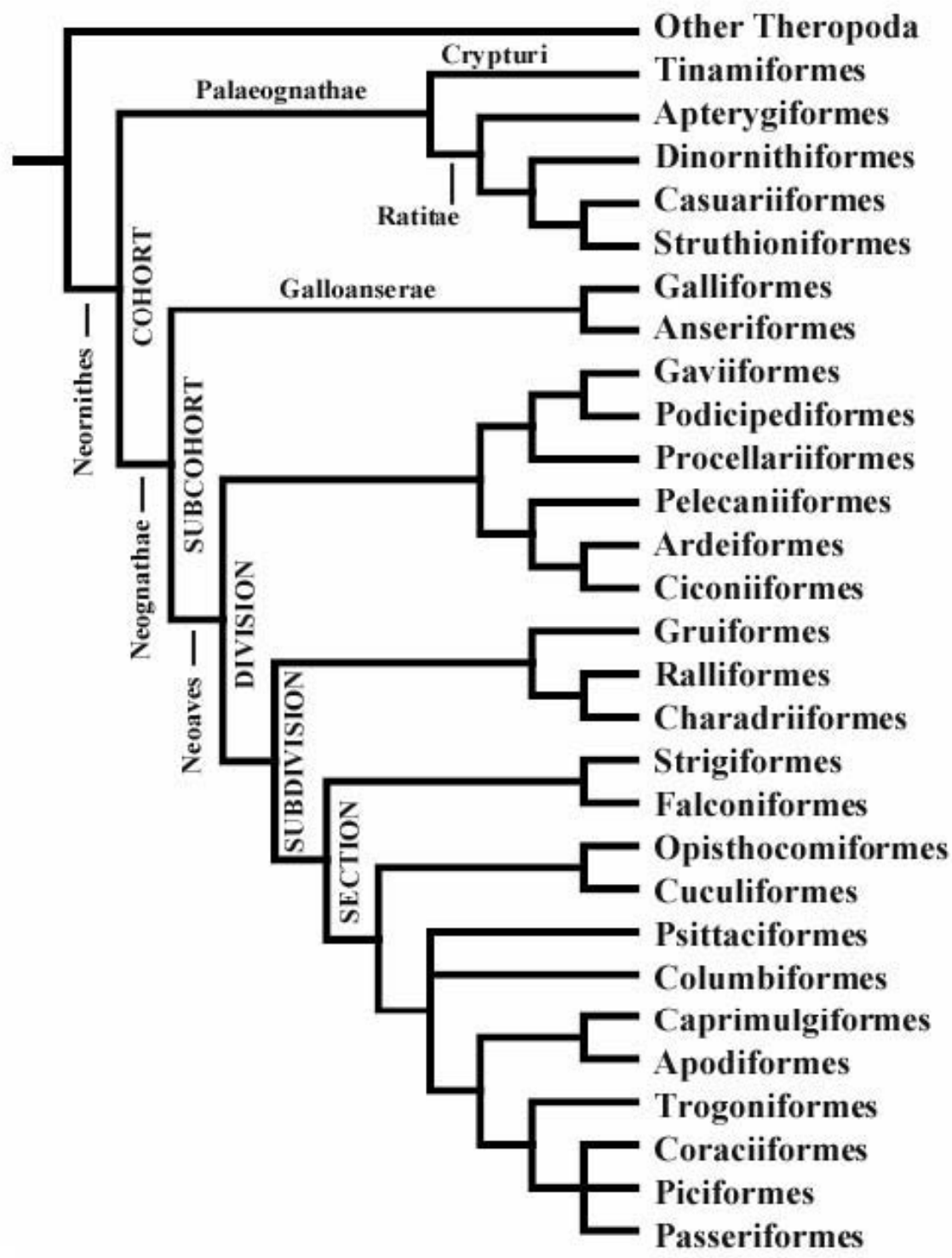

Figure 2–2. Summary phylogeny of extant avian orders. Simplified summary tree for uppermost, supraordinal ranks of avian classification for the taxa in this study, modified from Livezey and Zusi (2007).

integrating morphological and DNA-sequence data are needed to resolve avian relationships, however. Cracraft et al. (2004) present a summary phylogeny representing a total-evidence approach, and moreover a compromise between the 14 authors, that can best be described as a polytomy of all Neoavian taxa with a few well-supported internested clades. Despite its lack of resolution, this phylogeny does serve as a scaffold of sorts for investigating the fine-scale relationships of birds at the familial and lower terminal levels, especially when combined with more stable (but less inclusive) morphological analyses (e.g., Livezey and Zusi, 2007).

2.1.3. Evolution of the flight stroke

Decoupling of the forelimbs from the function of terrestrial locomotion ultimately permitted the evolution of wings in theropods, and decoupling of the tail from the hindlimb permitted its use as a supplementary flight structure useful in aerial coordination (Gatesy and Dial, 1996a). Although most modern birds do not rely on the tail to generate lift (Pennycuick, 1975), the tail is believed to have been an important flight surface in primitive birds, arguably to increase lift and stability in the pitch plane by shifting the center of mass posteriorly (Peters and Gutmann, 1985). Because the forelimbs had already been decoupled from locomotor function in bipedal theropods, the hindlimbs could not easily be integrated into a developing flight apparatus by protobirds, as they were by protobats. There is some evidence that dromaeosaurid relatives of avialans such as *Microraptor gui* used the tail both as a pitch dampener and lift surface during gliding flight (Chatterjee and Templin, 2007), and *Archaeopteryx* is thought to

have used its long, frond-shaped tail for pitch control (Gatesy and Dial, 1996b) and yaw control (Norberg, 1990). This configuration is inherently more stable—owing to the additional lift surface and stability in pitch afforded by the tail feathers—than in modern birds, which have a more anteriorly-shifted center of mass and benefit from increased instability with gains in turning performance (Maynard Smith, 1952). Maneuverability in flight was therefore limited in primitive avialans like *Archaeopteryx*, and nonsteady flight may have been impossible or highly restricted (Rayner, 2002). Modern birds have effectively shifted most lift function to the wings, relegating the shortened tail to the fine control of pitch (Thomas, 1993), the prevention of sideslip during banking maneuvers (ibid.), control during acute braking and turning (Gatesy and Dial, 1996b), or to no function at all during high speed forward flight when the tail is simply positioned in line with the body to minimize drag (Pennycuick, 1975).

Regarding the thoracic limb, the position of the glenoid is important for flapping flight function. In ornithurine birds and contentiously in basal avialans (Senter, 2006), the glenoid faces laterally to permit elevation of the humerus above the dorsum (Jenkins, 1993). This is an important reorientation of scapular position from the condition seen in most non-avian dinosaurs, where the scapulae are positioned laterally with glenoids facing ventrally. In the avian position (with glenoids lateralized), the ability of the humerus to elevate above the dorsum is critical to completing a full recovery stroke during flapping flight (Jenkins 1993; Poore et al., 1997). Arguments about the orientation of the glenoid in *Archaeopteryx* (most recently Senter, 2006) imply that flight stroke recovery was prevented in basal avialans and consequently *Archaeopteryx* was incapable of powered flight, though possibly gliding for flap-assisted gliding using downstroke

only. Rayner (2001) points out that *Archaeopteryx* was likely incapable of slow flight, since it lacked the necessary upstroke musculature (namely the wing elevator supracoracoideus), claiming that it probably used a continuous vortex gait (see section 2.2.2). As a means of lift production, this gait elevates the wing by aerodynamic forces rather than muscular effort (Rayner, 1988a, 2001). The result is a lower-amplitude wingbeat and recovery stroke of lesser magnitude, suggesting to me that a compromise may be possible between glenoid orientation (whatever its true position may be) and the necessary extent of humeral elevation during flapping flight in *Archaeopteryx*.

Evolution of the avian flight stroke and the behavioral conditions necessary as precursor to it, are matters of extreme, often hotly contested opinion. As mentioned above, decoupling of forelimb and hindlimb movements in basal dinosaurs freed the forelimb to be co-opted for lift production in flapping flight (Gatesy and Dial, 1996a), but exactly what stages did the forelimb go through to achieve its final modification as an airfoil? Numerous explanations have been put forward. Ostrom (1974) proposed the idea that a feathered forelimb could have been elongated to function as a net to trap insects, and that stereotyped motions associated with prey capture in this manner could lead evolutionarily and anatomically to an avian flight stroke. A similar hypothesis relating predatory motions of the hand in *Deinonychus* to avian wing movements was most recently advanced by Gishlick (2001) and refuted by Gatesy and Baier (2005). Chatterjee (1997) argued that forelimb motions used to climb trees would render possible a flight stroke. Others have argued that wingbeat movements could generate forward thrust during running (Burgers and Chiappe, 1999; Burgers and Padian, 2001) or when scaling trees and other inclines ("Wing Assisted Incline Running," or WAIR, Bundle and Dial,

2003; Dial, 2003). Alternately, as Bock has argued (1986), the flight stroke could have arisen de novo as a means to improve maneuvering and braking during gliding.

As Padian and Chiappe (1998) and Witmer (2002) point out, we must be careful when coupling the origin of flight to the origin of birds. The latter is necessarily a matter of phylogeny and not necessarily as a valid consequence of the former, which is a functional matter. Nevertheless, the phylogenetic definition of birds has usually implicitly or explicitly invoked the origin of flight or flight-related features, and the origin of birds is not entirely independent from the acquisition of flight characters. For over a century debate over the origin of flight has been framed in strongly simplified and contrasted terms, summarized in extreme forms by the arboreal, or "top-down" hypothesis, and the cursorial, or "ground-up" hypothesis. Proponents of the arboreal model argue that active bird flight proceeded from a scansorial, gliding stage, suited for leaping between trees. Under selective pressure for longer flight lengths and maneuverability, flapping wings and improved sense organs evolved and fully powered flight became possible. The arboreal model implies that bird ancestors possessed the antecedent ability to climb. While this model makes intuitive sense, there is little morphological or comparative evidence to support it (Padian and Chiappe, 1998). The first known fossil bird, *Archaeopteryx*, lacks features associated with typical vertebrate gliders, and it does not appear to be aerodynamically suited for gliding flight (Yalden, 1971; Padian, 1985; Rayner 1985c).

Workers who favor the cursorial model point to postcranial features of *Archaeopteryx* and argue from a functional and ecological standpoint that the earliest known bird was a strong, agile biped, ill-suited to life in the trees but capable of powered

take-off (e.g., Burgers and Chiappe, 1999). While there is agreement between derived theropod anatomy, phylogeny, and the predictions of the cursorial hypothesis, the model is subject to criticisms on energetic (Rayner, 1985b, c, 1988b, 1991b) and bioaerodynamic grounds (Norberg, 1985a, b, 1990). A modified version of the cursorial hypothesis was developed by Peters (1985), which argued that short glides were preceded by running take-offs. Some workers have considered these hypotheses untestable or a false dichotomy (reviewed in Padian, 2001).

Whatever the origin, primitive birds had a capacity for powered flight. The following section reviews the basic aerodynamics of flapping flight and considers the importance of vestibular control during maneuvering.

2.2. The aerodynamics of flapping flight

Powered flight requires a take-off event, acceleration to some cruising speed, typically a series of course corrections, ultimately concluding with a landing procedure. Rayner (2001) summarizes the basic biomechanical and aerodynamic adaptations necessary for powered flight. In order to fly, an animal must 1) have wings with an airfoil profile that can generate lift, 2) be able to flap its wings to generate thrust, and 3) be able to control its flight (Rayner, 2001). Birds must function as pilot and aircraft at the same time, taking into account a wide array of aerodynamic and structural limitations when executing maneuvers in an uneven locomotor substrate. They must possess control systems capable of responding rapidly to both intentional and unintentional course changes.

This section reviews the basic aerodynamic principles of flapping flight. More thorough treatments can be found in, for instance, Brown (1963), Pennycuick (1975), Ellington (1984a), Rayner (1988a), Biewener (2003), and many textbooks. The brief introduction that follows is adapted, in part, from these sources. The section is concluded with a pertinent discussion on aerial maneuvering and agility, with an assessment of the sensory systems necessary to permit controlled flight.

2.2.1. Introduction to basic principles

Flying birds are held aloft by forces generated by the flow of air over the outstretched wing. The force that supports the weight of the bird during flight is called lift, achieved primarily by beating the wing. Due to the asymmetrical shape of the wing, the air stream passing over the airfoil travels further and faster than the air stream passing beneath it. The undersurface of the wing is flatly contoured while the upper surface is convex in shape. This asymmetry, in conjunction with the angle at which the wings are tilted toward the oncoming air (angle of attack), produces lift by directing the flow of air downward. Generation of lift requires an expenditure of energy, provided by contraction of the bird's flight muscles (*m. pectoralis major*). The primary parameter for determining lift is the angle of attack with respect to oncoming air, with maximum lift obtained when the wing angle is held very near, but just below, the point of stalling (when air flow over the top of the wing becomes more turbulent and less flow is directed downward).

In order to fly level, air must be directed downward, to counteract gravitational acceleration and support the weight of the airborne animal, as well as backward, to

provide thrust. The thrust component of flapping flight is necessary to balance drag due to friction on the wings and body. In gliding flight, the wings balance the weight of the flier but do not provide thrust. Assuming the absence of environmental sources of energy, such as columns of rising air (thermals), the gliding bird loses altitude and/or speed due to induced drag encountered by the wings.

Because lift generation is proportional to the amount of air diverted down and back, lift is also related to the area of the wing, with maximum lift being proportional to (wing area) × (flight speed)^2 for any particular angle of attack. Because weight and lift must balance if the flier is to remain airborne, body mass is proportional to (wing area) × (minimum flight speed)^2. Minimum possible speed is therefore proportional to the square root of (body mass / wing area). The quantity (body mass / wing area) is typically referred to as wing loading. The larger the number, the smaller the wing in proportion to body mass and the faster the bird must fly to stay aloft.

Because the flow of air below the wing stagnates relative to air above the wing, positive pressure develops beneath the wing and negative pressure above it (Savile, 1957). Lift force is established; that is, air momentum is diverted behind and below the animal. In a fluid such as air, momentum can only be transported by a distribution of vortices (early vortex theory for avian wings was established by Rayner, 1979a, b, c and Ellington, 1984b; useful reviews are found in Rayner, 1988a, 1991a, 1994 and Tobalske, 2000). A vortex is a rotational motion in fluid caused by differences in pressure and velocity. The net circulation of air about the wing is represented as a bound vortex, the strength (circulation) of which is proportional to the degree of lift and the speed of movement. At all times, the bound vortex is abruptly shed from the wing tips as a pair of

separate trailing vortices. These constitute the "vortex wake." The distance between the axes of the two trailing vortices is slightly less than the maximum wingspan of the flying bird (length from wing tip to tip). Any change in the strength of the bound vortex, as during a wingbeat, will shed a transversely-directed vortex from the back of the wing, corresponding in strength to the change in bound circulation. Because these transverse vortices are formed when lift production starts and stops, their presence and structure reveals information about the pattern of wingbeat kinematics. By changing total wingspan or the circulation of the bound vortex (for instance, by changing the curvature of the airfoil, called wing camber, or the angle of attack), a bird can vary instantaneous lift production. Quantitative differences in the structure of wake vorticity caused by these changes are used to differentiate between distinct gaits in flying birds (Kokshaysky, 1979; Spedding et al., 1984; Spedding, 1986, 1987a,b; Rayner, 1991a; Hedrick et al., 2002).

2.2.2. Patterns of thrust generation in cruising flight

The purpose of wing flapping is to generate thrust, since body weight is adequately supported by the nonflapping wing. This can be readily appreciated by observing the shallow glide angles of most birds. The need for thrust in flapping flight, however, dictates that some form of geometric or aerodynamic asymmetry be adopted between the two stroke phases of the wingbeat. A bird flapping its wings with identical downstroke and upstroke kinematics cannot produce a horizontal thrust component to lift; any horizontal force generated by the downstroke would simply be cancelled by the

upstroke. Necessarily, the flying bird must somehow vary the kinematics of the stroke phases.

In the bird literature, aerial gait refers to the pattern of movement of the limbs at different speeds and locomotor modes. This is the same as for terrestrial animals, but the key difference is that gait transitions in flying birds are gradual and poorly understood (reviewed in Rayner, 1988a). Experimental analyses of wake vortices shed in clouds of neutrally buoyant particles have documented at least two kinds of flying gaits: the vortex ring gait and continuous-vortex gait (reviewed in Rayner, 1988a, 1991a, 1995). The primary difference between these gaits relates to controlled changes in the wing planform during the upstroke.

During the vortex ring gait, lift is entirely produced during the downstroke and the upstroke is aerodynamically inactive (Rayner 1979a, c). To achieve this during upstroke, the wing surface must be highly flexed to bring the wing tips close to the side of the bird's body. Deformation of the wing out of the stroke plane minimizes drag due to friction on the body (profile drag). After the wing is retracted, it is elevated by active contraction of the supracoracoideus and deltoid muscles. As the upstroke terminates, the wings are spread rapidly (Brown, 1963) but no lift is generated until initiation of the downstroke, when the wing depresses (Rayner, 1988a). In this gait, transverse vortices are shed from the trailing edge of the wing at the beginning and end of the downstroke, causing the wake to roll up into a chain of elliptical vortices, one closed ring for each downstroke (Rayner 1979a, b, c). This type of flight is typical of slow flight in all birds as well as fast flight in birds with rounded or square wings (low aspect ratio) (Rayner 1985b, 1988a, 1991a). The gait is also used by most small songbirds (passerines) at all

speeds, especially those that employ bounding or undulating flight modes (Rayner, 1985a).

Because lift production ceases during the upstroke with this type of flight, a bird will experience downward accelerations due to gravity and upward accelerations due to lift with each downstroke (Warrick et al., 2002). Therefore, in vortex ring gait, the weight of the animal is only supported during the downstroke. In many ways, this pattern is similar to the stresses encountered by terrestrial animals with each footfall, whereby ground reaction forces generated at touch-down by supporting limbs are transmitted to the axial skeleton, and thus to the inertially unstable head (refer to section 1.4.3) The difference is that volant birds would experience these oscillations at much higher frequencies during low speed flapping flight (~10 times per second, a typical avian wingbeat frequency) than would similarly sized cursorial bipeds. As pointed out by Warrick and colleagues (2002), visual and vestibular systems could be severely impacted by such rapidly alternating accelerations.

The continuous-vortex gait represents a simpler, more efficient gait than flight with an unloaded upstroke (Rayner, 1991a). In this gait, the upstroke is aerodynamically active and weight is supported throughout the wingbeat; air circulation around the wing is constant during both stroke phases. Net thrust is generated by the downstroke, which more than compensates for the retarding negative thrust incurred by the upstroke. The wing itself is raised by aerodynamic lift on the wing surface, requiring less active muscle contraction during upstroke (Rayner, 1988a; but see Olsen, 1993; Tobalske and Dial, 1994; Tobalske, 1995, and Tobalske et al., 1997 for evidence of wing elevator action during continuous-vortex gait). Geometric asymmetry of the wing is achieved during the

upstroke by sweeping or flexing the wing tips within the plane of the wing; i.e., effective wingspan is reduced by moving the wing tips back and slightly inwards at the wrist, while simultaneously avoiding rotation of the manus out of the wing plane (Rayner, 2001). As the name suggests, the vortex wake created by this gait is continuous. Paired trailing vortices are continuously shed from the wing tips in a smooth, unbroken pattern, undulating up and down with each stroke phase (Spedding, 1987a). No transverse vortices are created. This type of gait is used during fast flight in birds with long and/or narrow (high aspect ratio) wings, and also sometimes during deceleration in birds with low aspect ratio wings (Rayner 1985b, 1988a, 1991a; Tobalske and Dial, 1996). It is an inherently less perturbed (more stable) form of aerial locomotion. The large accelerations and decelerations associated with the wingbeat during vortex ring gait at lower speeds are absent (Aldridge, 1987). Accelerations experienced by the head are hypothesized to be lower. Continuous-vortex gait is less energetically expensive to maintain and is therefore favored by birds traveling over great distances at speed (exemplified in extreme form by the albatross). Birds using this gait typically have relatively small supracoracoideus muscles compared to birds using the vortex ring gait at all speeds (Rayner, 1988a).

Other gaits have been hypothesized for birds. Apodiforms (swifts and hummingbirds), for instance, are believed to shed vortex rings during the downstroke *and* upstroke of slow flight (the so-called "double-ring gait;" Rayner, 1979a, b, 1995; Tobalske, 2000), while during faster flight it is presumed that circulation is decreased during the upstroke, resulting in a characteristic ladder-like vortex-shedding regime ("ladder-wake gait;" Pennycuick, 1988). These gaits are conjectured to occur because neither swifts nor hummingbirds flex their wings considerably during upstroke at any

speed (Warrick, 1998), and because hummingbirds invert their wings during hovering (Rayner, 1988a). Recently, Warrick and colleagues (2005) visualized the wake of hovering rufous hummingbirds (*Selasphorus rufus*) using digital particle image velocimetry and reported preliminary findings on wake structure for the purpose of measuring force asymmetry during the stroke cycle, though they did not report explicitly on gait structure. Recent work quantifying wake vortices in the thrush nightingale suggest that graduated, intermediate vortex shedding regimes are present during gait transitions (Spedding et al., 2003). Complex vortical wake structures in bats have recently been documented (Tian et al., 2006).

In light of these exceptions, it is interesting that birds seemingly adopt one of only two gaits (vortex ring or continuous-vortex gait) during cruising flight. Rayner (2001) conjectures that other gait patterns could have evolved in birds, but only at higher aerodynamic energy costs. Natural selection seems therefore to have restricted the expression of such gaits. It is worth bearing in mind, however, that quite distinct and inherently more complex gait patterns are used by birds during takeoff and landing, and that the vortex ring and continuous-vortex gaits are primarily useful in describing steady-state (cruising) flight only.

Birds and bats are known to transition from a vortex-ring gait at slow speeds to a continuous-vortex gait at high speeds. The pigeon (*Columba livia*) is a well-documented example (e.g., Brown, 1963; Tobalske and Dial, 1996). Gait transition has also been studied experimentally in cockatiels (*Nymphicus hollandicus*) and ringed turtle-doves (*Streptopelia risoria*) (Hedrick et al., 2002). In this latter study, both species were observed to shift from a vortex-ring gait to a continuous-vortex gait at a flight speed of

7m s^{-1}, despite differences in wing shape (aspect ratio), body mass (76.5 and 76.9g for two cockatiels, and 152.0 and 128.9g for two ringed turtle-doves), and wing loading, and switching again to a ladder-wake gait at maximum flight speeds. Some comparative data indicates that the speed at which a bird changes from one gait to the other increases with body mass (summarized in Tobalske, 2000).

Another factor governing gait transition is instantaneous flight velocity. Kinematic evidence suggests the use of vortex-ring gait during acceleration and continuous-vortex gait during deceleration, depending on the gait in use before the change in velocity (Rayner et al., 1986, Rayner, 1991a, 1995; Tobalske and Dial, 1996; Hedrick et al., 2002). This occurs because the negative thrust generated during upstroke with a continuous-vortex gait tends to diminish acceleration and augment deceleration, and birds select gait accordingly (Tobalske, 2000). There may also be numerous physiological correlates of gait selection. Variations in muscle activity, such as wing elevator activation during upstroke, and respiratory patterns (which are known to coordinate with wingbeats; Berger et al., 1970) may be correlated with transitions in wing-beat gait. Lacking available kinematic and vortex visualization data, however, these physiological factors are difficult to ascertain at present.

2.2.3. Maneuvering during flight

All volant animals must be able to change their speed and trajectory during sustained flight. Many birds navigate and forage in densely cluttered environments, such as deciduous and mixed wooded areas, requiring an active and rapid control of aerial

movements to avoid collisions. Others pursue active prey, or must avoid predation with evasive responses. Aerial locomotion is characterized by movement across six degrees of kinematic freedom (three translational and three rotational), and given these freedoms rotational accelerations are likely to be more important in air than on land (Dudley, 2002). Although morphological correlates of turning performance predispose some birds for better or more efficient maneuverability, all birds that fly need to maneuver in an aerial habit.

Body mass, wing span, and wing area are the primary variables used in rating the performance of flying animals. From these variables are derived two important factors: wing loading and aspect ratio.

Wing loading

Wing loading is the weight (mass × gravitational acceleration) divided by the wing area, expressed in units N m^{-2} (Norberg and Rayner, 1987). Wing loading varies with increasing size, with larger birds having a higher wing load than smaller birds (Rayner, 1988a). The higher the wing load (i.e., the smaller the wing area in proportion to body weight), the faster the bird must fly to stay aloft. A low wing load enables birds to sustain flight at lower speeds and with greater maneuverability (ibid.). Birds that glide often have a low wing load relative to birds that employ active flapping flight, as do birds that inhabit dense environments and must fly at slower speeds to react to obstacles in their flight path.

Aspect Ratio

Aspect ratio is defined as the square of the wing span divided by the wing area (Norberg and Rayner, 1987). High aspect ratio wings tend to be long and narrow, whereas low aspect ratio wings are shorter and broader. This variable reflects the modification of the airfoil to accommodate a variety of flight behaviors, from gliding to rapid turning (Rayner, 1988a). Wings of high aspect ratio typically correspond with greater aerodynamic efficiency and lower energy costs in flight, ideal for fast flying at the expense of maneuverability. Reduction in maneuverability occurs because high aspect ratio wings inherently have a lower roll rate (the rate at which the bird can change its attitude in roll), due to the higher moment arm of parasite drag (drag due to shape) and greater moment of inertia associated with long wing morphs. Narrow wings have less inertia but have small wing areas and correspondingly high wing loading (lower maneuverability), unless they are also extremely long. Lower aspect ratios tend to be more stable in the pitch plane than high aspect ratio wings, conferring a handling advantage at slow speeds. Consequently, low aspect ratio wings are associated with slower flight strategies and higher maneuverability, the latter especially true when coupled with low wing loading (Norberg and Rayner, 1987).

It is inferred that specialization of bird wing morphology matches the aerodynamic requirements needed for optimal flight behaviors, given the body size of the animal in question (e.g., Norberg and Rayner, 1987; Spaar and Bruderer, 1997; Lockwood et al., 1998). However, it should be remembered that the aerodynamic properties of a wing are part of a larger mosaic of morphological traits related broadly to

ecology, physiology, and other adaptive aspects of an animal's behavior not limited to flight.

Following Norberg and Rayner (1987), the ability to execute a turn mid-flight is governed by two quantities: maneuverability and agility. These are defined below.

Maneuverability in turning flight

Maneuverability refers to the minimum space required by a flying animal to alter its flight path, traditionally defined by the radius of turn (Norberg and Rayner, 1987). The smaller the turn radius, the more maneuverable the flier and the more turns it can execute per unit time. To conduct a turn, lift must be redirected toward the center of curvature of the flight path, achieved by banking with the wings and body (Norberg and Norberg, 1971). To establish a bank angle and begin turning, a gliding bird must produce a lift force asymmetry between the two wings, initiating a bank and associated body roll, followed by another asymmetry to counteract the momentum of the turn and stabilize the roll along a new heading (e.g., Warrick et al., 2002). Birds in slow, flapping flight (using a vortex ring gait) produce a more complex series of lift force asymmetries over the course of the turn with each downstroke, due mainly to the saltatory nature of lift production (Warrick et al., 1998). When banking during slow flight, greater forces are produced on the outside wing with respect to the turn and moved incrementally through the duration of the maneuver (Warrick et al., 2002). Incremental force asymmetries are generated by downstroke velocity asymmetries, producing high angular accelerations with every downstroke, up to 2,000 radians sec^{-2} (determined experimentally for pigeons

by Warrick and Dial, 1998). Lateral accelerations are reported to peak during the sharpest point of a slow, flapping turn (Rayner and Aldridge, 1985; Aldridge 1986).

Degree of aerial maneuverability is determined by a bird's wing loading. Assuming constant lift, the minimum radius necessary to make a level banked turn is proportional to wing loading (Norberg and Rayner, 1987; Norberg, 1990). Flight speed is also proportional to wing load, and because of this, birds with low wing loads can travel at slower speeds without stalling (Ellington, 1984a; Rayner, 1988a). Stated simply, birds flying at slower absolute airspeeds can execute a smaller radius turn for any given maneuver. The optimal wing morphology for high maneuverability during slow flight is one with a large wing area relative to body mass (low wing loading) paired with a low aspect ratio (Pennycuick, 1975, Norberg, 1986, Norberg and Rayner, 1987; Warrick, 1998).

As Warrick and colleagues (2002) point out, correlating wing morphology to flight behavior in this way tacitly infers that maneuvering performance is somehow less important for birds lacking optimal or extreme wing shapes. The authors point out that any bird capable of slowing its flight speed can make turns of small radius regardless of wing shape (termed "facultative maneuverability," Warrick et al., 1998) and that the very act of taking off and landing—something all flying vertebrates must do at some point—requires often extreme feats of low-speed maneuverability many times per day. They argue that the ability to execute low-speed maneuvers is therefore critically important to all birds, regardless of wing size and shape, and that selection for this ability has likely been the defining pressure in avian evolution. The key point here is that wing loading is a good measure of the efficiency of turning performance; i.e., birds with low wing loads

can turn without reducing airspeed. Warrick and colleagues (2002) argue that wing loading should therefore be used as a measure of the ecomorpological specialization for turning (i.e., time spent turning during daily function), not a direct measure of absolute maneuverability.

Agility in turning flight

Agility refers in a general sense to the quickness of aerial movements, the rapidity with which a flight trajectory can be altered (Norberg and Rayner, 1987; Dudley, 2002). In a mechanical sense, it is defined as the "maximum roll acceleration during the initiation of a turn" (Norberg and Rayner, 1987), essentially the speed at which aerodynamic surfaces (wings) can be asymmetrically deployed to establish a directional change. These wing asymmetries might incorporate a differential change in wing flexion, pronation or supination of part of a wing, stalling one wing, or a change in angle of attack (ibid.). Both the inertia of the body and of the wings factor into the total roll moment of inertia, and therefore the requirements for good agility directly conflict with those for good maneuverability. Large wings are good for maneuvering but consequently increase inertial resistance to rotation, impeding the flier's ability to roll into a bank quickly. A decrease in either wing or body inertia favors agility, reducing the time taken to enter a turn and complete it. Relationships between wing morphology and agility are significantly more complex than for maneuverability, due to the fact that roll moments of inertia differ between the body and wings, and that both factors are difficult to calculate

without precise shape and weight data (measures not easily obtained and infrequently reported).

In a general sense, however, we may expect that airfoils having low wing loading (greater wing area) and low aspect ratio (less inertia) will favor agility at low speeds (Norberg and Rayner, 1987). Birds having such wings can initiate fast turns (agility) over short turn radii (maneuverability). Birds with exceptionally narrow, high aspect ratio wings also favor good rolling acceleration, especially when combined with low wing loading. Among avians, such a configuration is idealized in the man-o'-war birds (frigatebirds), five species that notoriously steal fish from other birds in flight. The huge wings of these birds are so highly adapted for flying that they cannot effectively swim or locomote on the ground, and can only take off from a height.

Of the two turning variables, maneuverability is inherently easier to work with, being inexorably linked to wing loading. As a characterization of overall turning ability, wing loading is likely to be more informative about the overall turning performance of a given flier. At the initiation of a turn, the input rotation will be determined by a flier's agility (the initial banking force asymmetry must cause a transient pulse in angular momentum), but throughout the turn differential downstroke velocities will produce a sequence of (often violent) angular accelerations, peaking with the sharpest point of the turn.

For a more thorough treatment on the subjects of aerial maneuverability and agility, the interested reader is referred to Norberg and Rayner (1987). Although this paper focuses on bat wing morphology, principles outlined therein apply well to vertebrate fliers in general.

2.2.4. Stability and head control during flight

Flying vertebrates locomote using an uneven and unpredictable substrate. Moving in such a low-viscosity and -density environment requires considerable control of movements. Turbulence-induced perturbations need to be countered effectively to maintain flight control. This source of rotational stimuli is of particular importance to canal function because voluntary movements are generated by central neural processes that may not produce significant perturbations on the time scale that stimulates the semicircular canals (sensu Muller, 1990). In the case of aerial locomotion, high frequency head perturbations associated with flapping flight and turning performance almost certainly produce canal-sensitive rotations, movements that must actively be countered by neck-stabilizing mechanisms to assure smooth vision. Canal-mitigated reflexes, by and large, must compensate for unpredictable environmental factors, as well as locomotor-induced perturbations, that might disrupt intentionally smooth execution of body movements.

As an external environmental source of perturbations, turbulence presents a greater challenge to gliders because such animals are dependent on prevailing wind conditions to generate lift. Altering the presentation of the wing to air flow by pronation and supination, or flexion and extension, enables a glider to actively counteract such perturbations. Deployment of tail feathers might provide a useful control surface in less perturbed flow fields (Thomas, 1993). Theoretically, neurotendinous organs in the wings (muscle spindles and Golgi tendon organs) could respond to turbulent air by activating spinal reflexes (Maier and Eldred, 1971; Haiden and Awad, 1981), though this has not

been demonstrated. Such an explanation was offered to explain floccular adaptations in gliding pterosaurs (Witmer et al., 2003), but the idea remains wholly speculative.

Despite the saltatory nature of force production in flapping flight, active flapping is thought to be inherently more stable than gliding (Warrick et al., 2002). Because the wings are at least partially folded during upstroke, according to gait parameters, the amount of surface area exposed to turbulence is overall reduced (Tobalske and Dial, 1994, 1996). Furthermore, as Warrick and colleagues (2002) point out, rapid wing beating creates a laterally projected centrifugal force that stabilizes the bird in yaw and roll axes, in the manner of a gyroscope. Importantly, however, the pitch axis remains unstable in this configuration. Maintaining pitch control under the rapidly oscillating conditions of low speed flapping flight might theoretically depend on activation of extensor muscles of the axial skeleton, muscles under direct reflexive control by excitation of anterior and lateral semicircular canals (Wilson and Maeda, 1974; Shinoda et al., 1996).

Additionally, the neck must act to reduce excessive perturbation of the head due to body oscillations and aspect changes, to effectively stabilize gaze on targets of interest (Wallman and Letelier, 1993; Wilson et al., 1995). Birds are remarkable in their ability to seemingly decouple the head from disturbances of extreme body rotations (Gioanni, 1988b; Erichsen et al., 1989; Wohlschlager et al., 1993; Wallman and Letelier, 1993; Haque and Dickman, 2005). X-ray cinematography of a black-billed magpie (*Pica pica*) flying in a wind tunnel showed that it was effective at isolating the head from vertical displacements when flying at a speed of 8 m sec^{-1} (Warrick et al., 2002), a typical velocity for the species. Under these conditions, vertical movement of the magpie's body

was measured at 1.44 ± 0.30 cm per upstroke, compared to 0.43 ± 0.21 cm for the head. The ability of maneuvering birds to stabilize their head in space during turns has long been appreciated (e.g., Money and Correia, 1972; Bilo and Bilo, 1983). In foraging swallows, body rolls during banking turns are completely counteracted by head rotation in the opposite direction, up to and exceeding 270º of body roll (Warrick et al., 2002). Such high degrees of cervical counter-rotation undoubtedly stem from neural control of neck muscles, though the inputs could come from many cues (vestibular, visual, proprioceptive).

Gioanni (1988a) demonstrated that eye movements in birds are more strongly coupled to head movements than in other tetrapods, indicating that effective gaze control strongly depends on head responses. Mechanically, gaze is affected by head inertial movements and contributions from the vestibuloocular (Gioanni, 1988b), vestibulocollic (Gioanni, 1988b; Gioanni and Sansonetti, 1999), and cervicocollic (Peterson et al., 1985) reflexes that work to balance these movements (see Chapter 1.5). In pigeons, it was experimentally shown that head movements were the major component of gaze during head-free rotations, and that such movements were in phase with sinusoidal body rotations (Haque and Dickman, 2005). In that same study, the more terrestrial Japanese quail was found to rely on both head and eye movements for gaze, suggesting that behaviors for gaze stabilization differ between terrestrial birds and active fliers (ibid.). This makes intuitive sense, in that flying birds typically operate in a more highly perturbed visual theater, one that must be compensated for by head movements to maintain gaze. Here, vestibular inputs are at a premium. The anterior and lateral semicircular canals are preferentially excited by pitching and rolling moments of the skull

and their activation may be used to directly offset head excursions induced by body rolls in aerial maneuvering.

Warrick and colleagues (2002) regard the head as residing in sensory isolation from body oscillations and rolling moments, but offer no mechanism to explain how this might be achieved if not by vestibular cues. Head stabilization is achieved explicitly by the vestibulocollic reflex (VCR), which operates in a feedback loop with canal input. Head rotations sensed by the canals trigger the VCR, which stabilizes the head and reduces input to the canals. Head perturbations and the sensory displacements are kept within operational limits by this feedback relationship (this process is reviewed in Spoor, 2003).

Vestibular signals are known to reflexively control muscles acting on the wing skeleton of restrained pigeons (Bilo and Bilo, 1978, 1983), so it reasonable to assume that vestibular cues are also used to adjust flight attitude, but this has not been determined in flying subjects.

2.2.5. How well could *Archaeopteryx* fly?

Although the wingbeat kinematics or the vortex wake shed by *Archaeopteryx* in flight cannot be known, key characteristics of its anatomy have been used to reconstruct its flying proficiency. Feather structure and wing plumage are very similar to modern birds and indicate aerodynamic function (Feduccia and Tordoff, 1979; Rietschel, 1985; Elzanowski, 2001). On the basis of wing shape, wing loading (39.27) and aspect ratio (6.73) are both low (computed from Burgers and Chiappe, 1999), suggesting a high

degree of maneuverability and aerial agility. However, *Archaeopteryx* is primitive in having a simple pectoral girdle, reminiscent of terrestrial theropods in lacking a triosseal canal (for passage of the supracoracoideus tendon, the main wing elevator), a strutlike coracoid, and a large, keeled sternum (for attachment of the pars thoracis portion of the pectoralis muscle, responsible for pronation of the humerus during downstroke and contributing to wing depression) (Elzanowski, 2002). These pectoral features suggest to some (e.g., Rayner, 1988a, b, 2001) that *Archaeopteryx* was weakly specialized for slow flapping flight. Further evidence comes from the bony, frond-like tail, useful for static stability in flight (Gatesy and Dial, 1996b; Norberg, 1990) while limiting control movements due to high inertial resistance to turning. The orientation of the semilunate carpal permitted fore-aft sweeping of the wing tip in the plane of the wing but limited rotation of the hand wing out of plane. These movements are identical to the asymmetrical repositioning of the wing during upstroke with a continuous vortex gait (Rayner, 2001). Arguing from this, Rayner suggests that the wing was likely incapable of the "complex twisting, folding, and flexing that must be used in slow flight" (p. 370, ibid.), as during vortex-ring gait. Rather, *Archaeopteryx* hypothetically favored a cruising, high-speed flight with poor maneuverability and agility, despite having a low aspect ratio wing with low wing loading, indicative of a continuous vortex gait (ibid.).

Chapter 3:
Research Design

3.1. Goals and predictions

The comparative anatomy of the bony labyrinth was first described by Retzius (1881, 1884) and later by Gray (1907, 1908) for diverse, but relatively small sets of vertebrates. More recent studies have looked at the labyrinth of humans (Spoor, 1993) and primitive hominids (Spoor et al., 1996), various nonhuman primates (Spoor and Zonneveld, 1998; Walker et al., 2003, 2004; Spoor et al., 2007), and cetaceans in reference to other mammals (Spoor et al., 2002). Gray's (1908) sample included 18 species of birds, and this remains the largest published data set of comparative bird semicircular canal morphology.

Functionally, the semicircular canal system senses angular accelerations experienced by the head and responds to motion by generating compensatory movements of the head, body, and eyes via nonconscious motor reflexes (Chapter 1). Increase in the length of the canal tubes is associated with greater sensitivity to rotational stimuli (Rabbitt et al., 2004). Previous comparative studies have demonstrated an association between canal size and locomotor behavior, with the common observation that, for any given body size, qualitatively more "agile" species have quantitatively larger-arced semicircular canals (Spoor, 1993; Spoor et al., 1996, 2007; Spoor and Zonneveld, 1998; Sipla et al., 2003; Walker et al., 2003, 2004; cf. Spoor et al., 2002). While these studies have established an empirical association between canal size (sensitivity) and locomotor preference, actual degree of maneuverability has not been quantitatively established for

the subjects examined. Instead, maneuverability has, by necessity, been framed in strongly simplified terms such as “acrobatic versus ponderous,” “fast versus slow,” “maneuverable verses cautious” (sensu Spoor, 2003), “terrestrial versus aquatic” (Georgi and Sipla, in press), “bipedal versus quadrupedal” (Sipla et al., 2004). Recently, Spoor et al. (2007) conducted a phylogenetically informed analysis of canal size in 91 primate species and assigned each taxon to one of six agility categories, from “extra slow” to “fast.” These agility scores were based on the qualitative observations of three field workers and were successfully used to demonstrate significant positive effects of body mass and locomotor agility on canal size, using conventional multiple regressions (ibid.).

Spoor and Zonneveld (1998) and Spoor and colleagues (2002) developed the technique of imaging the otic capsule of dry skull specimens using computed tomography (CT), and found consistent associations between canal size and inferred locomotor agility in both primate and cetacean groups, respectively. In the former study, a link between relatively large canal size and inferred active head movements was substantiated for a sample of 42 primate species. In the latter study, extant cetaceans were found to possess canal arc sizes three times smaller than other mammals (taking body mass into account), consistent with adaptations for dedicated agile swimming in a lineage with marked fusion of neck vertebrae and reduced neck motility. Analysis of fossil whales demonstrated that the acquisition of small semicircular canals and full independence from life on land was achieved early in cetacean evolution.

Among bird taxa, there are few comparative studies linking semicircular canal morphology and behavior. Using a sample of 17 birds taken from stereoscopic photographs in Gray (1908), Jones and Spells (1963) noted that bird canal dimensions

were, as a group, larger than other tetrapods relative to body size. Other studies have pointed out that species considered highly maneuverable, such as raptors, have larger semicircular canals relative to body size, whereas less maneuverable fliers, such as ducks and geese, have smaller canal dimensions (Tanturri, 1933; Hadziselimovic and Savkovic, 1964). Owls are known to possess large semicircular canals relative to body size, possibly due to the nature of their restricted eye movements (Money and Correia, 1972). But as yet, no comprehensive analysis of bird vestibular morphometrics and locomotion has been conducted.

Descriptions of semicircular canal morphology among theropod dinosaurs are rare. Typically, such descriptions are obtained from traditional endocasts or "digital endocasts" prepared from computed tomography (CT) scans. To date, digital endocasts have been published for the theropods *Tyrannosaurus* (Brochu, 2000), *Carcharodontosaurus* (Larsson et al., 2000; Larsson, 2001), and *Acrocanthosaurus* (Franzosa and Rowe, 2005). The doctoral dissertation of Jonathan Franzosa (2004) presents digitally prepared endocasts for a range of theropod dinosaurs, many of which preserve aspects of semicircular canal morphology. Digital treatment of the abelisaurid theropod *Majungasaurus* was recently published (Sampson and Witmer, 2007), and work on the Cleveland tyrannosaur skull is forthcoming (Witmer and Ridgely, in press). A digital reconstruction of the braincase of the London specimen of *Archaeopteryx* has also been published (Dominguez et al., 2004).

The major goal of this dissertation is to describe semicircular canal size variation in a large comparative sample of extant birds and extinct theropod dinosaurs, for the purpose of assessing vestibular evolution in these groups. A further objective is to

address the question, how are canal size and degree of locomotor agility related? Evidence that volant birds possess more sensitive canals than landbound birds and non-avian theropod dinosaurs would be a powerful test of the hypothesis that aerial maneuvering places higher demands on vestibular function than cursorial bipedalism, necessitating the evolution of sensors with higher gain. Additionally, it is desirable to find correlations, where they exist, between canal size and independent predictors of aerial maneuverability, namely wing-loading and aspect ratio. Covariance between these variables would quantitatively demonstrate whether a relationship between canal size and agility is a basic biological phenomenon of the vestibular system, as indicated by preliminary studies.

To explore these topics, the present study examined semicircular canal size in 178 species of extant birds, 10 species of non-avian theropod dinosaurs, 6 sauropod dinosaurs, and 10 ornithischian dinosaurs, using computed tomography. The canal morphology of the basal avialan *Archaeopteryx* was also assessed using data previously published in Dominguez et al. (2004). Results should provide evidence as to whether there is any relationship between canal size and volant behavior in modern birds. If changes in canal morphology are associated with evolution of the flight stroke and the transition of terrestrial theropod dinosaurs to volant birds, then the present study could be used to discriminate between diversely contrasted modes of flight in living birds, and inferentially to examine the evolution of flight capabilities—and associated neurosensory specializations—in basal birds and their ancestors. Furthermore, these data may indicate whether canal size and measures of aerial agility exhibit covariance, providing a means

Table 3–1: Definition of measurements

Measurement	Description
Canal measures	
ASCc	Anterior semicircular canal circumference (mm).*
PSCc	Posterior semicircular canal circumference (mm).*
LSCc	Lateral semicircular canal circumference (mm).*
ASCrel	Relative ASC = ASCc divided by cubed root of body mass.
PSCrel	Relative PSC = PSCc divided by cubed root of body mass.
LSCrel	Relative LSC = LSCc divided by cubed root of body mass.
SCc	Average circumference of ASCc + PSCc + LSCc (mm).
SCr	Average canal radius of ASCr + PSCr + LSCr (mm) (see text).
Other measures	
BM	Body mass (g). **
Velocity	Cruising airspeed velocity (m/sec). **
Wing loading	Wing loading (N m^{-2}), measured as the weight (mass times gravitational acceleration *g*) divided by the wing area. **
Aspect ratio	Aspect ratio, measured as the square of wingspan divided by wing area. **
BI	Brachial index, measured as the humerus length divided by ulna length. **

*See text for description of measurement.

**These data obtained from the literature or from museum records. Refer to Appendix 1 for references.

for future development of analytical tools to assess the locomotor behavior of extinct dinosaurian and avialan species, independent of postcranial evidence.

3.1.1. Hypotheses

This research allows the delineation of 6 broad hypotheses and their respective predictions, regarding semicircular canal size in theropods and birds:

Hypothesis 1 – Volant birds as a group have larger canals relative to body mass than bipedal dinosaurs.

> $H1_O$: There is no difference in relative size between the semicircular canals of volant birds and bipedal non-avian dinosaurs.
>
> $H1_1$: Overall, the semicircular canals of volant birds are larger (more sensitive) than similarly sized bipedal dinosaurs, to enable more precise vestibular control of head and body movements, and of vision, in a complex three-dimensional aerial environment.

Hypothesis 2 – Volant birds have larger canals relative to body mass than flightless birds.

$H2_O$: There is no difference in relative size between the semicircular canals of volant birds and secondarily flightless birds.

$H2_1$: The semicircular canals of volant birds are larger (more sensitive) than similarly sized flightless birds. It is hypothesized that full adaptation to aerial locomotion requires more effective balance sensors.

Hypothesis 3 – Semicircular canals expand differentially in relation to body size.

$H3_O$: There is no difference in the rate of expansion of the semicircular canals with increased body size, therefore use of the SCc metric or any single canal metric (ASCc, PSCc, LSCc) is reliable as a proxy for overall sensitivity. (Refer to Table 3–1: Measurements for definitions.)

$H3_1$: The anterior, posterior, and lateral semicircular canals expand differentially with increasing body size (i.e., their slopes are different), therefore use of the SCc metric is unreliable as a proxy for overall sensitivity.

$H3_2$: Compared to non-avian bipedal dinosaurs, volant birds have differentially larger anterior and lateral semicircular canals, due to the higher frequency of

uncompensated angular head rotations in the pitch plane associated with flapping flight.

Hypothesis 4 – Among volant birds, highly maneuverable species have larger (more sensitive) canals than less maneuverable species.

$H4_O$*:* There is no relationship between degree of aerial maneuverability and canal sensitivity.

$H4_1$*:* Taking body mass into account, relative canal size scales inversely with wing loading; i.e., as wing load increases, relative sensitivity decreases. The most maneuverable birds (low wing loading) are hypothesized to have larger canals to enable precise locomotor control and visual stability during banking.

$H4_2$*:* Taking body mass into account, birds that habitually fly at slower speeds have larger (more sensitive) canals. This is related to prediction $H4_1$, in that birds with low wing loading can maneuver at lower speeds.

$H4_3$*:* Taking body mass into account, birds that are both maneuverable (low wing loading) and agile (i.e., low aspect ratio + low wing loading) will have the largest relative canal sizes (all three canals). These species can *initiate* the fastest turns over the *smallest* minimum turn radii, and consequently these birds should have more effective sensors in roll, a movement which excites all three canals.

Hypothesis 5 – Archaeopteryx has canals that plot with low maneuverability flapping fliers, indicative of a bird restricted to steady forward flight using a continuous vortex gait (sensu Rayner, 2001).

$H5_O$: Archaeopteryx cannot be demonstrated to have canal measures similar to poorly maneuverable fliers.

$H5_1$: Archaeopteryx possesses canal dimensions that plot with poorly maneuverable fliers.

Hypothesis 6 – Canal size correlates with brachial index, a predictor of wing loading.

$H6_O$: There is no relationship between canal size and brachial index (BI).

$H6_1$: Taking body mass into account, relative canal size scales inversely with BI; i.e., as BI increases, relative sensitivity decreases.

Nudds and colleagues (2007) found a moderate but significant relationship between BI and wing loading for a large sample of extant birds (n=542) (r^2=0.49). If a relationship is substantiated between canal size and wing loading, then a similar relationship should hold independently true for BI.

3.2. Materials and Methods

3.2.1. Specimens

Dry skulls of adult, extant avians, representing 28 orders, 52 families, 131 genera, and 178 species obtained from several sources, were examined (see Appendix 1). 28 of 33 neornithine orders defined in the taxonomy of Livesy and Zusi (2007) were included, excluding only Aepyornithiformes (extinct elephant birds of Madagascar), Balaenicipitiformes (containing one species, *Balaeniceps rex*, the shoebill), Turniciformes (containing one family, the Turnicidae, with two genera of buttonquails), Coliiformes (a small group of near passerine birds, the mousebirds), and Sphenisciformes (penguins). The semicircular canal adaptations of penguins are being considered separately as part of an ongoing analysis of vestibular adaptations in secondarily aquatic taxa (e.g., Georgi and Sipla, in press). In addition to the high phylogenetic diversity of the sample, an effort was made to sample a broad range of body sizes, ranging from the 3 gram hummingbird *Metallura tyrianthina* to the 120 kilogram ostrich *Struthio camelus*. Due to the resolution limits of the primary medical CT scanner used in this analysis, lower body sizes (<125 grams) are underrepresented, and those few specimens included below this size limit were mostly scanned using a higher resolution micro-CT scanner. Consequently, the vast majority of small passeriforms (perching birds) and apodiforms (swifts and hummingbirds) are poorly sampled.

Wild-shot specimens were obtained whenever possible, and only those with intact otic capsules were selected for CT scanning. Each was inspected for the presence of

buckshot, signs of disease, necropsy, unusual preservational deformation, or postmortem damage that might interfere with scanning results (as by the intrusion of metallic buckshot) or the biological integrity of the canal system. Sample details are given in Appendix 1, including sample history, phylogenetic rank, and collection details.

Nonavian theropod specimens were obtained from several institutions. Comparative data on mammalian semicircular measurements were taken from Spoor et al. (2002). Cetaceans were excluded from this data set because of the highly derived nature of the vestibular system in these mammals, compared to non-cetacean mammals (ibid.). Data on the semicircular canals of *Archaeopteryx* were extrapolated from measures reported in Dominguez et al. (2004).

All species in the present analysis are represented by n=1 specimen. While it would certainly be more advantageous to use species means in statistical analyses to offset the effects of individuals, a decision was made to maximize interspecific diversity at the expense of high species sample sizes. The author recognizes that higher intraspecific sampling may yield more stable results.

3.2.2. CT scanning and image processing

Computed tomography (CT) has been used successfully to investigate a variety of complex skeletal morphologies in both fossil and living animals (Spoor et al., 2000). The technique employs an X-ray source and array of detectors that rotate about a specimen, generating a slice-shaped volume of cross-sectional scans. These images depict regions of low (black) to high (white) density and can be reoriented digitally, permitting the

visualization and measurement of structures in any desired slice plane. Given its non-invasive properties, CT is an ideal technique for the investigation of dry skull and fossil material. Micro-CT scanners produce images with significantly higher spatial resolution and smaller slice thickness than conventional medical CT scanners, but the cost to operate these scanners is prohibitively higher.

Most of the specimens used in this study were scanned using a conventional GE Medical Systems Lightspeed[16] computed tomography scanner located at Stony Brook University Hospital (Stony Brook, NY). A few smaller specimens were scanned using a high resolution Scanco Medical μCT 40 Desktop Cone-Beam MicroCT Scanner at Stony Brook University (Department of Biomedical Engineering). Additional scans of dinosaurian basicrania were obtained from scans conducted at UTCT high resolution x-ray CT facility (University of Texas at Austin) and Center for Quantitative Imaging at Penn State University (Penn State University).

Specimens were scanned individually. Crania were positioned on the surface of a foamed polystyrene board and each specimen was scanned in the best approximation of the coronal plane, except in a few instances when peculiar bill shapes or incompleteness of fossil material necessitated scanning in an alternate plane. A few heavier specimens (e.g., *Tyrannosaurus* AMNH 5029 braincase) were placed directly on the scanning bed and scanned without removing the specimen from its protective jacket.

Imaging parameters were optimized to yield the maximum possible resolution, given the size of each specimen relative to the image matrix, with voxel dimensions ranging from approximately 0.03 mm (Scanco) to 0.61 mm (Lightspeed). Data acquired from the scanners were saved as standardized DICOM files and imported to the Java-

based image processing and analysis software package ImageJ, available in the public domain (http://rsb.info.nih.gov/ij). CT volumes were edited in ImageJ to improve grayscale contrast and crop image size. The latter was done to isolate the otic capsule for measurement, remove extraneous image area, and increase image size, permitting a larger overall viewing area for taking measurements. Volumes were planar reformatted to demonstrate the full extent of each semicircular canal, using VoxBlast Measurement and Visualization Software 3.1.3 (VayTek). 3D reconstructions of the cranium and inner ear were rendered using 3D Slicer v.2.5 (http://www.slicer.org).

3.2.3. Measurements

All avian and non-avian dinosaur data of semicircular size were measured by the author, except *Archaeopteryx*. Additional measurements of body mass and all aspects of wing morphology were obtained from literary sources or museum records, as detailed below. Specific sources of all data are given in Appendix 1.

Although the dimensions of the membranous semicircular duct organ cannot be resolved using CT technology, the arc length of the bony semicircular canals (which contain the relevant duct organs) can be measured and compared to other scaling factors such as body mass.

Circumferential arc length of anterior, posterior, and lateral semicircular canal, *ASCc*, *PSCc*, *LSCc* (mm). Given that circumferential arc length of the canals (streamline length) is the most important measure of canal performance easily obtainable from CT

scans (after Spoor and Zonneveld, 1998), the following measures were taken to quantify this feature in a manner suitable for bivariate regression and discriminant function analyses. Linear raw measurements of canal length were obtained in the following manner. A minimum number of points were identified along the internal circumference of each canal necessary to adequately describe its shape, and the total distance connecting these points was measured. Points were targeted to the center of the canal lumen and to the border of the vestibule (Figure 3–1). The more a canal shape departed from true circularity and planarity, the more points were necessary to adequately describe its total streamline length (typically 7-20), depending on the shape of the canal in question. VoxBlast enables the user to take linear measurements in 3D space, allowing for proper measurement of bird canals that bend in and out of 2D planes. No measurements were taken of the cross-sectional area of the lumen as such dimensions do not adequately reflect the size of the enclosed membranous duct.

For comparisons with mammalian data (Spoor et al., 2002), circumferential arc lengths were transformed into radius of curvature values by computing the radius of a circle with given circumference (using the formula, e.g., [ASCc / π] /2). While this does not permit exact similarity between my measurements and those of the other authors, especially given that bird canals are not semicircular in shape like most mammals, this method does permit crude comparisons between both groups. For the mammalian data, Spoor and colleagues (2002) compute radius of curvature by the equation R = 0.5 x (height + width) / 2. While this estimates the radius of a circular object well, it is poorly suited to estimating the "radius" of noncircular shapes.

Raw linear measurements of the London *Archaeopteryx* specimen were not obtained directly, but were extrapolated from data published in Dominguez et al. (2004). Requests to obtain copies of the original CT scans were denied. As a substitute, and with the caveat that the crudeness of this approach undoubtedly suffers from measurement noise, the following method was used. Anterior canal diameter was reported in the original study (4.54mm) and was converted to ASCc by computing the circumference of a circle with diameter 4.54mm (=14.26mm). The anterior canal is the only complete canal preserved in the *Archaeopteryx* endocast, and the conversion done here is the only reliable measurement. The width of the PSC is given as 3.29mm. I estimated the height using the height/width ratio of the PSC in the closely related *Velociraptor* specimen (IGM 100/976); from the computed radius of curvature a circumference was obtained as described above. This is only an approximate measurement based on negative evidence and evidence from a different species. Finally, the LSC diameter is given as >3.75. I computed a circumference based on the lowest value of 3.75, so LSCc in my analysis must be regarded as a minimum measurement.

Body mass (g). For individual specimens, body masses were obtained from field measurements taken at time of death, whenever possible, for individual skulls, or taken from published estimates of species means. It should be noted that the body weight of birds generally varies seasonally, with the most dramatic changes occurring in long-distance migratory species (Clark, 1979). Many resident species increase in body mass during autumn months to store additional fat for winter (Haftorn, 1989). Other species vary little in body weight annually (e.g., Koenig et al., 2005). Given this variation, body mass estimates must be regarded as just that, *estimates*. Body masses reported in the

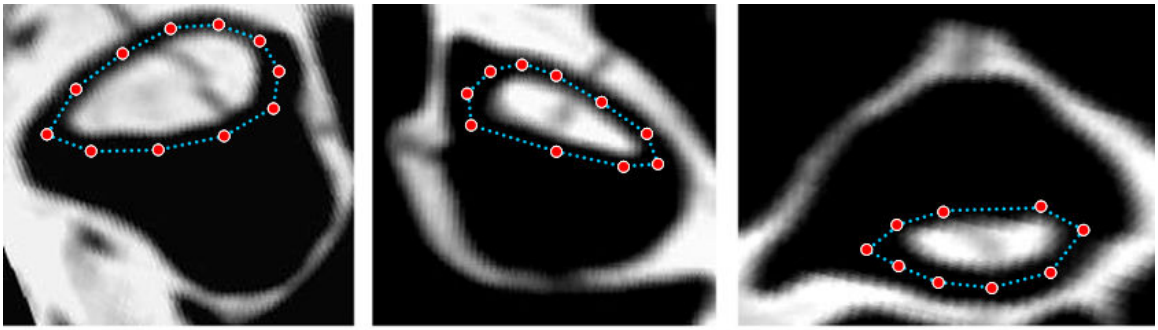

Figure 3–1. Definition of measurements. Planar reformatted images of the three semicircular canals for a specimen of Cuvier's dwarf caiman (*Paleosuchus palpebrosus*), demonstrating the full extent of each semicircular canal: a (ASC), b (PSC), c (LSC). Circumferential arc length of each canal (dotted lines) was quantified by measuring the total distance connecting a minimum number of points (in red) necessary to adequately describe the shape of each canal using VoxBlast v.3.1.3 software (VayTek).

literature rarely specify the time of the year or age of a weighed animal, and as such variation in body mass is an uncontrollable source of error in comparative studies.

Methods for calculating body mass in extinct dinosaurs are widely inconsistent (Peczkis, 1994) and can differ significantly when different methods are applied to the same specimen (Anderson et al., 1985). To minimize this variation in method error, I have chosen to rely on dinosaur measurements from a single source whenever possible, obtained using the 'polynomial method' described in Seebacher (2001). This technique was developed as an extension of methods used to calculate the body mass of extant crocodilians, where it was proven effective when validated against empirical data (Seebacher et al., 1999). Briefly, this method uses polynomial equations to describe body shape mathematically (shapes were obtained from published reconstructions and museum mounts), and then integrates to estimate the volume after correcting for body width (Seebacher, 2001). The validity of the technique has been tested using extant animals of diverse body shapes and known masses, and overall the mass estimates for dinosaurs produced by Seebacher's method agreed well with estimates from other sources, where available. For dinosaur masses not calculated by Seebacher, I used the technique of estimating weight from long-bone circumference described in Anderson et al. (1985).

All measurements are described on Table 3–1. All linear measurements were taken to the nearest hundredth of a millimeter.

3.2.4. Statistical analyses

Following transformation of raw data into $\log_{10}$ algorithms, bivariate associations were evaluated with Pearson's correlation coefficients (r) and trends were modeled with reduced major axis (RMA) regression of raw values using the freeware program SMATR (Warton et al., 2006). This was done to estimate the line best describing the bivariate scatter of Y and X points for any given comparison. RMA was the Model II line-fitting technique chosen for this study because measurement error and natural variation both affect dependent and independent variables in regression analyses, and the procedure to fit RMA lines does not assume that variance in either variable is more significant or influential (Sokal and Rohlf, 1995; Warton et al., 2006). Using SMATR, post-hoc multiple slope comparisons among groups were run if slopes were found to be significantly heterogeneous. Similarly, comparisons of lines with common slopes were run if slopes were not significantly heterogeneous, using a Wald statistic in SMATR (Warton et al., 2006). This last procedure measures the spread of data away from the fitted regression line and is analogous to the tests made in ANCOVA. Geometrically, ANCOVA asks whether a difference exists between the intercepts of two lines with common slope (Dawson and Trapp, 2004). Significance in the test for elevational differences indicates that the adjusted *Y mean* of each group is significantly different; i.e., at any given X value, Y is predictably larger or smaller in group A compared to group B.

Scatter plots were generated using SPSS 15.0 to allow for visual inspection of data distribution.

Previous studies have investigated the correlation between semicircular canal size and body mass (e.g., Spoor, 2003), noting that the physical dimensions of the canals increase with mass with strong negative allometry. Theoretical models of the canal system predict that the scaling exponent for this comparison should be between 0.08 and 0.33 (Jones and Spell, 1963), and previous studies have indeed shown that vertebrate canals scale to body mass with slopes falling in this range (Wilson and Melvill-Jones, 1979; Spoor and Zonneveld, 1998). A typical value of 0.14 was obtained for a recent analysis of 174 non-cetacean mammalian species (Spoor and Thewissen, in press). Regression slopes were compared to the theoretical range of 0.08–0.33 to determine if bird and dinosaur canal sizes scale similarly with mammals.

Testing hypotheses 1 – Volant birds as a group have larger canals relative to body mass than bipedal dinosaurs.

To test hypotheses 1 (section 3.1.1), the following bivariate regression was made and elevational differences calculated between paired slopes:

Log SCc vs. Log BM (volant bird line vs. dinosaur line)

Testing hypotheses 2 – Volant birds as a group have larger canals relative to body mass than flightless birds.

To test hypothesis 2, the following bivariate regression was made and elevational differences calculated between paired slopes:

Log SCc vs. Log BM (volant bird line vs. flightless bird line)

Testing hypothesis 3 – Semicircular canals expand differentially in relation to body size.

To test hypothesis 3, the following three comparisons were made and tested for common slope. Elevational differences were also examined to test whether ASCc, PSCc, and LSCc varied between birds and bipedal dinosaurs for each biplot:

Log ASCc vs. Log BM (bird line vs. dinosaur line)

Log PSCc vs. Log BM (bird line vs. dinosaur line)

Log LSCc vs. Log BM (bird line vs. dinosaur line)

Testing hypothesis 4 – Among volant birds, highly maneuverable species have larger (more sensitive) canals than less maneuverable species.

To test for covariance between canal size and wing parameters, a conventional least-squares multiple regression analysis was run for $\log_{10}$ average canal circumference (SCc) against $\log_{10}$ Body Mass, $\log_{10}$ Wing loading and $\log_{10}$ Aspect Ratio.

To further test hypotheses 4_1–4_2, the following bivariate regressions were made and evaluated for significance and correlation.

Hypothesis 4_1 – Relative canal size scales inversely with wing loading.

Log ASCrel vs. Log Wing Loading (volant birds)

Relative anterior canal size was chosen because this measure incorporates data from all specimens analyzed for which wing loading data is also available, including *Archaeopteryx* (for which the anterior canal is the only preserved canal circuit).

Hypothesis 4_2 – Relative canal size scales inversely with velocity.

Log ASCrel vs. Log Velocity (volant birds)

Testing hypothesis 4_3 – Taking body mass into account, birds that are both maneuverable (low wing loading) and agile (i.e., low aspect ratio + low wing loading) will have the largest relative canal sizes (all three canals).

To test hypothesis 4_3, birds were assigned to groups on the basis of wing loading and aspect ratio. First, mean wing loading (76.77) and aspect ratio (9.46) were determined for the total bird sample and specimens sorted according to their distribution above or below the mean for each variable. Specimens identified as having low wing loading (<76.77) were chosen for analysis. This subgroup was then further divided into low aspect ratio (<9.46) and high aspect ratio (>9.46) groups, and the following bivariate regressions were made and elevational differences calculated between paired slopes:

Log ASCc vs. Log BM (low aspect line vs. high aspect line)

Log PSCc vs. Log BM (low aspect line vs. high aspect line)

Log LSCc vs. Log BM (low aspect line vs. high aspect line)

Testing hypothesis 5 – Archaeopteryx has canals that plot with low maneuverability flapping fliers, indicative of a bird restricted to steady forward flight using a continuous vortex gait.

To test hypothesis 5, a discriminant function analysis (DFA) was performed on the logged relative circumference measurements of the three canals for all birds for which

wing loading and aspect ratio values could be obtained, including *Archaeopteryx* (n=110), plus all flightless birds and theropod dinosaurs.

Six groups were used, with *Archaeopteryx* unassigned to a group:

(1) Low wing loading, low aspect ratio

(2) Low wing loading, high aspect ratio

(3) High wing loading, high aspect ratio

(4) High wing loading, low aspect ratio

(5) Flightless bird

(6) Flightless non-avian theropod

Volant birds were assigned to groups on the basis of wing loading and aspect ratio. In both cases, mean wing loading (76.77) and aspect ratio (9.46) were determined for the total sample and specimens sorted according to their distribution above or below the mean for each variable. The group membership of *Archaeopteryx* as predicted by wing morphology is group 1 (*Archaeopteryx* has low wing loading and low aspect ratio wings). The group membership as predicted by skeletal morphology (Poore et al., 1997; Rayner, 2001) is group 3 or 4; that is, under highest discriminant classification, *Archaeopteryx* is expected to sort with birds having high wing loads, indicating poor aerial maneuverability despite wing morphology.

Testing hypothesis 6 – Canal size correlates with brachial index, a predictor of wing loading.

To test hypothesis 6, the following bivariate regression was made and evaluated for significance and correlation.

Hypothesis 6 – *Canal size correlates with brachial index.*

Log ASCrel vs. Log BI (all birds)

3.2.5. Bonferonni correction

Due to the high number of comparisons being made to analyze this data set, α was adjusted conservatively with a Bonferonni correction. This yielded an adjusted α of 0.05/22 comparisons=0.002. Null hypotheses were therefore rejected at p-values less than or equal to 0.002.

3.2.6. Phylogenetic constraints and "adjusted-N"

The goal of this study was to determine how semicircular canal size varied among birds, irrespective of phylogenetic relationships. Nevertheless, consideration of phylogenetic relationships has become an integral part of comparative analyses of the avian brain and sense organs (e.g., Nealen and Ricklefs, 2001; Iwaniuk and Hurd, 2005;

Hall and Ross, 2007). Failure to account for the influence of shared phylogenetic history increases the probability of committing type I error in comparative analyses, since species are not truly independent points (Felsenstein, 1985, Harvey and Pagel, 1991). The method of independent contrasts (Felsenstein, 1985; Harvey and Pagel, 1991) is a commonly used technique to adjust for phylogenetic effects, but this method requires *a priori* well-resolved phylogenetic relationships with reliable branch lengths. The current state of avian systematics is highly controversial and there is no commonly accepted phylogeny incorporating taxa from all (or indeed most) major clades. Multiple unresolvable polytomies are commonplace in avian systematics, especially when 'total evidence' procedures are used (e.g., Cracraft et al., 2004). Furthermore, the biogeographic, fossil, and molecular evidence for avian branch lengths is highly contradictory (Cracraft, 2001; Graur and Martin, 2004). Recent placement of the fossil taxon *Vegavis* as a basal anseriform confirms the origin of Neornithes by the latest Cretaceous and indicates that basal neornithine lineages were coexistent with non-avian dinosaurs (Clarke et al., 2005), but higher-order divergence dates remain controversial. Rather than setting branch lengths as arbitrarily "equal" throughout a composite of disparate phylogenies, I have chosen instead to account for phylogenetic effects and to ensure the statistical independence of data points by computing "effective" sample sizes (N_{eff}) using the method described in Smith (1994).

N_{eff} values were used to calculate new significance levels (P_{eff}) for all bivariate regression equations obtained using avian data points (for which adequate sample sizes and taxonomic diversity existed to permit such analysis). This was done to evaluate whether phylogenetic constraints on canal size or other variables had a significant effect

on independence of these points. Smith (1994) advocates using a phylogenetically reduced sample size computed from the smaller of two choices, either (1) N_{eff} for the y axis trait, or (2) mean of the N_{eff} scores for both axes. Variance components were partitioned using the fully nested ANOVA procedure in Minitab v. 15.1, using the phylogenetic hypothesis of Livezey and Zusi (2006, 2007). Seven nested levels of classification were used: cohort, subcohort, superorder, order, family, genus, and species (refer to Appendix 2).

Chapter 4:
The semicircular canals of birds and relationship to flight

In this chapter, I report on the canal morphology of birds and non-avian theropod dinosaurs as inferred from CT scans. First, I review the basic morphology of the semicircular canals in these taxa. Following from descriptions of basic morphology, I consider how semicircular canal size relates to degree of aerial maneuverability as inferred from wing morphology, and the relationship of these variables to body size. Statistical comparisons reveal underlying correlations between measures that predict canal sensitivity on the one hand, and aerial prowess on the other. Anatomical features of the avian bauplan influence the frequency content of aerial maneuvers and thus have a strong effect on turning agility, with implications for semicircular canal function.

4.1. Morphology of the semicircular canals of birds and their ancestors

The term 'semicircular' is something of a misnomer when applied to bird canals. This confusion stems from a mammalian-centric view of canal morphology. For the most part, mammal canals are indeed 'semicircular' in shape (e.g., Gray, 1907, 1908) and the description is warranted. Avian and non-avian theropod canals rarely approach circularity in shape, however, and in the case of the bird labyrinth all three canals typically undergo torsional excursions out of their respective planes.

4.1.1. The canals of birds

Gross anatomy of the semicircular canal system in birds has been described by others, being exquisitely detailed, for instance, by Retzius (1884) and Gray (1908). The basic organization of the vestibular system was described in Chapter 1 (see Figure 1–1). The overall size of the vestibular cavity is small in birds, compared to the majority of other diapsids including crocodilians, where the vestibule is the largest part of the labyrinth (Gray, 1908). In birds, as in mammals, the canals are considerably elevated from the vestibule, whereas in lower diapsids the canals are elevated only a small distance above the wall of the vestibular cavity and often appear to merge with it (Georgi and Sipla, in press).

Of all the lineages of vertebrates, Neornithes departs the most from the generalized vestibular configuration (Figure 4–1), especially where this concerns the anterior canal. Relative to the closest living relatives of birds, the crocodilians, there is a dramatic increase in anterior canal circumference achieved primarily via a hyper-elongation in the superoposterior direction (Sipla et al., 2003). Rather than passing directly superiorly as in most vertebrates, including non-avian theropods, the common crus is deflected in a posterolateral direction. The anterior canal branches from the crus at a sharp posteromedial angle. Thus, a significant portion of the anterior canal circuit travels posterior to the common crus before it curves superiorly and anteriorly to join the ampulla via a sharp ventral turn at the end of the circuit.

The morphology described is typical for volant birds, but the overall shape of the system is approximated in secondarily flightless birds. Among terrestrial bird taxa such

as *Struthio*, the anterior canal remains highly elevated, but the degree of posterior expansion is reduced.

In many species, anterior canal shape is further convoluted along its anterior aspect resulting from encroachment of the optic lobe of the brain into the developmental pathway of the canal during morphogenesis (Bissonnette and Fekete, 1996) (Figure 4–2). In embryonic chickens (*Gallus gallus domesticus*), the enlarged nature of the anterior canal, and the general shape and configuration of adult canal shapes for all three canals, is developmentally apparent by embryonic day 7 (Bissonnette and Fekete, 1996). Encroachment of the optic lobe into the developmental path of the anterior canal does not occur until embryonic day 11 (ibid.), at which point the anterior margin of the canal is subtly deflected posteriorly to accommodate the growing brain tissue. The optic lobe (mesencephalic tectum) receives projections from approximately 90% of retinal ganglion cell axons in lateral-eyed birds (Shimizu and Karten, 1991) and is thought to be homologous to the mammalian superior colliculus, exhibiting important characteristics for motion processing. Of all vertebrate classes, birds are the most visually dependent (Hodos, 1993), and birds exhibit proportionately large, laterally displaced optic lobes relative to non-avian reptiles. However, growth of the lobe does not affect the basic configuration of the canals until they are already deployed developmentally; that is, anterior canal enlargement in birds does not appear to be a result of optic lobe enlargement, but rather is predetermined genetically by the developing otocyst. If anything, the optic lobe reduces the overall size of the anterior canal by encroaching on its path. Furthermore, the optic lobe does not impinge on ASC shape equally in all birds,

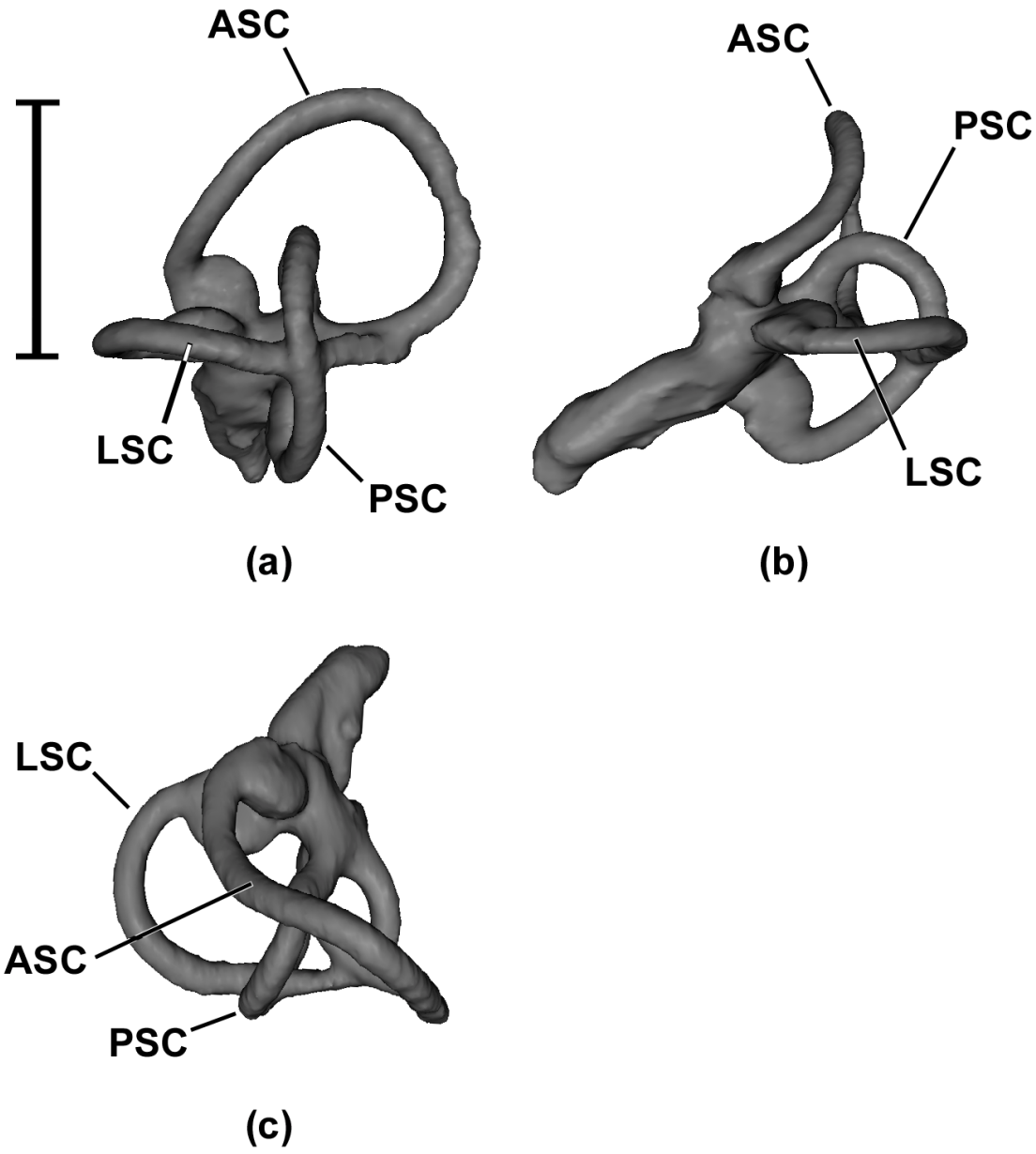

Figure 4–1. Morphology of bird semicircular canals. 3D digital endocasts of the left bony labyrinth in the Eurasian sparrowhawk (*Accipiter nisus*) reconstructed from μCT scans. Scale bar = 5 mm. Orientations as follows: (a) caudolateral view demonstrating extent of anterior semicircular canal (ASC); (b) rostrolateral view demonstrating extent of posterior semicircular canal (PSC); (c) dorsal view demonstrating extent of lateral semicircular canal (LSC). Note the extreme torsion and hyper-elongation of the ASC.

most notably passing over the ASC in owls without visibly distorting the canal arc (Figure 4–3).

Another feature of the brain that relates spatially to the anterior canal is the cerebellar flocculus (Figure 4–2). This small lobe projects from the caudolateral corner of the vestibulocerebellum, forming a recess into the bony space enclosed by the arc of the ASC (subarcuate fossa). The flocculus is qualitatively large in many bird taxa, especially among ducks and geese (Anseriformes), while smaller or not present in others (personal observation). In some taxa, the flocculus also invades the territory of the posterior and lateral canal arcs. Although flocculus size was not quantified for this study, it is important to note that protrusion of the floccular tissue into the anterior canal arc may have some relationship with ASC size. A study by Jeffery and Spoor (2006) found no such relationship between flocculus size and canal size in a sample of human and nonhuman primate fetuses, instead finding that ASC growth outpaced and often exceeded floccular growth, but the possibility remains unexplored in birds. Because the flocculus is functionally involved in the modulation of gain and phase dynamics for the optokinetic reflex (OKR) and vestibuloocular reflex (VOR), there may be an underlying structural as well as spatial link between the size of the floccular tissue and the size of the semicircular canals.

After branching from the common crus, the avian posterior canal (PSC) runs through a less elongate path than the ASC. At the most posterior extent of the PSC, where it bends ventrally, the bony posterior canal intersects, and is confluent with, the lateral canal (LSC), with the remaining course of the PSC lying ventral to the LSC plane. This communication between PSC and LSC has no known functional significance. It is a

feature of the perilymphatic space and is not shared by the endolymph-filled membranous ducts (Gray, 1908). In some taxa, the posterior portion of the lateral canal is hypertrophied to the extent that its utricular junction is located on the medial side of the posterior utricle (Figure 4–1c).

Despite the gross differences in canal morphology evinced by avians, the *functional* arrangement of the canals is unchanged from that of other vertebrates; that is, the three canals are arranged in approximately orthogonal planes (best demonstrated in dorsal view by Figure 4–1c) and the ampullae of the anterior and lateral canals are positioned at the anterior terminations of their respective circuits. The extreme shape differences exhibited by bird canals are most likely the result of tight packing in a limited space, and do not in all likelihood reflect special sensory attunements. Like mammals, the avian cranial cavity closely conforms to the shape of the brain (Zusi, 1993), a condition that departs greatly from the situation in lower diapsids, in which the brain does not entirely fill the endocranial space (Jerison, 1973, Hopson, 1977).

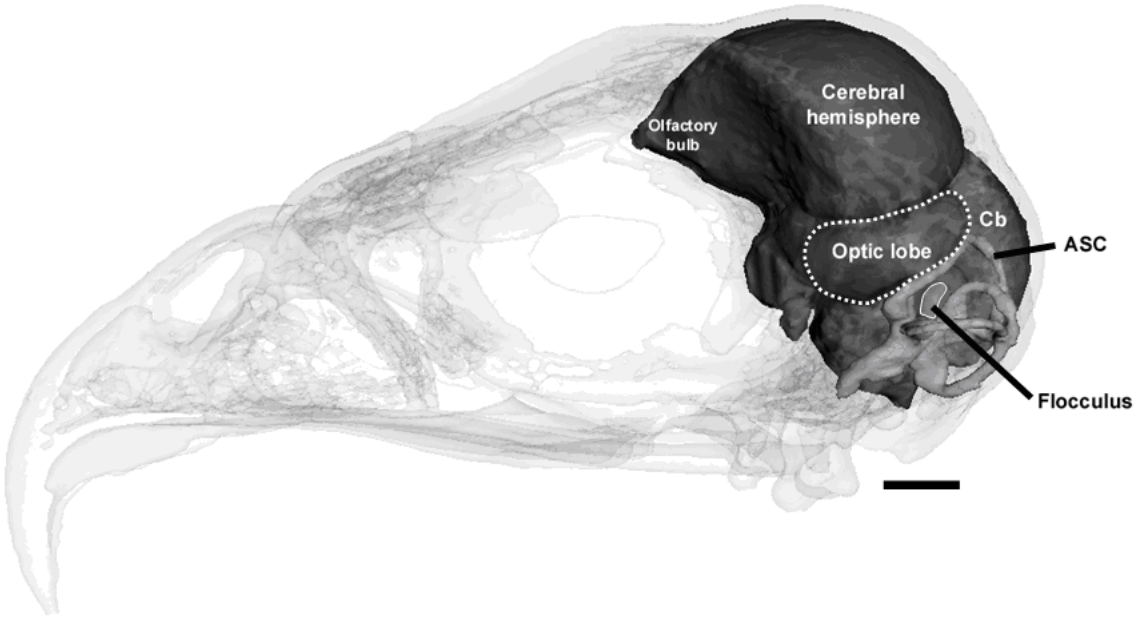

Figure 4–2. Relationship of canal morphology to neural structures. 3D digital endocasts of the brain and left semicircular canal system in the red-tailed hawk (*Buteo jamaicensis*). The outline of the skull is rendered to show the orientation of neural structures. ASC – anterior semicircular canal; Cb – cerebellum. Note the relationship of the optic lobe to the anterior margin of the ASC, as well as the position of the flocculus within the arc of the ASC. Scale bar = 5 mm.

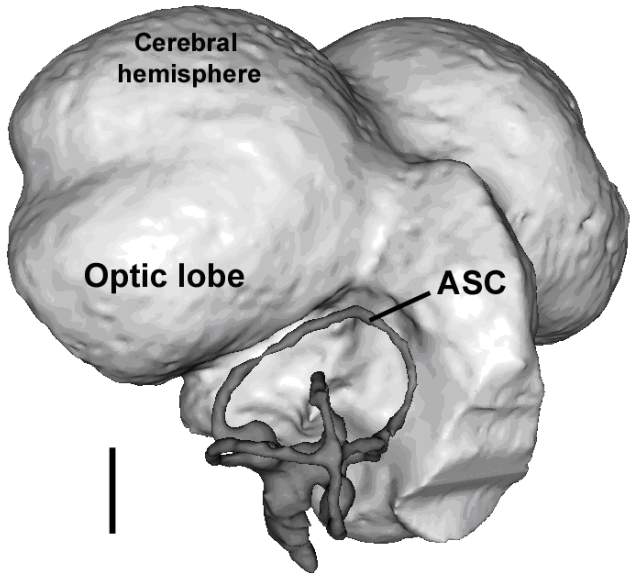

Figure 4–3. ASC shape in *Nyctea scandiaca*. 3D digital endocast of the brain and left semicircular canal system of the snowy owl (*Nyctea scandiaca*) in caudolateral view. ASC – anterior semicircular canal. Scale bar = 5 mm.

4.1.2. The canals of non-avian theropods

The semicircular canals of non-avian theropods possess a more typical vertebrate configuration, lacking the unusual shape seen in the avian system. The common crus passes directly superiorly or at a shallow posterosuperior angle, branching into an anterior canal passing anterolaterally, and a posterior canal posterolaterally. The ASC is dorsoventrally elongate compared to quadrupedal dinosaurs and crocodilians, as previously reported (Sipla et al., 2004). This pattern is not restricted to theropods, but is consistent across all bipedal dinosaur taxa irrespective of phylogeny or body size (Figure 4–4). A notable exception is found in the oviraptorids *Khaan* and *Citipati*, which demonstrate a more vertically compact and horizontally elongate shape than other bipeds (ASC wider than taller). Speculatively, this may relate to the overall lengthening of the braincase reported for oviraptorids (Osmólska et al., 2004), though higher maniraptorans also have elongate brains (Currie and Zhao, 1993; Burnham, 2004; Xu et al., 2002) and do not have this canal morphology. However, despite shape differences seen in the *Khaan* and *Citipati* labyrinths, the overall length of the anterior canal circuit in these taxa does not appear to vary significantly from the trend exhibited by other theropod dinosaurs (section 4.2.1). It is unclear what, if any, functional significance may be associated with this morphology, given that the chief functional parameter (canal streamline length) is unaffected.

Given the current lack of predictive models relating canal shape and canal function, it is difficult to interpret the functional significance of the dorsoventrally elongate ASC in bipeds, though it is argued from a comparative standpoint to indicate a

neurosensory specialization for bipedal locomotion. Basic physical principles suggest that the frequency content of head movements associated with bipedal maneuvering should differ from those incurred by four-legged animals. During bipedal walking and running in dinosaurs, the body's center of gravity is held forward of the point of ground support for a portion of each step cycle, causing the body to experience a pitch-down rotation in the sagittal plane. This movement pitches the head into a nose-down, vertex-up rotation—an acceleration amplified by relative motion of the body, resulting from the ground reaction force of the leading hind limb when it touches down. The ASC is more directionally sensitive to the detection of this pitch-down motion than either the PSC or LSC (Wilson and Melvill Jones, 1979). Conversely, during quadrupedal maneuvering, the body's center of gravity is more favorably stabilized over the limbs' triangle of support (Hildebrand, 1985), thereby subjecting the head to less pitch-down rotational acceleration over the course of the stride. The extent to which vertical expansion of the ASC in bipeds actually relates to head movements remains unknown, however.

Although the endocasts of advanced maniraptorans including troodontids (Currie and Zhao, 1993) and dromaeosaurids (Burnham, 2004) show evidence of ventrolaterally displaced optic lobes, none of these taxa show the characteristic deformation of the ASC seen in bird taxa. Despite recent assertions that *Archaeopteryx* did not have a comparatively large forebrain and lacked sensory specializations for active flight (Kurochkin et al., 2007), it is worth noting that the London *Archaeopteryx* specimen (BMNH 37001) does show a clear avian ASC morphology (Dominguez et al., 2004), with the ASC deflected partly backward by encroachment of the optic tectum. This

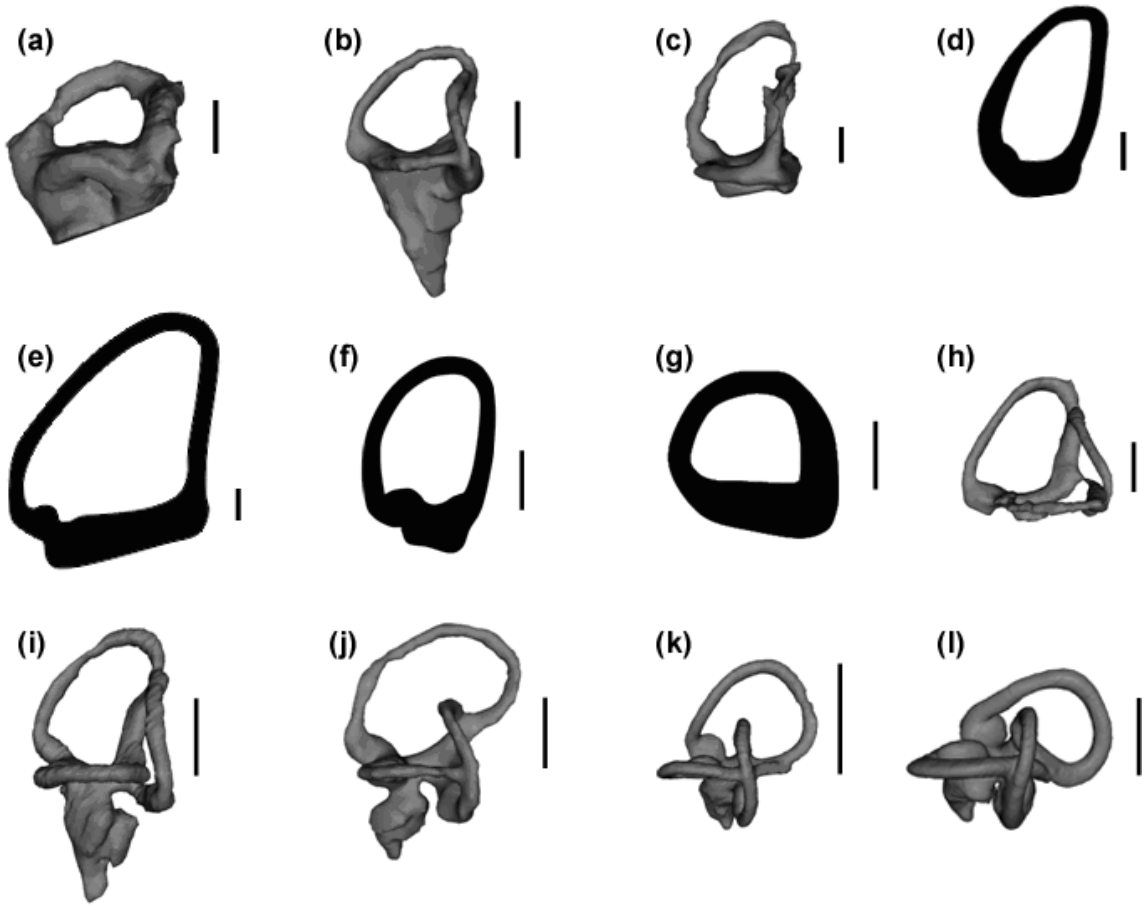

Figure 4–4. ASC morphology in Theropoda. 3D digital endocasts and silhouettes of the bony labyrinth oriented to show the anterior semicircular canal in AMNH 5337 *Euoplocephalus tutus* (a), IGM 100/1132 *Psittacosaurus mongoliensis* (b), MWC-1 *Ceratosaurus nasicornis* (c), YPM 14554 *Allosaurus fragilis* (d), AMNH 5029 *Tyrannosaurus rex* (e), AMNH 5355 *Struthiomimus altus* (f), IGM 100/973 *Khaan mckennai* (g), AMNH 5356 *Dromaeosaurus albertensis* (h), YPM 9207 *Dinornis struthoides* (i), AMNH 1503 *Struthio camelus* (j), AMNH 25244 *Accipiter nisus* (k), AMNH 24119 *Metallura tyrianthina* (l). All scale bars = 5 mm, except (l) = 1 mm.

morphology is characteristic of all avialan taxa observed to date, but unlike that of all non-avian theropod dinosaurs.

4.2. Canal size variation in birds and non-avian theropod dinosaurs

Here I present results from a comparative study of semicircular canal morphology for 178 species of extant birds, 10 species of non-avian theropod dinosaurs, 6 sauropod dinosaurs, and 10 ornithischian dinosaurs, using computed tomography. These results provide a benchmark for our current understanding of avian semicircular canal size, and how it varies with locomotor agility.

In this section, Model II bivariate regressions were used to evaluate structural relationships (covariance) between canal parameters and various aspects of biology, from body mass, to wing morphology and airspeed velocity, as described in the Methods section (section 3.2.4). Descriptive statistics for all comparisons are given in table 4–1.

4–1: Model II bivariate reduced major axis regression statistics

Comparison	Fig.	Slope	Intercept	r^2	n	p	N_{eff}	P_{eff}
SCr vs. BM (birds)	4–5	0.199	–0.197	0.425	178	<0.001	62	<0.001
SCr vs. BM (bipedal dinos)	4–5	0.183	–0.233	0.842	16	<0.001	—	—
SCr vs. BM (mammals)	4–5	0.15	–0.239	0.879	106	<0.001	—	—
SCc vs. BM (volant birds)	4–6	0.226	0.529	0.451	162	<0.001	71	<0.001
SCc vs. BM (bipedal dinos)	4–6	0.182	0.563	0.838	16	<0.001	—	—
SCc vs. BM (volant birds)	4–7	0.226	0.529	0.451	162	<0.001	71	<0.001
SCc vs. BM (flightless birds)	4–7	0.175	0.549	0.447	16	0.005	8	0.070^{NS}
ASCc vs. BM (birds)	4–8	0.217	0.631	0.437	178	<0.001	57	<0.001
ASCc vs. BM (bipeds)	4–8	0.196	0.591	0.866	16	<0.001	—	—
PSCc vs. BM (birds)	4–9	0.199	0.525	0.465	178	<0.001	66	<0.001
PSCc vs. BM (bipeds)	4–9	0.191	0.483	0.684	16	<0.001	—	—
LSCc vs. BM (birds)	4–10	0.198	0.575	0.292	178	<0.001	64	<0.001
LSCc vs. BM (bipeds)	4–10	0.183	0.497	0.747	16	<0.001	—	—
Velocity vs. Wing Loading	4–11	0.383	0.406	0.647	47	<0.001	—	—
ASCrel vs. Wing Loading	4–12	–0.522	1.242	0.562	116	<0.001	19	<0.001
ASCrel vs. Velocity	4–13	–1.313	1.733	0.347	50	<0.001	—	—
ASCc vs. BM (low aspect)	4–14	0.238	0.650	0.690	48	<0.001	—	—
ASCc vs. BM (high aspect)	4–14	0.224	0.672	0.745	19	<0.001	—	—
PSCc vs. BM (low aspect)	4–15	0.261	0.421	0.624	48	<0.001	—	—
PSCc vs. BM (high aspect)	4–15	0.221	0.485	0.657	19	<0.001	—	—
LSCc vs. BM (low aspect)	4–16	0.254	0.513	0.473	48	<0.001	—	—
LSCc vs. BM (high aspect)	4–16	0.219	0.513	0.568	19	<0.001	—	—
ASCrel vs. BI	4–18	–2.351	0.243	0.222	154	<0.001	26	0.015

N_{eff} = "effective n," following the method described by Smith (1994). P_{eff} = recalculated Significance levels using N_{eff} in place of actual n for the given comparison. Refer to text. All measurement terms defined in Table 3–1: Measurements.

4.2.1. Phylogenetic constraints and "adjusted-N"

Fully nested ANOVA for logged ASCc, PSCc, and LSCc using the phylogenetic hypothesis of Livezey and Zusi (2006, 2007) provides an estimate of the character variance attributable to a particular taxonomic level independent of other levels, as well as differences between clades at each taxonomic level (Bell, 1989). Seven nested levels of classification were used: cohort, subcohort, superorder, order, family, genus, and species, based on the taxonomy proposed for the higher-order classification of Class Aves by Livezey and Zusi (2007). Membership of individual species within these taxonomic groups is given in Appendix 1. The partition of variance components for all three canals between taxonomic levels is given in table 4–2.

Table 4–2. Fully nested ANOVA for Log-ASCc, Log-PSCc, and Log-LSCc in Class Aves (species n=178).

Level	ASCc variance component	PSCc variance component	LSCc variance component
Class	—	—	—
Cohort	–.006 (0.0%)	–.001 (0.0%)	–.002 (0.0%)
Subcohort	.006 (22.04%)	–.001 (0.0%)	–.000 (0.0%)
Superorder	.003 (11.09%)	.003 (17.18%)	.002 (12.92%)
Order	.005 (18.63%)	.004 (19.81%)	.005 (25.08%)
Family	.005 (18.30%)	.005 (24.76%)	.005 (28.09%)
Genus	.004 (16.39%)	.004 (20.37%)	.003 (16.57%)
Species	.003 (13.56%)	.003 (17.89%)	.003 (17.34%)
total	.026 (100.00%)	.019 (100.00%)	.018 (100.00%)

Variance components were obtained from the FULLY NESTED ANOVA procedure in Minitab 15.1.

ASC variance is most highly accumulated at the subcohort level, possibly reflecting primitive modification of the anterior semicircular canal in birds, either as a result of avian brain enlargement or some other factor, while this level accounts for no variance in PSCc or LSCc. The next highest partition of variance is found at the ordinal and familial levels for ASCc. The familial level represents the overall highest partition of variance for LSCc and PSCc. This is not surprising because avian species within families tend to have similar morphologies and locomotor habits. Indeed, many life history variables exhibit the highest variation at the family level in birds (Bennet and Owens, 2002). Canal variation at the cohort level is virtually nil, though a significant contributor of total variance is found at the lower superordinal level for all three canals. This is also expected because bird superorders (Chapter 2, Figure 2-2) often account for diversely contrasted locomotor behaviors. Galloanserimorphs and dromaeomorphs, for instance, represent large groups of poor-flying birds with few or no exceptional members. Falconimorphs (raptors, including hawks, falcons, and owls) exhibit some of the most agile behaviors in flight as a result of their predatory habits. More than half of all bird species are passerimorphs, or perching birds, and these typically employ high-amplitude, high-frequency wingbeats, critical to the execution of low speed maneuvers in cluttered environments. A sizeable amount of variation is still explained at the lower generic and species levels, permitting interpretation of species-specific vestibular adaptations to locomotor habits.

4.2.2. Allometry of bird and theropod canals

Bird semicircular canals have previously been noted for their relative largeness (Gray, 1908; Jones and Spells, 1963; Money and Correia, 1972; Sipla et al., 2003). Regression analysis of SCr versus body mass using 178 bird species (representing 24 orders), 16 bipedal nonavian dinosaurs, and 106 noncetacean mammals (Figure 4–5) confirms that bird canals ($\propto BM^{0.199}$) and dinosaur canals ($\propto BM^{0.183}$) scale with body mass with strong negative allometry, as with mammals ($\propto BM^{0.15}$). Expectations for isometry based purely on physical dimension (canal radius $\propto BM^{0.333}$) do not fall within the 95% lower and upper confidence limits of all three slopes, though it should be noted there is no expectation for physical isometry in the canals based on theory. Jones and Spells (1963) predict that the scaling exponent should be between 1/3 (derived by modeling the allometry of head movements based on geometric similarity) and 1/12 (based on elastic similarity), to permit "dynamic similarity" of canal function with increased body size.

Regarding hypothesis 1, that volant birds as a group have larger canals relative to body mass than bipedal dinosaurs, the slope of the volant bird regression for Log SCc vs. Log Body Mass is not significantly different from the bipedal dinosaur regression ($p=0.094$) (Figure 4–6). Elevation differences between the volant bird and dinosaur regressions are significant ($p<.001$). Hypothesis 1_O is rejected and support is found for hypothesis 1_1. That is, overall, the semicircular canals of volant birds are found to be larger (more sensitive) than similarly sized bipedal dinosaurs. However, there is no

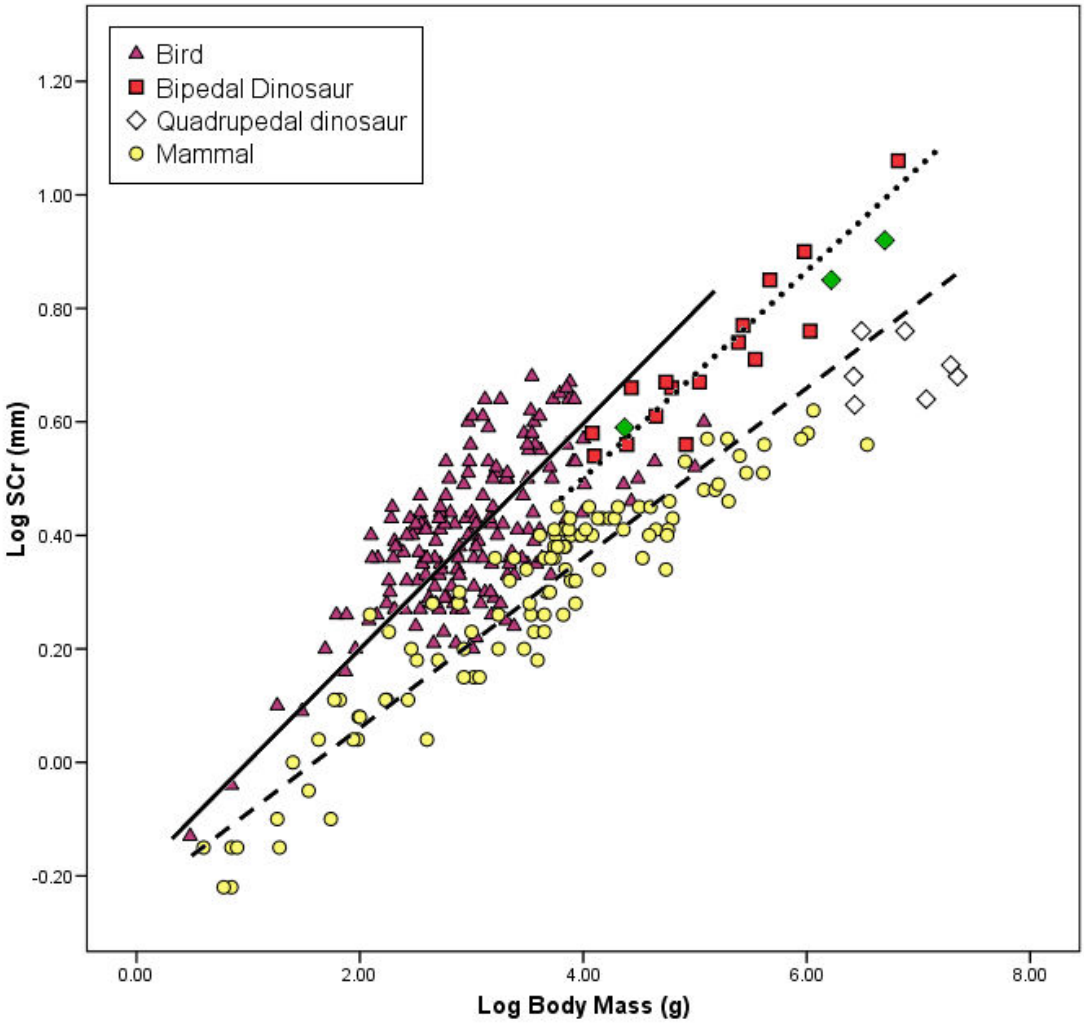

Figure 4–5. Bivariate plot of SCr vs. Body Mass for birds, dinosaurs, and mammals. Average semicircular canal radius (SCr) plotted against body mass (g) for 178 bird taxa, 16 bipedal nonavian dinosaurs, and 106 noncetacean mammals. 10 species of quadrupedal nonavian dinosaurs are also plotted (diamonds) onto the graph for comparison. Filled (green) diamonds indicate three quadrupedal ceratopsians. Fitted lines represent reduced major axis regressions for birds (solid line), bipedal dinosaurs (dotted line), and mammals (dashed line), respectively. The slope of the bird regression is not significantly different from the bipedal dinosaur regression (p=0.490), but is significantly different from the mammal regression (p=0.001). The slope of the bipedal dinosaur regression is not significantly different from the mammal regression (p=0.096). Regression statistics are summarized in table 4–1.

overlap in body size between the volant bird sample and dinosaurian sample, and the bipedal dinosaurian sample is comparatively small (n=16).

The bird regression in figure 4–6 is not well fit ($r^2 = 0.451$), probably because of poor sampling at lower body size (due to resolution lower limits of the medical CT scanner at Stony Brook Hospital used for the majority of specimens). It was hypothesized that overall increase in canal size would relate to the demands of aerial maneuvering in a highly perturbed, three-dimensional environment. While there is significant elevation of volant bird points relative to bipedal dinosaurs along the X-axis of figure 4–6 ($p<.001$), many poor-flying species overlap in scale with those of bipedal dinosaurs.

Regarding hypothesis 2, that volant birds have larger canals relative to body mass than flightless birds, the slope of the volant bird regression for Log SCc vs. Log Body Mass is not significantly different from the flightless bird regression ($p=0.227$) (Figure 4–7). Elevation differences between the volant and flightless bird regressions are significant ($p<.001$). Hypothesis 2_O is rejected and support is found for hypothesis 2_1. That is, at any given body mass, the semicircular canals of volant birds are predictably larger than those of flightless birds. There is however a great deal of overlap in relative canal size between the two samples. Secondary flightlessness does not *de facto* indicate a reduction in semicircular canal size relative to similarly sized fliers.

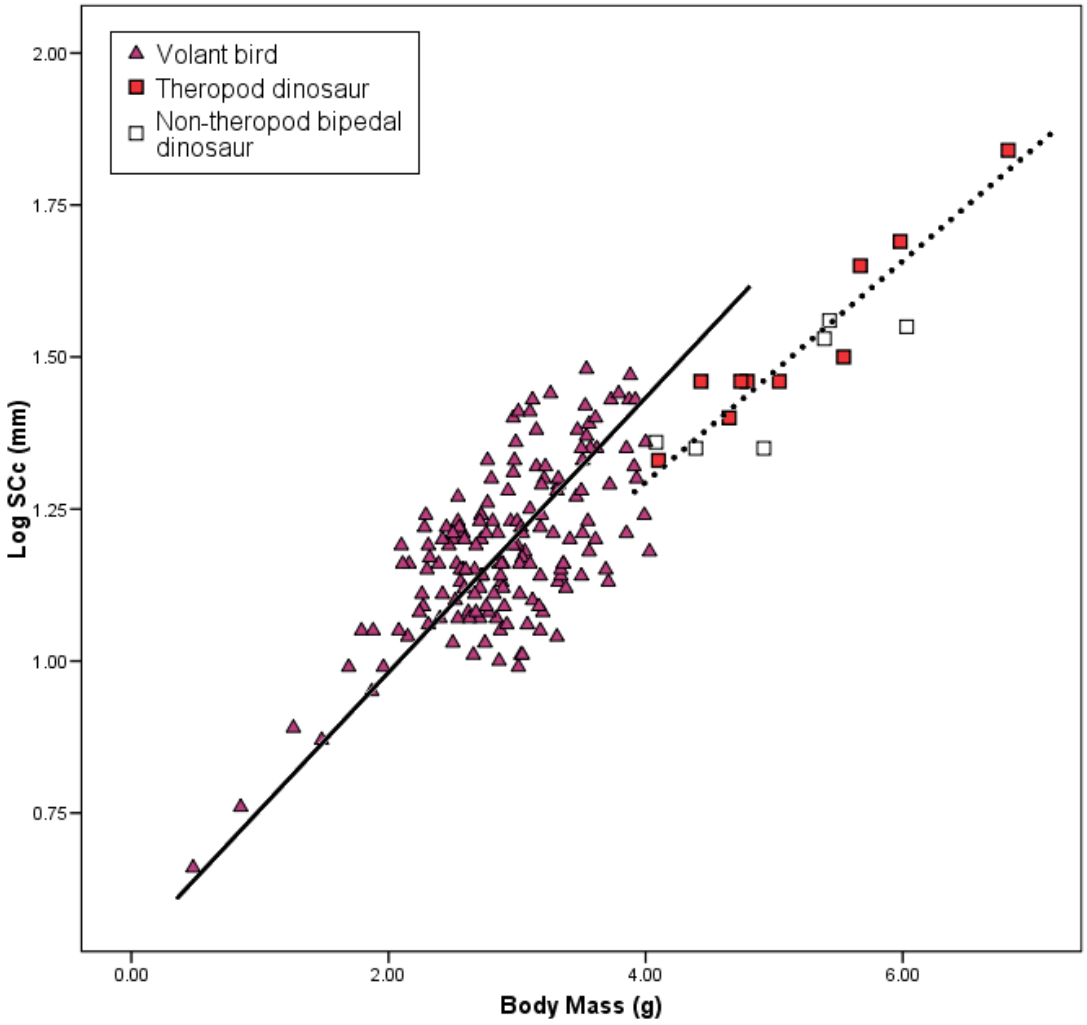

Figure 4–6. Bivariate plot of SCc vs. Body Mass for volant birds and bipedal dinosaurs. Average semicircular canal circumference (SCc) plotted against body mass (g) for 162 volant bird taxa and 16 bipedal nonavian dinosaurs (theropods and non-theropods). Fitted lines represent reduced major axis regressions for volant birds (solid line) and bipedal dinosaurs (dotted line). Slope equations are not significantly different ($p=0.094$), but there is significant elevation between slopes ($p<.001$). Regression statistics are summarized in table 4–1.

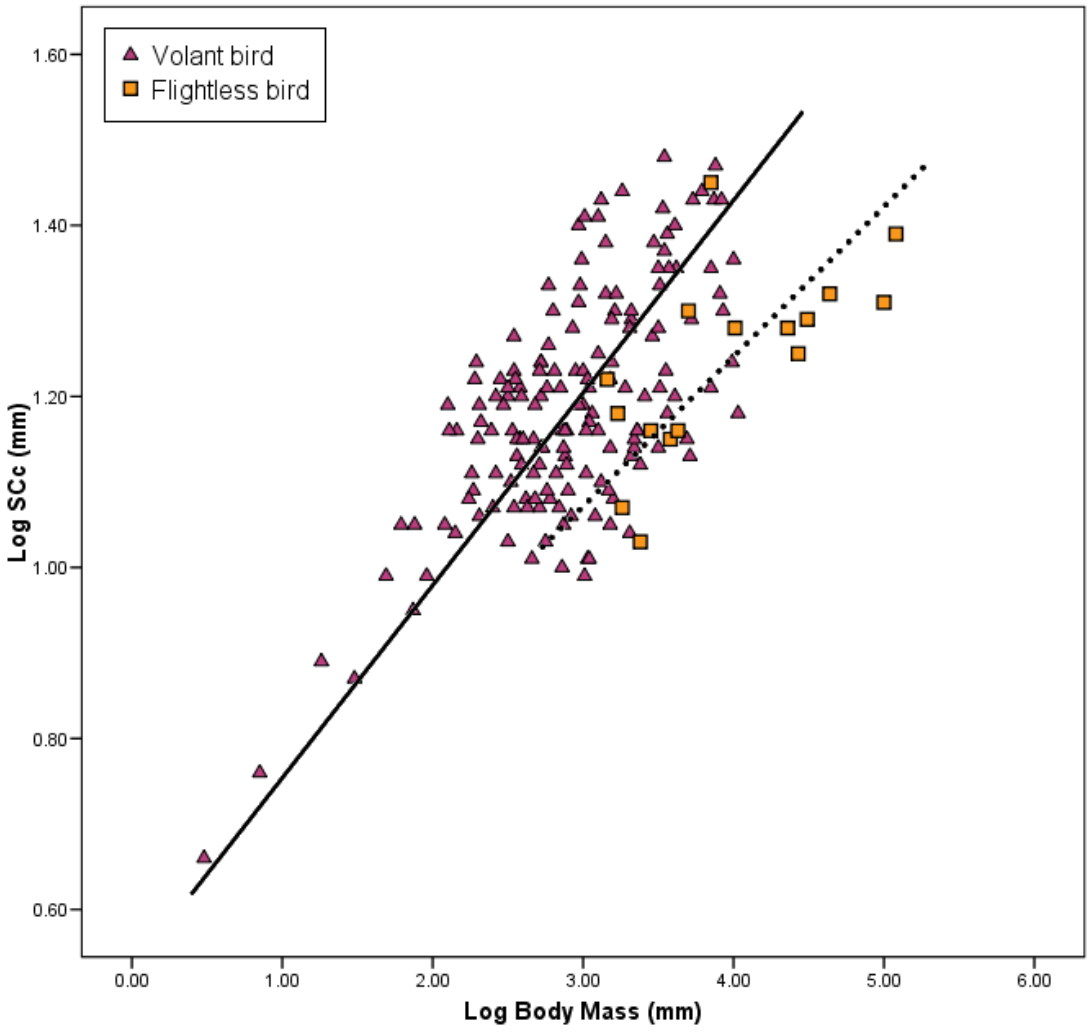

Figure 4–7. Bivariate plot of SCc vs. Body Mass for volant birds and flightless birds. Average semicircular canal circumference (SCc) plotted against body mass (g) for 162 volant bird taxa and 16 flightless bird taxa. Fitted lines represent reduced major axis regressions for volant birds (solid line) and flightless birds (dotted line). Slope equations are not significantly different ($p=0.227$), but there is significant elevation between slopes ($p<.001$). Overall, volant birds have larger canal dimensions than flightless birds at any given body mass. Regression statistics are summarized in table 4–1.

4.2.3. Differential expansion of the canals

To examine the possibility of differential expansion of the three semicircular canals, ASCc, PSCc, and LSCc were plotted separately against body mass (Figures 4–8, 4–9, and 4–10). None of the bird slopes were found to be significantly different from one another ($p>.05$). The plots indicate that expansion of individual canals is typically uniform in relation to body size. The null hypothesis $H3_0$ is not rejected. That is, there is no observed difference in the rate of expansion of the semicircular canals with increased body size.

A test for common slope across all three bird canals plotted in figures 4–8, 4–9, and 4–10 revealed a slope of 0.205, very close in value to the slope obtained for bird SCc vs. BM (0.199). Because all three canals scale proportionately to body mass, the SCc measure is found to be a good descriptor of overall canal size in birds, at the expense of masking some of the variability in LSC circumference. The lowest r^2 value of the three canal slopes for birds was obtained for LSCc ($r^2 = 0.292$), suggesting that LSC size is more variable with body size than either ASC ($r^2 = 0.437$) or PSC ($r^2 = 0.465$).

Regarding hypothesis $H3_2$, that birds have differentially larger anterior and lateral semicircular canals compared to non-avian bipedal dinosaurs, it is noted that ASCc and LSCc size are more significantly elevated ($p<.001$) than PSCc size ($p=.012$) in birds relative to dinosaurs. The difference in elevation between PSCc vs. BM in birds and dinosaurs is nonsignificant using the Bonferonni adjusted α (0.002). I speculate that increased anterior and lateral canal size in birds may relate specifically to the higher frequency pitch-down rotations experienced during flapping flight.

N_{eff} values were used to calculate new significance levels (P_{eff}) for the three bivariate regression equations obtained for figures 4–8, 4–9, and 4–10. Smith (1994) advocates using a phylogenetically reduced sample size computed from the smaller of two choices, either (1) N_{eff} for the y axis trait, or (2) mean of the N_{eff} scores for both axes. Significance at the .001 level was maintained for all three correlations using effective N for canal measures (N_{eff} = 69, 86, 84 for logged ASCc, PSCc, and LSCc, respectively) and body mass (N_{eff} = 49). N_{eff} scores reported in table 4–1 for these comparisons represent the mean of the canal N_{eff} and mass N_{eff}, because in all three instances mass N_{eff} was found to be lower.

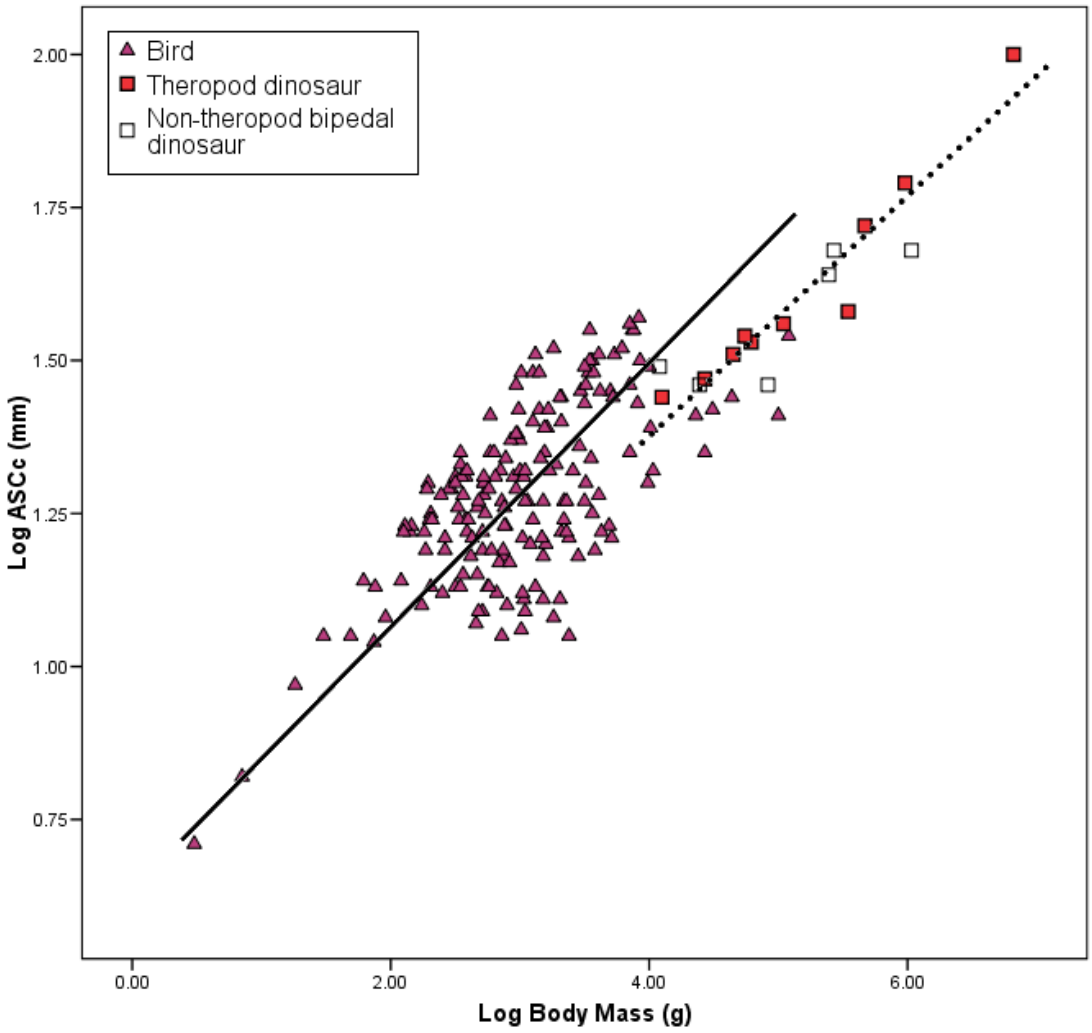

Figure 4–8. Bivariate plot of ASCc vs. Body Mass for birds and bipedal dinosaurs. Anterior canal circumference plotted against body mass for birds (n=178) and bipedal dinosaurs (n=16). Fitted lines represent reduced major axis regressions for birds (solid line) and bipedal dinosaurs (dotted line). Slope equations are not significantly different ($p>.05$), but there is significant elevation between slopes ($p<.001$). Regression statistics are summarized in table 4–1.

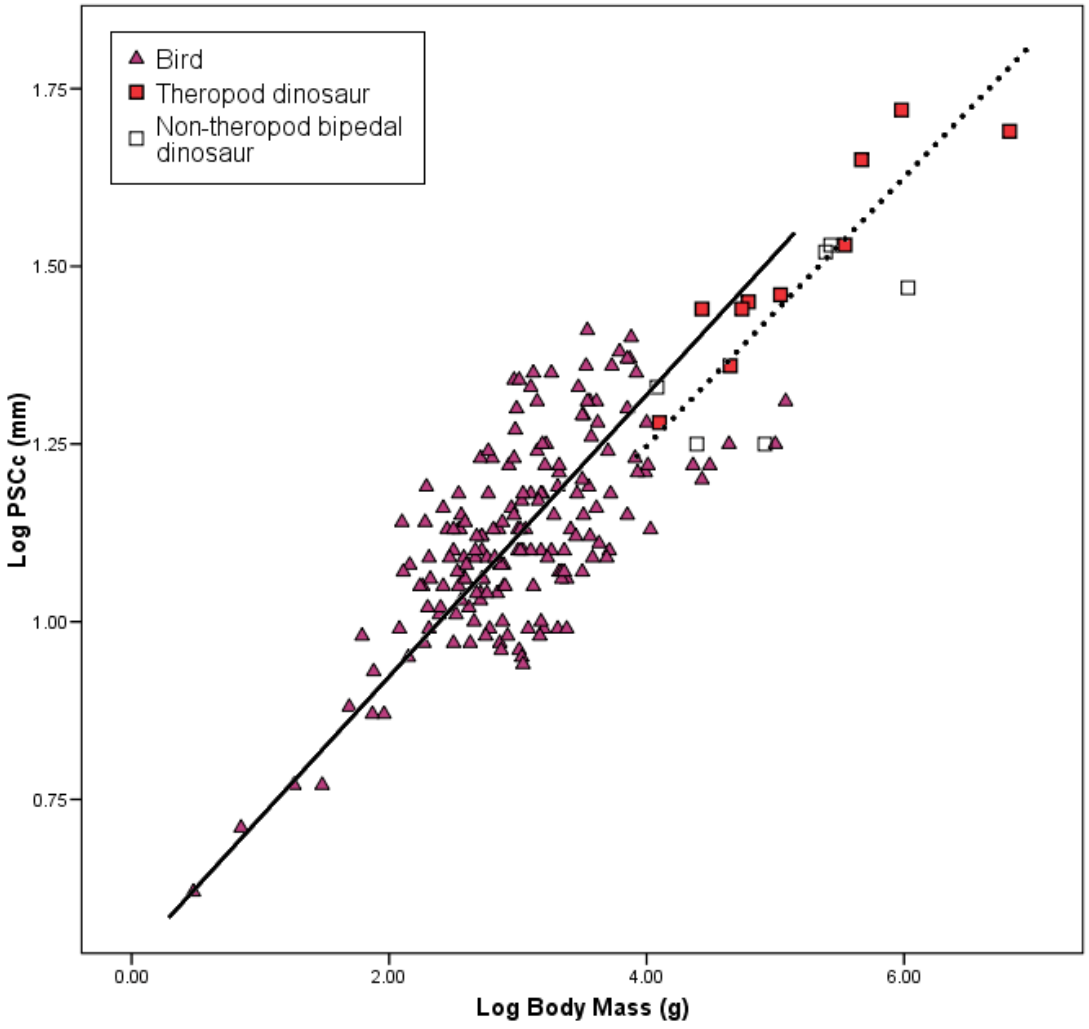

Figure 4–9. Bivariate plot of PSCc vs. Body Mass for birds and bipedal dinosaurs. Posterior canal circumference plotted against body mass for birds (n=178) and bipedal dinosaurs (n=16). Fitted lines represent reduced major axis regressions for birds (solid line) and bipedal dinosaurs (dotted line). Slope equations are not significantly different ($p>.05$), but there is significant elevation between slopes ($p=.012$). Using the Bonferonni Bonferonni adjusted α (0.002), the observed elevational difference is nonsignificant. Regression statistics are summarized in table 4–1.

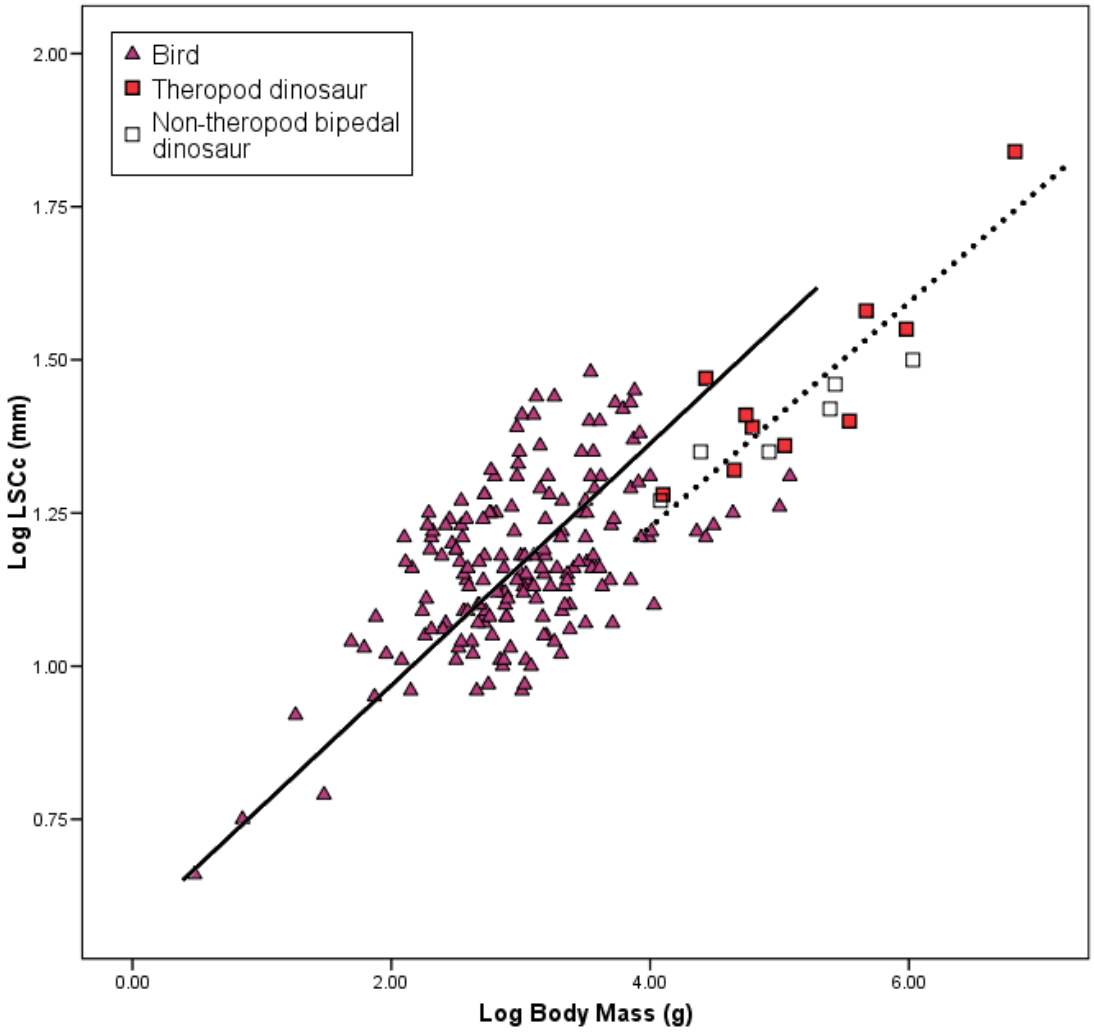

Figure 4–10. Bivariate plot of LSCc vs. Body Mass for birds and bipedal dinosaurs. Lateral canal circumference plotted against body mass for birds (n=178) and bipedal dinosaurs (n=16). Fitted lines represent reduced major axis regressions for birds (solid line) and bipedal dinosaurs (dotted line). Slope equations are not significantly different ($p>.05$), but there is significant elevation between slopes ($p<.001$). Regression statistics are summarized in table 4–1.

4.2.4. Relationship between semicircular canal size and morphological correlates of flight behavior

Conventional multiple regression of $\log_{10}$ SCc (average semicircular canal circumference) against $\log_{10}$ Body Mass, $\log_{10}$ Wing Loading, and $\log_{10}$ Aspect Ratio (n=106, incorporating all bird taxa for which wing measures could be obtained) is significant ($p<.001$) and given by the equation:

$$y = 0.229 (\log \text{body mass}) - 0.253 (\log \text{wing loading}) - 0.012 (\log \text{aspect ratio}) + 0.984.$$

The correlation coefficient for the plane described by this regression is 0.745 ($r^2 = 0.555$). Significant positive effects of log Body Mass and log Wing Loading on log SCc are indicated ($p<.001$ in both cases), but not Log Aspect Ratio ($p = 0.858$). This indicates strongly that despite the dependence of wing loading on body mass, wing loading is a good independent predictor of semicircular canal size.

Aspect ratio was not found to be a good predictor of semicircular canal size. This was expected, because in strict terms aerial maneuverability (minimum space required to turn) is proportional to wing loading. Aspect ratio doesn't factor into turning performance except at very low values in combination with low wing loading, or at high values combined with extremely narrow wings and low wing loads.

Figure 4–11 depicts the relationship between velocity and wing loading for 47 bird taxa used in this analysis where data could be obtained for both variables. Birds that have lower wing loads (larger wing area in proportion to body weight) can sustain flights

at lower speeds without stalling and consequently have greater maneuverability in flight (defined as a smaller minimum turn radius).

To test hypothesis 4_1 (relative canal size scales inversely with wing loading), ASCrel was plotted against wing loading (Figure 4–12), revealing a significant relationship ($p<0.001$, $r^2 = 0.562$). The null hypothesis 4_O is rejected. Support is therefore found for hypothesis 4_1. That is, taking body mass into account, there is an observed relationship between canal sensitivity and degree of aerial maneuverability as predicted by wing loading.

Adjusted for phylogenetic effects using a nested ANOVA, effective population size was dramatically reduced for this regression (ASCrel vs. wing loading; $N_{eff} = 19$ from original N = 117; refer to Table 4–1), though a significant correlation was still obtained ($p<0.001$).

Support is also found for hypothesis 4_2 (birds that habitually fly at slower speeds have larger canals). Regression of ASCrel vs. Velocity (Figure 4–13) revealed a significant but weak relationship ($p<0.001$, $r^2 = 0.347$).

To test hypothesis 4_3 (birds that are both highly maneuverable [low wing loading] and agile [low aspect ratio] have the largest relative canal sizes), bivariate regressions of ASCc, PSCc, and LSCc against Body Mass were calculated using birds categorized as having low wing loads (<76.77). These points were further parsed into high (>9.46) and low (<9.46) aspect categories and plotted on Figures 4–14 (ASC), 4–15 (PSC), and 4–16 (LSC).

Results show significant elevation differences between the regression slopes for both groups (low aspect vs. high aspect) in PSCc vs. BM (p=.035) and LSCc vs. BM

($p<.001$), but not ASCc vs. BM ($p=.349$). After Bonferonni correction, only the LSCc vs. BM comparison is significant.

Partial support is found for hypothesis 4_3. Birds with low wing loads and low aspect ratio wings have relatively enlarged LSC dimensions, though the separation between low aspect ratio and high aspect ratio groups is continuous and there is considerable overlap. Nevertheless, this is taken as evidence that enlarged lateral canal size correlates with degree of maneuverability and *agility* in birds. Contrary to prediction, however, ASC and PSC size are not predictably larger in highly maneuverable, agile birds.

Another way to improve agility in birds that are already highly maneuverable (low wing loading) is to have extremely narrow or thin wings. This combination is rarely achieved, but is exemplified by the long, thin wings of the common nighthawk (*Chordeiles minor*) and magnificent frigatebird (*Fregata magnificens*). Both of these birds have enlarged lateral canals, as shown in Figure 4–16. Tropicbirds (*Phaethon*) also have narrow, high aspect ratio wings and plot above the line for low aspect birds. Tropicbirds plunge-dive to capture prey below the waterline or by catching airborne flying fish on the wing, and the species is renowned for its synchronized, aerial courtship displays (Sibley, 2001).

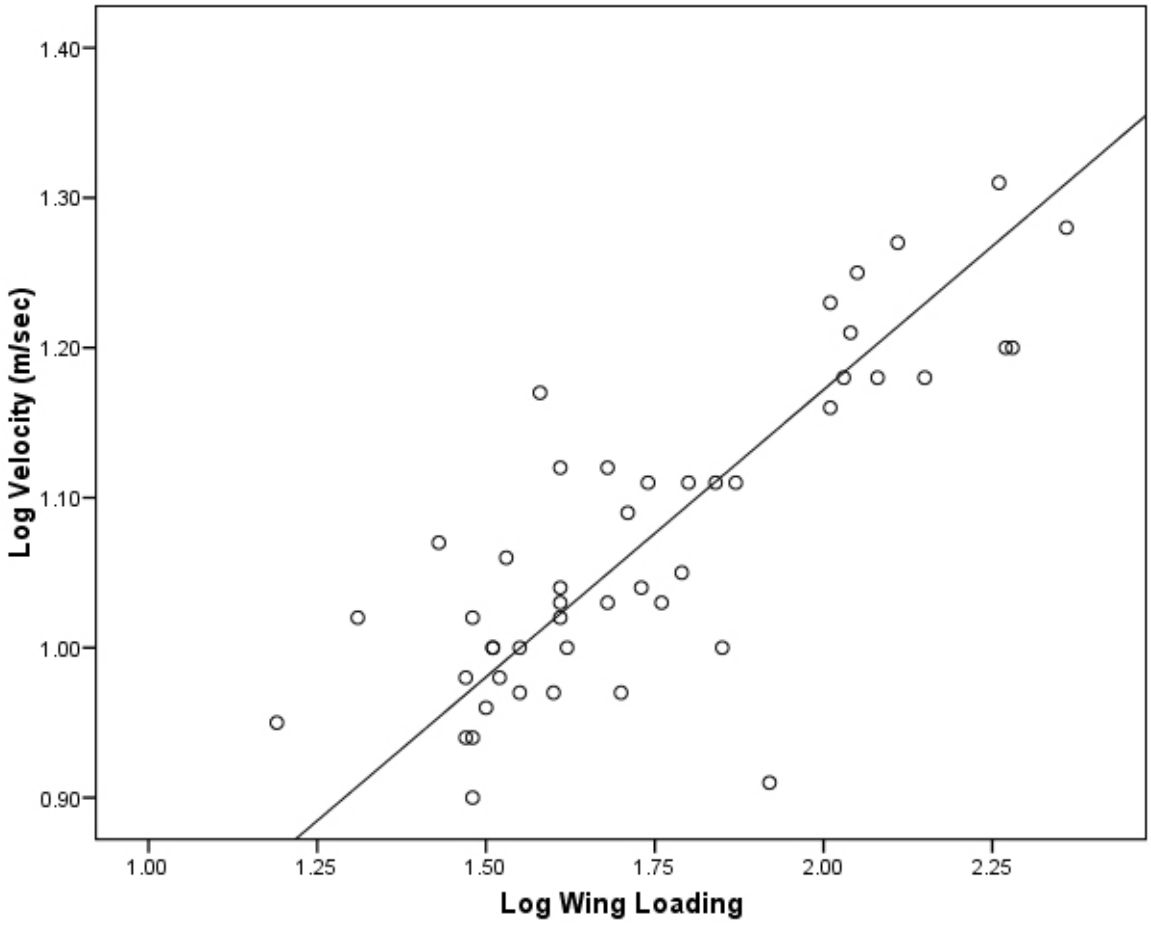

Figure 4–11: Bivariate plot of Velocity vs. Wing Loading for volant birds. Cruising airspeed velocity plotted against wing loading (units N m^{-2}) for n=47 birds using data obtained from the literature. Regression statistics are summarized in table 4–1.

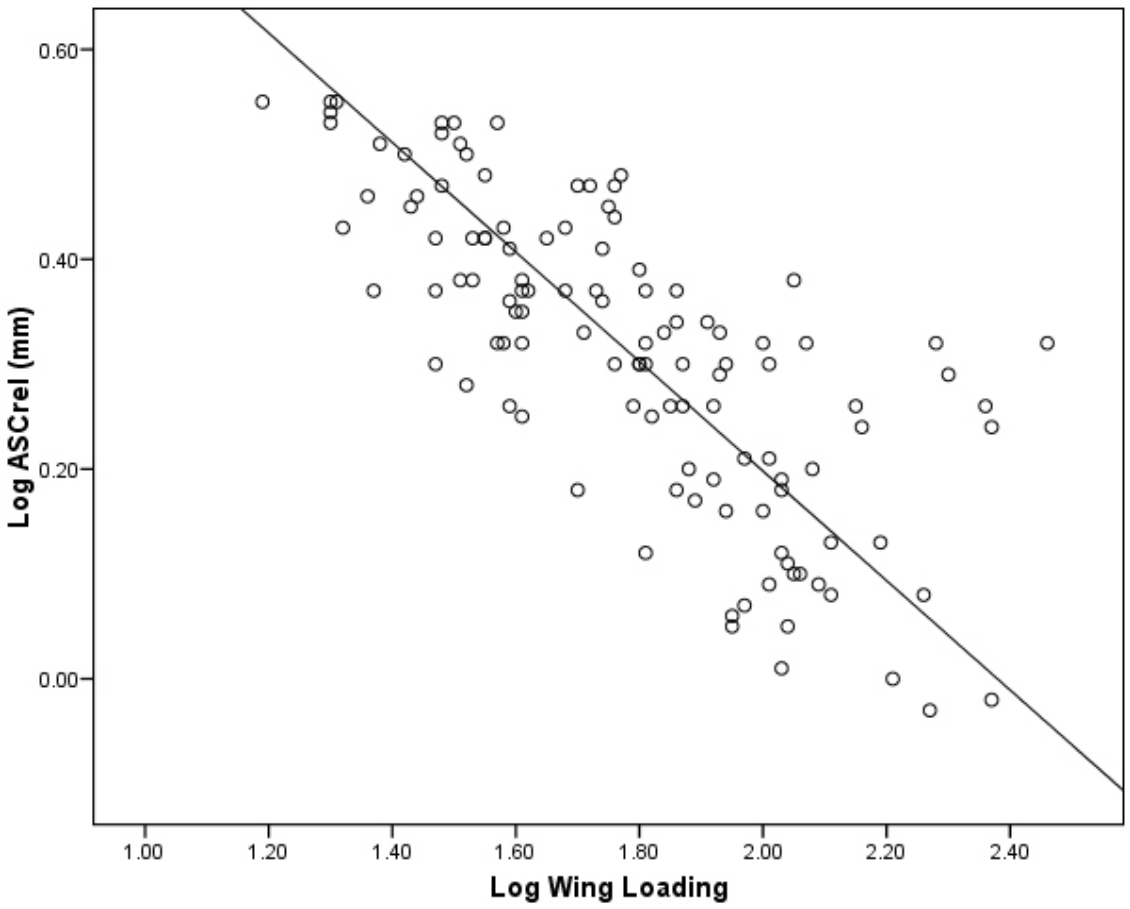

Figure 4–12: Bivariate plot of ASCrel vs. Wing Loading for volant birds. Relative anterior canal circumference plotted against wing loading (units N m^{-2}) for n=117 birds. Wing loading data obtained from the literature. Regression statistics are summarized in table 4–1.

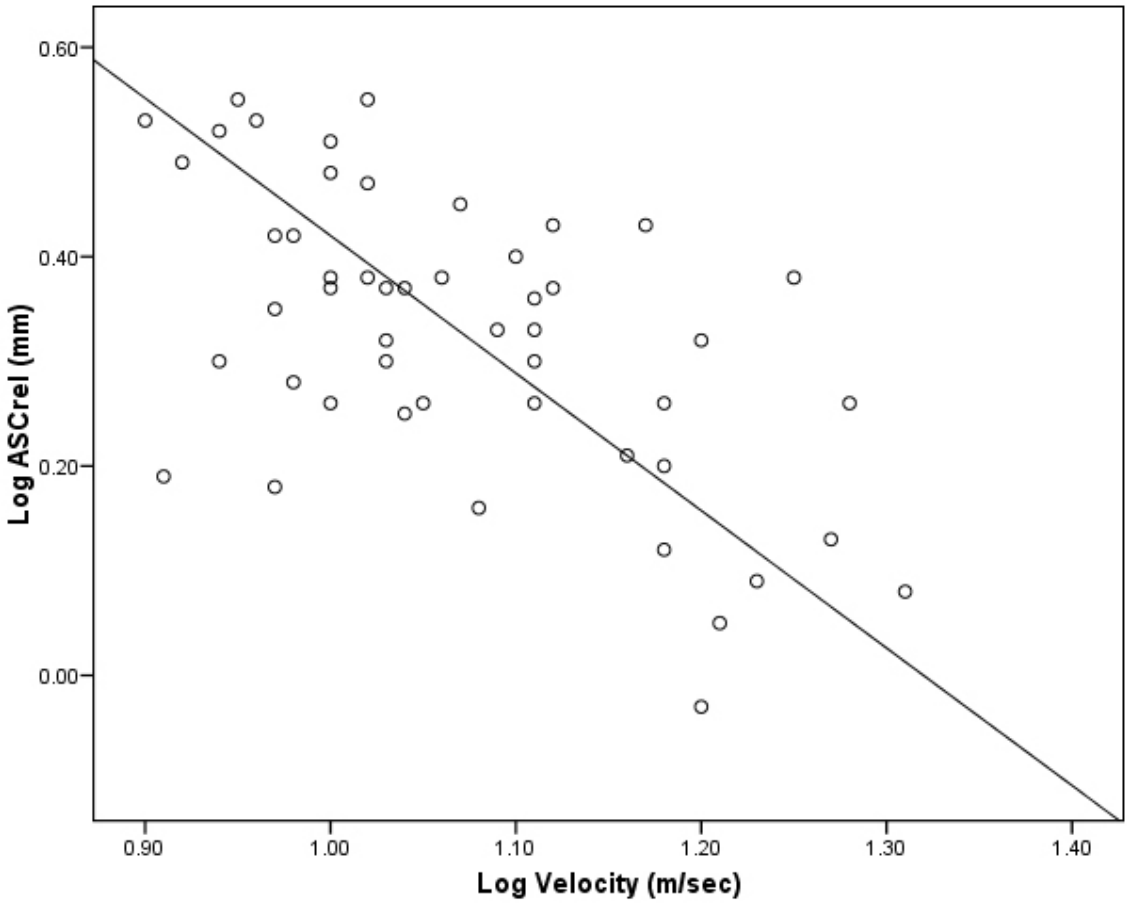

Figure 4–13: Bivariate plot of ASCrel vs. Velocity for volant birds. Relative anterior canal circumference plotted against average cruising airspeed velocity for n=47 birds. Velocity data obtained from the literature. Regression statistics are summarized in table 4–1.

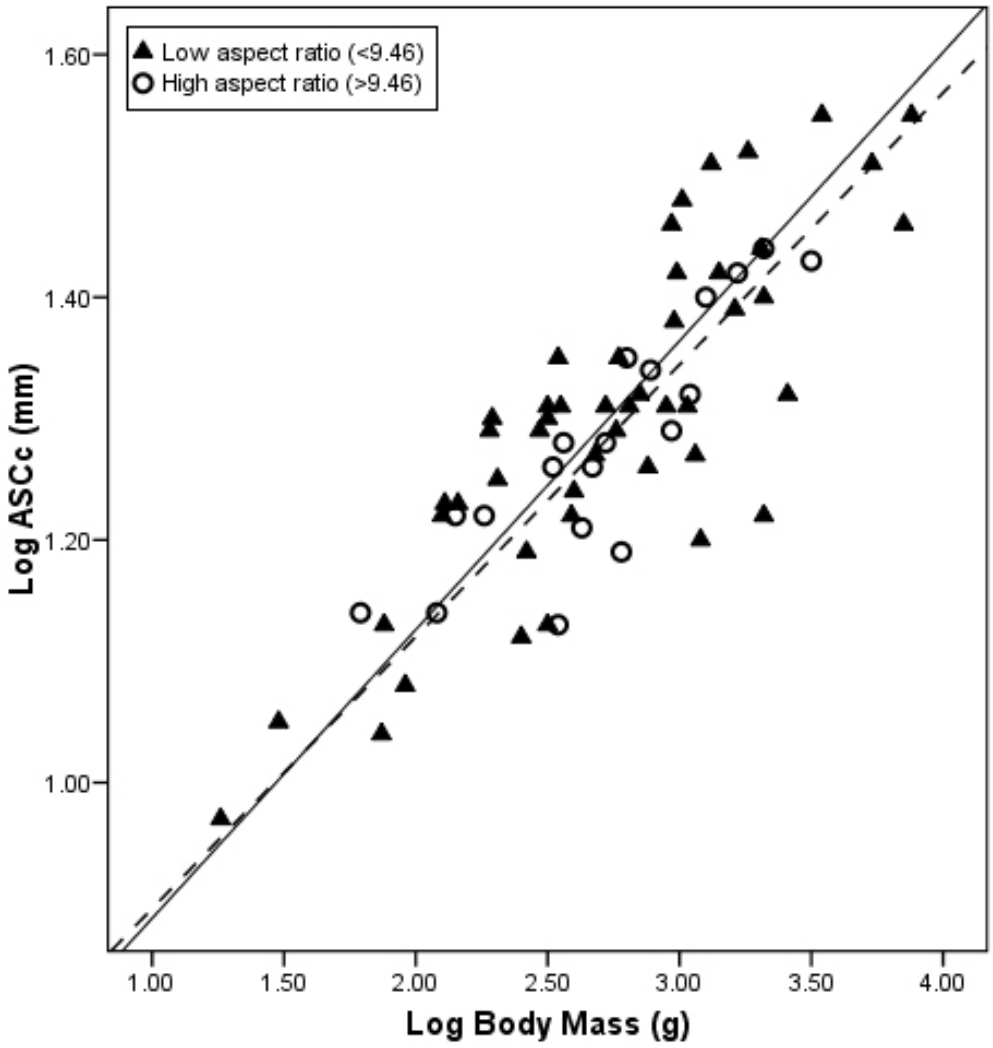

Figure 4–14. Bivariate plot of ASCc vs. Body Mass for highly maneuverable birds. Data points represent n=67 birds categorized by having low wing loads (<76.77, based on the mean wing loading of the entire bird sample). Triangles indicate those with low aspect ratio wings (<9.46) and the solid line indicates the reduced major axis regression for these points. Circles are fit to the dotted line and indicate those birds with high aspect ratio wings (>9.46). The slopes are not significantly different (p>.05) and are not significantly elevated (p>.05). Regression statistics are summarized in table 4–1.

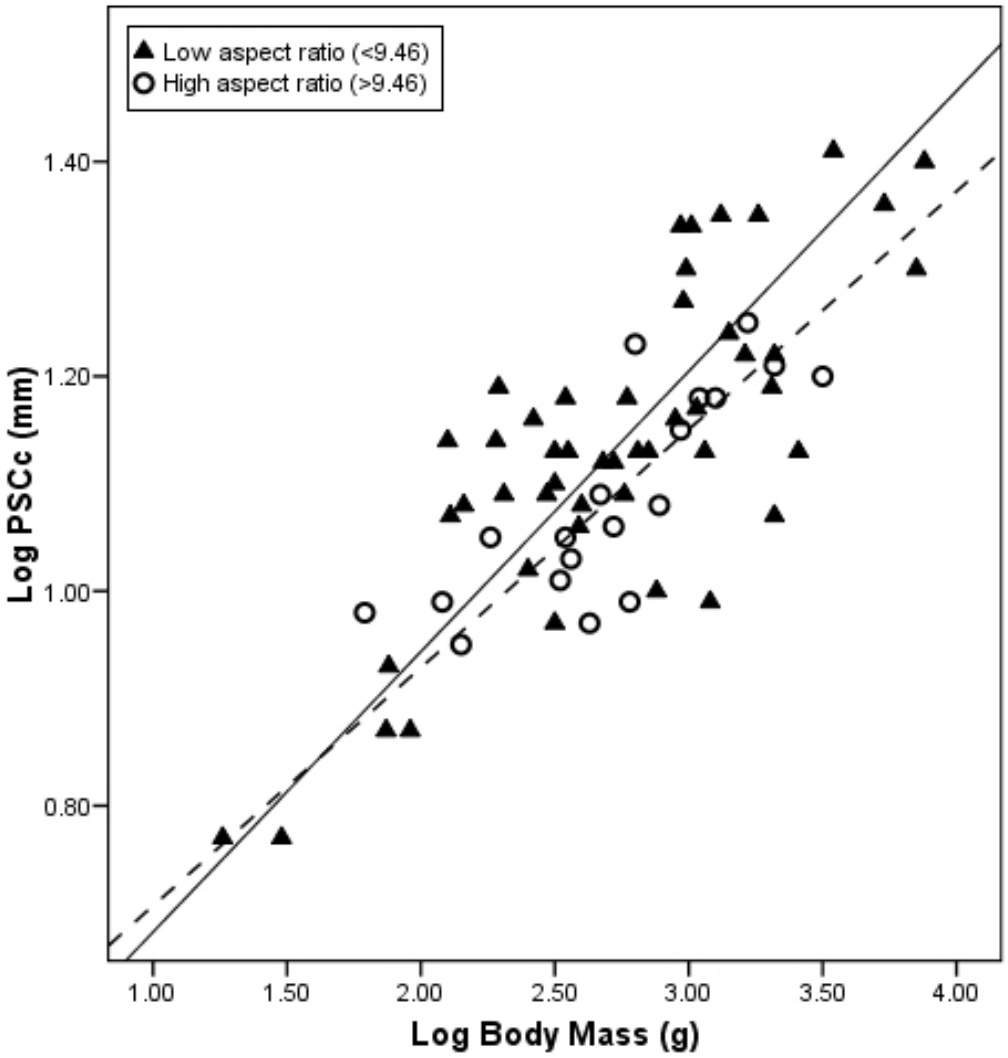

Figure 4–15. Bivariate plot of PSCc vs. Body Mass for highly maneuverable birds. Data points as indicated for figure 4–14. The slopes are not significantly different (p>.05) but are significantly elevated (p=.035). Using the Bonferonni adjusted α (0.002), the observed elevational difference is nonsignificant. Regression statistics are summarized in table 4–1.

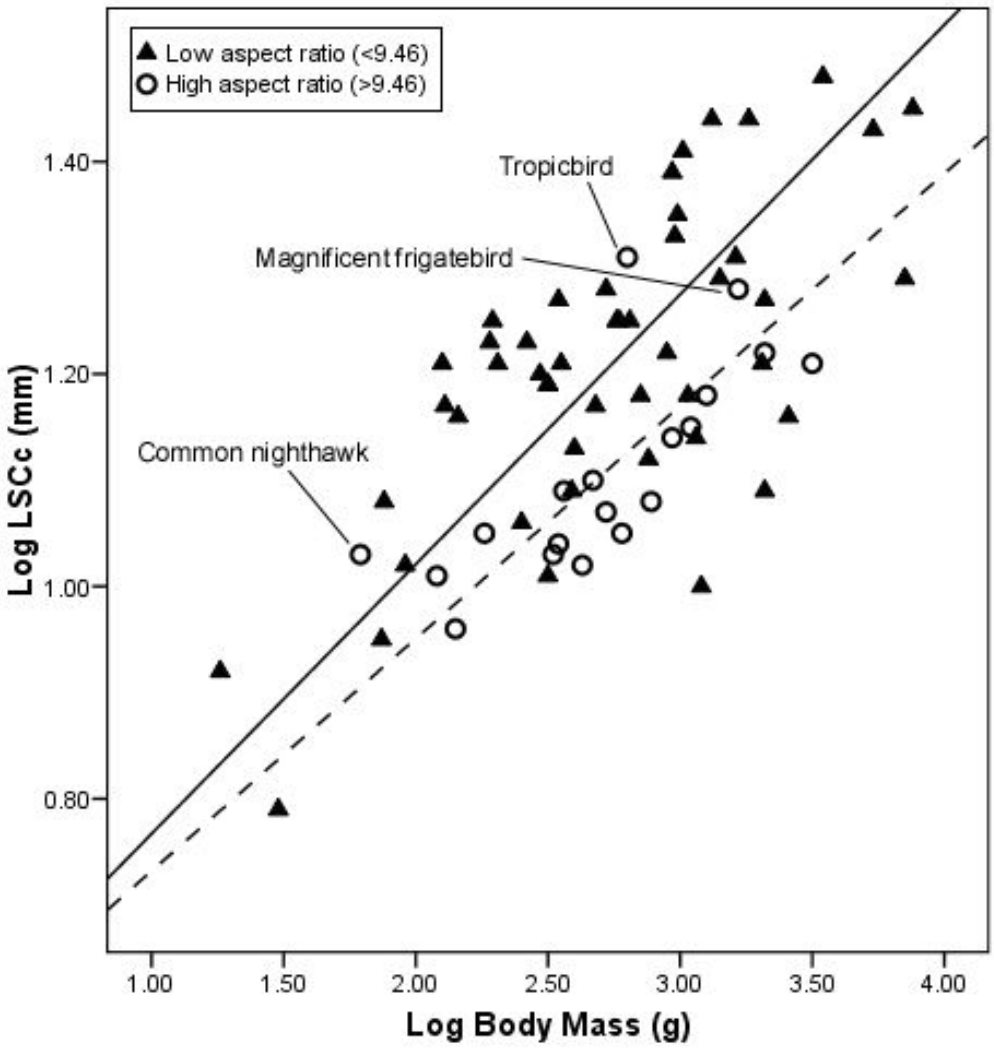

Figure 4–16. Bivariate plot of LSCc vs. Body Mass for highly maneuverable birds. Data points as indicated for figure 4–14. The slopes are not significantly different ($p>.05$) but are significantly elevated ($p<.001$), indicating that LSCc correlates with increased agility in birds with low wing loading and low aspect ratio. Birds with low wing loading and extremely thin high aspect ratio wings (as indicated) are also found to have enlarged LSCc dimensions. Regression statistics are summarized in table 4–1.

Results of the discriminant function analysis (DFA) are plotted on figure 4–17. This analysis was performed on the logged relative circumference measurements of the three canals for all birds for which wing loading and aspect ratio values could be obtained, including *Archaeopteryx* (n=110), plus all flightless birds and theropod dinosaurs. Specimens were grouped as follows:

(1) Volant (low wing loading, low aspect ratio
(2) Low wing loading, high aspect ratio
(3) High wing loading, high aspect ratio
(4) High wing loading, low aspect ratio
(5) Flightless bird
(6) Flightless non-avian theropod

Although there is considerable overlap between points (39 of 132 cases were assigned to different groups), group means appear to differ (Wilks' Lambda = 0.219, $p<.001$). Group centroids are spaced across function 1 (accounting for 88.2% of variance) in the following manner from left to right: flightless → high wing loading → low wing loading. All three canal measures are most highly correlated with function 1, with relative ASC size having the largest unique contribution to the discrimination specified by this function (table 4–3).

This indicates that overall canal size (all three canals) corresponds in trend from flightlessness to low-maneuverability flying to high-maneuverability flying, with ASC size contributing the most to variance. Despite clustering, relative canal measurements

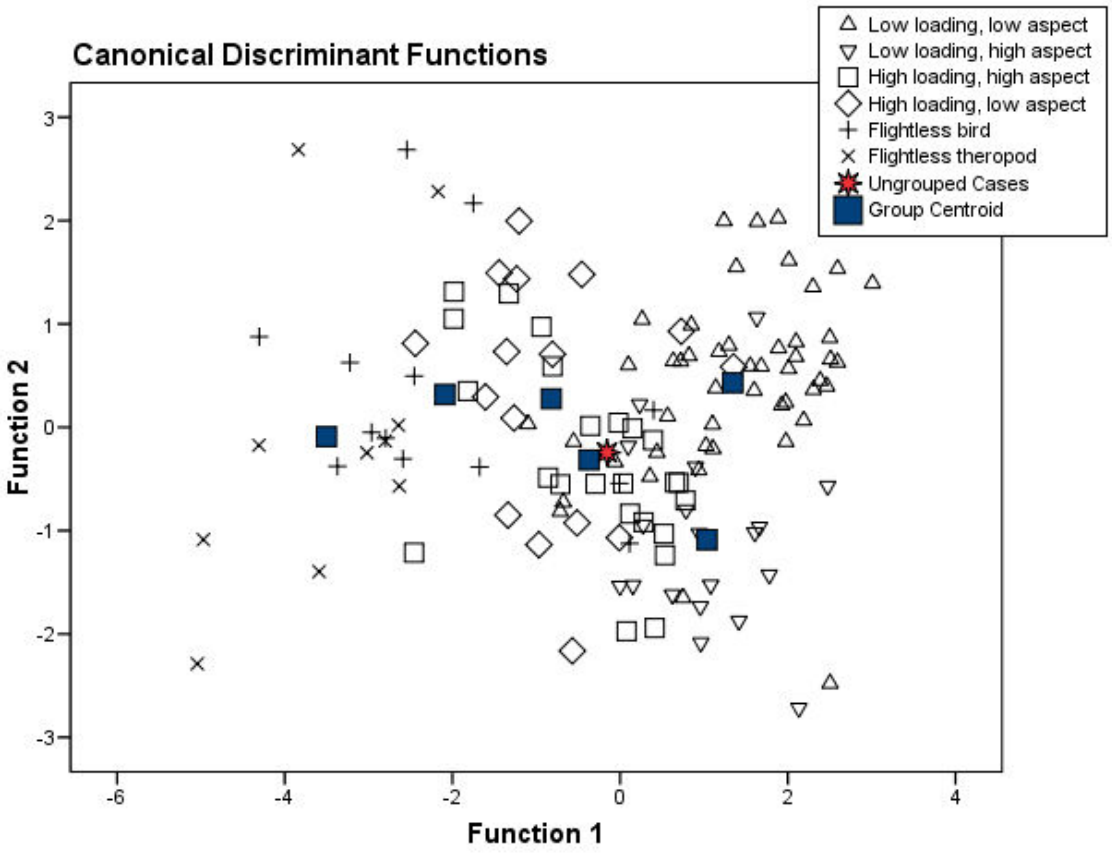

Figure 4–17. Plot of canonical discriminant functions. Scatterplot of the linear discriminant 1 versus linear discriminant 2 resulting from a discriminant function analysis of ASCrel, PSCrel, and LSCrel for n=109 volant birds, plus terrestrial birds and theropod dinosaurs. *Archaeopteryx* is indicated by the one ungrouped case. From left to right, group centroids are follows: flightless theropods, flightless birds, high wing loading/low aspect ratio birds, high wing loading/high aspect ratio birds, low wing loading/high aspect ratio birds, low wing loading/low aspect ratio birds.

can sort specimens into these basic flight categories. Furthermore, non-avian theropod dinosaurs do not overlap with low wing loading birds, nor does *Archaeopteryx* overlap with any non-avian theropod dinosaur points.

Under highest discriminate classification, *Archaeopteryx* is sorted with group 3 (high loading, high aspect ratio), as predicted by Hypothesis 5_1 (*Archaeopteryx* possesses canal dimensions that plot with poorly maneuverable fliers). *Archaeopteryx* does not sort with group 1 (low loading, low aspect ratio) as predicted on the basis of wing morphology alone.

There is also weak separation of species points along function 2 (10.7% of variance), however the largest absolute correlations were found between all three variables and function 1.

Table 4–3. Pooled within-groups correlations between the two linear discriminants resulting from multiple discriminant function analysis (DFA) of relative canal measures.

Level	Linear discriminant 1	Linear discriminant 2
Log10 ASCrel	.985(*)	–.129
Log10 PSCrel	.851(*)	.040
Log10 LSCrel	.914(*)	.274

* Largest absolute correlation between each variable and any discriminant function

Finally, in a preliminary effort to test whether canal size correlates with brachial index (hypothesis 6), a regression analysis of ASCrel was performed against BI data published in Nudds et al. (2007) using a bird sample subset of n=155. Brachial index is

defined as the humerus length/ulna length and has been shown to correlate significantly but weakly with wing loading (ibid.).

Although comparisons between BI and wing kinematics are in their infancy (Nudds et al., 2004a, 2007), it is interesting to note that canal measures correlate weakly ($r^2 = 0.243$) with BI ($p<.001$), providing additional confirmation that relative canal size and wing morphology covary even when body mass is removed from the wing measure. Weak support is found for hypothesis $H6_1$. That is, taking body mass into account, relative ASC size scales inversely with BI. However, using phylogenetically adjusted N for this comparison, $N_{eff} = 26$ and $P_{eff} = 0.015$ (nonsignificant using the Bonferonni correction; refer to Table 4–1).

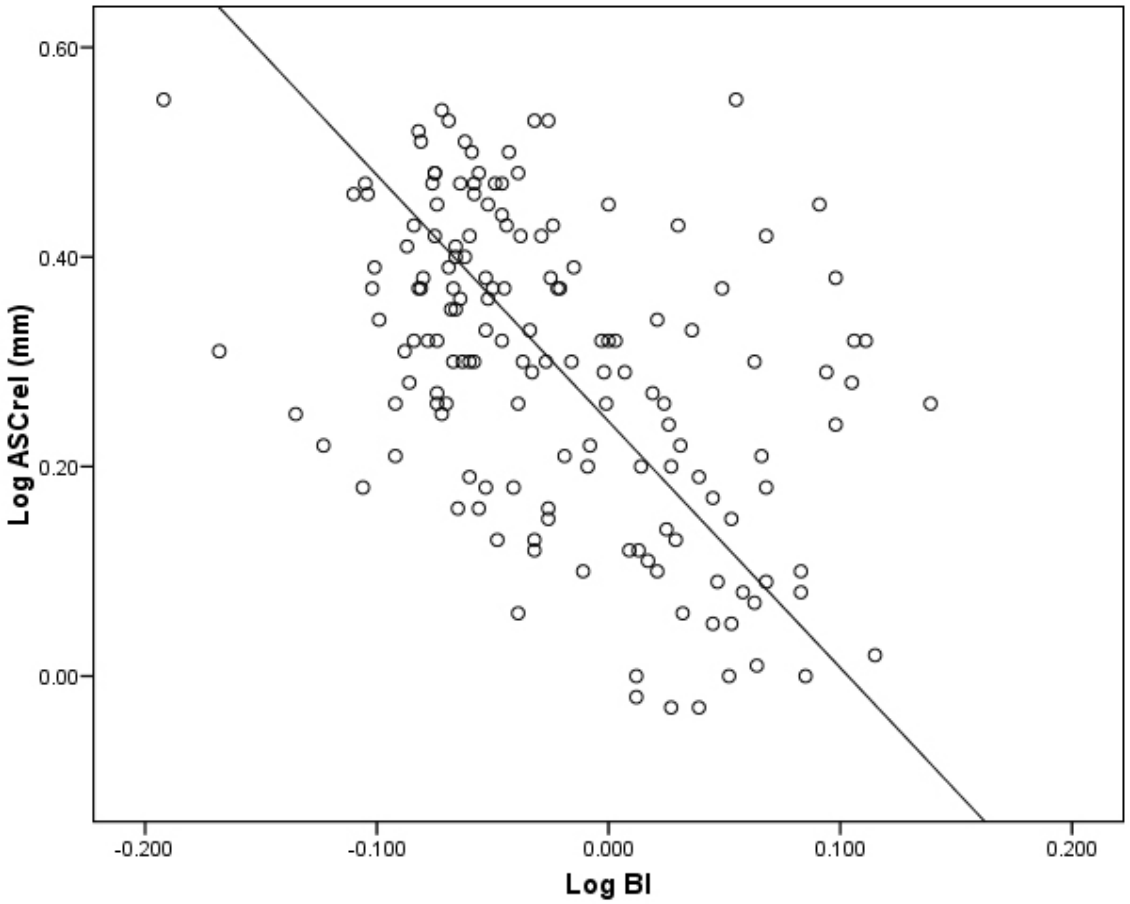

Figure 4–18. Bivariate plot of ASCrel vs. Brachial Index. BI data obtained from the literature. Regression statistics are summarized on Table 4–1.

4.3. Discussion

Bird semicircular canals have previously been noted for their relatively large size (Gray, 1908; Jones and Spells, 1963; Money and Correia, 1972; Sipla et al., 2003). Overall, the canal arcs of birds are shown here to be larger than same-sized mammals and bipedal dinosaurs. For instance, at roughly the same body mass, the golden eagle (*Aquila chrysaetos*) has canal dimensions exceeding 3 times those of the pale-throated three-toed sloth (*Bradypus tridactylus*). Deviations from the general scaling trends have been empirically demonstrated to represent functional attunement of the canal to the movement criteria of species (e.g., Spoor, 2003).

Bipedal dinosaurs are noted for having larger canals relative to similarly sized mammals, though not as large overall as birds. The bipedal dinosaur sample used in this analysis included 10 theropods, 3 prosauropods, 2 basal iguanodontians, and 1 basal ceratopsian for which body mass estimates could be obtained, with body masses ranging from the 12 kg *Psittacosaurus* to the 22,407 kg *Apatosaurus*. It is interesting to note that, overall, bipedal dinosaurs possess larger semicircular canals relative to body size than quadrupeds. There is no particular difference in scale noted between the canals of bipedal carnivores versus herbivores, nor between phylogenetically older or younger species, suggesting that increased arc size is directly related to moving in a cursorial, bipedal way, possibly due to the inertial instability of the head during this form of locomotion. Preliminary analyses of dinosaurian inner ear shape indicated that the anterior semicircular canal of bipedal dinosaurs is more elongate in the vertical dimension (taller inferosuperiorly than wide anteroposteriorly) than quadrupeds (Sipla et al., 2004, in

prep). It is noted here that the average canal radii of bipedal dinosaurs is concomitantly larger, indicating a functional increase in canal sensitivity for these animals.

Curiously, the only quadrupedal dinosaurs plotted on figure 4–5 that overlap with bipeds are the neoceratopsians *Protoceratops*, *Chasmosaurus*, and *Triceratops* (green diamonds). These herbivorous ornithischians possess extremely large, heavily ornamented heads (Dodson et al., 2004), exerting enormous head moments that hypothetically need to be counteracted by vestibular-mitigated neck reflexes. The gait of large-bodied ceratopsids (represented here by *Chasmosaurus* and *Triceratops*) is a matter of some debate. While undoubtedly quadrupedal, it has been claimed on the basis of anatomical and trackway evidence that large graviportal ceratopsids were capable of full galloping locomotion (Paul and Christiansen, 2000), in a manner similar to extant rhinoceroses. Such behavior, if substantiated, would result in high levels of uncompensated angular motion, especially in the pitch plane. Increased demands on neck stability in neoceratopsians may relate to the canal adaptations observed here. The large canal size observed for neoceratopsians may be an artifact of the technique used to estimate body mass for these specimens. Body mass for *Protoceratops* is estimated at 23.7 kg using the polynomial method (Seebacher, 2001), compared with a higher estimate of 177 kg using a scale model immersion technique (Colbert, 1962). Similarly, estimates for *Triceratops* give a polynomial mass of 4,963.6 kg, compared to other published estimates of 8,480 kg (Colbert, 1962) and 6,000 kg (Alexander, 1989). While the polynomial method performs rather conservatively for other taxonomic groups within Dinosauria, with estimates typically falling in the mid-range of other published values, in the case of Ceratopsia the method produces noticeably smaller values. Clearly, the poor

accuracy of dinosaurian body mass estimates is a hindrance to interpretation. It would be useful to devise alternate methods for comparing semicircular canal size across dinosaurian and bird taxa that don't rely on body mass. Unfortunately, given the variable and rarely complete nature of preservation in fossils, this remains a challenge.

Though extreme shape differences between birds and bipedal dinosaurs have been noted, especially in the anterior canal (section 4.1), comparative length of the canal circuit is found to be relatively similar in poor flying galloanserimorphs (waterfowl and gamefowl), dromaeomorphs (tinamous), and terrestrial ratites and bipedal dinosaurs. Collectively, these avian groups have the smallest canal dimensions relative to body size, even among bipedal dinosaurs, suggesting that the neurosensory demands of cursorial bipedalism do not differ significantly from those of high-speed aerial locomotion, in so far as such demands pertain to semicircular canal size.

However, ASC and LSC size (but not PSC size) were shown to be differentially expanded in birds compared to bipedal dinosaurs. This may relate to the higher frequency pitch-down rotations experienced during flapping flight and thus indicate a subtle difference in canal morphology between poor-flying volant bird taxa and flightless dinosaurs. This was confirmed by the discriminant function analysis, which separated flightless taxa from poor flying taxa on the basis of weight-adjusted canal measures. In that analysis, relative ASC and LSC size had larger unique contributions to the discrimination specified by function 1 than did relative PSC size (table 4–3).

By contrast, highly maneuverable birds of prey (falconiforms and strigiforms) have the largest overall canal dimensions relative to body mass, most plausibly to match the fast body rotations that characterize low speed maneuvering during pursuit.

A limitation of interpreting residuals is the poor fit of the bird regressions. Better sampling at low body mass—requiring more extensive use of microtomography scanning—would expectedly increase the correlation coefficient of the model lines. For instance, given the available data, SCc is highly correlated with body mass ($p<.001$) among volant birds, but the poor fit of the regression line (figure 4–5; $r^2 = 0.451$) indicates that factors other than simple size scaling contribute in a significant way to variation in bird canal size, more so than for bipedal dinosaurs ($r^2 = 0.838$). It is plausible that the demands of aerial maneuvering in a three-dimensional environment require greater adaptive plasticity of inner ear size, but this is cautiously unconfirmed by the present analysis. The better fit of the bipedal dinosaurian regression line may simply be an artifact of relatively poor sample size.

4.3.1. Interspecific variation in canal size

Regarding ASC circumference, there is very little difference between paleognaths (terrestrial ratites and poor-flying tinamous) and volant galloanseres. Consequently, the neoflightless condition in the galloanserean steamerducks (genus *Tachyeres*) does not correspond with reduced semicircular canal size relative to flighted galloanseres (figure 4–15).

The extinct moa *Dinornis* is noted for having particularly small semicircular canals. The unusual slowness of movement in moas is well documented by eighteenth century descriptions (Alexander, 1989), though recent mechanical models (Blanco and Jones, 2005) suggest that moas were biomechanically capable of extraordinary speed,

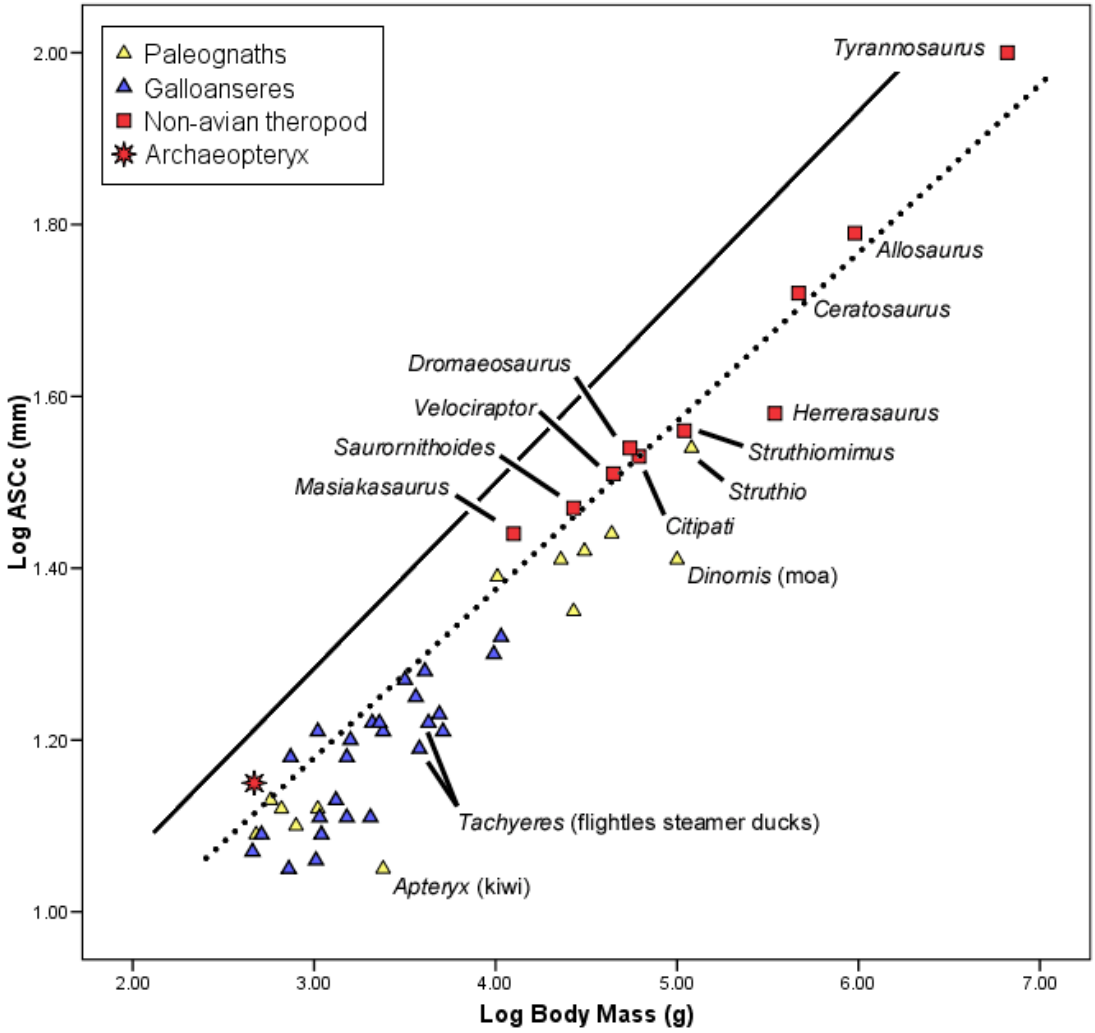

Figure 4–19. Bivariate plot of ASCc vs. BM for paleognaths, galloanseres, and non-avian theropod dinosaurs. Anterior semicircular canal circumference (ASCc) plotted against body mass (g) for paleognaths and galloanseres, and 10 non-avian theropod dinosaurs. Regression lines indicate reduced major axis regressions for all birds (solid line) and all bipedal dinosaurs (dotted line), as computed for figure 4–8.

even though it may not have been practiced. Similarly-sized ostriches are competent runners despite their large size (Hutchinson, 2004a), and have concomitantly larger anterior canal dimensions. The smallest (and least mobile) living ratite, the kiwi (*Apteryx*), has a very small anterior canal relative to body mass, even when compared to other ratites. Interestingly, the moa is the only neoavian taxon examined that lacks the characteristic bending of the common crus, or the posteromedial excursion of the anterior canal (figure 4–4i) seen in all other birds, including *Archaeopteryx*.

Because of their high wing loading, ducks, geese, pheasants, and tinamous all must fly rapidly by beating their wings to stay aloft, necessitating a high airspeed velocity with resultant poor maneuverability at low speeds. Many pheasants and especially tinamous move about mostly by walking, and several are prone to run rather than fly when alarmed (Proctor and Lynch, 1993). In phasianids, flight typically begins as a burst of high-frequency wingbeats, followed by short glides and a quick return to the ground (Sibley, 2001; Madge and MacGowan, 2002). Anseriforms (ducks and geese) are quite different in being highly migratory, often traveling considerable distances at high altitudes over water and land. Speed is argued to be a predominant factor selecting for small wing size (poor maneuverability, fast flight) in this lineage (Rayner, 1988a). Air currents during autumn migrations may be unfavorable, and higher flight speeds may give migrating ducks and geese greater headway during these conditions (ibid.). Waterfowl are also aquatic, and birds that swim underwater using their wings (e.g., auks, diving petrels) typically have small wing morphs. However, this does not explain the small wings of most ducks and geese (except eider ducks) that mostly swim with their

wings folded against the body (ibid.). Whatever the cause, high speed flight places limits on aerial maneuvering and the canals of galloanserimorphs reflect that limitation.

Regarding non-avian theropod dinosaurs, the primitive *Herrerasaurus* possesses the smallest anterior canal size relative to body size. As an early representative of both Dinosauria and Theropoda, *Herrerasaurus* is reconstructed as an agile, bipedal predator (Sereno and Novas, 1992). The hypothetical ancestor of Dinosauria is likely to have been a small biped (Sereno 1997; Gatesy, 2002) and the slightly smaller size of the anterior canal in *Herrerasaurus* may represent an early sensory attunement to habitual bipedal locomotion, though I can only speculate. Interpretations of theropod canal size must cautiously be checked by the lack of confidence in body mass estimates.

Tyrannosaurus has the largest anterior canal, in both relative and absolute size, of any bipedal dinosaur examined. Among tyrannosaurids and theropods in general, *Tyrannosaurus* is noted for its extreme large size (Erickson et al., 2004) and inferred slower body movements (Newman, 1970; Alexander, 1985, 1989; Farlow et al., 1995; Hutchinson and Garcia, 2002). Myological reconstructions of the *Tyrannosaurus* hindlimb indicate that it could probably not run at a fast pace (Hutchinson and Garcia, 2002), and others have demonstrated that such a large cursor would incur serious self-sustained injury if it tripped while doing so (Farlow et al., 1995), but it is likely that juveniles of *Tyrannosaurus* and smaller tyrannosaurids could maneuver at high speeds to acquire prey (Holtz, 2004). Another explanation for the large anterior canal size of *Tyrannosaurus* may be found in its inferred method of prey capture. Erickson and colleagues (1996) calculated the forces generated by *Tyrannosaurus* jaws and found them to among the highest of any known carnivores (as high as 13,400 N during feeding),

including other theropods. Puncture marks found on ornithischian bones from tyrannosaur-bearing deposits indicate the long teeth of tyrannosaurs frequently contacted bone (Erickson and Olson, 1996, Erickson et al., 1996). I suggest that the reaction forces encountered during such behavior, possibly resulting from increased reliance of tyrannosaurids on the jaws to acquire food (owing to their reduced forelimbs), may explain anterior canal enlargement in this taxon. The next largest carnivore analyzed here, *Allosaurus*, is reconstructed as having a significantly weaker bite force (~2,000 N) than *T. rex*, relying instead on "slash and tear" attacks rather than muscle-driven bites (Rayfield et al., 2001).

All other theropods are tightly fit to the ASCc vs. BM regression line ($r^2 = 0.87$) for bipedal dinosaurs (figure 4–19), including those closest in relation to *Archaeopteryx* (dromaeosaurids and troodontids). Hindlimb features of theropods are fairly conservative, and despite 150 million years of diversity the entire group employed the same primary locomotor mode: a "striding, digitigrade bipedalism" (Farlow et al., 2000, p. 659). It is not surprising that the canal adaptations of the group are also conservative and indiscernible in morphology from those of noncarnivorous dinosaurian bipeds. There is no evidence of increased canal size in maniraptorans relative to other coelurosaurs, other basal theropods, or other bipedal dinosaurs.

In the discriminant function analysis, *Archaeopteryx* was sorted with high loading/high aspect ratio birds, consistent with the hypothesis that it was poorly maneuverable in flight. The only semicircular canal that is entirely preserved in *Archaeopteryx* is the anterior canal, which is found to be scarcely larger than similarly sized tinamous and ducks. Reconstructions of *Archaeopteryx* as a fast-flying bird poorly

adapted to low-speed maneuvering may be valid, based on morphological evidence from the wing skeleton (e.g., Poore et al., 1997; Rayner, 2000) and is consistent from a neurosensory standpoint. Extreme enlargement of the ASC does not characterize basal Avialae, though it should be remembered that the *shape* of the ASC in *Archaeopteryx* is distinctly avian in character and departs noticeably from the maniraptoran configuration. This is most likely due to relative enlargement of the brain in basal Avialae, conceivably as a result of adaptation to the visual demands of flying.

The "preconditions" for vestibular attunement to high speed flapping flight, as far as canal size is concerned, were already present in nonavian bipedal dinosaurs. Subsequent enlargement of the cerebrum, optic tectum, and cerebellum in ornithurine birds (as demonstrated, for instance, by the Melovatka braincase [Kurochkin et al., 2007]) likely corresponds with acquisition of a more definitively shaped avian labyrinth, though this remains speculative until the canals can be visualized in ornithurine taxa.

More striking differences between volant forms and closely-related terrestrial taxa are demonstrated by plots of pellicaniform (figure 4–20), psittaciform (figure 4–21), and gruiform and ralliform (figure 4–22) taxa.

Storks and pelicans (figure 4–20) are heavy birds with wide wingspans. Both groups use a soaring, gliding flight, requiring constant, instantaneous adjustments of wing position during banking maneuvers (Pennycuick, 1975; Spear and Ainley, 1997). Overall, this group is marked by large anterior canal sizes. Brown pelicans (*Pelecanus occidentalis*) differ from other pelicans in using a peculiar form of plunge diving to acquire prey, and, interestingly, are found to have the largest canal dimensions of any pelicans. When foraging, the brown pelican enters a steep dive from flight, entering the

water head-first with the wings folded back (Sibley, 2001). Unlike sulids (boobies and gannets), these birds do not completely submerge but instead splash down on the water surface, coming to a percussive halt (ibid.). Other pelicans gather fish while floating on the waterline.

Boobies and gannets are skilled at diving from extreme heights (as much as 90 meters above the water surface) and pursuing fish underwater, using their wings for propulsion (Nelson, 1978), whereas cormorants dive from the surface and are observed to have markedly reduced canal sizes. The flightless cormorant, *Phalacrocorax harrisi*, has lost the ability to fly altogether, and has the smallest canals of any pelicanimorph, lying well below the regression line for bipedal dinosaurs. Exceptionally maneuverable frigatebirds, notable in having very low wing loads despite their large body size, have relatively large semicircular canals, possibly reflecting their habit of aerial kleptoparasitism.

Within closely related parrot species, volant parrots have larger canals than the critically endangered flightless kakapo (*Strigops habroptilus*) (figure 4–21). Parrots are generalist fliers, having wings of medium aspect ratio and medium loading (Rayner, 1988a). It should be noted that unlike most other terrestrial birds, the kakapo was found by Iwaniuk and colleagues to have a smaller relative brain volume than flying birds in general (Iwaniuk et al., 2004).

The situation with gruiforms and ralliforms is more complex, with flightless and weakly volant species often having larger canal sizes than volant forms (figure 4–22). In this lineage, the terrestrial phorusrhacoid "terror bird" *Psilopterus* (Mid-Miocene of Patagonia) is found to have relatively large canals compared to most volant (albeit poor-

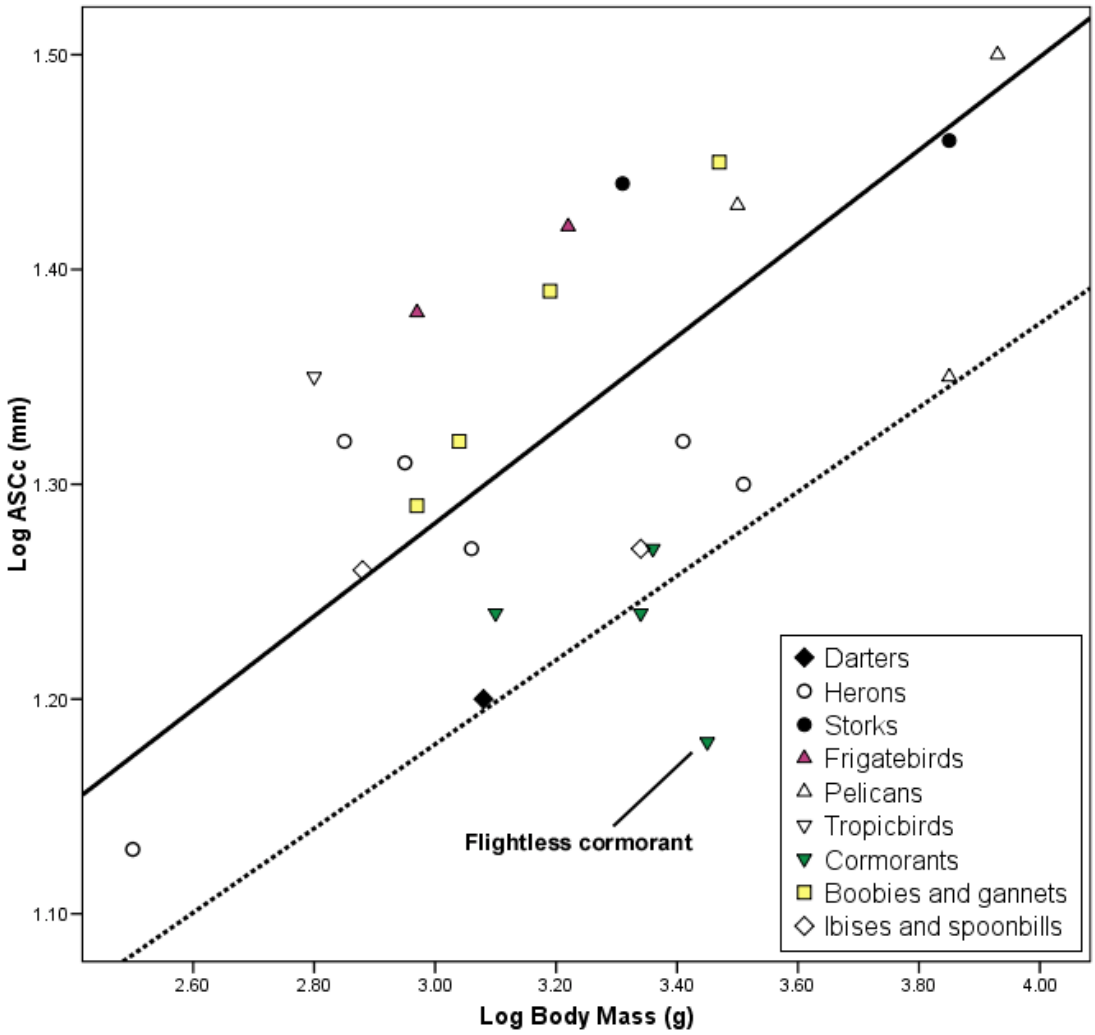

Figure 4–20. Bivariate plot of ASCc vs. BM for "pellicaniforms." Anterior semicircular canal circumference (ASCc) plotted against body mass (g) for pelicanimorphs and ciconiimorphs (sensu "pellicaniforms," Cracraft et al., 2004). Regression lines indicate reduced major axis regressions for all birds (solid line) and all bipedal dinosaurs (dotted line), as computed for figure 4–8.

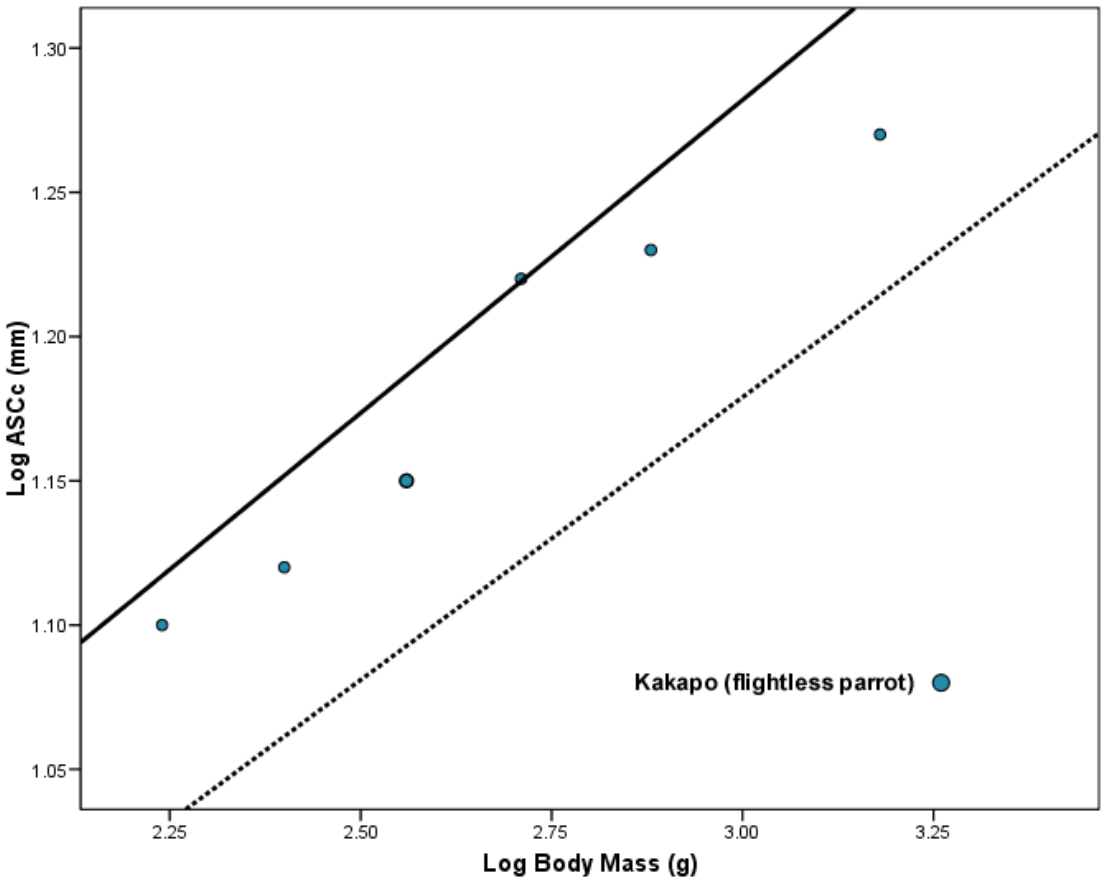

Figure 4–21. Bivariate plot of ASCc vs. BM for psittaciforms. Regression lines indicate reduced major axis regressions for all birds (solid line) and all bipedal dinosaurs (dotted line), as computed for figure 4–8.

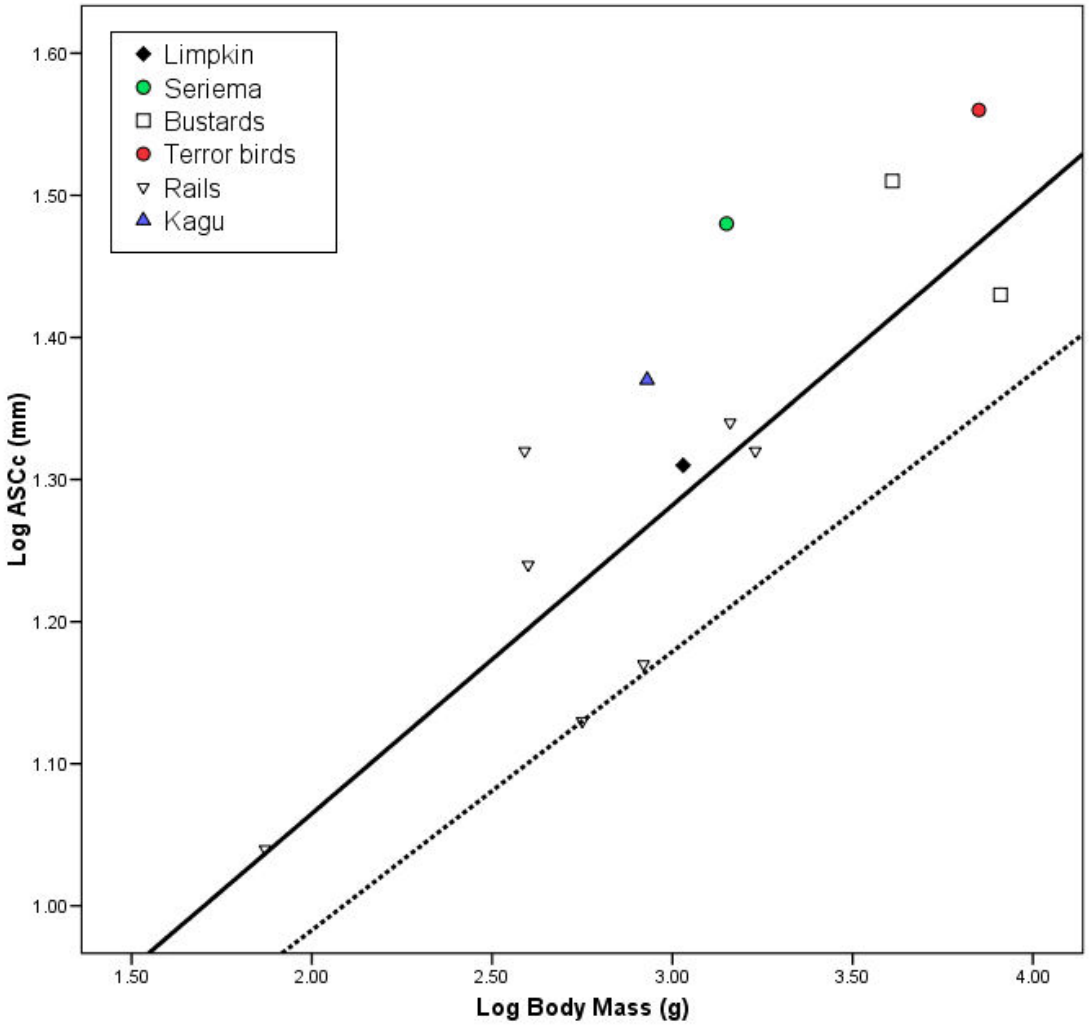

Figure 4–22. Bivariate plot of ASCc vs. BM for gruiforms and ralliforms. Regression lines indicate reduced major axis regressions for all birds (solid line) and all bipedal dinosaurs (dotted line), as computed for figure 4–8.

flying) rails. Now extinct, small-bodied (~7 kg) terror birds like *Psilopterus* are interpreted as lightly built, top-level predators, capable of high speed maneuvering on the ground comparable to the fastest extant mammalian carnivores (Blanco and Jones, 2005). Extant seriemas (*Cariama cristata*) are relatives of phorusrhacids (Alvarenga and Höfling, 2003) and frequently run rather than fly, here also found to possess relatively large canals. The kagu (*Rhynochetos jubatus*) also possesses relatively large canals. This predominantly terrestrial species is also a rapid runner, noted for locomoting in short, darting bursts, punctuated by brief episodes of motionlessness (Hunt, 1996). Most volant rails, on the other hand, have relatively smaller canals than these terrestrial taxa. Similar to galloanseriforms and tinamous, rails have highly loaded wings and poor maneuverability in flight. It is unclear why canal size does not seem to match expectations based on locomotor habit for the more terrestrial gruiforms and ralliforms. More work is needed to understand the factors underlying the unusual canal size of these birds.

Semicircular canal size does not correlate strictly with flightlessness in all clades. Many species that do not fly or fly infrequently are found to possess relatively large semicircular canals in some lineages (gruiforms), but relatively small canals in others (pelecaniforms, psittaciforms).

Primitive avialans like *Archaeopteryx* inherited inner ear sensors from animals already adapted to moving in a cursorial, bipedal manner (Hutchinson, 2004b). The demands of high speed flight, as employed for instance by galloanseriforms and *Archaeopteryx*, do not appear to require evolutionary modification for larger canals to successfully aerially locomote.

Secondary flightlessness in birds does not *de facto* indicate a reduction in canal size. Ground-dwelling phorusrhacids, seriemas, and kagus all have exceptionally large anterior semicircular canals, whereas the moa and kiwi canals are reduced in size. The difference between these birds is degree of terrestrial maneuverability, not shared flightlessness. Most secondarily flightless species, however, do possess overall reduced canal sizes relative to other birds, as seen in the flightless cormorant, flightless parrot, and all palaeognaths. Those neornithine birds lying outside the Neoaves radiation, specifically palaeognaths and galloanserimorphs, all appear to have retained a canal size proportionate to similarly sized bipedal dinosaurs. Secondarily flightless neoavian taxa may have simply retained larger canals from a volant ancestor, encountering no selective pressure to reduce canal size.

4.3.2. Canal size and flight behavior

There are no experiments known to this author that document the maximum rotational capabilities of vertebrate fliers. The reasons for this are mainly due to the technical challenges of reconstructing pitch, yaw, and roll angles during observable, aerial maneuvers (Dudley, 2002). Nor have the maximum or typical angular accelerations experienced during maneuvering been compared among different fliers (ibid.). As a result, we must presently look to descriptors of aerial maneuverability derived from wing theory, to assess in broad terms the ecomorphological specialization of taxa to turning performance.

Birds that frequently maneuver at lower speed do appear to possess more sensitive (larger) canals, reflecting their aerobatic proficiency (Figure 4–23). Comparisons between canal size and aspects of aerial maneuverability, as inferred from wing design, strongly support the conclusion that canal size and locomotor agility are indeed linked.

Birds characterized as highly maneuverable (low wing loading) and agile (low aspect ratio) were found to have relatively larger LSC dimensions than less agile birds (Figure 4–16). Birds turn in flight by initiating a rolling bank, a movement which excites all three semicircular canals. That LSC size was the only circuit found to be comparably larger in highly maneuverable and agile birds, may indicate a spatial constraint for extreme canal enlargement in these taxa. Hypertrophy of the lateral canal in falconiforms, strigiforms, apodiforms, and other aerobatic taxa is achieved by moving the origin of the lateral canal to the medial side of the posterior utricle (Figure 4–1c). The lateral canal originates from the posterior aspect of the utricle in less agile taxa.

Analysis indicates that *Archaeopteryx* had semicircular canals adapted for flight (a conclusion reached by Dominguez and coworkers [2004]) but not adapted for low speed maneuvering (predicted by, e.g., Poore and coworkers [1997] and Rayner [2001]). Reconstruction of the primitive avialan as a high speed flapping flier with poor aerial maneuverability is warranted. These findings must be cautiously checked, however, because only the ASC is completely preserved in the London *Archaeopteryx* specimen and the LSC and PSC values obtained for this analysis represent uncertain values. The same is true to a lesser extent for the ASC measurement, as I did not personally examine this specimen. The “external diameter of anterior canal” measure reported by Dominguez et al. (2004), on which my analysis was based, is slightly larger than would be obtained

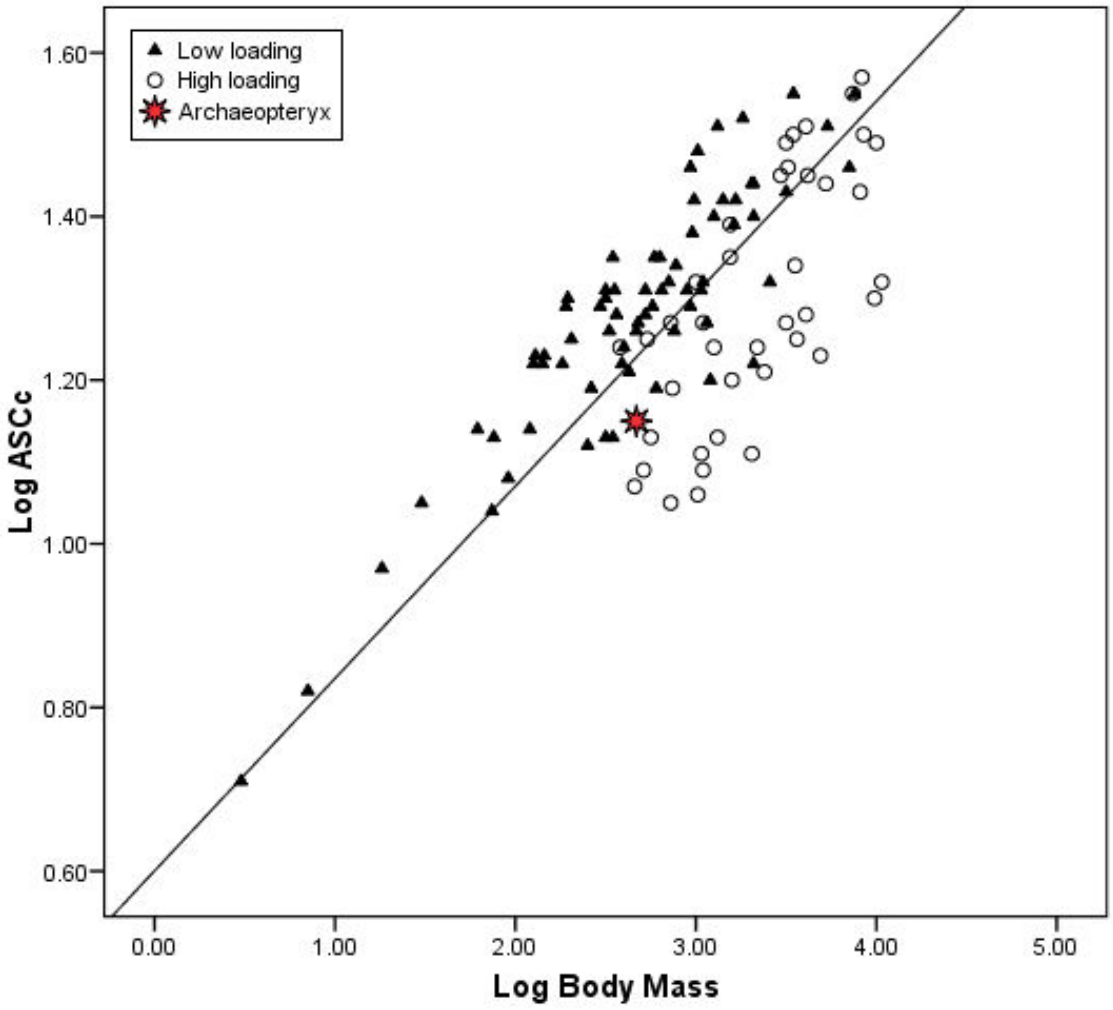

Figure 4–23. Bivariate plot illustrating the relationship between canal size and wing loading. ASCc plotted against BM for n=109 volant birds plus *Archaeopteryx*. Fitted line represents reduced major axis regression ($y=0.235x + 0.600$; $p<0.001$; $r^2 = 0.547$). Bird points are parsed into low wing loading (<76.77) and high wing loading (>76.77) groups to aid with visualization. Overall, birds with lower wing loads have larger semicircular canal dimensions than similarly sized birds with high wing loads. Wing shape data obtained from the literature.

by my methods. Furthermore, I transformed this measure to a circumference measurement by computing the circumference of a circle with the given diameter, so there is unavoidably some noise in the *Archaeopteryx* comparisons.

Given that wing outlines are rarely preserved in the fossil record (*Archaeopteryx*, *Confuciusornis*, *Eoalulavis*, and putative gliding taxa like *Microraptor gui* providing noteworthy dinosaurian exceptions), it is interesting to note that both wing loading and relative ASC size correlate (albeit weakly) with brachial index. It may therefore be possible to assess the maneuverability of fossil avian taxa using wing-bone proportions in combination with canal measures.

Overall, good corroboration was found between canal size and degree of aerial maneuverability (minimum turning radius) in birds, as predicted by wing theory, with the most maneuverable birds having the largest canals relative to body mass. The most agile birds (those capable of entering a roll quickly) were also found to have relatively larger LSC dimensions. Canal size correlates well with multiple ecomorphological aspects of flying behavior. For instance, higher wing loads necessitate faster minimum air speeds, requiring larger minimum turn radii (low maneuverability), and this is matched by relatively small canal sensors. The reverse pattern is also true. Lower wing loads permit slower air speeds and smaller minimum turn radii (high maneuverability), matched to relatively large canal sensors. Qualitative assessments of the relationship between locomotor "agility" and canal size (Spoor, 1993; Spoor et al., 1996, 2007; Spoor and Zonneveld, 1998; Sipla et al., 2003; Walker et al., 2003, 2004) are here confirmed by quantitative (though inferential) data derived from wing theory. To bolster these findings, future workers should ideally document kinematic patterns of head movements

experienced during flight and compare these findings with those predicted by wing theory. It is key to remember that wing loading does not indicate whether a flier can or cannot maneuver at low speeds—all birds have to maneuver slowly when they take off and land—but rather this indicates a general ecomorphological specialization for such ability. Maximum accelerations experienced in typical flight, and to which the canal apparatus may be attuned, may differ.

Chapter 5:
Synthesis

This analysis has been concerned primarily with establishing a correlation between relative canal arc size and locomotor repertoire in birds. Degree of aerial maneuverability was shown to have a significant relationship with semicircular canal arc size in birds that fly, with the most maneuverable and agile fliers having the largest canals relative to body size. This is taken as strong support for previously established links between canal arc size and locomotor behavior in other vertebrate groups. As well, it indicates that the neurosensory demands of low-speed flapping flight may be causal factors in selection for large canals.

5.1. Summary of the dissertation

The anterior and lateral canals of birds were found to be preferentially, albeit subtly, larger in relation to body size than those of nonavian theropod dinosaurs. These canals, particularly the anterior canal, are preferentially excited by pitch-down movements of the head, as would be experienced frequently in the natural course of wing-beating, particularly at low speed. Excitation of anterior and lateral canal afferents directly activates neck extensor muscles useful in counteracting these pitching moments and stabilizing the head. All birds must fly at slow speed, and though some birds exhibit ecomorphological specializations for slow flight speeds, and consequently have larger canals relative to body mass, slow maneuvering is essential for all birds during takeoff

and landing procedures, and to facilitate attitude corrections in response to unpredictable substrate variations.

As far as is known theoretically and experimentally, slow flight entails use of a vortex-ring gait by all birds, regardless of wing morphology (Rayner 1985b, 1988a, 1991a). Because the weight of the animal is only supported during the downstroke of this gait type, birds in slow flight experience frequent upward lift-generated accelerations with each downstroke (Warrick et al., 2002), similar in many ways to the stresses encountered by terrestrial bipedal dinosaurs during locomotion on a surface substrate. Relative enlargement of the anterior semicircular canal in all bipedal dinosaurs, including all theropods hitherto studied, this work inclusive, likely predisposed basal birds to the kinds of accelerations experienced during flapping flight. Once powered flight evolved, this system was modified to accommodate body oscillations associated with flapping flight occurring at much higher frequencies than during terrestrial maneuvering, upwards of 10 sec^{-1} for typical avian wingbeat frequencies. Furthermore, the saltatory nature of low speed flapping flight, combined with the incremental force asymmetries generated by the asymmetrically deployed wings during turning maneuvers, produce very high angular accelerations with each downstroke.

Selective pressure for increased anterior and lateral canal size relative to body mass was therefore favored by birds, presumably to increase the gain of the sensors largely responsible for offsetting head perturbations in the pitch plane through activation of the VCR (Wilson and Maeda, 1974; Shinoda et al., 1996). Active flapping flight provides inherent stability in the yaw and roll planes due to the laterally projected centrifugal forces created by the rapidly beating wings, but the pitch axis remains

unstable and must be counteracted. In maintaining axial balance, vestibular cues predominate over visual and somatosensory cues when maintenance of trunk posture is critical for good performance (Horak, 2007). Maintaining pitch control through enlargement of ASC and LSC dimensions in birds is one interpretation of the canal data obtained here, one that could be confirmed experimentally by analysis of flight kinematics over a range of flight behaviors, combined with electromyographic (EMG) recording of neck muscles during flight-generated oscillations.

Differences in ASC and LSC enlargement relative to PSC are small, however, and the overall enlargement of the canal system (all three canals) observed in birds would provide gain advantages during banking maneuvers. Birds turn by establishing a bank angle and executing a body roll, a movement which excites all three canal pairs if the maneuver is carried out during level, forward flight. Many birds, however, enter a diving roll when turning, as during the pursuit of prey, especially in raptors (personal observation), and here again the ASC and LSC are preferentially excited. That the most agile birds were found to have relatively larger LSC dimensions (but not ASC or PSC) permits one of three conclusions, either (1) initial banking force asymmetries during roll initiation cause higher amplitude lateral accelerations, reflected in greater LSC size for agile birds; (2) LSC enlargement in these birds has nothing to do with agility but instead reflects high aerial maneuverability, because lateral accelerations are known to peak during the sharpest point of a slow, flapping turn (Rayner and Aldridge, 1985; Aldridge 1986), not at turn initiation; or (3) some combination of both.

It should be remembered that the canals respond to angular head accelerations of any kind, not just those induced by locomotion. The degree to which feeding behaviors,

non-aerial courtship displays, and similar activities relate to canal size variation is presently unknown. Such influences on canal evolution may never be known, and would be difficult to assess experimentally. For this reason, canal sensors must be attuned to rather broad frequency spectra of possible movements encountered over the course of daily functioning, not necessarily the (potentially) narrower range of head movements experienced during locomotion.

This is not a hopeless view, however. Rotary head movements associated with gait are ubiquitous in cursorial animals, especially predators, and perhaps even more so in avian taxa. Birds are so definitely specialized for flight in nearly every aspect of their anatomy that it is reasonable to expect neurosensory specializations for flight to closely follow the kinematic particulars of their locomotion. Poor balance among terrestrial cursors may result in a fall, perhaps injury. Poor balance among flying taxa may result in fatality, especially given the cluttered habitats occupied by many highly maneuverable taxa (like passerimorphs and near-passerine birds) and the threat of predatory birds to avian prey in some areas. Lacking reliable somatosensory cues from interaction with a terrestrial substrate, birds in flight are hypothetically more reliant on vestibular cues than flightless relatives, and this may explain the general reduction in canal size evinced by such non-aerial exemplars as the flightless cormorant, kakapo, and ratite taxa. Not all flightless birds have relatively smaller canals, however, as seen in the flightless rails and gruiforms. Many of these taxa, such as the kagu, are described by field observers as making quick, darting movements on the ground, but higher-order derivates of head position with respect to time, such as the rate of change of acceleration (jerk), have not been quantified by observation. The large canals of these flightless taxa may simply be

due to retention of sensitive canal systems from a highly aerobatic ancestor, encountering no selective pressure to reduce canal size once landbound. In a recent morphological-based phylogeny (Livezey and Zusi, 2007), Gruiformes and Ralliformes were nested securely within the Subdivision Telmatorae, which has as its sister group the Subdivision Dendrornithes, a group that includes the highly aerobatic falconiforms and strigiforms. The large canals of terror birds and other gruiforms may simply be an artifact of phylogeny.

Figure 5–1 depicts a summary phylogeny of extant avian genera from this analysis whose relationships are resolved by the phylogeny of Livesy and Zusi (2007). A single discreet character was optimized on the tree, using Mesquite v. 1.12 (Maddison and Maddison, 2006). The character is 'average relative semicircular canal size' for each genus (specifically, average canal size for all three canals, divided by the cube root of body mass, then averaged for all species in the genus). The character was parsed into two states by comparing the value for each genus to the average relative SCc value for all birds (1.64). Below that number, taxa were assigned to state 0 (small canals). Above that number, taxa were assigned to state 1 (large canals). Because canal size data is not amenable to conversions into discreet states in this way, and because variation in canal size exists within genera, this is an extremely simplistic effort to look at canal size evolution in Neornithes. Nevertheless, the data generally show that there was an increase in canal size within Neoaves, and that Gruiformes and Ralliformes appear to retain large semicircular canals from a common ancestor, despite their general poor flying capabilities. However, the trend in reduction of canal size among flightless representatives of parrots, cormorants, and other taxa (not depicted in Figure 5–1),

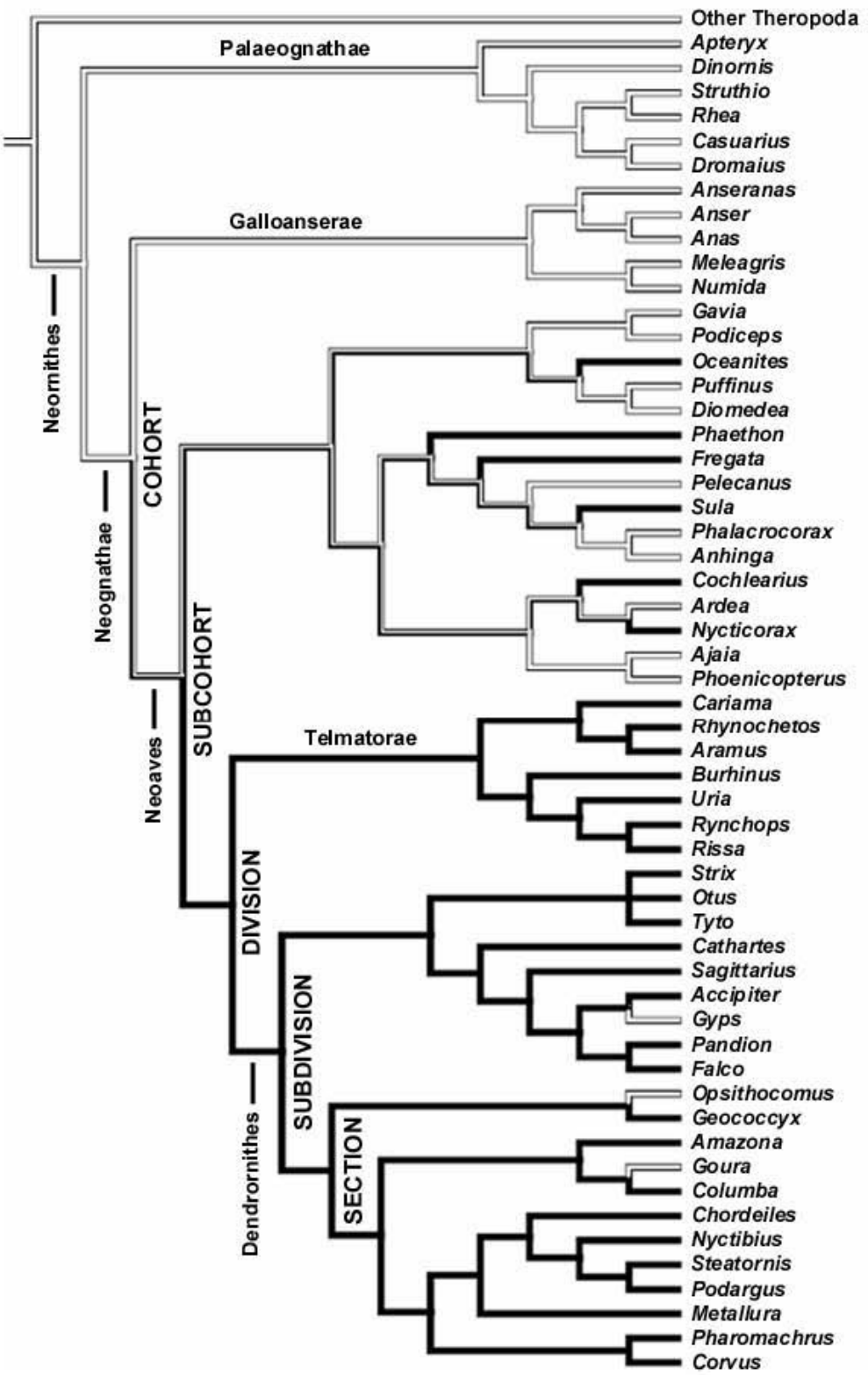

Figure 5–1. Evolution of canal size in Neornithes. Clades with open lines denote relative semicircular canal size below the average for all taxa in this study. Clades with solid lines denote canal dimensions above the average for all taxa. Refer to text.

compared with closely related volant allies, suggests that large canal size in flightless gruiformes is related to degree of terrestrial agility. Without kinematic descriptions of locomotor behavior, we can only speculate.

Many of the largest semicircular canal morphs were found among raptorial taxa (owls and falconiforms). Canal adaptations in these birds might best be understood in the context of their role in visual stabilization. Raptors must fixate their vision on frequently distant, often aerial targets, to acquire prey. These same birds typically employ a gliding or soaring flight that is inherently less stable than flapping flight due to susceptibility to turbulence. Visual acuity in these birds is an order of magnitude greater than, for instance, a common pigeon (Martin, 1993), and canal adaptations in raptors may relate more to high-gain control of the VOR to permit stable gaze during aerial maneuvering, than to maneuvering alone. Diurnal raptors possess two foveal specializations in each eye, with the temporal fovea being more pronounced in species that capture prey on the wing, compared to those that scavenge on the ground (Nalbach et al., 1993). More generally, the most impressive aspect of the avian brain relates to the size and development of the visual system, in particular the mesencephalic tectum (Shimizu and Karten, 1991), and the falconiforms share with corvids (crows) the distinction of having some of the largest brain volumes relative to body size of any bird taxa (Mlikovsky 1989a, b, c, 1990). It also happens that falconiforms have the most maneuverable and agile wing morphs, combined with the largest canals relative to body size, so teasing apart which aspects of canal morphology relate to flight behavior, and which relate to visual behavior, is presently impossible. Of course, both visual and vestibular systems are

operationally linked by the VOR and OKR, and relative largeness of scale between both systems may indicate mutually dependence of function.

Many of the smallest canal morphs among volant taxa were found for galloanserimorphs and tinamous. It is deduced that clade specificity of canal size within Neornithes is mostly due to the fact that birds of similar taxonomic rank fly with kinematic similarity and employ similar flight styles. Fully nested ANOVA indicated that variance in raw canal size was highly accumulated at the ordinal and familial levels. Phylogenetic effects certainly factor into relative canal size among avians. Interspecific differences of locomotor style within families are also important, as demonstrated by closely related flightless and volant taxa.

A more targeted analysis of semicircular canal size variation within a single family or even genus may prove fruitful in discriminating between finely contrasted modes of aerial maneuverability in bird taxa. The rationale of this study was to determine how semicircular canal morphology varied among bird taxa irrespective of phylogenetic relationships. Uncertain phylogenetic relationships among birds make difficult the interpretation of data from phylogenetically-corrected statistics. I recognize that inclusion of phylogenetic information, such as by independent-contrast analysis (Felsenstein, 1985; Harvey and Pagel, 1991), might alter my conclusions, and that by ignoring phylogenetic relationships there is an increased probability of committing type I error even when incorrect topology or unknown branch lengths confound relationships (as advocated, for instance, by Nunn and Barton, 2001). For the present analysis, the statistical independence of data points was estimated using effective sample sizes, as prescribed by

Smith (1994), and correlations between canal size and body mass were found to be strongly significant ($p<.001$) even after taxonomic partitioning of variance.

Although uniform canal enlargement in birds increases the gain (sensitivity) of the sensors, permitting finer discrimination between changes in angular acceleration and velocity, and hypothetically finer control of canal-mitigated reflexes, it does so at the expense of velocity-sensitive bandwidth (sensu Rabbitt et al., 2004; Highstein et al., 2005). It is assumed that bandwidth of the avian semicircular canal system is sufficient to operate within the normal range of head movements associated with flapping flight, but paradoxically the frequency content of such movements would expectedly occur over a wider bandwidth, not narrower, in aerial taxa. A wider repertoire of body movements is likely possible in air, especially forms of rotation that would be improbable on land. Unfortunately, bandwidth cannot be calculated from CT-based measurements of canal streamline length (which do not measure the diameter of the membranous duct lumen), and actual head rotations cannot be verified without kinematic data. Mechanical sensor gain may not even be the factor optimized by the canal system, especially since there are numerous post-mechanical mechanisms to adjust gain. Nevertheless, the empirically established relationship between canal size and degree of locomotor agility in birds strongly indicates that the demands of aerial locomotion are matched by a system of semicircular canals with greater mechanical gain.

5.1.1. Assessing the origin of flight

Theropod dinosaurs were found to have canal sizes and morphologies consistent with those of other bipedal dinosaurs from a range of taxonomic groups, with no particular difference in scale noted between bipedal carnivores and herbivores, nor between phylogenetically older or younger species. Cursorial bipedal locomotion is primitive for Dinosauria, and all bipedal dinosaurs so far studied, including the theropods examined here, seem to have retained a vertically elongate anterior semicircular canal (less pronounced in oviraptorids) and overall larger canal sensors relative to quadrupedal dinosaurs (except ceratopsids) and mammals of similar size. Hypothetically, enlargement of the ASC in bipeds represents a functional attunement to the frequent occurrence of pitch-down rotations experienced by the head during bipedal locomotion. That the ASC is further enlarged in volant bird descendents suggests attunement to the higher frequency rotations experienced during flapping flight, while the peculiar warp of the semicircular canal system in birds is undoubtedly due to enlargement of the forebrain and cerebellum.

The evidence suggests that the flight capabilities of basal avialans were marked by structural and behavioral adaptations to high-speed flight with poor maneuverability. Aspects of the pectoral skeleton of *Archaeopteryx* indicate strongly that it was restricted to high air speeds and poorly adapted to low-speed maneuvering. This is also in concordance with the bony, frond-like tail of *Archaeopteryx*, which would have provided a considerable measure of static stability in flight, limiting control movements. Evaluation of the inner ear of *Archaeopteryx* conducted by me supports this prediction, but the accuracy of the measurements used in the analysis is highly questionable. Access

to the original CT data sets generated for BMNH 37001 would permit analysis of ASC shape and circumference using the same methods used to measure extant birds and extinct theropods, with less inherent error.

Whether flight proceeded from the ground up or the trees down, or through some other preconditions, cannot be determined directly by canal data. Inferentially, by supporting the predictions of Rayner (2001), this analysis suggests that *Archaeopteryx* was limited to flight using a continuous vortex gait. This manner of flight is aerodynamically easier to achieve by a gliding animal. Though *Archaeopteryx* does not possess any special adaptations for dedicated gliding or parachuting, aerodynamic lift in continuous vortex gait would have elevated the wing of *Archaeopteryx* despite the lack of elevating musculature, providing a solid mechanism for powered flight (Rayner, 2001). The canal adaptations of *Archaeopteryx*, as inferred from the present analysis, support this interpretation. It is intuitively more likely that primitive avialans could have achieved speeds necessary for fast flight from an inclined take-off, such as a tree perch, in the manner of gliding animals, rather than by a running take-off from horizontal ground, though others have argued that wingbeat movements could generate significant forward thrust during running take-off (Burgers and Chiappe, 1999; Burgers and Padian, 2001). Rayner (1985b, c, 2001) estimated that speeds on the order of 6–8 m sec^{-1} would have been necessary for the optimal origin of this type of flight, inferring that such ground-based velocities were unlikely for cursorial maniraptoran bipeds. The reversed hallux of *Archaeopteryx* suggests that it was at least partially capable of arboreal habits, and may have initiated flight from a perched position. Whether it practiced these habits or not is a matter of debate I cannot address. Recent reconstruction of the arboreal-gliding affinities

of *Microraptor*, a non-avian dromaeosaurid, suggest that it was adapted for undulatory "phugoid" gliding between trees, using its feathered tail for stability and pitch control (Chatterjee and Templin, 2007). This offers tantalizing support that flight in dromaeosaurids proceeded from an arboreal stage.

Like *Archaeopteryx*, basal neornithine birds such as galloanseres are high speed, poorly maneuverable fliers and possess canal dimensions that scale closely with non-avian theropod dinosaurs. A limitation of the present analysis is the poor overlap in body size between nonavian theropods and birds, and the poor reliability of body mass estimates for extinct taxa. Inclusion of smaller theropod taxa with estimable body masses (such as the maniraptoran *Mei*) would predictably show that these smaller dinosaurs scaled with slightly smaller anterior and lateral canals than volant galloanseres, indicating that canal size in poorly maneuverable birds reflects an underlying avian attunement to flapping flight despite overlap in scale with the regression line for larger-bodied, non-volant theropods. Discriminant function analysis using mass-adjusted canal measures effectively separated theropod and poor-flying taxa in this manner. Adaptations for increased canal size with respect to body mass are found throughout bird taxa, with interspecific variation closely linked to wing loading, and thus degree of aerial maneuverability.

Presently, we may conjecture as others have (Maynard Smith, 1952) that early avian flight proceeded through a relatively stable phase with poor attitude control, possibly as a result of insufficiently adapted neural control for aerial maneuvering. The current evidence for the sequence of avian brain evolution demonstrates that cerebellum size increased dramatically from the condition seen in primitive Avialae (Dominguez et

al., 2004) up through the phylogenetically derived orthithurine lineage (Kurochkin et al., 2007) and culminating with the large hindbrains of neornithine birds. Ornithurine birds are reconstructed as being more aerially maneuverable than *Archaeopteryx* (Chiappe and Witmer, 2002). Enlarged cerebellar surface area in ornithurine birds would indicate enhanced calibration and timing of motor activities and vestibular reflexes, and predictably, these birds should have larger semicircular canals. Future examination of ornithurine braincase evolution will cast light on the neurosensory and vestibular adaptations to flight that coincide with increased aerial maneuverability.

5.2. Future directions

A hindrance to this study was the resolution limits of the medical CT scanner at Stony Brook Hospital. Consequent to this, birds are underrepresented below a body mass of ~125 grams, which includes the vast majority of passerine and apodiform taxa (in total, around 60% of all extant bird species). Future work will address this gap by increasing the number of taxa sampled using μCT scanners, which accurately permit reconstruction and measurement of labyrinth structures at any size range.

Better sampling of small-bodied theropod dinosaur taxa, in particular small maniraptoran taxa, is needed to extend the dinosaurian body mass range into an area of overlap with most birds. Unfortunately, although small theropods were relatively common animals in the late Triassic to latest Cretaceous biota, very few are represented by intact basicranial remains. I am presently working with CT volumes of the small-

bodied troodontids *Mei long* (IVPP V12733) and *In ga* (gen. et sp. nov.), and discoveries of new taxa may one day improve the situation.

Especially important to future work is evaluation of ornithurine taxa intermediate to *Archaeopteryx* and neornithine birds. Though few intact three-dimensional basicrania exist for these taxa, examination of these specimens will help elucidate the evolution of canal size variation in Neornithes. Predictably, these taxa will evince canal sizes that scale with theropod dinosaurs and poor-flying galloanseriforms, but it would be informative to discover if, for instance, the volant *Ichthyornis* (Clarke, 2004) possessed larger canals than the nonflying *Hesperornis* (Marsh, 1880). Further analysis of the London (BMNH 37001) and Thermopolis (WDC-CSG-100) braincase specimens of *Archaeopteryx* are needed to confidently measure canal size in basal Avialae and to bolster the preliminary findings reported here.

While the size of the canals in nonflying theropods, basal avialans, and galloanserine birds is generally small with respect to body mass (compared to more agile flyers), the shape of the canals in basal avialans and modern birds is distinct, with the anterior canal deflected partly backward by encroachment of the enlarged optic tectum. Quantification of shape differences among avialan canals may cast further light on adaptations specific to flying behavior, if, and when, the effect of canal shape on endolymph flow can be modeled.

Finally, wireless triaxial accelerometers are becoming more commonplace in experimental settings, as well as becoming physically smaller, and may one day be fitted to birds permitted to locomote in natural flying conditions. Such devices could provide experimental data on actual head and body accelerations experienced during natural

flying movements, and would provide a powerful test of hypotheses supported by inferential, though compelling ecomorphological data derived from wing shape.

Literature Cited

Aldridge HDJN. 1986. Manoeuvrability and ecology in British bats. Myotis 23-24:157-160.

Aldridge HDJN. 1987. Body accelerations during the wingbeat in six bat species: the function of the upstroke in thrust generation. J Exp Biol 130:275-293.

Alexander RMcN. 1985. Mechanics of posture and gait of some large dinosaurs. Zool J Linn Soc 83:1-25.

Alexander RMcN. 1989. Dynamics of Dinosaurs and Other Extinct Giants. New York: Columbia University Press.

Alvarenga MFH, Höfling E. 2003. Systematic revision of the Phorusrhacidae (Aves: Ralliformes). Pap Avulsos Zool. 43: 55-91.

Anderson JF, Hall-Martin A, Russell DA. 1985. Long-bone circumference and weight in mammals, birds and dinosaurs. J Zool Lond 207:53-61.

Anderson JH, Blanks RHI, Precht W. 1978. Response characteristics of semicircular canal and otolith systems in cat: I. Dynamic responses of primary vestibular fibers. Exp. Brain Res. 32:491-507.

Angelaki DE, Dickman JD. 2000. Spatiotemporal processing of linear acceleration: primary afferent and central vestibular neuron responses. J. Neurophysiol. 84:2113-2132.

Assad JA, Shepherd GM, Corey DP. 1991. Tip-link integrity and mechanical transduction in vertebrate hair cells. Neuron 7:985-994.

Baird IL. 1974. Anatomical features of the inner ear in submammalian vertebrates; pp. 159-212 in Keidel WD, Neff WD (eds.), Handbook of Sensory Phsyiology. Berlin: Springer-Verlag.

Baird RA, Desmadryl G, Fernández C, Goldberg JM. 1988. The vestibular nerve of the chinchilla. II. Relation between afferent response properties and peripheral innervation patterns in the semicircular canals. J Neurophysiol 60:182-203.

Baloh RW, Honrubia V, Konrad HR. 1977. Ewald's second law re-evaluated. Acta Otolaryngol 83:475-479.

Bell, G. 1989. A comparative method. Am Nat 133:553-571.

Bellrose FC, Crompton RC. 1981. Migration speeds of three waterfowl species. Wilson Bull 93:121-124.

Bennett PM, Owens IPF. 2002 Evolutionary ecology of birds: life histories, mating systems and extinction. Oxford University Press.

Berg CVD, Rayner JMV. 1995. The moment of inertia of bird wings and the inertial power requirement for flapping flight. J Exp Biol 198:1655-1664.

Berger M, Roy OZ, Hard IS. 1970. The co-ordination between respiration and wing beats in birds. Z Vgl Physiol 66:190-200.

Bertelli S, Tubaro PL. 2002. Body mass and habitat correlates of song structure in a primitive group of birds. Biol J Linn Soc 77:423-430.

Birt-Friesen VL, Montevecchi WA, Cairns DK, Macko SA. 1989. Activity-specific metabolic rates of free-living northern gannets and other seabirds. Ecology 70:357-367.

Biewener AA. 2003. Animal locomotion. Oxford: Oxford University Press.

Bilo D, Bilo A. 1978. Wind stimuli control and vestibular and optokinetic reflexes in the pigeon. Naturwissenschaften 65:161-162.

Bilo D, Bilo A. 1983. Neck flexion related activity of flight control muscles in the flow stimulated pigeon. J Comp Physiol 153:111-122.

Bissonnette JP, Fekete DN. 1996. Standard atlas of the gross anatomy of the developing inner ear of the chicken. J Comp Neurol 368:620-630.

Blanco RE, Jones WW. 2005. Terror birds on the run: a mechanical model to estimate its maximum running speed. Proc R Soc B 272:1769-1773.

Blanks RHI, Estes MS, Markham CH. 1975. Physiological characteristics of vestibular first-order neurons in the cat. II. Response to angular acceleration. J Neurophysiol 38:1250-1268.

Blanks RHI, Curthoys IS, Bennett ML, Markham CH. 1985. Planar relationships of the semicircular canals in rhesus and squirrel monkeys. Brain Res 340:315-324.

Bock WJ. 1986. The arboreal origin of avian flight; pp. 57-72 in Padian K (ed.), The Origin of Birds and the Evolution of Flight. San Francisco: Memoirs of the California Academy of Sciences.

Boord RL, Karten HJ. 1979. Neuroanatomical aspects of the vestibular system of the Pigeon; pp. 255-265 in Granda AM, Maxwell J (eds.), Neural Mechanisms of Behavior in the Pigeon. New York: Plenum Press.

Boyle R, Carey JP, Highstein SM. 1991. Morphological correlates of response dynamics and efferent stimulation in horizontal semicircular canal afferents of the toadfish, *Opsanus tau*. J Neurophysiol 66:1504-1521.

Breuer J. 1874. Über die funktion der bogengänge des ohrlabyrinthes. Wien Med Jahrb 4:72– 124.

Brichta AM, Goldberg JM. 1998. The papilla neglecta of turtles: a detector of head rotations with unique sensory coding properties. J. Neurosci. 18:4314-4324.

Brochu CA. 2000. A digitally-rendered endocast for *Tyrannosaurus rex*. Journal of Vertebrate Paleontology 20:1-6.

Brodal A. 1974. Anatomy of the vestibular nuclei and their connections; pp. 239-352 in Kornhuber HH (ed.), Handbook of Sensory Physiology: Vestibular System. New York: Springer-Verlag.

Brooks VB, Thatch WT. 1981. Cerebellar control of posture and movement; pp. 877-946 in Brookhart JM, Mountcastle VB (eds.), Handbook of Physiology, Section I: The Nervous System, Volume II: Motor Control. Bethesda, MD: American Physiological Society.

Brown RHJ. 1963. The flight of birds. Biol Rev 38:460-489.

Brush AH. 1996. On the origin of feathers. J Evol Biol 9:131-142.

Brush AH. 2000. Evolving a protofeather and feather diversity. Amer Zool 40:631-639.

Bühler P. 1985. On the morphology of the skull of *Archaeopteryx*; pp. 135-140 in Hecht MK, Ostrom JH, Viohl G, Wellnhofer P (eds.), The Beginnings of Birds. Germany: Freunde des Jura-Museums, Eichstätt.

Bunce M, Worthy TH, Ford T, Hoppitt W, Willerslev E, Drummond A, Cooper A. 2003. Extreme reversed sexual size dimorphism in the extinct New Zealand moa *Dinornis*. Nature 425: 172-175.

Bundle MW, Dial KP. 2003. Mechanics of wing-assisted incline running (WAIR). J Exp Biol 206:4553-4564.

Burgers P, Chiappe LM. 1999. The wing of *Archaeopteryx* as a primary thrust generator. Nature 399:60-62.

Burgers P, Padian K. 2001. Why thrust and ground effect are more important than lift in the evolution of sustained flight; pp. 351-361 in Gauthier J, Gall LF (eds.), New Perspectives on the Origin and Early Evolution of Birds. New Haven: Peabody Museum of Natural History.

Burnham DA. 2004. Anatomy of *Bambiraptor*; pp. 61-111 in Currie PJ, Koppelhus EB, Shugar MA, Wright JL (eds.), Feathered Dragons. Bloomington: Indiana University Press.

Butler PJ, Woakes AJ. 1980. Heart rate, respiratory frequency and wing beat frequency of free flying barnacle geese *Branta Leucopsis*. J Exp Biol 85:213-236.

Butler RJ, Upchurch P. 2007. Highly incomplete taxa and the phylogenetic relationships of the theropod dinosaur *Juravenator starki*. J Vert Paleo 27:253-256.

Camis M. 1930. The Physiology of the Vestibular Apparatus. Oxford: Clarendon Press.

Carrano MT. 2007. The appendicular skeleton of *Majungasaurus crenatissimus* (Theropoda: Abelisauridae) from the Late Cretaceous of Madagascar. Memoirs of the Society of Vertebrate Paleontology, J Vert Paleo 27 (Supplement to 2):163-179.

Carrano MT, Sampson SD, Forster CA. 2002. The osteology of *Masiakasaurus knopfleri*, a small abelisauroid (Dinosauria: Theropoda) from the Late Cretaceous of Madagascar. J Vert Paleo 22:510-534.

Chatterjee S. 1997. The Rise of Birds. Baltimore: Johns Hopkins Press.

Chatterjee S. 1998. Counting the fingers of birds and dinosaurs. Science 280:355-356.

Chatterjee S, Templin RJ. 2004. Feathered coelurosaurs from China: New light on the arboreal origin of avian flight; pp. 251-281 in Currie PJ, Koppelhus EB, Shugar MA, Wright JL (eds.), Feathered Dragons. Bloomington: Indiana University Press.

Chatterjee S, Templin RJ. 2007. Biplane wing planform and flight performance of the feathered dinosaur *Microraptor gui*. Proc Nat Acad Sci USA 104:1576-1580.

Chen P-J, Dong Z-M, Zhen S-N. 1998. An exceptionally well-preserved theropod dinosaur from the Yixian Formation of China. Nature 391:147-152.

Chiappe LM. 1995. The first 85 million years of avian evolution. Nature 378:349-354.

Chiappe LM. 2001. Phylogenetic relationships among basal birds; pp. 125-139 in Gauthier J, Gall LF (eds.), New Perspectives on the Origin and Early Evolution of Birds. New Haven: Peabody Museum of Natural History.

Chiappe LM, Dyke GJ. 2002. The Mesozoic radiation of birds. Annu Rev Ecol Syst 33:91-124.

Chure DJ, Madsen JH. 1996. On the presence of furculae in some non-maniraptoran theropods. J Vert Paleo 16:573–577.

Clark GA Jr. 1979. Body weights of birds: a review. Condor 81:193-202.

Clark JM, Norell MA, Makovicky PJ. 2002. Cladistic approaches to the relationships of birds to other theropod dinosaurs; pp. 31-61 in Chiappe LM, Witmer LM (eds.), Mesozoic Birds: Above the Heads of Dinosaurs. Berkeley: University of California Press.

Clarke J. 2004. The morphology, phylogenetic taxonomy and systematics of *Ichthyornis* and *Apatornis* (Avialae: Ornithurae). Bull Am Mus Nat Hist 286:1-179.

Clarke J, Tambussi CP, Noriega JI, Erickson GM, Ketcham RA. Definitive fossil evidence for the extant avian radiation in the Cretaceous. Nature 433:305-308.

Cohen B. 1984. Erasmus Darwin's observations on rotation and vertigo. Hum Neurobiol 3:121-128.

Cohen B, Raphan T. 2004. The physiology of the vestibuloocular reflex (VOR); pp. 235-285 in Highstein SM, Fay RR, Popper AN (eds.), The Vestibular System. New York: Springer-Verlag.

Cohen B, Suzuki J, Bender MB. 1964. Eye movements from semicircular canal nerve stimulation in the cat. Ann Otol Rhinol Laryngol 73:153-169.

Colbert EH. 1962. The weights of dinosaurs. Am Mus Novit 2076:1-16.

Cooper RG. 2005. Growth in the ostrich (*Struthio camelus* var. *domesticus*). Anim Sci J 76:1-4.

Corey DP, Hudspeth AJ. 1979. Ionic basis of the receptor potential in a vertebrate hair cell. Nature 281:675-677.

Corey DP, Hudspeth AJ. 1983. Kinetics of the receptor current in bullfrog saccular hair cells. J. Neurosci 3:962-976.

Corwin JT. 1981. Peripheral auditory physiology in the lemon shark: evidence of parallel otolithic and nonotolithic sound detection. J Comp Physiol 142:379-390.

Cracraft J. 1981. Toward a phylogenetic classification of birds of the world (class Aves). Auk 98: 681-714.

Cracraft, J. 1988. The major clades of birds; pp. 333-355 in Benton MJ (ed.), The Phylogeny and Classification of the Tetrapods. Systematics Assoc Special Vol 35A. Oxford: Clarendon Press.

Cracraft J. 2001. Avian evolution, Gondwana biogeography and the Cretaceous–Tertiary mass extinction event. Proc Roy Soc Lond B 1466:459-469.

Cracraft J, Barker FK, Braun MJ, Harshman J, Dyke GJ, Feinstein J, Stanley S, Cibois A, Schikler P, Beresford P, García-Morena J, Sorenson MD, Yuri T, Mindell DP. 2004. Phylogenetic relationships among modern birds (Neornithes): toward an avian tree of life; pp. 468-489 in Cracraft J, Donoghue MJ (eds.), Assembling the Tree of Life. New York: Oxford University Press.

Crum Brown A. 1874. On the sense of rotation and the anatomy and physiology of the semicircular canals of the inner ear. J Anat Physiol 8:327-331.

Cruz I, Elkin D. 2003. Structural bone density of the lesser rhea (*Pterocnemia pennata*) (Aves: Rheidae). Taphonomic and archaeological implications. J Archaeol Sci 30:37-44.

Currie PJ, Zhao X-J. 1993. A new troodontids (Dinosauria, Theropoda) braincase from the Dinosaur Park Formation (Campanian) of Alberta. Can J Earth Sci 30:2231-2247.

Currie PJ, Chen P-J. 2001. Anatomy of *Sinosauropteryx prima* from Liaoning, northeastern China. Can J Earth Sci 38:1705-1727.

Curthoys IS, Markham CH, Curthoys EJ. 1977. Semicircular duct and ampulla dimensions in cat, guinea pig and man. J Morphol 151:17-34.

Curthoys IS, Oman CM. 1986.Dimensions of the horizontal semicircular duct, ampulla and utricle in rat and guinea pig. Acta Oto-Laryngol 101:1-10.

Curthoys IS, Oman CM. 1987. Dimensions of the horizontal semicircular duct, ampulla and utricle in human. Acta Oto-Laryngol 103:254-261.

Damiano ER. 1999. A poroelastic continuum model of the cupula partition and the response dynamics of the vestibular semicircular canal. J Biomech Eng 121:449-461.

Darwin E. 1796. Zoonomia, or, the Laws of Organic Life. London: J. Johnson.

Davis PG, Briggs DEG. 1992. Fossilization of feathers. Geology 23:783-789.

Dawson B, Trapp RG. 2004. Basic and Clinical Biostatistics, 4th ed. New York: McGraw-Hill.

De Zeeuw CI, Koekkoek SKE. 1997. Signal processing in the C2 module of the flocculus and its role in head movement control. Prog Brain Res 114:299-321.

De Zeeuw CI, Koekkoek SKE, van Alphen AM, Luo C, Hoebeek F, van der Steen J, Frens MA, Sun J, Goossens HHLM, Jaarsma D, Coesmans MPH, Schmolesky MT, De Jeu MTG, Galjart N. Gain and phase control of compensatory eye movements by the flocculus of the vestibulocerebellum; pp. 375-422 in Highstein SM, Fay RR, Popper AN (eds.), The Vestibular System. New York: Springer-Verlag.

Dial KP. 2003. Wing-assisted incline running and the evolution of flight. Science 299:402-404.

Dickman JD. 1996. Spatial orientation of semicircular canals and afferent sensitivity vectors in pigeons. Exp Brain Res 111:8-20.

Dickman JD, Fang Q. 1996. Differential central projections of vestibular afferents in pigeons. J Comp Neurol 367:110-131.

Dietz, V. 1992. Human neuronal control of automatic functional movements: Interaction between central programs and afferent input. Physiol Rev 72:33-69.

Dietz V, Horstmann GA, Berger W. 1989. Interlimb coordination of leg-muscle activation during perturbation of stance in humans. J Neurophysiol 62:680-693.

Dodson P, Forster CA, Sampson SD. 2004. Ceratopsidae; pp. 494-513 in Weishampel DB, Dodson P, Osmolska H, The Dinosauria, 2nd edition. Berkeley: University of California Press.

Dominguez PA, Milner AC, Ketcham RA, Cookson MJ, Rowe TB. 2004. The avian nature of the brain and inner ear of *Archaeopteryx*. Nature 430:666-669.

Dominguez-Bello MG, Michelangeli F, Ruiz MC, Garcia A, Rodriguez E. 1994. Ecology of the folivorous hoatzin (*Opisthocomus hoazin*) on the Venezuelan plains. Auk 111:643-651.

Dudley R. 2002. Mechanisms and implications of animal flight maneuverability. Integ and Comp Biol 42:135-140.

Dunning JB. 1993. CRC Handbook of Avian Body Masses. Boca Raton: CRC.

Eatock RA. 2000. Adaptation in hair cells. Annu Rev Neurosci 23:285-314.

Edington GH, Miller AE. 1941. The avian ulna: its quill-knobs. P Roy Soc Edinb 61:138-148.

Ellington CP. 1984a. The aerodynamics of flapping animal flight. American Zoologist 24:95-105.

Ellington CP. 1984b. The aerodynamics of hovering insect flight. V. A vortex theory. Philos Trans R Soc Lond B 305:115-144.

Elzanowski A. 2001. A new genus and species for the largest specimen of *Archaeopteryx*. Acta Palaeontol Pol 46:519-532.

Elzanowski A. 2002. Archaeopterygidae (Upper Jurassic of Germany), pp. 129-159 in Chiappe L, Witmer L (eds.), Mesozoic Birds: Above the Heads of Dinosaurs. Berkeley: University of California Press.

Erichsen JT, Hodos W, Evinger C, Bessette BB, Phillips SJ. 1989. Head orientation in pigeons: postural, locomotor and visual determinants. Brain Behav Evol 33: 268-278.

Erickson GM, Olson KH. 1996. Bite marks attributable to *Tyrannosaurus rex*: preliminary description and implications. J Vert Paleo 16:175-178.

Erickson GM, Van Kirk SD, Su J, Levenston ME, Caler WE, Carter DE. 1996. Bite-force estimation for *Tyrannosaurus rex* from tooth-marked bones. Nature: 382:706-708.

Erickson GM, Makovicky PJ, Currie PJ, Norell MA, Yerby SA, Brochu CA. 2004. Gigantism and comparative life-history parameters of tyrannosaurids dinosaurs. Nature 430:772-775.

Estes MS, Blanks RHI, Markham CH. 1975. Physiologic characteristics of vestibular first-order neurons in the cat. I. Response plane determination and resting discharge characteristics. J Neurophysiol 38:1239-1249.

Ewald JR. 1892. Physiologische Untersuchungen über das Endorgan des Nervus Octavus. Wiesbaden: Bergmann.

Ezure K, Graf W. 1984. A quantitative analysis of the spatial orientation of the vestibulo-ocular reflexes in lateral- and frontal-eyed animals. I. Orientation of semicircular canals and extra-ocular muscles. Neuroscience 12:85-93.

Farlow JO, Smith MB, Robinson JM. 1995. Body mass, bone "strength indicator," and cursorial potential of *Tyrannosaurus rex*. J Vert Paleo 15:713-725.

Farlow JO, Gatesey SM, Holtz TR Jr., Hutchinson JR, Robinson JM. Theropod locomotion. Amer Zool 40:640-663.

Fay RR, Kendall JI, Popper AN, Tester AL. 1975. Vibration detection by the macula neglecta of sharks. Comp Biochem Physiol 47A:1235-1240.

Feduccia A, Tordoff HB. 1979. Feathers of *Archaeopteryx:* Asymmetric vanes indicate aerodynamic function. Science 203:1021-1022.

Felsenstein J. 1985. Phylogenies and the comparative method. Am Nat 125:1-15.

Flock, Å. 1964. Structure of the macula utriculus with special reference to directional interplay of sensory responses as revealed by morphological polarization. J Cell Biol 22:413-431.

Flourens M-J-P. 1824. Recherches expérimentales sur les propriétés et les fonctions du système nerveux dans les animaux vertébrés. Paris: Crevot.

Flourens M-J-P. 1830. Experiences sur les canauz semicirculaires de l'oreille. Mém Acad Roy Sci (Paris) 9:455-477.

Forster CA, Sampson SD, Chiappe LM, Krause DW. 1998. The theropod ancestry of birds: new evidence from the Late Cretaceous of Madagascar. Science 279:1915-19.

Franzosa J. 2004. Evolutin of the Brain in Theropoda (Dinosauria). Unpublished Ph.D. dissertation. Austin: University of Texas at Austin.

Franzosa J, Rowe TB. 2005. Cranial endocast of the cretaceous theropod dinosaur *Acrocanthosaurus atokensis*. J Vert Paleo 25:859-864.

Fritzsch B. 1987. The inner ear of the coelacanth fish *Latimeria* has tetrapod affinities. Nature 327:153-154.

Fritzsch B. 1988. The amphibian octavo-lateralis system and its regressive and progressive evolution. Acta Biol. Hung. 39: 305-322.

Fritzsch B, Beisel KW. 2001. Evolution and development of the vertebrate ear. Brain Res Bull 55:711-721.

Fritzsch B, Wake MH. 1988. The inner ear of gymnophine amphibians and its nerve supply: a comparative study of regressive events in a complex sensory system (Amphibia, Gymnophiona). Zoomorphology 108:201-217.

Fuchs AF, Kimm J. 1975. Unit activity in vestibular nucleus of the alert monkey during horizontal angular acceleration and eye movement. J Neurophysiol 38:1140-1161.

Gatesy SM. 1995. Functional evolution of the hind limb and tail from basal theropods to birds; pp. 219-234 in Thomason JJ (ed.), Functional Morphology in Vertebrate Paleontology. New York: Cambridge University Press.

Gatesy SM. 2002. Locomotor evolution on the line to modern birds; pp. 432-447 in Chiappe LM, Witmer LM (eds.), Mesozoic Birds: Above the Heads of Dinosaurs. Berkeley: University of California Press.

Gatesy SM, Dial KP. 1996a. Locomotor modules and the evolution of avian flight. Evolution 50:331-340.

Gatesy SM, Dial KP. 1996b. From frond to fan: *Archaeopteryx* and the evolution of short-tailed birds. Evolution 50:2037-2048.

Gatesy SM, Baier DB. 1995. The origin of the avian flight stroke: a kinematic and kinetic perspective. Paleobiology 31:382-399.

Gauthier J. 1986. Saurischian monophyly and the origin of birds. Mem Calif Acad Sci 8:1-55.

Gauthier J, de Queiroz K. 2001. Feathered dinosaurs, flying dinosaurs, crown dinosaurs, and the name "Aves"; pp. 7-41 in Gauthier J, Gall LF (eds.), New Perspectives on the Origin and Early Evolution of Birds. New Haven: Peabody Museum of Natural History.

Georgi JA, Sipla JS. In press. Balance: comparative anatomy and physiology in secondarily aquatic reptiles and birds; in Thewissen JGM, Nummela S (eds.), Senses on the Threshold: Form and Function of the Sense Organs in Secondarily Aquatic Tetrapods. Berkeley: University of California Press.

Gibson JJ. 1954. The visual perception of object motion and subjective movement. Psychol Rev 61:304-314.

Gill RE Jr., Piersma T, Hufford G, Servranckx R, Riegen A. 2005. Crossing the ultimate ecological barrier: Evidence for an 11 000-km-long nonstop flight from Alaska to New Zealand and Eastern Australia by bar-tailed godwits. Condor 107:1-20.

Gioanni H. 1988a. Stabilizing gaze reflexes in the pigeon (*Columba livia*). I. Horizontal and vertical optokinetic eye (OKN) and head (OCR) reflexes. Exp Brain Res 69: 567-582.

Gioanni H. 1988b. Stabilizing gaze reflexes in the pigeon (*Columba livia*). II. Vestibulo-ocular (VOR) and vestibulo-collic (closed-loop VCR) reflexes. Exp Brain Res 69: 583-593.

Gioanni H and Sansonetti A. Characteristics of slow and fast phases of the optocollic reflex (OCR) in head free pigeons (*Columba livia*): influence of flight behaviour. Eur J Neurosci 11: 155–166, 1999.

Gishlick AD. 2001. The function of the manus and forelimb of *Deinonychus antirrhopus* and its importance for the origin of avian flight; pp. 301-318 in Gauthier J, Gall LF (eds.), New Perspectives on the Origin and Early Evolution of Birds. New Haven: Peabody Museum of Natural History.

Göhlich U, Chiappe LM. 2006. A new carnivorous dinosaur from the Late Jurassic Solnhofen archipelago. Nature 440:329-332.

Goldberg JM. 1996. Theoretical analysis of intercellular communication between the vestibular type I hair cell and its calyx ending. J Neurophysiol 76:1942-1957.

Goldberg JM, Fernández C. 1971. Physiology of peripheral neurons innervating semicircular canals of the squirrel monkey. I. Resting discharge and response to constant angular accelerations. J. Neurophysiol 34:635-660.

Goldberg JM, Lysakowski A, Fernández C. 1990. Morphophysiological and ultrastructural studies in the mammalian cristae ampullares. Hear Res 49:89-102.

Goldberg ME, Hudspeth AJ. 2000. The vestibular system; pp. 801-815 in Kandel ER, Schwartz JH, Jessel TM (eds.), Principles of Neural Science, Fourth edition. New York: McGraw-Hill.

Goodman MB, Art JJ. 1996a. Positive feedback by a potassium-selective inward rectifier enhances tuning in vertebrate hair cells. Biophys J 72:430-442.

Goodman MB, Art JJ. 1996b. Variations in the ensemble of potassium currents underlying resonance in turtle hair cells. J Physiol 497:395-412.

Gould SJ, Vrba ES. 1982. Exaptation—a missing term in the science of form. Paleobiology 8:4-15.

Graf W. 1988. Motion detection in physical space and its peripheral and central representation. Ann NY Acad Sci 545:154-169.

Graur D, Martin W. 2004. Reading the entrails of chickens: molecular timescales of evolution and the illusion of precision. Trends Genet 20:80–86.

Gray AA. 1907. The Labyrinth of Animals, Volume 1. London: Churchill.

Gray AA. 1908. The Labyrinth of Animals, Volume 2. London: Churchill.

Griffiths PJ. 1996. The isolated *Archaeopteryx* feather. Archaeopteryx 14:1-26.

Grossman GE, Leigh RJ, Abel LA, Lanska DJ, Thurston SE. 1988. Frequency and velocity of rotational head perturbations during locomotion. Exp Brain Res 70:470-476.

Grüsser O-J. 1984. J. E. Purkyne's contributions to the physiology of the visual, the vestibular and the oculomotor system. Hum Neurobiol 3:129-144.

Hadziselimovic H, Savkovic LJ. 1964. Appearance of semicircular canals in birds in relation to mode of life. Acta Anat 57:306-315.

Haftorn S. 1989. Seasonal and diurnal body weight variations in titmice, based on analyses of individual birds. Wilson Bulletin 101:217-235.

Haiden GJ, Awad EA. 1981. The ultrastructure of the avian Golgi tendon organ. Anat Record 200:153-161.

Hain TC, Helminski JO. 2007. Anatomy and physiology of the normal vestibular system; pp. 2-18 in Herdman SJ (ed.), Vestibular Rehabilitation, Third edition. Philadelphia: F. A. Davis.

Hall MI, Ross CF. 2007. Eye shape and activity pattern in birds. J Zool 271:437-444.

Halmagyi GM, Curthoys IS, Cremer PD, Henderson CJ, Staples M. 1990. Head impulses after unilateral vestibular deafferentation validate Ewald's second law. J Vestib Res 1:187-197

Haque A, Dickman JD. Vestibular gaze stabilization: different behavioral strategies for arboreal and terrestrial avians. J Neurophysiol 93:1165-1173.

Harvey PH, Pagel MD. 1991. The comparative method in evolutionary biology. Oxford: Oxford University Press.

Hawkins JE, Schacht J. 2005. Sketches of otohistory. Part 8: The emergence of vestibular science. Audiol Neurotol 10:185-190.

Hecht MK.1985. The biological significance of *Archaeopteryx*; pp. 149-160 in Hecht MK, Ostrom JH, Viohl G, Wellnhofer P (eds.), The Beginnings of Birds. Germany: Freunde des Jura-Museums, Eichstätt.

Hedrick TL, Tobalske BW, Biewener AA. 2002. Estimates of circulation and gait change based on a three-dimensional kinematic analysis of flight in cockatiels (*Nymphicus hollandicus*) and Ringed Turtle-doves (*Streptopelia risoria*). J Exp Biol 205:1389-1409.

Helling K, Clarke AH, Watanabe N, Scherer H. 2000. Morphological studies of the form of the cupula in the semicircular canal ampulla. HNO 48:822-827.

Hertel F, Balance LT. 1999. Wing ecomorphology of seabirds from Johnston Atoll. Condor 101:549-556.

Highstein SM, Rabbitt RD, Boyle RD. 1996. Determinants of semicircular canal afferent response dynamics in the toadfish, *Opsanus tau*. J Neurophsiol 75:575-596.

Highstein SM, Rabbitt RD, Holstein GR, Boyle RD. 2005. Determinants of spatial and temporal coding by semicircular canal afferents. J Neurophysiol 93:2359-2370.

Hildebrand M. 1985. Walking and running; pp. 38-57 in Hildebrand M, Bramble DM, Liem KF, Wake DB (eds.), Functional Vertebrate Morphology. Cambridge: Belknap Press.

Hillman DE. 1977. Relationship of the sensory cell cilia to the cupula; pp. 415-420 in Johari O, Becker RP (eds.), Scanning Electron Microscopy, Volume 2. Chicago: ITT Res Inst.

Hillman DE, McLaren JW. 1979. Displacement configuration of semicircular canal cupulae. Neuroscience 4:1989-2000.

Hodos W. 1993. The visual capabilities of birds; pp. 63-76 in Zeigler HP, Bischof H-J (eds.), Vision, Brain, and Behavior in Birds. Cambridge: MIT Press.

Holstein GR, Martinelli GP, Boyle R, Rabbitt RD, Highstein SM. 2004. Ultrastructural observations of efferent terminals in the crista ampullaris of the toadfish, *Opsanus tau*. Exp Brain Res 155:265-273.

Holtz TR. 1994. The phylogenetic position of the Coelurosauria (Dinosauria: Theropoda). J Paleontol 68:1100-1117.

Holtz TR. 1998. A new phylogeny of the carnivorous dinosaurs. Gaia 15:5-61.

Holtz TR. 2004. Tyrannosauroidea; pp. 111-136 in Weishampel DB, Dodson P, Osmolska H, The Dinosauria, 2nd edition. Berkeley: University of California Press.

Hopkins M. 1906. On the relative dimensions of the osseous semicircular canals of birds. Bull Marine Biol Lab Woods Hole 11:253-264.

Hopson J. 1977. Relative brain size and behaviour in archosaurian reptiles. Annu Rev Ecol Syst 8:429-448.

Horak FB. 2007. Role of the vestibular system in postural control; pp. 32-51 in Herdman SJ (ed.), Vestibular Rehabilitation, Third edition. Philadelphia: F. A. Davis.

Horak FB, Macpherson JM. 1996. Postural orientation and equilibrium; pp. 255-292 in Rowell L, Shepherd JT (eds.), Regulation and integration of multiple systems. New York: Oxford University Press.

Hou L-H, Zhou Z, Martin LD, Feduccia A. 1995.A beaked bird from the Jurassic of China. Nature 377:616-618.

Howard IP, Templeton WB. 1966. Human Spatial Orientation. New York: Wiley.

Howard J, Hudspeth AJ. 1988. Compliance of the hair bundle associated with gating of mechanoelectrical transduction channels in the bullfrog's saccular hair cell. Neuron 1:189-199.

Hudspeth AJ. 1982. Extracellular current flow and the site of transduction by vertebrate hair cells. J Neurosci 2:1-10.

Hudspeth AJ. 2000. Sensory transduction in the ear; pp. 614-624 in Kandel ER, Schwartz JH, Jessel TM (eds.), Principles of Neural Science, Fourth edition. New York: McGraw-Hill.

Hudspeth AJ, Jacobs R. 1979. Stereocilia mediate transduction in vertebrate hair cells. Proc Natl Acad Sci USA 76:1506–1509.

Hudspeth AJ, Gillespie PG. 1994. Pulling springs to tune transduction: adaptation by hair cells. Neuron 12:1-9.

Hunt GR. 1996. Family Rhynochetidae (Kagu); pp. 218-225 in del Hoyo J, Elliot A, Sargatal J (eds.), Handbook of Birds of the World, Vol. 3. Barcelona: Lynx Edicions.

Hunter-Duvar IM, Hinojosa R. 1984. Vestibule: sensory epithelia; pp. 211-244 in Friedmann I, Ballantyne J (eds.), Ultrastructural Atlas of the Inner Ear. London: Butterworths.

Hurlburt GR. 1994. Were Dinosaurs Cold- or Warm-blooded?: An Exercise in Scientific inference; pp. 181-214 in Goldman CA (ed.), Proceedings of the 15th Workshop/ Conference of the Association for Biology Laboratory Education.

Hutchinson JR, Garcia M. 2002. *Tyrannosaurus* was not a fast runner. Nature 415 :1018-1021.

Hutchinson JR. 2004a. Biomechanical modeling and sensitivity analysis of bipedal running ability. I. Extant taxa. J Morph 262:421-440.

Hutchinson JR. 2004b. Biomechanical modeling and sensitivity analysis of bipedal running ability. II. Extant taxa. J Morph 262:441-461.

Huxley TH. 1868. Remarks upon *Archaeopteryx lithographica*. Proc R Soc Lond 16:243-248.

Huxley TH. 1870. Further evidence of the affinity between dinosaurian reptiles and birds. Q J Geol Soc Lond 26:12-31.

Ito M. 1984. The Cerebellum and Neural Control. New York: Raven Press.

Iwaniuk AN, Hurd PL. 2005. A multivariate analysis of cerebrotypes in birds. Brain Behav Evol 65:215-230.

Iwaniuk AN, Nelson JE, James HF, Olson SL. 2004. A comparative test of the correlated evolution of flightlessness and relative brain size in birds. J Zool Lond 263:317-327.

Jaeger R, Takagi A, Haslwanter T. 2002. Modeling the relation between head orientations and otolith responses in humans. Hear Res 173:29-42.

Jenkins FA Jr. 1993. The evolution of the avian shoulder joint. Am J Sci 293A:253-267.

Jerison H. 1973. Evolution of the Brain and Intelligence. New York: Academic Press.

Ji Q, Currie PJ, Norell MA, Ji S-A. 1998. Two feathered dinosaurs from northeastern China. Nature 393:753-761.

Jørgensen JM. 1988. The number and distribution of calyceal hair cells in the inner ear utricular macula of some reptiles. Acta Zool (Stockh) 69:169-175.

Keller EL. 1978. Gain of the vestibulo-ocular reflex in monkey at high rotational frequencies. Vision Res 18:311-315.

Keshner EA, Peterson BW. 1992. Multiple control mechanisms contribute to functional behaviors of the head and neck; pp. 381-386 in Berthoz A, Graf W, Vidal PP (eds.), The Head-Neck Sensory Motor System. New York: Oxford University Press.

Keshner EA, Peterson BW. 1995. Mechanisms controlling human head stabilization. I. Head-neck dynamics during random rotations in the horizontal plane. J Neurophysiol 73:2293-2301.

Keshner EA, Cromwell RL, Peterson BW. 1995. Mechanisms controlling human head stabilization. II. Head-neck characteristics during random rotations in the vertical plane. J Neurophysiol 73:2302-2312.

King OS, Seidman SH, Leigh RJ. 1992. Control of head stability and gaze during locomotion in normal subjects and patients with deficient vestibular function; pp. 568-570 in Berthoz A, Graf W, Vidal PP (eds.), The Head-Neck Sensory Motor System. New York: Oxford University Press.

Koenig WD, Walters EL, Walters JR, Kellam JS, Michalek KG, Schrader MS. 2005.Seasonal body weight variation in five species of woodpeckers. Condor 107:810-822.

Kokshaysky NV. 1979. Tracing the wake of a flying bird. Nature 279:146-148.

Kurochkin EN, Dyke GJ, Saveliev SV, Pervushov EM, Popov EV. 2007. A fossil brain from the Cretaceous of European Russia and avian sensory evolution. Biol Lett 3:309-313.

Larsson HCE. 2001. Endocranial anatomy of *Carcharodontosaurus saharicus* (Theropoda: Allosauridae) and its implications for theropod brain evolution; pp. 19-33 in Tanke DH and Carpenter K (eds.), Mesozoic Vertebrate Life. New Research Inspired by the Paleontology of Philip J. Currie. Bloomington: Indiana University Press.

Larsson HCE, Sereno PC, Wilson JA. 2000. Forebrain enlargement among nonavian theropod dinosaurs. J Vert Paleo 20:615–618.

Leshem Y, Yom-Tov Y. 1996. The use of thermals by soaring migrants. Ibis 138:667-674.

Lewis ER, Leverenz EL, Bialek WS. 1985. The vertebrate inner ear. Boca Raton: CRC Press.

Lindenlaub T, Burda H, Nevo E. 1995. Convergent evolution of the vestibular organ in the subterranean mole-rats, *Cryptomys* and *Spalax*, as compared with the aboveground rat, *Rattus*. J Morphol 224:303-311.

Linnaeus C. 1758. Systema naturae per regna tria naturae, 10th ed. Vol 1, Regnum animale [photographic facsimile]. London: Trustees, British Museum (Natural History), 1939.

Livezey BC. 1988. Morphometrics of flightlessness in the Alcidae. Auk 105:681-698.

Livezey BC, Humphrey PS. 1986. Flightlessness in steamer-ducks (Anatidae: *Tachyeres*): its morphological bases and probable evolution. Evolution 40:540-558.

Livezey BC, Zusi RL. 2006. Higher-order phylogeny of modern birds (Theropoda, Aves: Neornithes) based on comparative anatomy: I. Methods and characters. Bull Carnegie Mus Nat Hist 37:1-556.

Livezey BC, Zusi RL. 2007. Higher-order phylogeny of modern birds (Theropoda, Aves: Neornithes) based on comparative anatomy. II. Analysis and discussion. Zool J Linnean Soc 149:1-95.

Lockwood, R, Swaddle JP, and Rayner JMV. 1998. Avian wingtip shape reconsidered: wingtip shape indices and morphological adaptations to migration. J Avian Biol 29: 273-292.

Loe PR, Tomko DL, Werner G. 1973. The neural signal of angular head position in primary afferent vestibular nerve axons. J. Physiol. 230: 29–50.

Lorente de Nó R. 1927. Contribucion al estudio matematico del organo del equilibrio. Trab Publ En La 7:202-206.

Lowenstein O, Wersäll J. 1959. A functional interpretation of the electron-microscopic structure of the sensory hairs in the cristae of the elasmobranch *Raja calvata* in terms of directional sensitivity. Nature 184:1807-1808.

Lowenstein O, Roberts TDM. 1951. The localization and analysis of the response to vibration from the isolated elasmobranch labyrinth. A contribution to the problem of the evolution of hearing in vertebrates. J Physiol (Lond) 114:471-489.

Lowenstein O, Thornhill RA. 1970. The labyrinth of *Myxine:* anatomy, ultrastructure and electrophysiology. Proc R Soc Lond B 176:21-42.

Lysakowski A. 1996. Synaptic organization of the crista ampullaris in vertebrates. Ann NY Acad Sci 781:164-182.

Lysakowski A, Goldberg JM. 2004. Morphophysiology of the vestibular periphery; pp. 235-285 in Highstein SM, Fay RR, Popper AN (eds.), The Vestibular System. New York: Springer-Verlag.

Mach E. 1873. Physikalische versuche über den Gleichgewichtssinn des Menschen. S Ber Akad Wiss Wien Math Naturw K1 68:124-140.

Mach E. 1875. Grundlinien der Lehre von den Bewegungsempfindugen.Leipzig: Engelmann.

Maderson PFA. 1972. On how an archosaurian scale might have given rise to an avian feather. Am Nat 176:424-428.

Maderson PFA, Alibardi L. 2000. The development of the sauropsid integument: a contribution to the problem of the origin and evolution of feathers. Am Zool 40:513-529.

Madge SP, McGowan P. 2002. Pheasants, Partridges and Grouse: A guide to the pheasants, partridges, quails, grouse, guineafowl, buttonquails and sandgrouse of the world. London: Christopher Helm.

Maddison WP, Maddison DR. 2006. Mesquite: a modular system for evolutionary analysis. Version 1.12. http://mesquiteproject.org

Maier A, Eldred E. 1971. Comparisons in the structure of avian muscle spindles. J Comp Neur 143:25-40.

Makovicky PJ, Currie PJ. 1998. The presence of a furcula in tyrannosaurid theropods, and its phylogenetic and functional implications. J Vert Paleo 18:143-149.

Marsh OC. 1880. Odontornithes, a Monograph on the Extinct Toothed Birds of North America. Washington, DC: Government Printing Office.

Martin GR. 1993. Producing the image; pp. 5-24 in Zeigler HP, Bischof H-J (eds.), Vision, Brain, and Behavior in Birds. Cambridge: MIT Press.

Matano S, Kubo T, Günther M. 1985. Semicircular canal organ in three primate species and behavioural correlations. Fortschr Zool 30:677-680.

Matano S, Kubo T, Matsunaga T, Niemitz C, Günther M. 1986. On the basis of the semicircular canal organ in the *Tarsius bancanus*; pp. 122-129 in Taub DM, King FA (eds.), Current Perspectives in Primate Biology. New York: Van Nostrand Reinhold.

Maynard Smith J. 1952. The importance of the nervous system in the evolution of animal flight. Evolution 6:127-129.

Mayne R. 1950. The dynamic characteristics of the semicircular canals. J Comp Physiol Psychol 43:309-319.

Mayne R. 1965. The “match” of the semicircular canals to the dynamic requirements of various species; pp. 57-67 in Symposium on the Role of the Vestibular Organs in the Exploration of Space. Washington, D.C.: National Aeronautics and Space Administration, SP-77.

Mayo H. 1837. Outlines of Human Physiology, Fourth edition. London: Henry Renshaw and J. Churchill.

Mayr G, Pohl B, Peters DS. 2005. A well-preserved *Archaeopteryx* specimen with theropod features. Science 310:1483-1486.

Mayr G, Pohl B, Hartman S, Peters DS. 2007. The tenth skeletal specimen of *Archaeopteryx*. Zool J Linnean Soc 149:97-116.

McLaren JW, Hillman DE. 1979. Displacement of the semicircular canal cupula during sinusoidal rotation. Neuroscience 4:2001-2008.

McVean A. 1999. Are the semicircular canals of the European mole, *Talpa europaea*, adapted to a subterranean habit? Comp Biochem Physiol A 123:173-178.

Melvill Jones G, Milsum JH. 1971. Frequency response analysis of central vestibular unit activity resulting from rotational stimulation of the semicircular canals. J Physiol 219:191-215.

Miller MR, Takekawa JY, Fleskes JP, Orthmeyer DL, Casazza ML, Haukos DA, Perry WM. 2005. Flight speeds of northern pintails during migration determined using satellite telemetry. Wilson Bull 117:364-374.

Mindell DP, Sorenson MD, Dimcheff DE. 1998. Multiple independent origins of mitochondrial gene order in birds. Proc Natl Acad Sci USA 95:10693-10697.

Mlikovsky J. 1989a. Brain size in birds: 1. Tinamiformes through ciconiiformes. Vest Cs Spolec Zool 53: 33-47.

Mlikovsky J. 1989b. Brain size in birds: 2. Falconiformes through gaviiformes. Vest Cs Spolec Zool 53: 200-213.

Mlikovsky J. 1989c. Brain size in birds: 3. Columbiformes through piciformes. Vest Cs Spolec Zool 53: 252-264.

Mlikovsky J. 1990. Brain size in birds: 4. Passeriformes. Acta Soc Zool Bohemoslov 54: 27-37.

Money KE, Correia MJ. 1972. The vestibular system of the owl. Comp Biochem Physiol 42:353-358.

Muller M. 1990. Relationships between semicircular duct radii with some implications for time constants. Neth J Zool 40:173-202.

Muller M. 1994. Semicircular duct dimensions and sensitivity of the vertebrate vestibular system. 1994. J Theor Biol 167:239-256.

Muller M. 1999. Size limitations in semicircular duct systems. J Theor Biol 198:405-437.

Muller M. 2000. Biomechanical aspects of the evolution of semicircular duct systems. Neth J Zool 50:279-288.

Muller M, Verhagen JHG. 1988a. A new quantitative model of total endolymph flow in the system of semicircular ducts. J Theor Biol 134:473-501.

Muller M, Verhagen JHG. 1988b. A mathematical approach enabling calculation of the total endolymph flow in the semicircular ducts. J Theor Biol 134:503-529.

Muller M, Verhagen JHG. 2002a. Optimization of the mechanical performance of a two-duct semicircular duct system. Part 1: Dynamics and duct dimensions. J Theor Biol 216:409-424.

Muller M, Verhagen JHG. 2002b. Optimization of the mechanical performance of a two-duct semicircular duct system. Part 2: Excitation of endolymph movements. J Theor Biol 216:425-442.

Muller M, Verhagen JHG. 2002c. Optimization of the mechanical performance of a two-duct semicircular duct system. Part 3: The positioning of the ducts in the head. J Theor Biol 216: 443-459.

Nalbach H-O, Wolf-Oberhollenzer F, Remy M. 1993. Exploring the image; pp. 25-46 in Zeigler HP, Bischof H-J (eds.), Vision, Brain, and Behavior in Birds. Cambridge: MIT Press.

Nealen PM, Ricklefs RE. 2001. Early diversification of the avian brain:body relationship. J Zool Lond 253:391-404.

Nelson JB. 1978. The Sulidae – Gannets and Boobies. Oxford: Oxford University Press.

Newman BH. 1970. Stance and gait in the flesh-eating dinosaur *Tyrannosaurus*. Biol J Linn Soc 2:119-123.

Norberg RÅ, Norberg UM. 1971. Take-off, landing, and flight speed during fishing flights of *Gavia stellata*. Orn Scand 2:55-67.

Norberg RÅ. 1985. Function of vane asymmetry and shaft curvature in bird flight feathers; Inferences on flight ability of *Archaeopteryx*; pp. 303-318 in Hecht MK, Ostrom JH, Viohl G, Wellnhofer P (eds.), The Beginnings of Birds. Germany: Freunde des Jura-Museums, Eichstätt.

Norberg UM. 1985a. Evolution of vertebrate flight: an aerodynamic model for the transition from gliding to active flight. Am Nat 126:303-327.

Norberg UM. 1985b. Evolution of flight in birds: aerodynamic, mechanical, and ecological aspects; pp. 293-302 in Hecht MK, Ostrom JH, Viohl G, Wellnhofer P (eds.), The Beginnings of Birds. Germany: Freunde des Jura-Museums, Eichstätt.

Norberg UM. 1986. Evolutionary convergence in foraging niche and flight morphology in insectivorous aerial-hawking birds and bats. Ornis Scand 17:253-260.

Norberg UM. 1990. Vertebrate flight. Berlin: Springer-Verlag.

Norberg UM, Rayner JMV. 1987. Ecological morphology and flight in bats (Mammalia; Chiroptera): wing adaptations, flight performance, foraging strategy and echolocation. Phil Trans R Soc Lond B 316:335-427.

Norell MA, Makovicky PJ, Clark JM. 1998. A *Velociraptor* wishbone. Nature 389:447.

Norell MA, Clark JM, Makovicky PJ. 2001. Phylogenetic relationships among coelurosaurian theropods; pp. 49-67 in Gauthier J, Gall LF (eds.), New Perspectives on the Origin and Early Evolution of Birds. New Haven: Peabody Museum of Natural History.

Norell MA, Xu X. 2005. Feathered dinosaurs. Annu Rev Earth Planet Sci 33:277-299.

Norell MA, Clark JM, Turner AH, Makovicky PJ, Barsbold R, Rowe T. 2006. A new dromaeosaurid theropod from Ukhaa Tolgod (Ömnögov, Mongolia). Am Mus Novit 3545:1-51.

Northcutt, RG. 1989. The phylogenetic distribution and innervation of craniate mechanoreceptive lateral lines; pp. 17-78 in Coombs S, Görner P, Münz H (eds.), Mechanosensory Lateral Line: Neurobiology and Evolution. New York: Springer-Verlag.

Nudds RL, Dyke GJ, Rayner JMV. 2004a. Forelimb proportions and the evolutionary radiation of Neornithes. Proc R Soc B 271: S324-S327.

Nudds RL, Taylor GK, Thomas ALR. 2004b. Tuning of Strouhal number for high propulsive efficiency accurately predicts how wingbeat frequency and stroke amplitude relate and scale with size and flight speed in birds. Proc R Soc Lond B 271:2071-2076.

Nudds RL, Dyke GJ, Rayner JMV. 2007. Avian brachial index and wing kinematics: putting movement back into bones. J Zool 272: 218-226.

Nunn CL, Barton RA. 2001. Comparative methods for studying primate adaptation and allometry. Evol Anthrop 10:81–98.

Ohmori H. 1985. Mechano-electrical transduction currents in isolated vestibular hair cells of the chick. J Physiol 359:189-217.

Oman CM. 1980. The influence of duct and utricular morphology in semicircular canal response; pp. 251-274 in Gualtierotti T (ed.), Vestibular Function and Morphology. New York: Springer-Verlag.

Oman CM, Young LR. 1972. The physiological range of pressure difference and cupula deflections in the human semicircular canal. Acta Otolaryngol 74:324-331.

Oman CM, Marcus EN, Curthoys IS. 1987. The influence of semicircular canal morphology on endolymph flow dynamics. Acta Otolaryngol 103:1-13.

Osmólska H, Currie PJ, Barsbold R. 2004. Oviraptorosauria; pp. 165-183 in Weishampel DB, Dodson P, Osmolska H, The Dinosauria, 2nd edition. Berkeley: University of California Press.

Ostrom JH. 1969. Osteology of *Deinonychus antirrhopus*, an unusual theropod from the lower Cretaceous of Montana. Bull Peabody Mus Nat Hist 30:1-165.

Ostrom JH. 1973. The ancestry of birds. Nature 242:136.

Ostrom JH. 1974. *Archaeopteryx* and the origin of flight. Q Rev Biol 49:27-47.

Ostrom JH. 1976. *Archaeopteryx* and the origin of birds. Biol J Linn Soc 8:91-182.

Padian K. 1985. The origins and aerodynamics of flight in extinct vertebrates. Paleontology 28:413-433.

Padian K. 2001. Cross-testing adaptive hypotheses: Phylogenetic analysis and the origin of bird flight. Amer Zool 41:598-607.

Padian K, Chiappe LM. 1998. The origin and early evolution of birds. Biol Rev 73:1-42.

Paul GS, Christiansen P. 2000. Forelimb posture in neoceratopsian dinosaurs: implications for gait and locomotion. Paleobiology 26: 450-465.

Pearson RG.1972. The Avian Brain. London: Academic Press.

Peczkis J. 1994. Implications of body-mass estimates for dinosaurs. J Vert Paleo 14:520-533.

Pennycuick CJ. 1975. Mechanics of flight; pp. 1-75 in Farner DS, King JR, Avian Biology, vol. 5. Academic Press.

Pennycuick CJ. 1988. On the reconstruction of pterosaurs and their manner of flight, with notes on vortex wakes. Biol Rev 63:209-231.

Pennycuick CJ. 1996. Wingbeat frequency of birds in steady cruising flight: New data and improved predictions. J Exp Biol 199:1613-1618.

Peters DS. 1985. Functional and constructive limitations in early evolution of birds; pp. 243-249 in Hecht MK, Ostrom JH, Viohl G, Wellnhofer P (eds.), The Beginnings of Birds. Germany: Freunde des Jura-Museums, Eichstätt.

Peters DS, Gutmann WF. 1985. Constructional and functional preconditions for the transition to powered flight in vertebrates; pp. 233-242 in Hecht MK, Ostrom JH, Viohl G, Wellnhofer P (eds.), The Beginnings of Birds. Germany: Freunde des Jura-Museums, Eichstätt.

Peterson BW, Boyle RD. 2004. Vestibulocollic reflexes; pp. 343-374 in Highstein SM, Fay RR, Popper AN (eds.), The Vestibular System. New York: Springer-Verlag.

Peterson BW, Goldberg J, Bilotto G, Fuller JH. 1985. Cervicocollic reflex: its dynamic properties and interaction with vestibular reflexes. J Neurophysiol 54: 90-109.

Phillimore AB, Freckleton RP, Orme CDL, Owens IPF. 2006. Ecology predicts large-scale patterns of phylogenetic diversification in birds. Am Nat 168:220-229.

Pickles JO, Corey DP. 1992. Mechanoelectrical transduction by hair cells. Trends Neurosciencei 15:254-259.

Poore SO, Sanchez-Haiman A, Goslow GE Jr. 1997. Wing upstroke and the evolution of flapping flight. Nature 387:799-802.

Pozzo T, Berthoz A, Lefort L. 1990. Head stabilization during various locomotor tasks in humans. I. Normal subjects. Exp Brain Res 82:97-106.

Proctor N, Lynch P. 1993. Manual of Ornithology. New Haven: Yale University Press.

Prum RO. 2002. Why ornithologists should care about the theropod origin of birds. The Auk 119:1-17.

Purkyně JE. 1820. Beiträge zur näheren Kenntnis des Schwindels aus heutognostischen Daten. Medizinische Jahrbücher des Kaiserlich-Königlichen Österreichischen Staates 6:79-125.

Rabbitt RD. 1999. Directional coding of three-dimensional movements by the vestibular semicircular canals. Biol Cybern 80:417-431.

Rabbitt RD, Boyle R, Highstein SM. 1995. Mechanical indentation of the vestibular labyrinth and its relationship to head rotation in the toadfish, *Opsanus tau*. J Neurophysiol 73:2237-2260.

Rabbitt RD, Boyle R, Highstein SM. 1998. Responses of patent and plugged semicircular canals to linear and angular acceleration. Soc Neurosci Abstr 24:1653.

Rabbitt RD, Damiano ER, Grant JW. 2004. Biomechanics of the semicircular canals and otolith organs; pp. 153-201 in Highstein SM, Fay RR, Popper AN (eds.), The Vestibular System. New York: Springer-Verlag.

Ramprashad F, Landolt JP, Money KE, Laufer J. 1984.Dimensional analysis and dynamic response characterization of mammalian peripheral vestibular structures. Am J Anat 169:295-313.

Ramprashad F, Landolt JP, Money KE, Laufer J. 1986. Comparative morphometric study of the vestibular system of the vertebrata: reptilia, aves, amphibia, and pisces. Acta Otolaryngol Suppl. 427:1-42.

Rawles ME. 1963. Tissue interactions in scale and feather development as studied in dermal-epidermal recombinations. J Embryol Exp Morph 11:765-789.

Rayfield EJ, Norman DB, Horner CC, Horner JR, Smith PM, Thomason JJ, Upchurch P. 2001. Cranial design and function in a large theropod dinosaur. Nature 409:1033-1037.

Rayner JMV. 1979a. A new approach to animal flight mechanics. J Exp Biol 80:17-54.

Rayner JMV. 1979b. A vortex theory of animal flight. Part 1. The vortex wake of a hovering animal. J Fluid Mech 91:697-730.

Rayner JMV. 1979c. A vortex theory of animal flight. Part 2. The forward flight of birds. J Fluid Mech 91:731-763.

Rayner JMV. 1985a. Bounding and undulating flight in birds. J Theor Biol 117:47-77.

Rayner JMV. 1985b. Mechanical and ecological constraints on flight evolution; pp. 279-288 in Hecht MK, Ostrom JH, Viohl G, Wellnhofer P (eds.), The Beginnings of Birds. Germany: Freunde des Jura-Museums, Eichstätt.

Rayner JMV. 1985c. Cursorial gliding in proto-birds: an expanded version of a discussion contribution; pp. 289-292 in Hecht MK, Ostrom JH, Viohl G, Wellnhofer P (eds.), The Beginnings of Birds. Germany: Freunde des Jura-Museums, Eichstätt.

Rayner JMV. 1988a. Form and function in avian flight; pp. 1-66 in Johnston RF (ed.), Current Ornithology, vol. 5. New York: Plenum Press.

Rayner JMV. 1988b. The evolution of vertebrate flight. Biol J Linn Soc 34:269-287.

Rayner JMV. 1991a. Wake structure and force generation in avian flapping flight. Acta XX Congr Int Ornithol 2:702-715.

Rayner JMV. 1991b. Avian flight evolution and the problem of *Archaeopteryx*; pp. 183-212 in Rayner JMV and Wootton RJ, Biomechanics and Evolution. Cambridge: Cambridge Univ. Press.

Rayner JMV. 1994. Aerodynamic corrections for the flight of birds and bats in wind tunnels. J Zool (Lond) 234:537-563.

Rayner JMV. 1995. Dynamics of the vortex wakes of flying and swimming vertebrates; pp. 131-155 in CP Ellington, TJ Pedley (eds.), Symposia of the Society for Experimental Biology XLIX. Cambridge: Company of Biologists.

Rayner JMV. 2001. On the origin and evolution of flapping flight aerodynamics in birds; pp. 363-385 in Gauthier J, Gall LF (eds.), New Perspectives on the Origin and Early Evolution of Birds. New Haven: Peabody Museum of Natural History.

Rayner JMV, Aldridge HDJN. 1985. Three-dimensional reconstruction of animal flight paths and the turning flight of microchiropteran bats. J Exp Biol 118:247-265.

Reisine H, Simpson JI, Henn V. 1988. A geometric analysis of semicircular canals and induced activity in their peripheral afferents in the rhesus monkey. Ann NY Acad Sci 445:163-172.

Retzius G. 1881. Das Gehörorgan der Wirbelthiere: I. Das Gehörorgan der Fische und Amphibien. Stockholm: Centraldruckerei.

Retzius G. 1884. Das Gehörorgan der Wirbelthiere: II. Das Gehörorgan der Amnioten. Stockholm: Stockholm: Centraldruckerei.

Ricci AJ, Fettiplace R. 1998. Calcium permeation of the turtle hair cell mechanotransducer channel and its relation to the composition of endolymph. J Physiol
506:159-173.

Rietschel S. 1985. Feathers and wings of *Archaeopteryx*, and the question of her flight ability; pp. 251-265 in Hecht MK, Ostrom JH, Viohl G, Wellnhofer P (eds.), The Beginnings of Birds. Germany: Freunde des Jura-Museums, Eichstätt.

Robinson DA. 1976. Adaptive gain control of vestibuloocular reflex by the cerebellum. J Neurophysiol 39: 954-969.

Sampson SD, Witmer LM. 2007. Craniofacial anatomy of *Majungasaurus crenatissimus* (Theropoda: Abelisauridae) from the Late Cretaceous of Madagascar. Memoirs of the Society of Vertebrate Paleontology, J Vert Paleo 27 (Supplement to 2):32-102.

Sanz JL, Chiappe LM, Perez-Moreno BP, Buscalioni AD, Moratella JJ, Ortega F, Poyato-Ariza FJ. 1996. An Early Cretaceous bird from Spain and its implications for the evolution of avian fight. Nature 382:442-445.

Savile DBO. 1957. Adaptive evolution in the avian wing. Evolution 11:212-224.

Schellart NAM, Wubbels RJ. 1998. The auditory and mechanosensory lateral line system; pp. 283-312 in Evans DH (ed.), The physiology of fishes, 2nd ed. New York: CRC Press.

Schnell GD, 1965. Recording the flight-speed of birds by doppler radar. Living Bird 4:79-87.

Schnell GD, Hellack JJ. 1979. Bird flight speeds in nature: optimized or a compromise? Am Nat 113:53-66.

Schöne H. 1984. Spatial Orientation: The Spatial Control of Behavior in Animals and Man. Princeton: Princeton University Press.

Schweigart G, Maurer C, Mergner T. 2003. Combined action of smooth pursuit eye movements, optokinetic reflex and vestibulo-ocular reflex in macaque monkey during transient stimulation. Neurosci Lett 340:217-220.

Schweitzer MH, Watt JA, Avci R, Knapp L, Chiappe L, Norell M, Marshall M. 1999. Beta-keratin specific immunological reactivity in feather-like structures of the Cretaceous alvarezsaurid, *Shuvuuia deserti*. J Exp Zool 285:146-157.

Seebacher F, Grigg GC, Beard LA. 1999. Crocodiles as dinosaurs: behavioural thermoregulation in very large ectotherms leads to high and stable body temperatures. J Exp Biol 202:77–86.

Seebacher F. 2001. A new method to calculate allometric length-mass relationships of dinosaurs. J Vert Paleo 21:51-60.

Senter P, Robins JH. 2003. Taxonomic status of the specimens of *Archaeopteryx*. J Vert Paleo 23:961-965.

Senter P. 2005. Function in the stunted forelimbs of *Mononykus olecranus* (Theropoda), a dinosaurian anteater. Paleobiology 31:373-381.

Senter P. 2006. Scapular orientation in theropods and basal birds, and the origin of flapping flight. Acta Palaeontol Pol 51:305-313.

Sereno PC, Novas FE. 1992. The complete skull and skeleton of an early dinosaur. Science 258:1137-1140.

Sereno PC. 1997. The origin and evolution of dinosaurs. Annu Rev Earth Planet Sci 25:435-489.

Sereno PC. 1999. The evolution of dinosaurs. Science 284: 2137-2147.

Shimizu T, Karten HJ. 1991. Central visual pathways in reptiles and birds: Evolution of the visual system; pp. 421-441 in Cronly-Dillon JR, Gregory RL (eds.), Vision and Visual Dysfunction, Vol. 2. Boca Raton: CRC.

Shinoda Y, Sugiuchi Y, Futami T, Kakei S, Izawa Y, Na J. 1996. Four convergent patterns of input from the six semicircular canals to motoneurons of different neck muscles in the upper cervical cord. Ann NY Acad Sci 781:264-274.

Sibley CG, Ahlquist JE. 1990. Phylogeny and classification of birds: a study in molecular evolution. New Haven: Yale University Press.

Sibley DA. 2001. The Sibley Guide to Bird Life and Behavior. New York: Alfred A. Knopf.

Simpson JI. 1984. The accessory optic system. Rev Neurosci 7:13-41.

Simpson JI, Giolli RA, Blanks RHI. 1988. The pretectal nuclear complex and the accessory optic system. Rev Oculomot Res 2:335-364.

Sipla JS. 2002. Kinematics of head posture during galloping locomotion in *Erythrocebus patas*. J Vestibular Res Suppl. 11: 193.

Sipla JS, Ross CF, Larson SG. 2002. Kinematics and EMG activation of head-neck muscles during locomotion in *Erythrocebus patas*. Am J Phys Anthrop Suppl. 36:193.

Sipla JS, Georgi JA, Forster CA. 2003. The semicircular canal dimensions of birds and crocodilians: Implications for the origin of flight. J Vert Paleo Suppl 23:97.

Sipla JS, Georgi JA, Forster CA. 2004. The semicircular canals of dinosaurs: Tracking major transitions in locomotion. J Vert Paleo Suppl 24:113.

Sipla JS, Spoor F. In press. The physics and physiology of balance; in Thewissen JGM, Nummela S (eds.), Senses on the Threshold: Form and Function of the Sense Organs in Secondarily Aquatic Tetrapods. Berkeley: University of California Press.

Smith CA, Sjöstrand F. 1961. A synaptic structure in the hair cells of the guinea pig cochlea. J Ultrastruct Res 5:184-192.

Smith RJ. 1994. Degrees of freedom in interspecific allometry: an adjustment for the effects of phylogenetic constraint. Am J Phys Anthropol 93:95-107.

Sokal RR, Rohlf FJ. 1995. Biometry, 3rd ed. New York: WH Freeman and Co.

Spaar R and Bruderer B. 1997. Optimal flight behavior of soaring migrants: a case study of migrating steppe buzzards *Buteo buteo vulpinus*. Behav Ecol 8: 288-297.

Spear LB and Ainley DG. Flight behaviour of seabirds in relation to wind direction and wing morphology. Ibis 139:221-233.

Spedding GR. 1986. The wake of a jackdaw (Corvus monedulus) in slow flight. J Exp Biol 125:287-307.

Spedding GR. 1987a. The wake of a kestrel (*Falco tinnunculus*) in flapping flight. J Exp Biol 127:59-78.

Spedding GR. 1987b. The wake of a kestrel (*Falco tinnunculus*) in gliding flight. J Exp Biol 127:45-57.

Spedding GR, Rayner JMV, Pennycuick CJ. 1984. Momentum and energy in the wake of a pigeon (*Columba livia*) in slow flight. J Exp Biol 111:81-102.

Spedding GR, Rosén M, Hedenström A. 2003. A family of vortex wakes generated by a thrush nightingale in free flight in a wind tunnel over its entire natural range of flight speeds. J Exp Biol 206:2313-2344.

Spoendlin H. 1966.Some morphofunctional and pathological aspects of the vestibular sensory epithelia; pp. 99- 115 in Second Symposium on the Role of the Vestibular Organs in Space Exploration. Washington, DC: U.S. Government Printing Office, NASA SP-115.

Spoor F. 1993. The comparative morphology and phylogeny of the human bony labyrinth. Ph.D. Dissertation. University of Utrecht, Utrecht.

Spoor F. 2003. The semicircular canal system and locomotor behaviour, with special reference to hominin evolution. Cour Forsch Inst Senck 243:93-104.

Spoor F, Zonneveld F. 1998. A comparative review of the human bony labyrinth. Yrbk Phys Anthropol 41:211-251.

Spoor F, Thewissen JGM. In press. In Thewissen JGM, Nummela S (eds.), Senses on the Threshold: Form and Function of the Sense Organs in Secondarily Aquatic Tetrapods. Berkeley: University of California Press.

Spoor F, Wood B, Zonneveld F. 1996. Evidence for a link between human semicircular canal size and bipedal behaviour. J Hum Evol 30:183-187.

Spoor F, Jeffery N, Zonneveld F. 2000. Imaging skeletal growth and evolution; pp. 123-161 in O'Higgins P, Cohn M (eds.), Development, Growth and Evolution. London: Academic Press.

Spoor F, Bajpai S, Hussain ST, Kumar K, Thewissen JGM. 2002. Vestibular evidence for the evolution of aquatic behaviour in early cetaceans. Nature 417:163-166.

Spoor F, Garland T Jr., Krovitz G, Ryan TM, Silcox MT, Walker A. 2007. The primate semicircular canal system and locomotion. Proc Nat Acad Sci USA 104:10808-10812.

Steinacker A. 2004. Sensory processing and ionic currents in vestibular hair cells; pp. 202-234 in Highstein SM, Fay RR, Popper AN (eds.), The Vestibular System. New York: Springer-Verlag.

Steinhausen W. 1931. Über den Nachweis der Bewegung der Cupula in der intaktene Bogengangsampulle des Labyrinthes bei der naturlichen rotatorischen und calorischen Reizung. Pflugers Archiv 225:322-328.

Steinhausen W. 1933. Über die Beobachtungen der Cupula in den Bogengangsampullen des Labyrinthes des Lebendes Hechts. Pflugers Archiv 232:500-512.

Sterling P, Matthews G. 2005. Structure and function of ribbon synapses. Trends Neurosci 28:20-29.

Strait DA, Ross CF. 1999. Kinematic data on primate head and neck posture: Implications for the evolution of basicranial flexion and an evaluation of registration planes. Am J Phys Anthrop 108:205-222.

Suedmeyer WK, Bermudez AJ, Barr BC, Marsh AE. 2001. Acute pulmonary *Sarcocystis falcatula*-like infection in three Victoria crowned pigeons (*Goura Victoria*) housed indoors. J Zoo Wildlife Med 32:252-256.

Suzuki JI, Cohen B. 1964. Head, eye, body and limb movements from semicircular canal nerves. Exp Neurol 10:393-405.

Tanturri V. 1933. Zur Anatomie and Physiologie des Labyrinthes der Voegel. Mschr Ohrenheilk. Laryngo-Rhinol 67:1-27.

Tellegen AJ, Arends JJA, Dubbeldam JL. 2001. The vestibular nuclei and vestibuloreticular connections in the mallard (*Anas platyrhynchos* L.), an anterograde and retrograde tracing study. Brain Behav Evol 58:205–217

Ten Kate JH, Barneveld HH, Kuiper JW. 1970. The dimensions and sensitivities of semicircular canals. J Exp Biol 53:501-514.

Thomas ALR. 1993. On the aerodynamics of birds' tails. Phil Trans Royal Soc London B 340:361-380.

Thulborn RA. 1984. The avian relationships of *Archaeopteryx*, and the origin of birds. Zoo J Linn Soc 82:119-158.

Tian X, Iriarte-Diaz J, Middleton K, Galvao R, Israeli E, Roemer A, Sullivan A, Song A, Swartz S, Breuer K. 2006. Direct measurements of the kinematics and dynamics of bat flight. Bioinsp Biomim 1:S10-S18.

Tobalske BW. 1995. Neuromuscular control and kinematics of intermittent flight in European starlings {*Sturnus vulgaris*). J Exp Biol 198:1259-1273.

Tobalske BW. 2000. Biomechanics and physiology of gait selection in flying birds. Physiol Biochem Zool 73:736-750.

Tobalske BW, Dial KP. 1994. Neuromuscular control and kinematics of intermittent flight in budgerigars (*Melopsittacus undulatus*). J Exp Biol 187:1-18.

Tobalske BW, Dial KP. 1996. Flight kinematics of black-billed magpies and pigeons over a wide range of speeds. J Exp Biol 199:263-280.

Tobalske BW, Olson NE, Dial KP. 1997. Flight style of the black-billed magpie: variation in wing kinematics, neuromuscular control, and muscle composition. J Exp Zool 279:313-329.

Tucker VA, Schmidt-Koenig K. 1971. Flight speeds of birds in relation to energetics and wind directions. Auk 88:87-107.

Tukewitsch BG. 1934. Zur Anatomie des Gehörorgans der Vögel (Canales semicirculares). Z Anat Entwicklungsgesch 103:551-608.

Tykoski RS, Forster CA, Rowe T, Sampson SD, Munyikwa D. 2002. The presence of a furcula in the coelophysid theropod (Dinosauria: Saurischia) *Syntarsus*. J Vert Paleo 22:728-733.

van Bergeijk WA. 1966. Evolution of the sense of hearing in vertebrates. Am Zool 6:371-377.

Van Buskirk WC. 1987. Vestibular mechanics; pp. 31.1-31.17 in Skalak R, Chien S (eds.), Handbook of Bioengineering. New York: New York Academy of Sciences.

Van Buskirk WC, Watts RG, Liu YK. 1976. The fluid mechanics of the semicircular canals. J Fluid Mech 78:87-98.

van Egmond AAJ, Groen JJ, Hulk J, Jongkees LBW. 1948. The turning test with small regulable stimuli. V. Is Ewald's law valid in men? J. Laryngol. Otol. 62: 299-305.

van Egmond AAJ, Groen JJ, Jongkees LBW. 1949. The mechanics of the semicircular canal. J Physiol 110:1-17.

Videler JJ, Groenewegen A, Gnodde M, Vossebelt G. 1988. Indoor flight experiments with trained kestrels: II. The effect of added weight on flapping flight kinematics. J Exp Biol 134:185-199.

von Gersdorff H. 2001. Synaptic ribbons: versatile signal transducers. Neuron 29:7-10.

von Meyer H. 1861. *Archaeopteryx lithographica* (Vogel-Feder) und *Pterodactylus* von Solnhofen. Neues Jb Miner Geol Palaeontol 1861:678-679.

Wagner GP, Gauthier JA. 1999. 1,2,3 = 2,3,4: A solution to the problem of the homology of the digits in the avian hand. Proc Nat Acad Sci USA 96:5111-5116.

Walker A, Silcox MT, Bloch JI, Spoor F, Krovitz G. 2003. The semicircular canals of plesiadapiform primates and their functional significance. J Vert Paleo 23:107A.

Walker A, Krovitz GE, Silcox MT, Simons EL, Spoor F. 2004. The semicircular canals of subfossil lemurs and their functional significance. Am J Phys Anthropol 38 (Suppl): 202.

Wallman J, Letelier J-C. 1993. Eye movements, head movements, and gaze stabilization in birds; pp. 244-263 in Zeigler HP, Bischof H-J (eds.), Vision, Brain, and Behavior in Birds. Cambridge: Bradford.

Warrick DR. 1998. The turning- and linear-maneuvering performance of birds: the cost of efficiency for coursing insectivores. Can J Zool 76:1063-1079.

Warrick DR, Dial KP. 1998. Kinematic, aerodynamic, and anatomical mechanisms in the slow maneuvering flight of pigeons. J Exp Biol 201:655-672.

Warrick DR, Dial KP, Biewener AA. 1998. Asymmetrical force production in the maneuvering flight of pigeons. The Auk 115:916-928.

Warrick DR, Bundle MW, Dial KP. 2002. Bird maneuvering flight: blurred bodies, clear heads. Integ and Comp Biol 42:141-148.

Warton DI, Wright IJ, Falster DS, Westoby M. 2006. Bivariate line-fitting methods for allometry. Biol Rev 81:259-291.

Wellnhofer P. 2004. The plumage of *Archaeopteryx:* Feathers of a dinosaur?; pp. 282-300 in Currie PJ, Koppelhus EB, Shugar MA, Wright JL (eds.), Feathered Dragons. Bloomington: Indiana University Press.

Wersäll J. 1956. Studies on the structure and innervation of the sensory epithelium of the cristae ampullares in the guinea pig. A light and electron microscopic investigation. Acta Otolaryngol Suppl 126:1-85.

Wersäll J. 1968. Efferent innervation of the inner ear; pp. 123-139 in von Euler C, Skoglund C, Söderberg U (eds.), Structure and Function of Inhibitory Neuronal Mechanisms. Oxford: Pergamon.

Wersäll J, Bagger-Sjöbäck D. 1974. Morphology of the vestibular sense organ; pp. 123-170 in Kornhuber HH (ed.), Handbook of Sensory Physiology: Vestibular System. New York: Springer-Verlag.

Williamson MR, Dial KP, Biewener AA. 2001. Pectoralis muscle performance during ascending and slow level flight in mallards (*Anas platyrhynchos*). J Exp Biol 204:595-507.

Wilson VJ, Maeda M. 1974. Connections between semicircular canals and neck motoneurons in the cat. J Neurophysiol 37:346-357.

Wilson VJ, Melvill Jones G. 1979. Mammalian Vestibular Physiology. New York: Plenum Press.

Wilson VJ, Boyle R, Fukushima K, Rose PK, Shinoda Y, Sugiuchi Y, Uchino Y. 1995. The vestibulocollic reflex. J Vestib Res 5: 147-170.

Witmer LM. 1991. Perspectives on avian origins; pp. 427-465 in Schultze H-P, Trueb L (eds.), Origins of the Higher Groups of Tetrapods. Ithica: Cornell University Press.

Witmer L. 2002. The debate on avian ancestry: phylogeny, function, and fossils; pp. 3-30 in Chiappe LM, Witmer LM (eds.), Mesozoic Birds: Above the Heads of Dinosaurs. Berkeley: University of California Press.

Witmer LM and RC Ridgely. In press. The Cleveland tyrannosaur skull (*Nanotyrannus* or *Tyrannosaurus*): new findings based on CT scanning, with special reference to the braincase. Kirtlandia.

Witmer LM, Chatterjee S, Franzosa J, Rowe T. 2003. Neuroanatomy of flying reptiles and implications for flight, posture and behavior. Nature 425:950-953.

Wohlschlager A, Jager R, Delius JD. 1993. Head and eye movements in unrestrained pigeons (*Columba livia*). J Comp Psych 107: 313-319.

Wold, JE. 1976. The vestibular nuclei in the domestic hen (*Gallus domesticus*) I. Normal anatomy. Anat Embryol 149:29-46.

Xiong G, Nagao S. 2002.The lobulus petrosus of the paraflocculus relays cortical visual inputs to the posterior interposed and lateral cerebellar nuclei: an anterograde and retrograde tracing study in the monkey. Exp Brain Res 147:252-263.

Xu X, Tang Z-L, Wang X-L. 1999a. A therizinosauroid dinosaur with integumentary structures from China. Nature 399:350-354.

Xu X, Wang X-L, Wu X-C. 1999b. A dromaeosaurid dinosaur with a filamentous integument from the Yixian Formation of China. Nature 401:262-266.

Xu X, Zhou Z, Wang X. 2000. The smallest known non-avian theropod dinosaur. Nature 480:705-708.

Xu X, Zhou Z-H, Prum RO. 2001. Branched integumental structures in *Sinornithosaurus* and the origin of feathers. Nature 410:200-204.

Xu X, Norell MA, Wang X, Makovicky PJ, Wu X. 2002. A basal troodontid from the early Cretaceous of China. Nature 415:780-784.

Xu X, Zhou Z, Wang X, Kuang X, Zhang F, Du X. 2003. Four-winged dinosaurs from China. Nature 421, 335-340.

Xu X, Norell MA, Kuang X, Wang X, Zhao Q, Jia C. 2004. Basal tyrannosauroids from China and evidence for protofeathers in tyrannosauroids. Nature 431:680-684.

Yalden DW. 1971. The flying ability of *Archaeopteryx*. Nature 231:127.

Yamauchi AM, Rabbitt RD, Boyle R, Highstein SM. 2002. Relationship between inner-ear fluid pressure and semicircular canal afferent nerve discharge. J Assoc Res Otolaryngol 3:26-44.

Zhou Z-H, Wang X-L. 2000. A new species of *Caudipteryx* from the Yixian Formation of Liaoning, northeast China. Vert PalAs 38:113-130.

Zhou Z-H, Wang X-L, Zhang F-C, Xu X. 2000. Important features of *Caudipteryx*—Evidence from two nearly complete new specimens. Vert PalAs 38:241-254.

Zusi R. 1993 Patterns of diversity in the avian skull; pp. 391-437 in Hanken J, Hall BK (eds.) The Skull, vol. 2. Chicago: University of Chicago Press.

Appendix 1 – Raw Morphometric Data

Data on aspect ratio and wing loading are from Birt-Friesen et al. (1989), Berg and Rayner (1995), Pennycuick (1996), Hertel and Balance (1999), Williamson et al. (2001), and Nudds et al. (2004b, 2007). Data on airspeed velocity are from Schnell (1965), Tucker and Schmidt-Koenig (1971), Schnell and Hellack (1979), Butler and Woakes (1980), Bellrose and Crompton (1981), Videler et al. (1988), Leshem and Yom-Tov (1996), Nudds et al. (2004b), and Miller et al. (2005). Data on brachial index are from Nudds et al. (2007). Sources of body mass estimates are indicated for each specimen (see footnotes at bottom of table). Flightless bird species are indicated by the superscript $^{(FL)}$ after the species name. Bipedal non-avian dinosaurs are indicated by the superscript $^{(2P)}$. Quadrupedal dinosaurs are indicated by the superscript $^{(4P)}$. All other specimens represent volant birds.

Abbreviations: ASCc – anterior semicircular canal circumference (mm), PSCc – posterior semicircular canal circumference (mm), LSCc – lateral semicircular canal circumference (mm), SCc – average semicircular canal circumference (mm), AR – aspect ratio, WL – wing loading (N m^{-2}), VEL – airspeed velocity (m sec^{-1}), BI – brachial index, M – Body Mass (g), Source – source of body mass estimate (itemized at bottom of table.)

Specimens referred to in this appendix are maintained in the collections of the following institutions, abbreviated as follows:

AMNH – American Museum of Natural History, New York
CM – Carnegie Museum of Natural History, Pittsburgh
IGM – Institute of Geology, Mongolian Academy of Sciences, Ulaan Bataar
LACM – Natural History Museum of Los Angeles County, Los Angeles
MAD – Madagascar specimen field number, Mahajanga Basin Project, Stony Brook University, Stony Brook
MCZ – Museum of Comparative Zoology, Harvard University, Cambridge
MWC – Museum of Western Colorado, Fruita
UTMP – University of Texas Museum of Paleontology, Austin
YPM – Peabody Museum of Natural History, Yale University

TAXON	SPECIMEN	ASCc	PSCc	LSCc	SCc	AR	WL	VEL	BI	M	Source
NEOGNATH BIRDS											
ORDER ANSERIFORMES											
Anas acuta	AMNH 24208	11.39	9.19	9.06	9.88	10.05	109.14	16.19	1.13	1035	a
Anas clypeata	AMNH 25362	11.77	10.03	9.13	10.31	9.84	108.39	—	1.17	460	b
Anas penelope	AMNH 5984	11.11	9.27	9.93	10.11	10.04	101.62	17.10	1.17	724	a
Anas platyrhynchos	AMNH 16240	12.79	8.91	9.31	10.34	8.61	113.76	—	1.21	1082	a
Anas rubripes	AMNH 10666	12.38	8.71	10.27	10.45	8.87	128.53	—	1.21	1100	a
Anser fabalis	AMNH 4028	18.51	11.79	11.79	14.03	8.17	112.72	—	1.05	3198	a
Anseranas semipalmata	AMNH 1772	16.70	11.72	12.19	13.53	6.03	64.86	—	1.02	2070	a
Branta leucopsis	AMNH 11437	15.83	9.79	11.27	12.29	15.52	130.01	18.70	1.07	1586	a
Cairina moschata	AMNH 11024	12.93	9.80	10.53	11.08	21.07	107.15	—	1.16	2022	a
Cygnus atratus	AMNH 945	16.12	12.72	11.65	13.50	—	—	—	1.09	5100	a
Cygnus buccinator	AMNH 4365	21.03	13.34	12.45	15.61	13.84	232.81	—	1.03	10701	a
Cygnus columbianus	AMNH 18674	16.82	12.34	13.72	14.29	10.09	160.69	—	1.13	4900	b
Cygnus olor	AMNH 1075	19.97	16.31	16.24	17.50	9.16	184.08	16.00	1.06	9670	a
Somateria mollissima	AMNH 19574	16.13	11.38	12.54	13.35	9.06	182.39	20.20	1.14	2400	b
Tachyeres leucocephalus (FL)	AMNH 8513	15.60	12.31	14.39	14.10	—	—	—	1.22	3808	c
Tachyeres pteneres (FL)	AMNH 1222	16.76	12.99	13.45	14.40	—	—	—	1.30	4228	a
ORDER APODIFORMES											
Campylopterus duidae	AMNH 18150	6.54	5.17	5.65	5.79	—	—	—	—	7	b
Metallura tyrianthina	AMNH 24119	5.17	4.12	4.61	4.63	—	—	—	—	3	b
ORDER ARDEIFORMES											
Ardea cinerea	AMNH 25358	18.79	13.62	13.91	15.44	8.05	41.02	11.00	0.85	1150	b
Ardea cocoi	AMNH 3620	19.89	14.10	14.85	16.28	—	—	—	0.90	3200	a
Ardea herodias	AMNH 27250	20.67	13.58	14.59	16.28	7.67	50.35	9.40	0.89	2576	a
Cochlearius cochlearius	AMNH 2424	20.66	13.59	15.05	16.43	5.79	38.82	—	0.89	712	a
Egretta caerulea	AMNH 26358	13.43	9.35	10.13	10.97	7.62	29.58	8.80	0.86	315	a
Nycticorax nycticorax	AMNH 20571	20.21	14.55	16.52	17.09	6.89	38.28	—	0.90	883	a

ORDER CAPRIMULGIFORMES											
Chordeiles minor	AMNH 15623	13.76	9.65	10.61	11.34	9.91	19.77	—	0.85	62	a
Nyctibius griseus	AMNH 10021	15.50	9.43	12.75	12.56	—	21.04	—	0.95	185	a
Podargus strigoides	AMNH 12462	21.40	13.50	16.86	17.25	—	—	—	0.84	350	a
Steatornis caripensis	AMNH 22733	15.13	10.47	10.87	12.16	—	—	—	0.68	414	a
ORDER CHARADRIIFORMES											
Alca torda	AMNH 2764	18.82	11.95	13.05	14.61	12.25	190.98	16.00	1.29	719	a
Burhinus magnirostris	AMNH 4000	23.28	13.58	15.11	17.33	—	—	—	0.95	1000	a
Cerorhinca monocerata	AMNH 19586	15.34	11.01	13.66	13.34	—	—	—	1.27	510	b
Fratercula arctica	AMNH 16726	17.54	11.36	13.89	14.26	8.79	111.69	17.60	1.25	381	a
Larus argentatus	AMNH 5462	25.38	14.98	15.28	18.55	10.69	54.08	10.90	0.89	1247	b
Larus atricilla	AMNH 9914	18.40	10.34	10.70	13.15	10.35	29.72	9.50	0.92	334	b
Larus canus	AMNH 21456	19.20	11.46	11.88	14.18	10.33	34.20	11.60	0.89	525	b
Larus marinus	AMNH 16600	27.41	16.19	16.54	20.05	11.43	68.71	12.90	0.89	2100	b
Larus ridibundus	AMNH 25365	16.62	8.88	9.12	11.54	10.38	32.28	10.10	0.87	140	b
Pinguinus impennis (FL)	AMNH "1"	27.91	17.37	16.88	20.72	—	—	—	—	5000	d
Rissa tridactyla	AMNH 18566	18.98	10.68	12.38	14.01	11.97	48.08	13.10	0.90	360	b
Rynchops niger	AMNH 23538	13.46	11.13	10.85	11.81	15.67	33.04	9.50	0.82	350	b
Scolopax rusticola	AMNH 5053	20.29	12.52	15.51	16.11	7.14	58.34		0.91	313	a
Stercorarius parasiticus	AMNH 22352	18.38	12.33	12.65	14.45	10.54	40.36	13.30	0.95	470	b
Sterna fuscata	AMNH 9055	16.64	11.10	11.28	13.01	11.38	29.99	10.40	0.86	180	a
Sterna hirundo	AMNH 17840	13.82	9.84	10.12	11.26	14.16	27.04	11.62	0.84	120	a
Sterna maxima	AMNH 12991	21.71	11.90	12.03	15.21	13.84	42.07	10.00	0.83	775	b
Uria aalge	AMNH 20645	18.81	12.60	13.90	15.10	12.94	229.61	19.10	1.38	1100	b
Uria lomvia	AMNH 22332	20.96	12.46	14.05	15.82	15.74	285.76	—	1.28	1000	b
ORDER CICONIIFORMES											
Ajaia ajaja	AMNH 27251	18.49	11.60	12.66	14.25	6.91	—	11.90	0.88	2163	b
Eudocimus albus	AMNH 25871	18.17	10.00	13.14	13.77	7.18	63.53	12.90	0.94	764	a
Leptoptilos crumeniferus	AMNH 5862	29.11	19.83	19.65	22.87	7.59	71.94	—	0.78	7100	a
Mycteria americana	AMNH 26362	27.62	15.66	16.24	19.84	6.78	72.44	—	0.80	2050	a
Phoenicopterus minor	AMNH 26170	21.28	13.97	14.36	16.54	—	—	—	—	1900	a

Phoenicopterus ruber	AMNH 11656	21.88	15.55	14.57	17.33	7.52	87.10	—	0.94	3540	a
ORDER COLUMBIFORMES											
Caloenas nicobarica	AMNH 1092	20.18	12.71	15.11	16.00	—	—	—	0.87	530	a
Columba fasciata	AMNH 22784	16.38	11.31	11.77	13.15	—	54.83	—	0.86	264	b
Columba livia	AMNH 20013	16.48	11.42	12.22	13.37	7.18	55.21	12.80	0.86	385	b
Columba picazuro	AMNH 25629	17.42	11.84	14.80	14.69	—	—	—	0.86	340	b
Goura victoria	AMNH 1236	22.96	15.26	17.83	18.68	—	—	—	0.81	2900	f
ORDER CORACIIFORMES											
Coracias garrulus	AMNH 12839	16.89	12.16	14.42	14.49	7.67	24.04	—	0.83	146	a
ORDER CUCULIFORMES											
Geococcyx californianus	AMNH 15978	20.51	12.18	17.37	16.69	—	—	—	1.23	376	a
ORDER FALCONIFORMES											
Accipiter gentilis	AMNH 17947	28.99	22.12	24.68	25.26	7.00	52.97	—	0.89	943	b
Accipiter nisus	AMNH 25244	16.91	11.83	14.66	14.47	6.50	30.41	8.70	0.83	130	b
Aquila chrysaetos	AMNH 1058	35.32	25.95	29.96	30.41	7.43	71.94	—	0.86	3477	a
Buteo buteo	AMNH 23691	26.16	19.81	22.62	22.86	6.70	35.40	9.30	0.84	969	a
Buteo jamaicensis	AMNH 18336	29.95	21.83	25.65	25.81	7.40	50.35	—	0.88	1028	a
Cathartes aura	AMNH 17842	24.46	16.44	20.24	20.38	7.33	40.36	10.60	0.84	1622	b
Circus aeruginosus	AMNH 24085	20.38	13.64	17.81	17.28	8.61	29.24	—	0.83	639	b
Circus cyaneus	AMNH 22598	20.31	13.45	16.40	16.72	7.60	27.48	—	0.88	358	a
Circus pygargus	AMNH 4209	19.38	12.43	15.80	15.87	8.24	22.70	—	0.78	295	a
Coragyps atratus	AMNH 26552	25.26	16.58	18.75	20.20	6.19	58.21	10.80	0.87	2081	a
Elanus caeruleus	AMNH 22920	22.39	15.29	18.57	18.75	8.28	26.42	—	0.87	350	a
Falco peregrinus	AMNH 26368	24.01	18.60	21.47	21.36	8.83	63.68	—	0.85	952	a
Falco sparverius	AMNH 16681	16.78	13.79	16.27	15.61	8.09	31.33	9.10	0.93	125	b
Falco tinnunculus	AMNH 25246	19.83	15.34	17.58	17.58	8.22	30.20	7.90	0.85	197	b
Gymnogyps californianus	AMNH 1937	31.14	18.95	20.29	23.46	9.48	100.92	—	0.86	10104	a
Gyps fulvus	AMNH 918	35.60	23.21	23.54	27.45	6.81	83.37	—	0.81	7436	a
Haliaeetus leucocephalus	AMNH 24193	31.99	23.06	27.20	27.42	6.64	61.51	11.20	0.91	5350	a
Harpia harpyja	AMNH 1383	33.15	24.14	26.58	27.96	—	—	—	0.85	6200	a
Ictinia plumbea	AMNH 22854	19.60	13.56	17.32	16.83	—	—	—	0.88	280	b

Milvus migrans	AMNH 9593	22.34	15.20	17.96	18.50	8.15	35.40	—	0.87	596	a
Pandion haliaetus	AMNH 27190	26.45	17.46	19.43	21.11	7.46	47.75	10.60	0.79	1403	a
Sagittarius serpentarius	AMNH 9165	31.69	20.40	22.22	24.77	—	65.01	—	0.99	3607	a
Sarcoramphus papa	AMNH 877	30.50	23.13	24.98	26.20	—	—	—	0.82	3400	a
Spizaetus ornatus	AMNH 2972	30.42	21.14	25.59	25.71	—	56.10	—	0.89	1270	a
Torgos tracheliotus	AMNH 2990	35.18	25.37	28.22	29.59	6.92	66.83	—	0.73	7500	a
ORDER GALLIFORMES											
Alectura lathami	AMNH 1388	16.76	12.57	14.14	14.49	—	—	—	0.98	2300	a
Chrysolophus amherstiae	AMNH 3589	15.11	12.13	14.30	13.84	—	—	—	1.07	738	a
Lagopus lagopus	AMNH 13873	12.34	10.72	11.94	11.67	6.97	108.14	—	1.09	516	a
Lophura erythrophthalma	AMNH 11090	16.15	13.46	13.57	14.40	—	75.36	—	0.98	1043	a
Meleagris gallopavo	AMNH 18704	17.63	13.07	15.14	15.28	4.47	89.33	—	1.08	3600	b
Numida meleagris	AMNH 23327	12.91	9.97	11.22	11.37	—	88.31	—	1.11	1500	b
Pavo cristatus	AMNH 16428	18.98	14.48	14.49	15.98	4.71	93.11	—	1.16	4089	a
Phasianus colchicus	AMNH 24592	13.50	11.30	13.00	12.60	5.79	122.46	—	1.11	1317	a
Syrmaticus reevesii	AMNH 1078	15.13	12.53	14.13	13.93	—	—	—	1.03	1529	a
ORDER GAVIIFORMES											
Gavia immer	AMNH 26307	28.01	19.06	20.47	22.51	13.80	232.27	—	1.25	4134	a
Gavia stellata	AMNH 16091	22.42	15.05	15.21	17.56	16.26	199.53	—	1.24	1551	a
ORDER GRUIFORMES											
Aramus guarauna	AMNH 26373	20.59	14.89	15.14	16.87	7.59	63.24	—	0.96	1080	a
Cariama cristata	AMNH 1722	30.37	20.29	22.96	24.54	—	—	—	1.07	1400	a
Neotis denhami	AMNH 1967	32.14	20.25	25.15	25.85	9.14	88.10	—	0.87	4120	a
Otis tarda	AMNH 1706	26.99	17.11	20.16	21.42	8.13	153.82	—	0.93	8091	b
Psilopterus lemoinei (FL)	YPM 15109	36.31	23.60	26.98	28.96	—	—	—	—	7000	e
Rhynochetos jubatus	AMNH 1326	23.30	16.79	18.04	19.38	—	—	—	0.97	860	a
ORDER OPISTHOCOMIFORMES											
Opisthocomus hoazin	AMNH 12127	14.63	10.90	10.23	11.92	—	—	—	0.98	696	g
ORDER PASSERIFORMES											
Corvus brachyrhynchos	AMNH 5897	20.04	13.20	19.22	17.49	—	—	12.69	—	524	b
Corvus corone	AMNH 27117	19.68	12.29	17.74	16.57	6.65	40.55	10.50	0.83	570	a

Corvus frugilegus	AMNH 24645	20.64	13.24	18.99	17.63	7.01	38.55	—	0.82	528	b
Corvus monedula	AMNH 3490	18.90	10.34	15.20	14.82	—	—	—	—	246	a
Hirundo rustica	AMNH 17265	9.34	5.84	8.31	7.83	8.24	15.63	8.90	0.64	18	b
Molothrus ater	AMNH 26836	11.25	7.66	10.84	9.92	—	—	8.23	—	49	a
Pica pica	AMNH 25395	17.96	12.28	16.34	15.53	5.66	35.24	10.00	0.84	205	b
Procnias nudicollis	AMNH 5894	17.35	10.49	15.50	14.45	—	—	—	0.79	200	a
Rupicola rupicola	AMNH 18169	17.23	11.43	16.42	15.03	—	—	—	0.79	210	b
Sturnus vulgaris	AMNH 14558	12.01	7.47	10.52	10.00	7.10	37.84	14.70	0.82	91	b
Turdus migratorius	AMNH 15705	13.51	8.49	12.00	11.33	6.46	32.96	—	0.91	76	b
ORDER PELECANIFORMES											
Anhinga anhinga	AMNH 9859	15.68	9.81	10.08	11.86	8.77	77.27	—	1.11	1192	b
Fregata magnificens	AMNH 2351	26.26	17.61	19.12	21.00	12.85	40.07	9.30	—	1667	a
Fregata minor	AMNH 25843	24.19	17.16	20.28	20.55	—	—	—	0.79	927	a
Morus bassanus	AMNH 16840	28.35	21.24	22.28	23.95	12.98	101.41	—	1.16	2932	a
Pelecanus erythrorhynchos	AMNH 27222	22.17	14.11	13.92	16.73	—	—	—	0.91	7000	a
Pelecanus occidentalis	AMNH 3618	26.94	16.02	16.14	19.70	10.57	70.63	10.10	0.84	3174	a
Pelecanus onocrotalus	AMNH 5251	31.30	16.22	16.16	21.23	9.48	83.37	8.11	0.87	8500	a
Phaethon rubricauda	AMNH 5410	22.39	17.10	20.36	19.95	12.76	33.65	—	0.94	624	a
Phalacrocorax auritus	AMNH 23109	17.33	12.59	13.38	14.43	10.43	101.62	14.50	0.96	1260	b
Phalacrocorax carbo	AMNH 10380	17.24	11.79	13.64	14.23	9.95	107.65	15.00	0.93	2172	a
Phalacrocorax harrisi (FL)	AMNH 2312	15.02	13.28	14.78	14.36	—	—	—	—	2787	a
Phalacrocorax urile	AMNH 18390	18.52	11.75	13.91	14.73	—	—	—	0.94	2300	b
Sula dactylatra	AMNH 1452	24.50	17.79	17.28	19.86	12.16	84.76	—	0.93	1539	a
Sula leucogaster	AMNH 1885	20.79	15.07	13.97	16.61	12.14	64.06	—	0.88	1093	a
Sula sula	AMNH 1208	19.51	14.06	13.86	15.81	13.90	73.79	—	0.92	938	a
ORDER PICIFORMES											
Dryocopus pileatus	AMNH 22600	15.58	14.50	17.08	15.72	4.42	32.35	9.90	0.94	266	a
ORDER PODICIPEDIFORMES											
Aechmophorus occidentalis	AMNH 18782	16.06	9.65	12.01	12.57	—	—	—	1.13	1477	a
Podiceps cristatus	AMNH 25241	15.65	9.08	10.16	11.63	10.54	143.88	—	1.06	738	a

ORDER PROCELLARIIFORMES											
Daption capense	AMNH 3126	16.20	9.26	10.44	11.97	11.91	50.82	12.30	1.09	428	a
Diomedea exulans	AMNH 1440	37.07	22.30	23.75	27.70	17.74	139.96	15.00	1.00	8400	a
Diomedea immutabilis	AMNH 25838	29.00	19.66	17.72	22.12	15.56	85.51	—	1.00	3230	a
Diomedea irrorata	AMNH 1628	30.24	18.38	19.64	22.75	—	—	—	1.02	3750	a
Diomedea melanophrys	AMNH 23506	31.46	20.20	20.53	24.07	16.11	100.69	—	1.01	3500	b
Diomedea nigripes	AMNH 25837	30.67	19.30	18.44	22.81	14.96	116.41	—	1.00	3148	a
Fulmarus glacialis	AMNH 19553	15.43	9.88	11.28	12.20	11.40	73.45	13.00	1.06	600	b
Macronectes giganteus	AMNH 27156	27.50	15.26	17.34	20.03	12.22	120.23	15.20	1.03	5190	a
Oceanites oceanicus	AMNH 23547	11.10	5.90	6.16	7.72	8.85	20.37	10.40	1.14	30	b
Puffinus griseus	AMNH 23544	17.17	11.23	12.03	13.48	—	—	—	1.05	775	b
Puffinus tenuirostris	AMNH 17336	17.75	11.60	12.34	13.90	12.88	81.85	—	1.05	543	a
ORDER PSITTACIFORMES											
Alisterus scapularis	AMNH 9321	12.47	11.13	12.38	11.99	—	—	—	0.86	175	b
Amazona ochrocephala	AMNH 2766	16.69	16.89	17.37	16.98	—	—	—	0.84	510	a
Anodorhynchus hyacinthinus	AMNH 2777	18.80	15.20	15.50	16.50	—	—	—	0.75	1500	a
Nestor meridionalis	AMNH 27323	13.99	14.20	13.98	14.06	—	—	—	0.93	360	b
Probosciger aterrimus	AMNH 11351	17.02	13.87	12.56	14.48	—	—	—	0.84	760	a
Psittacus erithacus	AMNH 12777	13.11	10.43	11.59	11.71	7.83	37.33	—	0.82	250	a
Strigops habroptilus (FL)	AMNH 2079	12.07	12.54	10.93	11.85	—	—	—	1.03	1814	a
ORDER RALLIFORMES											
Aramides cajanea	AMNH 1909	17.41	11.98	13.44	14.27	5.21	64.71	—	1.12	397	a
Diaphorapteryx hawkinsi (FL)	AMNH 4667	20.86	12.43	13.64	15.64	—	—	—	—	1706	b
Fulica americana	AMNH 26371	13.48	9.65	9.24	10.79	7.82	93.76	—	1.16	560	a
Himantornis haematopus	AMNH 4183	20.71	13.73	14.40	16.28	—	—	—	1.00	390	a
Porphyrio hochstetteri (FL)	AMNH 26211	21.65	14.82	14.55	17.01	—	—	—	—	1456	b
Porphyrio porphyrio	AMNH 5052	14.92	9.59	10.78	11.76	—	—	—	1.06	840	a
Porzana carolina	AMNH 23161	11.05	7.35	9.00	9.13	6.17	44.16	—	1.17	75	a
ORDER STRIGIFORMES											
Asio flammeus	AMNH 24180	20.09	13.50	15.66	16.42	8.00	26.67	—	0.84	315	a
Bubo virginianus	AMNH 26702	32.35	22.23	27.55	27.38	6.58	57.94	—	0.90	1318	a

Nyctea scandiaca	AMNH 8	33.17	22.38	27.59	27.71	7.11	58.21	—	0.90	1806	a
Otus asio	AMNH 18290	19.66	13.69	16.88	16.74	5.90	37.15	—	0.94	191	b
Strix occidentalis	AMNH 26464	25.88	17.54	21.06	21.50	—	—	—	—	591	b
Tyto alba	AMNH 10691	18.53	13.11	14.95	15.53	7.26	23.23	—	0.90	479	a
ORDER TROGONIFORMES											
Pharomachrus mocinno	AMNH 8735	13.37	9.74	11.61	11.57	—	40.93	—	0.86	206	a
PALAEOGNATH BIRDS											
ORDER APTERYGIFORMES											
Apteryx australis (FL)	AMNH 27328	11.30	9.84	11.43	10.86	—	—	—	—	2403	a
ORDER CASUARIIFORMES											
Casuarius casuarius (FL)	AMNH 1516	27.78	17.84	17.97	21.20	—	—	—	—	44000	a
Casuarius unappendiculatus (FL)	AMNH 2729	24.56	16.73	16.77	19.35	—	—	—	—	10116	b
Dromaius novaehollandiae (FL)	AMNH 1708	26.15	16.51	16.88	19.85	—	—	—	—	31160	a
ORDER DINORNITHIFORMES											
Dinornis struthoides (FL)	YPM 9207	25.76	17.76	18.23	20.58	—	—	—	—	100500	h
ORDER STRUTHIONIFORMES											
Rhea americana (FL)	AMNH 2300	25.42	16.42	16.53	19.46	—	—	—	—	23000	a
Rhea pennata (FL)	AMNH 12891	22.48	15.81	16.29	18.19	—	—	—	—	27000	i
Struthio camelus (FL)	AMNH 1506	34.92	20.20	20.60	25.24	—	—	—	—	119300	j
ORDER TINAMIFORMES											
Crypturellus noctivagus	AMNH 5871	12.71	11.22	12.80	12.24	—	—	—	1.06	800	a
Eudromia elegans	AMNH 11435	13.05	12.21	13.21	12.82	—	—	—	0.91	660	a
Nothoprocta cinerascens	AMNH 6509	12.25	11.01	12.52	11.92	—	—	—	—	475	k
Nothoprocta ornata	AMNH 6502	13.62	11.02	12.14	12.26	—	—	—	—	572	k
Tinamus major	AMNH 5283	13.13	12.54	13.15	12.94	—	110.15	—	1.04	1052	a
BASAL AVIALANS											
Archeopteryx lithographica	BMNH 37001	14.26	12.47	11.78	12.84	6.73	39.27	—	1.15	468	l

NON-AVIAN THEROPOD DINOSAURS

Allosaurus fragilis (2P)	YPM 14554	61.31	52.64	35.33	49.76	—	—	—	—	952000	m
Ceratosaurus nasicornis (2P)	MWC-1	52.86	44.28	37.75	44.96	—	—	—	—	472600	m
Citipati osmolskae (2P)	IGM 100/978	33.64	28.15	24.66	28.82	—	—	—	—	62153	n
Dromaeosaurus albertensis (2P)	AMNH 5356	34.90	27.51	25.64	29.35	—	—	—	—	55000	o
Herrerasaurus ischigualastensis (2P)	MCZ 7063R	37.98	33.52	25.14	32.21	—	—	—	—	347800	m
Masiakasaurus knopfleri (2P)	MAD 03174	27.73	19.24	18.92	21.96	—	—	—	—	12513	p
Saurornithoides junior (2P)	IGM 100/1	29.33	27.85	29.81	29.00	—	—	—	—	27000	m
Struthiomimus altus (2P)	AMNH 5355	36.65	28.68	22.69	29.34	—	—	—	—	110000	m
Tyrannosaurus rex (2P)	AMNH 5029	99.29	48.52	69.63	72.48	—	—	—	—	6650900	m
Velociraptor mongoliensis (2P)	IGM 100/976	32.50	22.88	21.09	25.49	—	—	—	—	44300	m

SAUROPODOMORPH DINOSAURS

Anchisaurus polyzelus (2P)	YPM 1883	28.60	17.63	22.18	22.81	—	—	—	—	84000	m
Plateosaurus fraasianus (2P)	AMNH 6810	47.66	29.49	31.49	36.22	—	—	—	—	1072600	m
Thecodontosaurus antiquus (2P)	YPM 2192	28.60	17.63	22.18	22.81	—	—	—	—	24600	m
Apatosaurus ajax (4P)	YPM 1860	38.76	29.74	22.08	30.20	—	—	—	—	22407200	m
Diplodocus longus (4P)	AMNH 694	40.21	30.46	22.92	31.20	—	—	—	—	19654600	m
Camarasaurus lentus (4P)	CM 11969	35.34	24.91	22.68	27.64	—	—	—	—	11652200	m

ORNITHISCHIAN DINOSAURS

Psittacosaurus mongoliensis (2P)	IGM 100/1132	31.00	21.19	18.70	23.63	—	—	—	—	12100	m
Protoceratops andrewsi (4P)	IGM 100/1246	28.71	27.14	18.29	24.71	—	—	—	—	23700	m
Triceratops sp. (4P)	LACM 150168	55.10	61.76	39.89	52.25	—	—	—	—	4964000	m
Chasmosaurus mariscalensis (4P)	UTMP 42313-1	55.27	48.37	30.41	44.68	—	—	—	—	1658700	m
Stegosaurus sp. (4P)	YPM 1853	35.12	34.26	20.09	29.82	—	—	—	—	2610600	m
Euoplocephalus tutus (2P)	AMNH 5337	32.90	24.70	22.16	26.58	—	—	—	—	2675900	m
Camptosaurus dispar (2P)	YPM 1854	48.20	34.00	29.15	37.12	—	—	—	—	268400	m

Tenontosaurus tilletti [4P]	AMNH 3014	44.11	33.03	26.36	34.50	—	—	—	—	242900	m
Edmontosaurus sp. [4P]	AMNH 427	41.52	39.15	27.54	36.07	—	—	—	—	7594400	m
Corythosaurus sp. [4P]	AMNH 5433	42.52	35.27	30.95	36.25	—	—	—	—	3078500	m

Sources of Body Mass Estimates:

a. Dunning (1993).
b. Museum archive.
c. Livezey and Humphrey (1986).
d. Livezey (1988).
e. Alvarenga and Höfling (2003).
f. Suedmeyer et al. (2001).
g. Dominguez-Bello et al. (1994).
h. Bunce et al. (2003).
i. Cruz and Elkin (2003).
j. Cooper (2005).
k. Bertelli and Tubaro (2002).
l. Dominguez et al. (2004).
m. Seebacher (2001).
n. Franzosa (2004).
o. Peczkis (1994).
p. Estimated from equation in Anderson et al. (1985) using long-bone circumference measurements published in Carrano et al. (2002).

Appendix 2 – Taxonomic Ranks of Bird Specimens

Bird specimens in this study were assigned to taxonomic ranks using a phylogenetic hypothesis modified from Livezey and Zusi (2006, 2007). These ranks were used to compute "effective n" for bivariate regression equations using bird data points (Table 4–1) and to estimate the character variance attributable to particular taxonomic levels independent of other levels for logged ASCc, PSCc, and LSCc (Table 4–2), using fully nested ANOVA (after Smith, 1994). References for each rank are given in Livezey and Zusi (2007). Specimens were ranked as follows:

Subclass Avialae

Superorder Archaeornithes
Order Archaeopteryiformes
Family Archaeopterygidae
Archaeopteryx lithographica

Cohort Palaeognathae
Subcohort Crypturi
Superorder Dromaeomorphae
Order Tinamiformes
Family Tinamidae
Crypturellus noctivagus (yellow-legged tinamou)
Eudromia elegans (elegant crested tinamou)
Nothoprocta cinerascens (brushland tinamou)
Nothoprocta ornata (ornate tinamou)
Tinamus major (great tinamou)
Subcohort Ratitae
Superorder Apterygimorphae
Order Apterygiformes
Family Apterygidae
Apteryx australis (brown kiwi)
Order Dinornithiformes
Family Dinornithidae
Dinornis struthoides (moa)
Superorder Casuariimorphae
Order Casuariiformes
Family Casuariidae
Casuarius casuarius (southern cassowary)
Casuarius unappendiculatus (northern cassowary)
Family Dromaiidae
Dromaius novaehollandiae (emu)

Superorder Struthionimorphae
Order Struthioniformes
Family Struthionidae
Struthio camelus (ostrich)
Family Rheidae
Rhea americana (greater rhea)
Rhea pennata (lesser rhea)

Cohort Neognathae
Subcohort Galloanserae
Superorder Galloanserimorphae
Order Galliformes
Family Megapodiidae
Alectura lathami (Australian brush-turkey)
Family Phasianidae
Chrysolophus amherstiae (Lady Amherst's pheasant)
Lagopus lagopus (willow grouse)
Lophura erythrophthalma (crestless fireback)
Meleagris gallopavo (wild turkey)
Numida meleagris (helmeted guineafowl)
Pavo cristatus (Indean peafowl)
Phasianus colchicus (common pheasant)
Syrmaticus reevesii (Reeves's pheasant)
Order Anseriformes
Family Anseranatidae
Anseranas semipalmata (magpie-goose)
Family Anatidae
Anas acuta (northern pintail)
Anas clypeata (northern shoveler)
Anas penelope (Eurasian wigeon)
Anas platyrhynchos (mallard)
Anas rubripes (American black duck)
Anser fabalis (bean goose)
Branta leucopsis (barnacle goose)
Cairina moschata (Muscovy duck)
Cygnus atratus (black swan)
Cygnus buccinator (trumpeter swan)
Cygnus columbianus (tundra swan)
Cygnus olor (mute swan)
Somateria mollissima (common eider)
Tachyeres leucocephalus (Chubut steamerduck)
Tachyeres pteneres (flightless steamerduck)

Subcohort Neoaves

Superorder Gaviomorphae

Order Gaviiformes

Family Gaviidae

Gavia immer (common loon)

Gavia stellata (red-throated loon)

Order Podicipediformes

Family Podicipedidae

Aechmophorus occidentalis (western grebe)

Podiceps cristatus (great crested grebe)

Superorder Procellariimorphae

Order Procellariiformes

Family Oceanitidae

Oceanites oceanicus (Wilson's storm petrel)

Family Procellariidae

Daption capense (Cape petrel)

Fulmarus glacialis (northern fulmar)

Macronectes giganteus (southern giant petrel)

Puffinus griseus (sooty shearwater)

Puffinus tenuirostris (short-tailed shearwater)

Family Diomedeidae

Diomedea exulans (wandering albatross)

Diomedea immutabilis (Laysan albatross)

Diomedea irrorata (waved albatross)

Diomedea melanophrys (black-browed albatross)

Diomedea nigripes (black-footed albatross)

Superorder Pelecanimorphae

Order Pelecaniformes

Family Phaethontidae

Phaethon rubricauda (red-tailed tropicbird)

Family Fregatidae

Fregata magnificens (magnificent frigatebird)

Fregata minor (great frigatebird)

Family Pelecanidae

Pelecanus erythrorhynchos (American white pelican)

Pelecanus occidentalis (brown pelican)

Pelecanus onocrotalus (great white pelican)

Family Sulidae

Morus bassanus (northern gannet)

Sula dactylatra (masked booby)

Sula leucogaster (brown booby)

Sula sula (red-footed booby)

Family Phalacrocoracidae

Phalacrocorax auritus (double-crested cormorant)

Phalacrocorax carbo (great cormorant)

Phalacrocorax harrisi (flightless cormorant)
Phalacrocorax urile (red-faced shag)
Family Anhingidae
Anhinga anhinga (anhinga)

Superorder Ciconiimorphae
Order Ciconiiformes
Family Ciconiidae
Leptoptilos crumeniferus (marabou stork)
Mycteria americana (wood stork)
Family Phoenicopteridae
Phoenicopterus minor (lesser flamingo)
Phoenicopterus ruber (Caribbean flamingo)
Family Threskiornithidae
Ajaia ajaja (roseate spoonbill)
Eudocimus albus (white ibis)

Superorder Charadriimorphae
Order Gruiformes
Family Otididae
Neotis denhami (Stanley bustard)
Otis tarda (great bustard)
Family Cariamidae
Cariama cristata (red-legged seriema)
Family Phorusrhacidae
Psilopterus lemoinei (terror bird)
Family Rhynochetidae
Rhynochetos jubatus (kagu)
Family Aramidae
Aramus guarauna (limpkin)
Order Ralliformes
Family Rallidae
Aramides cajanea (grey-necked wood-rail)
Diaphorapteryx hawkinsi (Hawkins' rail)
Fulica americana (American coot)
Himantornis haematopus (Nkulengu rail)
Porphyrio hochstetteri (southern takahe)
Porphyrio porphyrio (purple swamphen)
Porzana carolina (sora)
Order Charadriiforme
Family Scolopacidae
Scolopax rusticola (Eurasian woodcock)
Family Burhinidae
Burhinus magnirostris (stone-plover)
Family Alcidae
Alca torda (razorbill)
Cerorhinca monocerata (rhinoceros auklet)

Fratercula arctica (Atlantic puffin)
Pinguinus impennis (great auk)
Uria aalge (common murre)
Uria lomvia (thick-billed murre)

Family Stercorariidae
Stercorarius parasiticus (arctic skua)

Family Laridae
Larus argentatus (herring gull)
Larus atricilla (laughing gull)
Larus canus (common gull)
Larus marinus (great black-backed gull)
Larus ridibundus (common black-headed gull)
Rissa tridactyla (black-legged kittiwake)
Sterna fuscata (sooty tern)
Sterna hirundo (common tern)
Sterna maxima (royal tern)

Family Rynchopidae
Rynchops niger (black skimmer)

Superorder Falconimorphae

Order Falconiformes

Family Cathartidae
Cathartes aura (turkey-vulture)
Coragyps atratus (black vulture)
Gymnogyps californianus (California condor)
Sarcoramphus papa (king vulture)

Family Sagittariidae
Sagittarius serpentarius (secretary bird)

Family Falconidae
Falco peregrinus (peregrine falcon)
Falco sparverius (American kestrel)
Falco tinnunculus (common kestrel)

Family Pandionidae
Pandion haliaetus (osprey)

Family Accipitridae
Accipiter gentilis (northern goshawk)
Accipiter nisus (Eurasian sparrowhawk)
Aquila chrysaetos (golden eagle)
Buteo buteo (common buzzard)
Buteo jamaicensis (red-tailed hawk)
Circus aeruginosus (western marsh harrier)
Circus cyaneus (northern harrier)
Circus pygargus (Montagu's harrier)
Elanus caeruleus (black-winged kite)
Gyps fulvus (Eurasian griffon)
Haliaeetus leucocephalus (bald eagle)

Harpia harpyja (harpy eagle)
Ictinia plumbea (plumbeous kite)
Milvus migrans (Australian black kite)
Spizaetus ornatus (ornate hawk-eagle)
Torgos tracheliotus (lappet-faced vulture)

Order Strigiformes

Family Tytonidae

Tyto alba (barn owl)

Family Strigidae

Asio flammeus (short-eared owl)
Bubo virginianus (great horned owl)
Nyctea scandiaca (snowy owl)
Otus asio (eastern screech owl)
Strix occidentalis (spotted owl)

Superorder Cuculimorphae

Order Opisthocomiformes

Family Opisthocomidae

Opisthocomus hoazin (hoatzin)

Order Cuculiformes

Family Cuculidae

Geococcyx californianus (greater roadrunner)

Superorder Psittacimorphae

Order Psittaciformes

Family Psittacidae

Alisterus scapularis (Australian king-parrot)
Amazona ochrocephala (yellow-crowned parrot)
Anodorhynchus hyacinthinus (hyacinth macaw)
Nestor meridionalis (kaka)
Probosciger aterrimus (palm cockatoo)
Psittacus erithacus (grey parrot)
Strigops habroptilus (kakapo)

Order Columbiformes

Family Columbidae

Caloenas nicobarica (Nicobar pigeon)
Columba fasciata (band-tailed pigeon)
Columba livia (common pigeon)
Columba picazuro (Picazuro pigeon)
Goura victoria (Victoria crowned-pigeon)

Superorder Cypselomorphae

Order Caprimulgiformes

Family Caprimulgidae

Chordeiles minor (common nighthawk)

Family Nyctibiidae
Nyctibius griseus (common potoo)
Family Podargidae
Podargus strigoides (tawny frogmouth)
Family Steatornithidae
Steatornis caripensis (oilbird)
Order Apodiformes
Family Trochilidae
Campylopterus duidae (buff-breasted sabrewing)
Metallura tyrianthinas (Tyrian metaltail)

Superorder Trogonomorphae
Order Trogoniformes
Family Trogonidae
Pharomachrus mocinno (resplendent quetzal)

Superorder Passerimorphae
Order Coraciiformes
Family Coraciidae
Coracias garrulus (European roller)
Order Piciformes
Family Picidae
Dryocopus pileatus (pileated woodpecker)
Order Passeriformes
Family Corvidae
Corvus brachyrhynchos (American crow)
Corvus corone (carrion crow)
Corvus frugilegus (rook)
Corvus monedula (Eurasian jackdaw)
Pica pica (common magpie)
Family Cotingidae
Procnias nudicollis (bare-throated bellbird)
Rupicola rupicola (Guianan cock-of-the-rock)
Family Hirundinidae
Hirundo rustica (barn swallow)
Family Icteridae
Molothrus ater (brown-headed cowbird)
Family Sturnidae
Sturnus vulgaris (European starling)
Family Turdidae
Turdus migratorius (American robin)